

**Synthesis and properties of
new heterocyclic metallised dyes**

Kevin J. Boyle BSc. (Hons).

Thesis presented for the degree of
Doctor of Philosophy,
The University of Edinburgh,
January 2005

Declaration

I declare that this thesis is my own composition, that the work which is described has been carried out by myself, unless otherwise stated, and that it has not been submitted in any previous application for a higher degree.

This thesis describes the results of research carried out in the Department of Chemistry, University of Edinburgh, under the supervision of Dr Hamish McNab, since 1-4-01, the date of my admission as a research student.

Signed:-

Date:-

Acknowledgements

I would like to thank my supervisor Dr. Hamish McNab for his constant enthusiasm, support and advice over the last three years.

I would like to thank Dr Prakash Patel, Dr Mark Kenworthy, Dr Graeme Watson and Dr Doug Spencer (all Avecia) for their invaluable help and support. I would also like to thank Mr Chris Nally, Dr Patricia Dunwoody and Dr Marie Holmes for their help while at Avecia (Grangemouth and Blackley). Thanks again to Avecia, in particular to Dr Colin Robertson, for their funding of this research.

I would like to thank the technical staff at the University of Edinburgh, especially Mr J. A. R. Millar (NMR) and Mr A. T. Taylor (Mass Spec.).

Thanks to all the McNab research group past and present, especially Mr Stuart Wharton for all the NMR work.

Lecture Courses Attended

Organic Research Seminars, Edinburgh University, School of Chemistry (3 years attendance).

Organic Colloquia, Edinburgh University, School of Chemistry (3 years attendance).

Royal Society of Chemistry, Perkin Division, Annual Scottish Meeting (3 years attendance).

Organometallics and Synthesis, Dr A. Hulme (5 lectures).

Royal Society of Chemistry, Perkin Division, RSC-SCI Joint Meeting (International Conference) on Heterocyclic Chemistry, Edinburgh (3 days).

Liquid and Solid State NMR Spectroscopy in Drug Discovery and Development, Edinburgh University, School of Chemistry (6 lectures).

Modern Colourant Chemistry, Avecia, Grangemouth (8 lectures).

Sigma-Aldrich Contemporary Organic Synthesis, Postgraduate symposium, Edinburgh University, School of Chemistry (4 lectures).

Strategies for Synthesis, Postgraduate Symposium, Edinburgh University School of Chemistry (3 lectures).

Contemporary Synthetic techniques, Postgraduate Symposium, Edinburgh University School of Chemistry (3 lectures).

SCI Symposium, Edinburgh University, School of Chemistry (4 lectures).

Abstract

Various 3-substituted isoquinolin-4-ols have been successfully synthesised by two different methodologies. Treatment of isoquinoline *N*-oxide with *p*-toluenesulfonyl chloride, provided 4-(*p*-toluenesulfonyloxy)isoquinoline in 30% yield and high purity, *via* rearrangement of an intermediate *N*-(*p*-toluenesulfonyloxy) compound. Isoquinolin-4-ol was then obtained, after acid hydrolysis of 4-(*p*-toluenesulfonyloxy)isoquinoline. 3-Methylisoquinolin-4-ol has been synthesised in a similar manner and yield, from 3-methylisoquinoline *N*-oxide *via* 3-methyl-4-(*p*-toluenesulfonyloxy)isoquinoline. 4-(*p*-Nitrobenzenesulfonyloxy)isoquinoline has been obtained from the reaction between isoquinoline *N*-oxide and *p*-nitrobenzenesulfonyl chloride. The regioselectivity of these rearrangements was in contrast to that of isoquinoline *N*-oxide with 2,4-dinitrobenzenesulfonyl chloride, which gave 1-(2,4-dinitrobenzenesulfonyloxy)isoquinoline.

The Mannich reaction was used to functionalise isoquinolin-4-ol at the 3-position, giving 3-(dimethylaminomethyl)isoquinolin-4-ol and sodium 3-aza-3-methyl-4(4-hydroxyisoquinolin-3-yl)butane-1-sulfonate. These derivatives however, proved unstable to attempted azo coupling at the unsubstituted 1-position.

FVP of various 5-aryloxy-5-methyl Meldrum's acid derivatives has provided a novel reduction of the azo group to the corresponding hydrocarbon, but the reaction was shown to take place in the FVP inlet, and due to the low yields is of limited synthetic use.

3-Phenylisoquinolin-4-ol has been synthesised *via* an isoindolone precursor in 20% yield, under FVP conditions, but the method has proved inapplicable to alkyl derivatives.

A novel azo cyan dye was synthesised from the reaction between 3-phenylisoquinolin-4-ol and a diazonium salt derived from 2-amino-6-chloro-4-sulfonamidophenol. The metallised complex of the azo dye was then obtained after reaction with nickel (II) acetate tetrahydrate.

Diazoindazole was synthesised from 3-aminoindazole in high yield, and its coupling reactions were investigated. Reaction with active methylene compounds provided a model series of water insoluble yellow derivatives. 3-Aminoindazole was then

sulfonated and coupled under standard conditions to a sulfonated β -ketoamide, providing a novel water soluble yellow dye.

Water soluble magenta dyes have been obtained *via* coupling reactions between diazoindazole and various sulfonated naphthol derivatives. The ligands obtained were reacted with nickel (II) acetate tetrahydrate, and their metallised complexes were readily formed.

A water soluble analogue was obtained when the diazonium salt derived from 3-amino-1,2-benzisoxazole was successfully coupled under standard aqueous conditions to disodium 2-naphthol-3,7-disulfonic acid, but the ligand proved to be far less reactive towards metallisation than the corresponding indazole analogue. A further analogue was obtained when the diazonium salt derived from 1-benzyl-3-aminoindazole was coupled to disodium 2-naphthol-3,7-disulfonic acid; the ligand readily formed its metallised complex when reacted with nickel (II) acetate tetrahydrate.

Several dyes were selected for applications testing, where their stability upon exposure to light and ozone was examined, as well as quantifying their colour properties.

Contents

1. INTRODUCTION

Preamble	1
1.1 Ink Jet Printing	1
1.2 History and Concept	1
1.3 Continuous Technology	2
1.4 Drop-on-demand Technology	4
1.5 Ink Jet Triumvirate	6
1.6 Composition of the ink	6
1.7 Colourants	7
1.8 UV-Vis Spectroscopy	8
1.9 The origin of colour	9
1.10 Describing Colour	10
1.11 Dye Requirements	14
1.12 Papers	14
1.13 Kogation	15
1.14 Ames Testing	16
1.15 Impurities	16
1.16 Solubility	17
1.17 Structure of the Dye	17
1.18 1 st Generation Dyes	19
1.19 2 nd Generation Dyes	22
1.20 Current Trends	24
1.21 Fading	26
1.22 Metallisation	29

2. DISCUSSION

3-Substituted Isoquinolin-4-ols	34
2.1 Synthesis from <i>N</i> -oxides	34
2.2 Synthesis <i>via</i> dihydro intermediates	39
2.3 Synthesis from isoquinolin-4-ol	43

2.4 Other methods	46
2.6 Metallised isoquinolin-4-ol dyes	50
2.7 New Routes to isoquinolin-4-ols	51
2.8 Characterisation of isoquinolin-4-ols	51
2.9 Synthesis of isoquinolin-4-ol	52
2.10 Other rearrangements	60
2.11 Reactions of isoquinolin-4-ol	66
2.12 FVP methods	74
2.13 Synthesis of azo dye	96
2.16 Literature synthesis of diazoindazole	105
2.17 Literature synthesis of diazoindazole derivatives	107
2.19 Literature reactions of diazoindazole	110
2.22 Benzimidazole derivatives	123
2.24 Synthesis of diazoindazole	125
2.25 Yellow dyes	127
2.26 Magenta dyes	142
2.27 Benzisoxazole derivatives	158
2.28 1-Benzyl-3-aminoindazole	167
2.29 UV-Vis data for sulfo F-acid derivatives	171
2.30 Metallised complex geometry	171
2.31 Applications testing	173
3. EXPERIMENTAL	
3.1 Abbreviations	185
3.2 Instrumentation	189
3.3 Flash Vacuum Pyrolysis	192
3.4 General Synthesis of <i>N</i> -Oxides	193
3.5 Rearrangement reactions	194
3.7 Reactions of isoquinolin-4-ol derivatives	200
3.10 Synthesis and FVP of Imine Precursors	205
3.11 Methyl Meldrum's acid precursors	207
3.12 FVP of Methyl Meldrum's Acid Derivatives	210

3.13 Synthesis and FVP of isoindolone precursors	212
3.15 Synthesis of sulfonamide	215
3.16 Synthesis of azo dye	217
3.17 Synthesis of diazoindazole	218
3.18 Reactions of diazoindazole	219
3.21 Synthesis of benzisoxazole derivatives	228
3.23 Synthesis and reaction of 1-benzyl-3-aminoindazole	231
3.24 UV-Vis studies	233
3.33 Quantitative addition of nickel (II) acetate tetrahydrate	245
3.35 Large scale metallisations	247
3.37 Stability studies	248
3.40 Applications testing	251
4. REFERENCES	253
5. APPENDICES	259

1. INTRODUCTION

Preamble

There are many important features involved in the success of modern ink jet printing systems. Progression and development of this technology has been rapid over recent years, and will continue to grow further in the future. Section 1.1 highlights many of these advances and the key elements required in this field.

The role of the colourant (dyes and pigments) is an important feature, which is of great interest to the chemist. The colourant is responsible for the reliability and the bright attractive colours that are required for the ink to be a success; development of the colourant has therefore initiated much research. In this thesis, the synthesis and properties of many novel heterocyclic dyes are discussed.

1.1 Ink jet printing

Ink jet printing can be described as today's leading non-impact printing technology.^{1a} Until 20 years ago, impact printers dominated office and home printing. However, there were many drawbacks to this technology, mainly that it was too slow, too noisy and was restricted to text and monochrome.^{1b} Clearly a very lucrative market and opportunity therefore existed for non-impact technologies to exploit.

Due to its low cost, ever improving high quality, reasonable speed, capability of printing on a variety of substrates, and ability to produce text or graphics in monochrome and colour, ink jet now leads the way in this market. Applications cover a wide range, from simple home and office use, to printing sell-by-dates on cornflakes packets and printing of colour filters used in flat screen displays.^{1a}

1.2 History and concept

The mechanism, by which a liquid stream breaks up into droplets, was discovered as far back as 1878 by Lord Rayleigh,^{1b} and is now the basis for modern day ink jet technology. The first use of ink jet in recording devices dates to the 1930s,^{1b,3} but it took until 1951 for the production of the first successful product, when Seimens patented the first practical Rayleigh break-up device, the Mingograph.^{3,4} This device was one of the first commercial ink jet chart recorders. The 50s and 60s saw a great advance in computer systems, which meant that there was a need for high speed electronic printing methods. A further breakthrough occurred in the early 1960s,

when Sweet developed continuous ink jet technology (see Section 1.3).^{1b,6} This technology had many advantages over the early printers, mainly in its speed, quiet operation and non-contact imaging.⁵ Hertz further modified this in 1967 (see Section 1.3), by developing a method which allowed access to the grey scale and also produced commercial high quality colour images.⁴ The main drawbacks of the continuous technology were the cost, poor print quality and poor reliability.⁵

Today's leading technology is drop-on-demand ink jet printing.^{1a} The first method, known as the piezoelectric method (see Section 1.4.1), was pioneered by Zoltan in 1972.^{1b,3,6} Immediate advantages over the continuous technology were apparent. The system was simpler, more reliable and less expensive.⁵ Piezoelectric ink jet was by no means perfect, even though it had improved upon the continuous method. Nozzles were still prone to clogging and the images were inconsistent. New problems also arose with the introduction of the bulky printhead, which was expensive.^{1b,4} Another landmark was the first near letter quality ink jet product pioneered by IBM in the 70s, but still the images produced were not reliable.

The discovery of thermal or bubble ink jet printing technology was the major breakthrough, changing the technical picture completely, simultaneously pioneered by Canon and Hewlett-Packard in 1979.^{1a,1b,3,4,6} The very simple idea of the growth and collapse of a bubble to force out droplets of ink was used (see Section 1.4.2). Hewlett-Packard marketed the first low-cost thermal ink jet printer in 1984, which used disposable printheads. The idea of the disposable printhead and ink cartridge was brilliant and original, eliminating the previous reliability and cost problems.⁵ The combined factors of low cost, simplicity, full colour and high quality images, make thermal ink jet technology dominant in this market.^{1b} The introduction of this technology ended the use of continuous printers in the office.

However, problems do still exist with ink jet technology, such as the drying time of the ink and throughput speeds; more significant problems are associated with the development of the colourant (see Sections 1.21 and 1.22).⁵

1.3 Continuous Technology/Mechanism

Sweet's technology was the first example of continuous ink jet printing. He demonstrated that by applying a pressure wave to an orifice, the ink jet stream could

be broken into droplets of uniform size and spacing. An electrical charge can then be applied onto the drops selectively and reliably, as they are formed out of the continuous stream. The drops then pass through a high voltage electric field, where upon they are deflected.⁴ There are two different deflection methods, either binary or multiple (raster scan), as illustrated below in Figure 1.

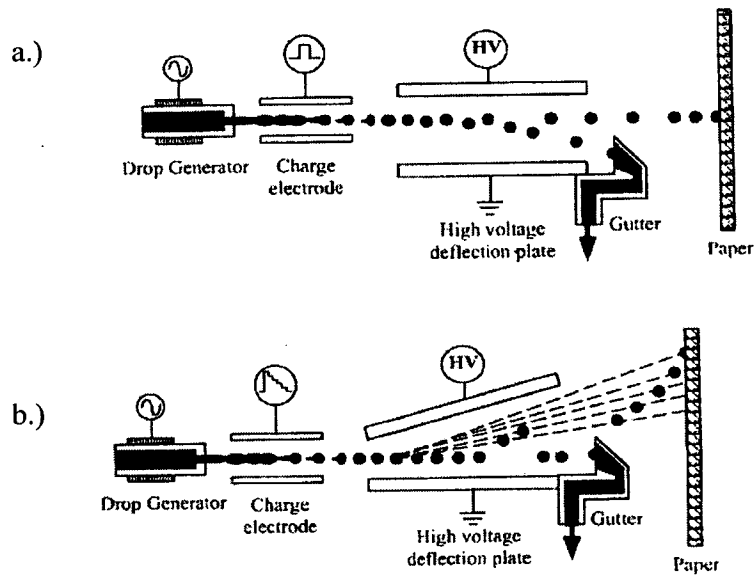


Figure 1 The two different deflection methods used in continuous ink jet printing, a.) binary deflection and b.) multiple deflection.⁴

In both cases, the drops are either charged or uncharged. The uncharged drops in binary deflection fly directly onto the medium to form the image, while the charged drops are deflected into the gutter for recirculation. In multiple deflection, the charged drops are deflected onto the medium at different levels, while the uncharged drops go straight back to the gutter.^{3,6} Both of these methods are suited to monochrome printing, and are used in the industrial coding, marking and labelling markets.^{3,4} The very high drop production capabilities enables these printers to write on irregular surfaces at high speeds on the production line.

Hertz's modified continuous technology, which was based on the binary deflection method, allowed access to the grey scale by controlling the number of drops

deposited on each pixel. By varying the number of drops laid down, the volume of ink in each pixel was controlled, resulting in irregular sized ink drops being formed, and therefore, the density of each colour could be adjusted to give the desired tone.⁶ This method is more suited for colour images than the previous two methods, and is commonly used in the graphics art market, still employed by Iris.^{4,5}

1.4 Drop-on-demand Technology

Four major drop-on-demand methods currently exist, thermal, piezoelectric, acoustic and electrostatic, although acoustic and electrostatic are still in the early stages of development. Almost all of the drop-on-demand printers in use today are either thermal or piezoelectric; the vast majority of which are thermal.⁴

The big advantage that drop-on-demand has over continuous, is that it is more efficient. Drops are only ejected when required, and therefore, every drop produced is used in forming the image, resulting in lower cost.^{3,6}

As no deflection methods are involved, the complexities of charging the drops, the deflection hardware and the unreliability of ink recirculation, typical of continuous technology, are all eliminated.^{4,6} Printheads are as close to the substrate as possible, so the droplets travel a short distance to the desired point, producing high quality and accurate images. This is in contrast to continuous technology, where the drops travel greater distances, and is therefore used for printing on irregular surfaces such as cardboard boxes.⁶

1.4.1 Piezoelectric Technology/Mechanism

The principle of this method is to convert a pulse of electrical energy into a mechanical pressure pulse, that is sufficient enough to overcome surface tension forces holding ink at the nozzle. The droplet ejection is controlled by an electrical signal that produces a deformation in a piezoelectric crystal, resulting in a pressure wave in the ink, which is subsequently forced out. There are four main piezoelectric methods used, depending on the mode of deformation of the crystal; bend (Figure 2), push, squeeze and shear^{1a}

Despite the current dominance of thermal ink jet printers (Hewlett Packard and Lexmark particularly in the US), the piezoelectric method still has a place in the

market.² Seiko Epson (SEC) produce only piezoelectric printers, and can compete commercially with thermal printers;^{1a,1b} SEC and Canon currently dominate the Japanese market; and SEC are looking to double their share in the US which is currently around 11%.²

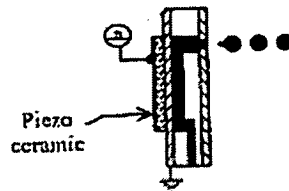


Figure 2 An example of one of the technologies used in piezoelectric ink jet printing.^{1b}

1.4.2 Thermal Technology/Mechanism

Printers that use this method contain an ink chamber with a heater and a nozzle nearby. A short pulse of current (lasting for less than a few microseconds) is passed through the heater, in the tip of the nozzle, to the ink. A rapid temperature rise results, and at ~ 300 °C, a tiny bubble is formed in water based inks. The bubble then exerts pressure causing an ultra-fine droplet of ink to be ejected from the nozzle (Figure 3). A vacuum is created as a result of the bubble collapsing after the droplet is ejected, drawing new ink in to replace the ejected ink. The whole bubble formation and collapsing process takes less than ten microseconds. The ink recirculation takes ~ 80 - 200 μ s.^{1a,3} This process is repeatable and reproducible, as at the superheated temperature of 300 °C, the behaviour of the water becomes predictable. The bubble involved in this process, is steam and not air, as an air bubble would not redissolve quickly enough.⁷

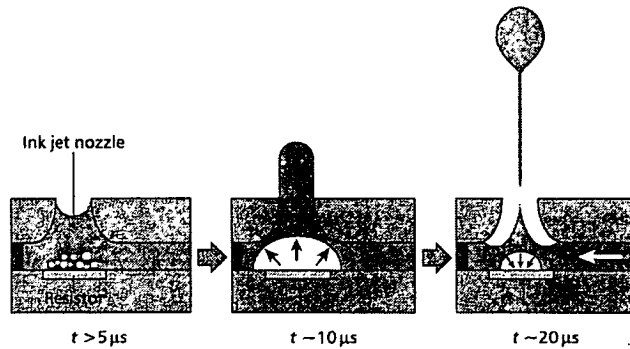


Figure 3 The mechanism of action in thermal drop-on-demand ink jet printing.^{1a}

Advances on the present technology are always being sought. The introduction of faster, better and cheaper printers is always the goal, and there is great incentive for ink jet companies such as Hewlett Packard, SEC, Canon and Lexmark.^{1a,1b} New applications such as colour copying saw an explosion in unit volume of ink jet products in the 1990s. The introduction of specialised media has also added many vendors to the market, and attracted many ink suppliers who sell the bulk inks, a consequence of the high profit margins available.

1.5 Ink jet Triumvirate

The combination of the ink, printhead and media are all very closely linked, and are collectively known as the triumvirate. The interaction and relationship between these components is very important and determines the potential success of an ink jet product. Inks are much easier and cheaper to develop than printheads, mirrored in the fact that there are only around twelve organisations worldwide investing in printhead manufacture. Great expense, technical skills and advanced equipment are required; inks however, are far easier to manufacture but difficult to design.⁷

1.6. Composition of the ink

The three types of inks commonly used in ink jet systems are aqueous, solvent and phase change based.^{3,6} Drop-on-demand printers use aqueous based inks, whereas continuous printers use either solvent inks, or phase change inks.⁶ Continuous or

piezoelectronic methods are used when non-aqueous inks are required. Table 1 summarises the essential components involved in a typical aqueous ink.^{1a}

Component	%
Dye (Water soluble)	~ 3-6%
Water	~ 70-80%
Humectant	~ 5-10%
Surfactant	~ 1%
Penetrant	~ 2-10%

Table 1 The various components involved in a typical ink.^{1b}

Water is used as the solvent in drop-on-demand inks, as it is excellent for the anionic water-soluble dyes used in ink jet printing, it is better than any other solvent for bubble formation, and it is safe/low cost. Water also has its drawbacks, as it is a good medium for growth of bacteria/fungi, leading to nozzle clogging, and it is a good corrosion promoter.^{3,6}

Humectants are high boiling water-miscible compounds such as diethylene glycol or 2-pyrrolidone, which prevent evaporation of water from the printhead nozzle when the printer is not in use. Any evaporation causes the dye to crystallise from the ink, blocking the nozzle.

The surfactant/penetrant lowers surface tension and effects rapid penetration of the ink into the medium. A typical penetrant is pentane-1,5-diol and a typical surfactant is Surfynol 465.^{1a}

Due to the high importance of the role of the dye in an ink, a full discussion will be provided below forming the remainder of this introduction.

1.7. Colourants

The colourant is the key element in the ink, producing a bright well defined image.⁸ The two main classes of colourant are dyes and pigments. Dyes have traditionally been used almost exclusively in ink jet printing, as pigments are insoluble, and

consequently clog the nozzle; they also tend to be duller.⁶ However, ink jet pigments are now becoming more common. Recent advances have led to Hewlett Packard using a black pigment in thermal printers, and the leading piezoelectric technology pioneered by SEC uses only pigments which display high fastness properties, but are expensive.

The three subtractive primary colours yellow, cyan and magenta, the most vivid colours available, plus black, are used in imaging systems.^{1a} Due to the amount of printed text, black is the most important colour.⁶

A 2-D representation of colour, is shown below in Figure 4, with yellow, cyan and magenta at the extremities. Any colour desired can be obtained by various combinations of these three colours.

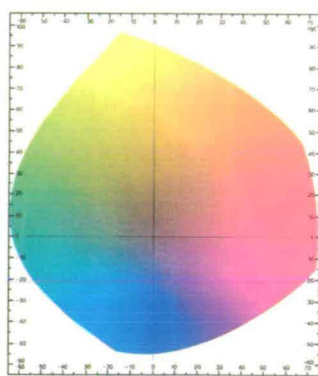


Figure 4 Colour map showing yellow, magenta and cyan.

1.8 UV-Vis spectra

All coloured substances give characteristic absorption curves or spectra, in which the degree of absorption is plotted against wavelength or frequency, an example of which is shown in Figure 5. An ultra-violet (~200-380 nm) or visible (~380 nm-760 nm) absorption curve is obtained which gives an accurate indication of the shade of the dye. The key parameters which are obtained from any UV-Vis curve, are the absorption maxima or peak wavelength (λ_{\max}), which describes the colour of the dye, and the shape of the absorption curve. A symmetrical curve is desirable with no extra absorption areas evident, especially at high wavelengths; “high wavelength tails” are observed when the curve does not fall directly to the baseline, but “tails” off at a

much shallower gradient, and can contribute to an undesirable hue. The width of the curve at half the maximum absorption (half-band width, $w_{1/2}$) is also important; bright dyes exhibit narrow absorption curves ($w_{1/2} < 100$ nm) and sharp peaks, giving a comprehensive balanced colour gamut.⁹ On the other hand, dull dyes have much broader and less well defined peaks, due to unwanted absorptions outside the desired range.^{6,10}

A bathochromic shift is observed in the UV-Vis spectrum, if substitution of one group for another causes absorbance at a higher wavelength. The opposite is true for a hypsochromic shift.^{10,11} Typical absorbances for ideal yellow, magenta and cyan dyes would be observed at approximately 440 nm, 540 nm and 640 nm respectively.

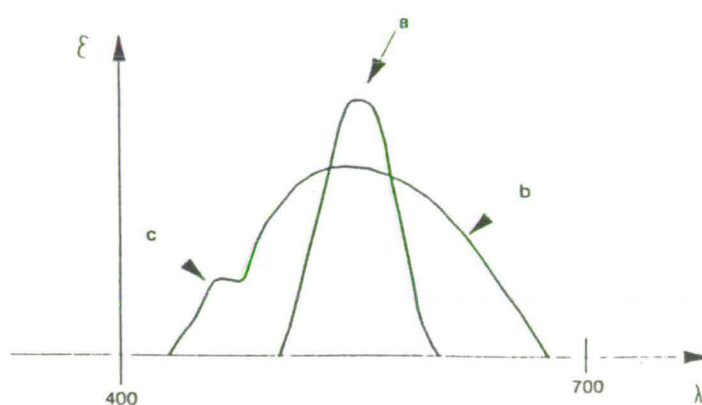


Figure 5 An example of a typical absorption curve obtained for: a.) a bright ideal magenta dye and b.) a duller, nonideal magenta dye with unwanted secondary absorptions at c.)⁶

1.9 The origin of colour in dyes.

In general, the colour of a material is due to absorption of light, resulting in the promotion of an electron, usually from the ground state (HOMO), to a higher unoccupied orbital (LUMO). The colour obtained depends on the wavelength of the light absorbed, which depends on the difference in energy between the orbitals in question. This difference in the energy levels depends on the structure of the dye involved.^{10,11}

The chromophore, generally electron withdrawing groups such as azo, nitro, methine or carbonyl containing groups, is principally responsible for the colour observed. The addition of groups conjugatively linked to the chromophore called auxochromes (generally electron donating groups containing atoms such as nitrogen, oxygen and halogens) can cause a bathochromic shift, providing a more intense colour.^{6,7}

Conjugation is a common feature often referred to when describing coloured compounds.^{10,12} As a general rule, the longer the conjugated system, then the more bathochromic a shift that will be observed.⁷

1.10 Describing Colour

Various ways have been used to quantify colour and one common way to do this is by using a colour space, which is simply an arrangement of colours in some orderly fashion.

In 1905, the artist Albert H. Munsell originated a colour ordering system or colour scale, which is still used today. This system is historically significant as it is based on human perception, and was devised before instrumentation was available for measuring and specifying colour. Many different types of colour space are based on Munsell's.^{13,14}

Colour spaces evolved out of the necessity to provide a uniform method to spread colours relative to their visual differences and to describe colour in numerical terms that makes sense to us.¹⁵

1.10.1 The CIE

Any system of measurement requires a repeatable set of standard scales. This led to the formation of the CIE (International Commission on Illumination), whose ultimate goal was to develop a repeatable system of colour communication standards for manufacturers of paints, inks, dyes and other colourants, and to provide a universal framework for colour matching. In 1931, the CIE established standards for a series of colour spaces that represent the visible spectrum. They utilised three coordinates to locate a colour in space that are device independent, and therefore, a range of colours is not limited to a particular device or the visual skills of the observer.^{13,15}

Every measurement is related to a standard observer, which describes how an average human sees colour. A standard observer aperture angle or field of view, of 2° was established in 1931, and another of 10° in 1964. The 10° view is much more commonly used today than the 2°, and was introduced as it was found to be more accurate.¹⁵

Another problem was that lighting conditions influence the appearance of colours, and therefore standard illuminants had to be developed. The spectral quality of natural daylight constantly changes from hour to hour, day to day, season to season and place to place. Natural daylight is not available at night or in interior rooms, therefore, technologies that simulate daylight phases were developed. Daylight sources are the preferred sources for colour evaluation, due to their equal energy distribution, which other light sources do not exhibit. The best sources are through filtered tungsten halogen sources. Illuminants called D₅₀ and D₆₅ are used to simulate daylight conditions (at colour temperatures of 5000 K and 6407 K respectively). Colour temperature can best be described with the analogy of an iron bar that is placed in a furnace. The iron bar changes colour as the temperature increases, going from an initial dull red, becoming brighter, and eventually going through to blue-white. In the same way, a filament in a lamp changes colour as varying voltages are applied. D₆₅ has the entire spectrum in close to equal amounts, and simulates average north sky daylight, conforming with international standards in Europe, Orient and South America.¹⁵

1.10.2 CIELab and CIELCh Colour Systems

The CIELab system is based on the theory that a colour cannot be both green and red at the same time nor blue and yellow, resulting in a system that defined numbers that could be used to represent a colour.

L - a measure of the lightness of an object (0 black to 100 white)

a - a measure of redness (positive a) or greenness (negative a)

b - a measure of yellowness (positive b) or blueness (negative b)

The a and b values approach zero for neutral colours (white, grey and black), while the higher a and b are, the more saturated a colour is.

In addition, colours can also be defined by lightness, chroma and hue (CIELCh). This system is based on CIELab but describes the location of a colour in space by use of polar coordinates rather than rectangular coordinates. Hue (colour) is the way in which someone would distinguish red from green, chroma is the saturation/intensity of a particular colour (see Equation 1), or the degree of departure from the neutral colour, and lightness distinguishes between dark and light colours.

$$\text{Chroma} = \sqrt{a^2 + b^2} \quad \text{Equation 1}$$

Lightness, similarly to the Lab system, is the central axis, chroma is the horizontal axis that extends from the lightness axis, and the hue is an angle at which the chroma axis extends from the lightness axis. Typical hue values are around 340°, 90° and 190° for magenta, yellow and cyan dyes respectively.^{7,14,15}

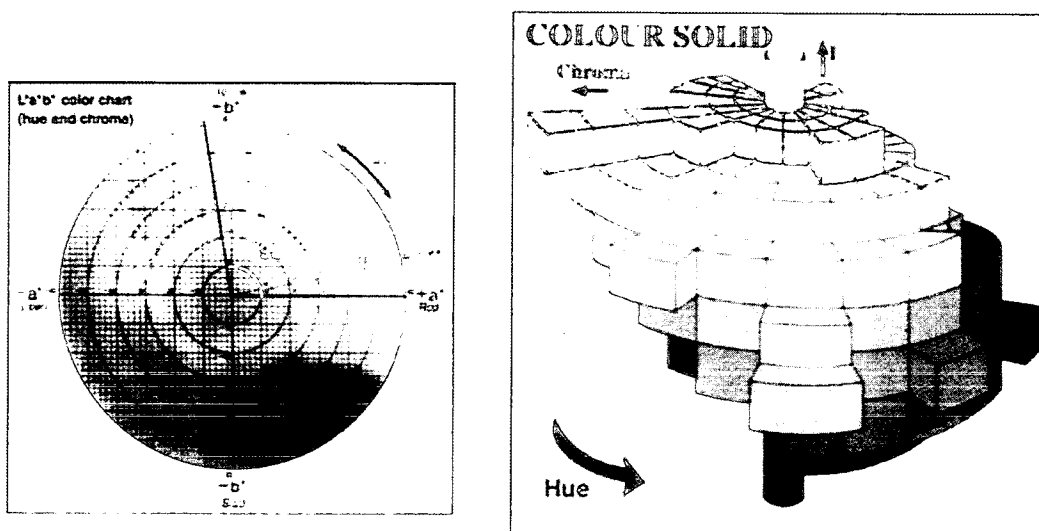


Figure 6 Two representations of CIE colour systems, showing L, a, b, C and h.

The a and b values approach zero for neutral colours (white, grey and black), while the higher a and b are, the more saturated a colour is.

In addition, colours can also be defined by lightness, chroma and hue (CIELCh). This system is based on CIELab but describes the location of a colour in space by use of polar coordinates rather than rectangular coordinates. Hue (colour) is the way in which someone would distinguish red from green, chroma is the saturation/intensity of a particular colour (see Equation 1), or the degree of departure from the neutral colour, and lightness distinguishes between dark and light colours.

$$\text{Chroma} = \sqrt{a^2 + b^2} \quad \text{Equation 1}$$

Lightness, similarly to the Lab system, is the central axis, chroma is the horizontal axis that extends from the lightness axis, and the hue is an angle at which the chroma axis extends from the lightness axis. Typical hue values are around 340°, 90° and 190° for magenta, yellow and cyan dyes respectively.^{7,14,15}

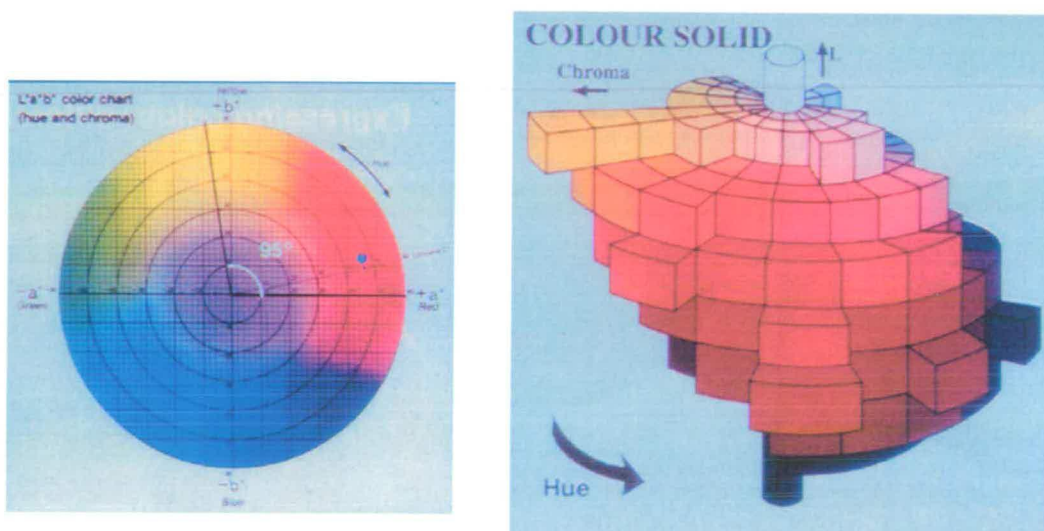


Figure 6 Two representations of CIE colour systems, showing L, a, b, C and h.

1.10.3 Measurement

The mixing of different wavelengths of energy to create white light is known as the additive colour process, such as used in a colour television, using the three colours red, green and blue. On the other hand, the subtractive colour process is used in the printing industry. Any material containing dyes or pigments will reflect, absorb or transmit light energy, resulting in a colour being produced according to the subtractive colour theory, using the colours cyan, yellow and magenta. A cyan colourant will absorb red energy (subtraction), and reflect the remaining light as cyan energy (combination of blue and green), similarly, yellow subtracts blue, while magenta subtracts green. The combination of all three colours produces black light, where all light is absorbed.¹⁵

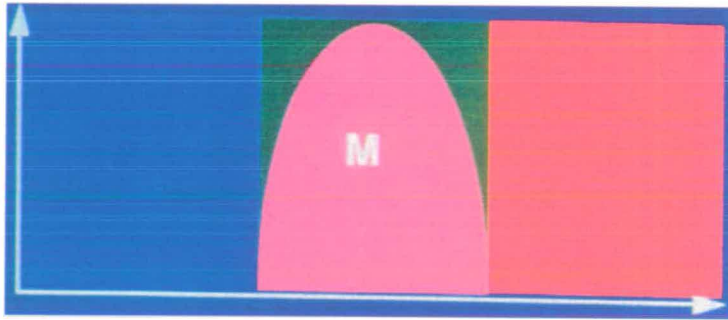


Figure 7 The subtractive curve for magenta, showing the absorbance of green energy, and reflectance of blue and red, to give magenta.

There are various devices used to measure colour, such as a colorimeter or spectrophotometer, made by companies such as X-Rite or Gretag Macbeth. These are photoelectric devices that simply measure and compute how much of a known amount of light is reflected from an object. The amount of reflectance is measured and translated into ROD (Reflectance Optical density) values using Equation 2.¹⁴

$$\text{Density (ROD)} = \log_{10} 1/R, \text{ where } R = \text{reflectance} \quad \text{Equation 2}$$

Light is shone through coloured filters and the appropriate colours, as described above, are removed by these filters. The filters remove light at specific wavelengths, and at these points, the reflectance, which is at a minimum (maximum absorbance),

is measured, and reported as ROD values, using Equation 2. Black exhibits almost no reflectance.¹⁵

1.11 Dye Requirements

Dyes used in ink printing technology have to meet many requirements. The prints must display the same shade across a range of substrates, which is very difficult to achieve due to a huge variety of substrate properties, different textures, adsorption characteristics, additives, pH *etc.*, and ideally a dye which is insensitive to such factors is required.⁷ Important factors include colour (hue), chroma (vividness), good light fastness (see Section 1.20), wet fastness and ozone fastness, high aqueous solubility (see Section 1.15) and high thermal stability (see Section 1.14).^{1b}

The dyes' ability to resist fading upon exposure to light and ozone, both of which are major problems, is currently generating great research.

1.12 Papers

The media used with ink jet applications include all of the materials used by other marking technologies. An ink jet system is expected to write successfully on plain papers that are used in other technologies. If other substrates *e.g.* plastic film, fabrics and specialised papers, are to be used, then an absorptive coating is required.⁷

The interaction of the ink on plain paper is one of the most important characteristics for product success, as well as one of the most difficult to control. This is because plain paper is a very chaotic material in a physical sense and different papers have widely varying chemical properties. The structure of a plain paper consists of a matted tangle of cellulose fibres which have different lengths and cross-sections, which does not make a smooth surface; the areas in-between the fibres are called voids and vary in size. Small white particles called fillers are added to improve brightness, and to make the paper smoother.¹⁷ Different paper mills drawing from different fibre stocks, chemicals and process hardware produce tangled nests with different void structures, fibre characteristics and chemistries. Ink jet formulations do not perform well on plain papers in general, and the majority of plain papers are not intentionally manufactured to suit the ink jet system.⁷

Aqueous ink jet inks have the viscosity and hydrophilic components that set up surface tension and capillary forces that pull the ink along the paper fibres into the voids and fibre tubes. The rate of penetration of the ink into the paper can be increased by the addition of a co-solvent that assists wetting, such as an alcohol, for two primary purposes; to yield faster ambient drying and to reduce lateral or intercolour bleed. The trade-off is that the image will be less saturated or may show through the other side. The raggedness of the edges will also increase, since the penetration will cause the ink to follow and mark the tangled structure itself.

If special coated media (swellable polymer or microporous) rather than plain paper can be used, then the image permanence problems (water/light fastness) that are frequently encountered (see Sections 1.17 and 1.20) can be controlled.

When the ink is fired at the paper, the polymers (*e.g.* polyvinyl alcohol, gelatin) swell, and absorb the ink. The polymer returns to its original size after absorbing all the ink, which is encapsulated within the coating. With microporous coatings such as alumina or silica, the ink is absorbed into the coating through microscopic pores.¹⁷

The result of these coatings is that the dye is held close to the surface providing maximum optical density, since the dye is not dispersed in the fibrous paper structure, providing high quality glossy images. The coatings also interact with the ink to promote rapid ink absorption, to generate the required spot diameter/shape by controlling the spread of ink on the paper, and provide high water/light fastness. However, all these additions adds to the expense, and a large portion of the ink jet market requires plain papers.^{7,16}

The ideal situation is for the ink jet printhead/ink supplier to specify the optimised media.⁷

1.13 Kogation

Dyes must be thermally stable up to temperatures of 300 °C in ink jet systems, due to the mechanism involved in bubble formation (see Section 1.4.2). The build up of impurities (kogation) on the heating element can be a problem. Any impurities have the potential to act as an insulating barrier and can hinder the heat flow from the heater to the ink, causing the element to overheat. Good kogation (low concentration

of impurities) can be achieved by having sulfonic acid groups on each fragment of the dye, so that any decomposed fragments are all water soluble.⁶

1.14 Ames Testing

A requirement for ink jet dyes is that they must be classed as Ames-safe (or Ames negative). This is an environmental safety screening test performance. The material in question is fed to colonies of several strains of the bacterium salmonella. These bacteria can mutate from one form to another if subjected to toxic agents. A control set of salmonella colonies is fed a standard metabolic enzyme so a comparison of colonies can be made after allowing a standard time for a biological response (mutation) to occur.

A material passes (Ames-safe) if it does not cause more than twice the number of colony mutations that the control does. A ratio of 4:1 fails (Ames positive).

This test is not infallible, a material may still be carcinogenic or poisonous, but materials that pass the Ames test are very likely to pass any others. In the 1980s, this test alone eliminated the majority of commercially available water soluble dyes.⁷

1.15 Impurities

The dye must be highly water soluble in the aqueous ink vehicle. Water, however, promotes corrosion and encourages growth of bacteria/fungi, therefore, a biocide is required to prevent this. The colourant is dissolved in the ink vehicle at the appropriate pH (8-10) that already contains the biocide, and any solubilising or dispersing agents. The synthesis of a pure dye is essential and filtering is usually required to remove any insolubles.⁹

The presence of electrolytes/metals, normally sulfates and chloride, are undesirable as they promote corrosion. Divalent metals are also a problem as they can precipitate with anions such as sulfate or with the dye itself. Cu^{2+} is particularly effective at initiating precipitation at low concentrations.⁹ Orifice diameters in printheads range from 10 μm - 40 μm , therefore the potential for clogging is clear if particles larger than this exist. Chelating agents such as EDTA can be added to remove these ions as soluble complexes. Impurities can also be removed by ultrafiltration or dialysis

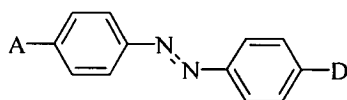
(process used to remove salts) by selecting a membrane impervious to the higher molecular weight.⁷

1.16 Solubility

The dyes used in ink jet printing have to be highly soluble in water to minimise crystallisation and nozzle blockage.⁶ Water solubility in dye systems is increased by the presence of at least one salt forming group. The most commonly used of these is the sulfonic acid group, and generally the greater the number of sulfonic acid groups *per* molecule, then the greater the water solubility that results. Carboxylic acid groups, sulfonamides and alkyl sulfonyl groups are also said to improve solubility, but to a lesser degree.^{6,10,18} Dyes with such solubilising groups are rarely present as the free acid but rather as a metal salt. Sodium is most commonly used as the cation, but other metals such as lithium have been used, as have some non metals, such as ammonium ions.⁶

1.17 Structure of the dye

The majority of dyes synthetically manufactured today are the product of an azo coupling reaction, in which the target molecule contains an azo group linking two fragments together. The trans conformation of the azo group is the most stable, where both nitrogen atoms are sp^2 hybridised giving carbon-nitrogen bond angles of 120° .⁹



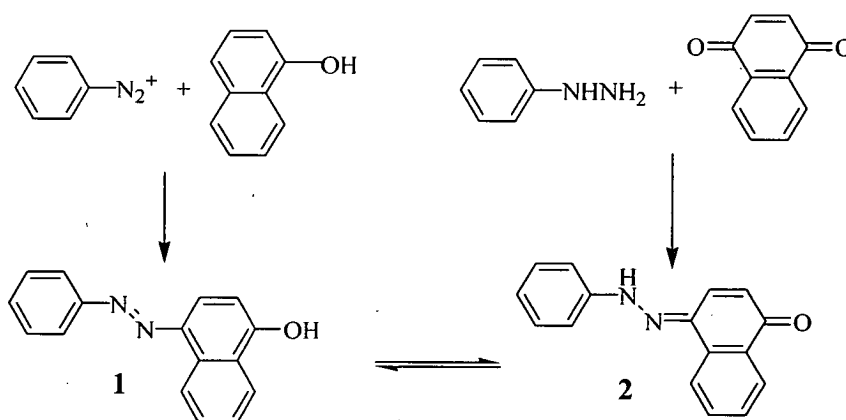
Most azo dyes are based on a structure similar to that above, with electron donating (D) and electron withdrawing groups (A) conjugatively linked (*o/p*) *via* the azo group, known as a push/pull mechanism, in reference to the delocalisation of the π electrons. By increasing the strength of the electron donating group (or groups) (D), and/or the electron withdrawing group (or groups) (A), then a bathochromic shift will be observed. Further additions of electron donating/withdrawing groups in the appropriate ring (D and A respectively) will also cause a bathochromic shift, whereas

electron donating/withdrawing groups in A and D respectively would cause a hypsochromic shift.

1.17.1 Azo/Hydrazone Tautomerism

The possibility that an azo compound (with an OH present) can exist in either its azo or hydrazone tautomer has been known since 1884, proposed by Zincke and Binderwald. The azo dye **1** and the hydrazone **2** were the expected products from the respective reactions in Scheme 1, but instead the same product was observed from both reactions, a tautomeric mixture of **1** and **2**, and therefore, the authors suggested that an equilibrium must exist.⁹

A dye will have different properties, such as colour and fastness properties, depending on which tautomer predominates. This tautomerism can depend on various factors, such as the solvent, pH and substituents in the dye molecule.



Scheme 1

Generally, more polar solvents such as water, formamide and acetic acid, favour the hydrazone form, presumably due to intermolecular hydrogen bonding, compared with less polar solvents such as pyridine, alcohols and hydrocarbons, which favour the azo form. If a molecule contains an *ortho* substituent capable of intramolecular hydrogen bonding then the hydrazone form will dominate. Many commercial dyes are based on a hydrogen bonded structure, as they are exceptionally stable. Compounds in this form can be insensitive to pH and solvent, and therefore make

ideal colourants. In comparison with the azo form, the hydrazone form exhibits a bathochromic shift, and an increase in the extinction coefficient, both of which are desirable properties.

Azo compounds derived from naphthols predominantly exist in the hydrazone form, whereas phenols are in the azo form, and are weak and hypsochromic.¹⁹

1.18 1st Generation Dyes.

The three types of dye originally used in ink jet printing, were acid, direct and food dyes, as they were readily available and provided vivid colours.²

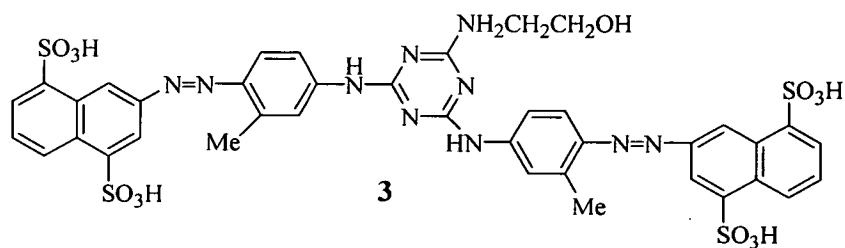
Acid dyes were initially used to dye protein fibres, and derived their name from the acidic conditions used in this process.^{21b} They were small in size with low molecular weight, and had high aqueous solubility, but they suffered from poor light and wet fastness on most substrates. Typical acid dyes used were Acid Red 52 **7**, Acid Blue 9 **8**, (both shown below) and Acid Red 37 **18** (see Section 1.20.2).

Direct dyes were initially used to dye cellulosic fibres, and were the first dyes that could be directly applied to the fibre without the need for a fixation process.^{21b} These dyes, such as **3** shown below, had higher molecular weight than acid dyes, which increased their affinity for the medium, but their large planar aromatic rings meant they were less soluble in water than the acid dyes. They were also not as bright as acid dyes. They did however, exhibit better fastness properties, and were the most common dyes used.^{3,8}

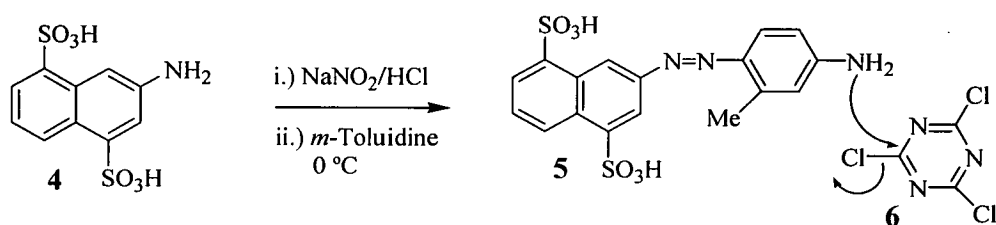
The best example of a food dye was Food Black 2 **12**, used in colouring liquorice and winegums, and is discussed in more detail in Section 1.18.4.

Several of the original dyes and their syntheses are shown in the following discussion; those that are outlined are used to demonstrate the various steps of a typical azo dye synthesis.

1.18.1 Yellow Dyes



Dyes which contain a 1,3,5-triazine structural element are well known as reactive dyes in textiles. Azo dye synthesis utilising cyanuric chloride is also common in ink jet printing systems; the cyanuric chloride provides a convenient linkage between the two azo components. The dye CI Direct yellow 86 **3**, synthesised in this way, is shown above.²⁰



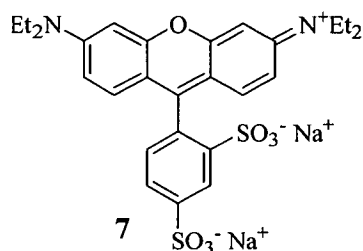
Scheme 2

An azo coupling reaction would firstly take place between the diazonium salt derived from the sulfonated amine **4**, and *m*-toluidine. Using two moles of **5**, two nucleophilic substitution reactions with cyanuric chloride **6** could then take place. The third chlorine atom could be substituted with a colourless “capping” compound such as ethanolamine to give **3**; phenol or aniline are also commonly used. The reactivity of cyanuric chloride is reduced with each substitution, as the ring becomes less electron deficient with the replacement of each chlorine atom. This means that the temperature must be increased for each subsequent substitution.^{21a}

1.18.2 Magenta Dyes

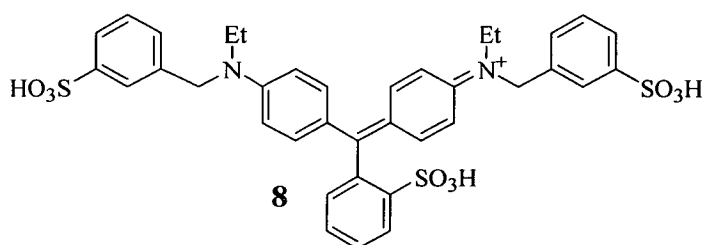
Early magenta dyes were based on xanthene structures such as Acid Red 52 **7**, giving excellent brightness with narrow absorption curves (λ_{\max} 565 nm, ϵ 89 000 l mol⁻¹ cm⁻¹), but had very poor fastness properties. Dyes such as these gave bluish shades of magenta, as reflected in the high λ_{\max} value.³ The water fastness again can be

improved by replacing the sulfonic acid groups with carboxylic acid groups, and early magenta dyes such as 7, have been superseded by the dyes in Section 1.21.2.²²



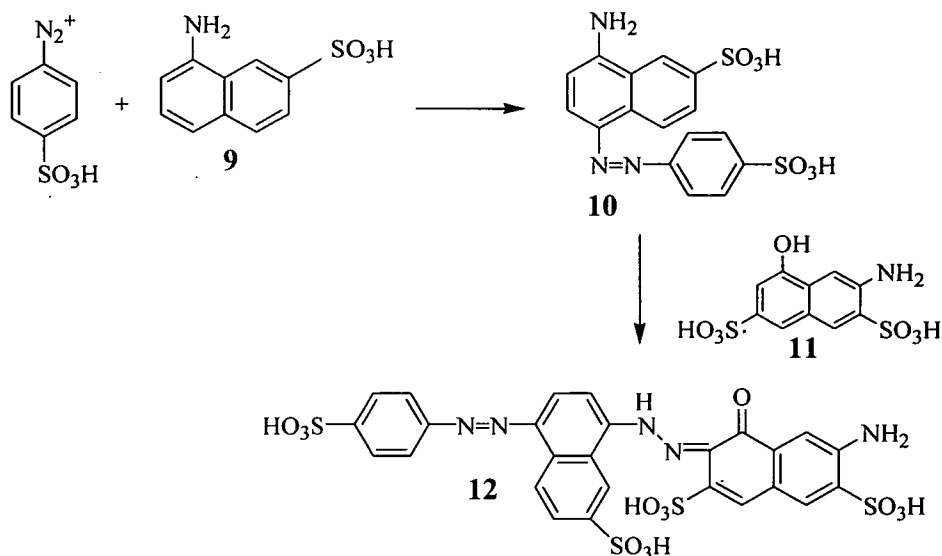
1.18.3 Cyan Dyes

The first cyan dyes used were based on triphenylmethane structures, such as the very bright Acid Blue 9 8 shown below, but again this displayed very poor fastness properties.^{1a,21a}



1.18.4 Black Dyes

The first generation black dye was CI Food Black 2 12, chosen for its high water solubility, but this high solubility also gave it poor water fastness on paper. This dye gave attractive neutral shades of black and was toxicologically safe.³ It could be synthesised firstly by coupling the diazonium salt derived from sulfanilic acid to the amine 9, and then coupling the resulting azo compound 10, under basic conditions, to 2R-Acid 11.



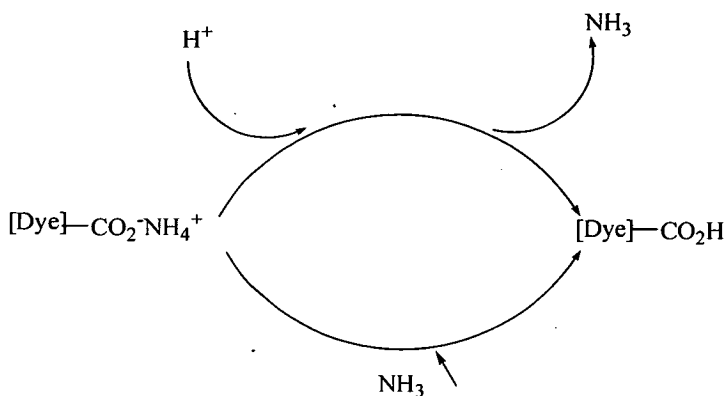
Scheme 3

1.19 2nd Generation Dyes

The problem of poor water fastness, as in CI Food Black 2 **12**, does not occur in laser printers. A solution was found for ink jet systems by using the two simple principles of differential solubility and smelling salts.^{1b,6} The dye was required to have high water solubility in the water-based ink, but zero water solubility when on the paper. The ink jet inks are normally alkaline (pH 8-10), whereas most papers are slightly acidic to neutral (pH 4-7). Less acidic groups such as a carboxylic acid were incorporated, to produce dyes that are highly soluble in the ink (acid group is ionised and is water soluble), but have very low water solubility on the paper (acid group is in its non-ionised form).^{1b,6} This improved the water fastness but it was still unsatisfactory.

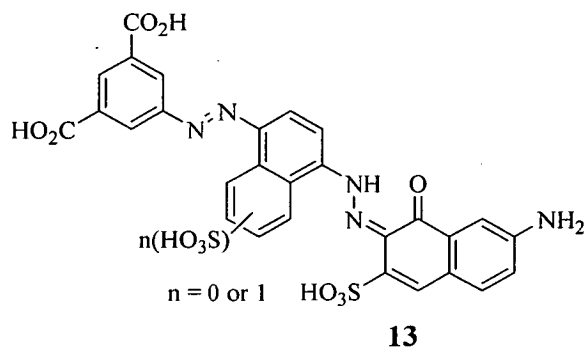
Further improvement of the water fastness level (approaching 100%), was achieved by utilising the smelling salts principle, shown in Scheme 4. Smelling salt is ammonium carbonate, the salt of a weak acid, carbonic acid, and a weak base, ammonia. This salt is unstable and decomposes into water vapour, carbon dioxide and ammonia. Changing the sodium salt of the dye to the ammonium salt, therefore, introduced another mechanism to form the insoluble free acid form of the dye.

Working on the same principle as the smelling salts, the ammonium carboxylate is unstable and loses ammonia by evaporation (which takes several hours), producing the free carboxylic group.^{1b,3,6}



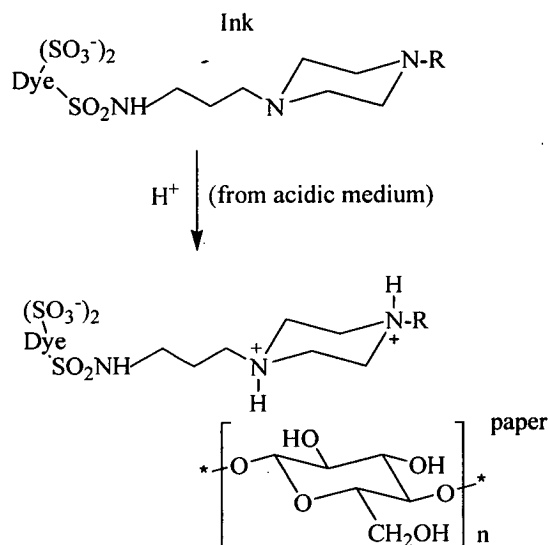
Scheme 4

These principles are used to produce the black dye, Pro-Jet Fast Black 2 **13**, which can be found in many printers. The number of sulfonic acid groups has been reduced and replaced with carboxylic acid groups to improve the water fastness.



The second generation yellow, magenta and cyan dyes were also produced in this manner, and were classed as modified dyes. Simple modifications of the first generation dyes shown above were introduced; examples of which are replacement of sulfonic acid groups with carboxylic acid groups in Acid Red 52 **7**, magenta dyes derived from H-acid, yellow dyes such as **3** and copper phthalocyanines **20**.^{1b,3,6,8} Instantaneous 100% water fastness is the ultimate goal for ink jet dyes, whilst maintaining their chroma, light fastness and reliability. A new approach utilised to

try to achieve this is by using a combination of zwitterion formation and stereochemistry, shown in Scheme 5. The dyes contain piperazino groups, which may be bonded to a sulfonamido group directly, or *via* a spacer group, and sulfonic acid groups. The dyes are soluble in the alkaline ink due to the sulfonate group. The dyes are water fast on the paper, due to zwitterion formation between the protonated amino groups (protonation from acidic medium) and the sulfonate groups, leading to insolubility and strong hydrogen bonding between the dye and cellulose (on the medium), because of the stereochemical fit allowing close interactions.^{1b}

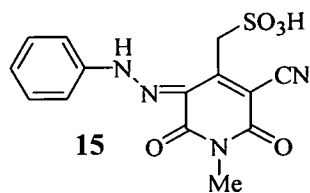
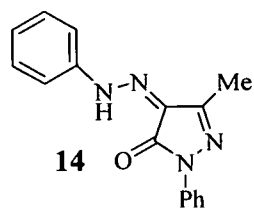


Scheme 5

1.20 Current Trends

1.20.1 Yellow Dyes

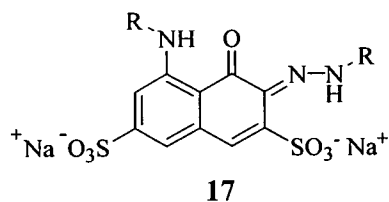
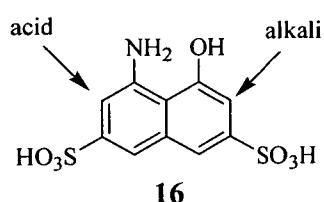
Yellow dyes are currently based on azopyrazolones **14** or azopyridone **15** structures, shown below. Both of these compounds can be made by a simple azo coupling reaction from the respective pyrazolone and pyridone, and exist in the hydrazone form. Pyrazolones are synthesised from the condensation of a hydrazine with a β -ketoester.⁹ Pyridones are obtained, from the condensation of ethyl acetoacetate and an amide. Yellow azo dyes such as **3**, as discussed in Section 1.18.1, are still used today.



1.20.2 Magenta Dyes

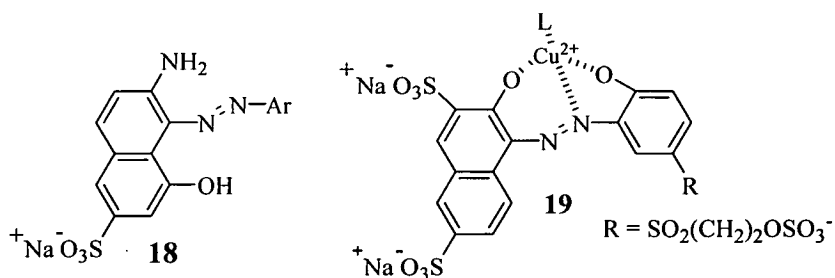
Magenta dyes have at best moderate light fastness and fade before yellow dyes. It is these unequal fade rates that are most noticeable, and the aim is to produce dyes with low and equal fade rates.^{1b} Magenta dyes that exhibit optimal hue and brightness, high light and water fastness, and good solubility are proving particularly difficult to design.^{7,22}

Current magenta dyes are based on mono aminoazobenzenes and azonaphthol structures. Many different naphthols are used, but the majority of magenta dyes are derived from H-acid 16, giving dyes such as 17 with good shades of magenta,⁶ reflected in the number of patent applications for dyes of this type.²² The site of coupling can be chosen by varying the pH of the reaction mixture. Below pH 7, only the free amine is available for coupling since the naphtholate is not present in solution ($pK_a > pH$). At high pH, both the free amine and naphtholate are present, but the naphtholate couples much faster than the amine. This means that monoazo and disazo compounds can be selectively prepared. In disazo synthesis the acid side must be coupled first in order to prevent the deactivation caused by coupling first to the alkali side.⁹



These dyes exhibit enhanced light fastness over the xanthenes, high brightness, and moderate wet fastness. Another naphthol derivative, gamma acid, is also commonly used. Dyes derived from gamma acid exist in the azo form and show improvements in light fastness, such as the Acid Red dye 18.

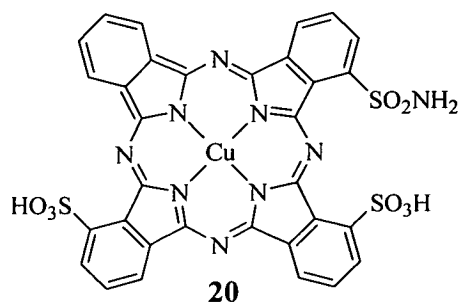
Even better fastness is achieved by metallised complexes such as the Reactive Red dye **19**, but at the expense of brightness. Compounds **18** and **19** are easily synthesised by azo coupling reactions from the appropriate naphthol derivative and an aromatic amine. Despite these advances made in the synthesis of superior magenta dyes, all the targets have still not been met.^{21a,22}



1.20.3 Cyan Dyes

Copper phthalocyanines, such as CI Direct Blue 199 **20** below, are the pinnacle of cyan dyes. These systems are continuously conjugated, allowing a large number of resonance structures to be drawn, and are probably the strongest, brightest and most stable of all colourants used today.⁶

These dyes are made by the reaction of readily available sulfonated copper phthalocyanine and chlorosulfonic acid, followed by amidation. The closeness in structure to natural pigments such as porphyrins is clear to see, which also readily form metal complexes.^{9,23} Despite the excellent properties shown by these dyes, there is still room for improvement, as solubility maybe a problem due to aggregation.



Along with the phthalocyanines, various heterocyclic azo compounds can be used in the synthesis of cyan dyes, such as azo isoquinolines. As will be discussed in Section 2.6, the metallised complexes of these species are very important.

1.21 Fading of the Dye

Dyes fade to varying degrees when in contact with the atmosphere, the media and components in the ink.⁷ A dye that fades within weeks of manufacture is obviously unsatisfactory, and therefore the high quality colour images that are produced are required to have excellent stability.⁹ The main problem of fastness on prolonged exposure to light remains a very difficult problem to overcome in the design of ink jet dyes. The understanding of the controlling mechanisms is somewhat limited, although certain parameters and guidelines have been helpful in developing correlations with dye structure.⁷

1.21.1 Fading Mechanisms

When a molecule absorbs a photon of light energy, it is raised to an excited level, where photochemical reactions can occur. The capacity of coloured substances for storage of the absorbed energy is limited, and the excited molecule can lose its energy by a variety of processes, such as luminescence or heat, to return to the ground state. It can also decompose or react with another molecule.^{9,10} In general, the longer the lifetime of the excited state, then the more chance there is for it to react. Other factors such as the absorption characteristics of the dye, the nature of the solvent and substrate, and the presence of air or moisture, can all play a part in photochemical reactions.⁹

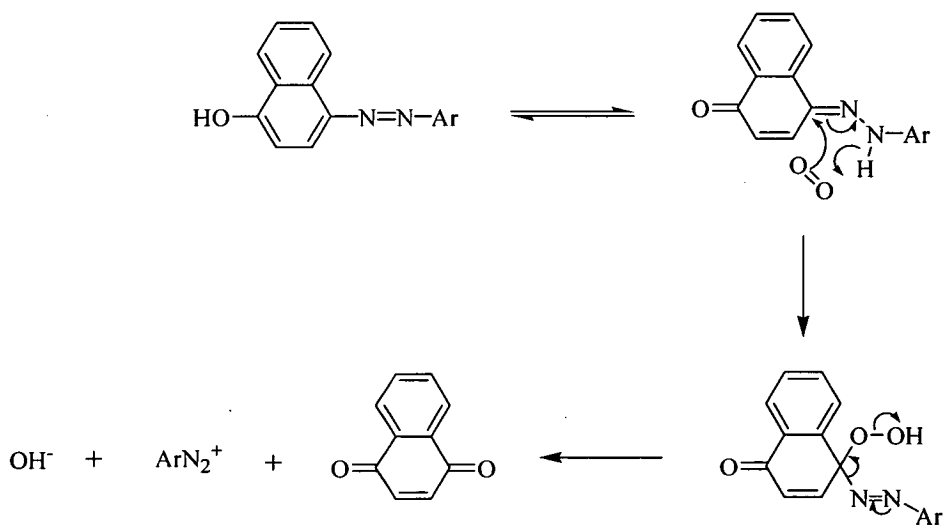
The chromophore is believed to be most important in this photodegradation process, but the nature and position of the substituents is also believed to play a part.^{8,24} By varying the substituent and keeping the chromophore constant, differences in the relative light stabilities are observed. Generally, electron withdrawing groups improve light stability, whereas electron donating groups cause deterioration. Groups such as OH, NH₂ and NHR in azo dye systems have been studied, and all cause a decrease in light stability. Too many electron withdrawing groups, however, also has a negative effect.²⁴

The two recognised pathways by which azo dyes can fade are by photo-reduction or photo-oxidation. These reactions depend on the chemical environment of the dye as determined by the media, components in the ink and the surrounding atmosphere.

The understanding of the chemical environment is critical in protection against these mechanisms.⁷

Under anaerobic conditions an azo dye can be reduced to its amines by abstracting a hydrogen atom from a hydrogen donor. Such a decomposition is accelerated when the hydrogen donor or the dye is photoexcited. Common hydrogen donor groups include alcohols, amines, ketones, carboxylic acids, ethers and esters.⁷

Oxidative fading mechanisms can be caused by direct photoreactions of the dye, *i.e.* from the excited state, or indirect, caused by another photoexcited molecule *e.g.* singlet oxygen. The fading process is believed to be a consequence of the hydrazone form rather than the azo.⁹ Magenta dyes that are in the hydrazone form, show poorer light fastness than those in the azo form.²² The mechanism firstly involves the attack of singlet oxygen on the hydrazone tautomer, a 6- π electron thermally allowed process (Ene reaction), forming an unstable peroxide, which then decomposes to products, as shown below in Scheme 6. Singlet oxygen sensitisers such as anthraquinones promote this reaction by transferring their energy to the oxygen upon excitation. A molecule locked in the azo form is thought to be more resistant to attack.^{7,9}



Scheme 6

Both the reduction and oxidation degradation reactions are affected by the substituents in the dye and hydrogen donor. Since hydrogen is abstracted by

electrophiles, fading should increase with more electron withdrawing groups relative to the hydrogen. On the other hand singlet oxygen is electrophilic and attacks areas of high electron density, promoted by electron donating substituents. For this reason, metallised dyes with their electron withdrawing metal atom are particularly stable, and this is an area that is currently generating great interest and is discussed in detail in Section 1.22.⁷

1.22 Metallisation

In an attempt to improve the light fastness properties, metallised dyes are now becoming increasingly common. Dyes which are neutral metallised complexes in general, have excellent durability and fastness to light, but this tends to be at the expense of brightness, which is assumed to be due to the formation of aggregates.^{1b,9,18}

In the design of a suitable system for potential use as an ink jet dye, certain basic requirements have to be met. The ligand must be designed to coordinate to the metal centre; Figure 7 shows one possible generic structure than can be drawn to meet such a requirement. The metal must coordinate to the azo group, and also with the two components involved in the synthesis of the dye, therefore suitable amines and couplers must be chosen.

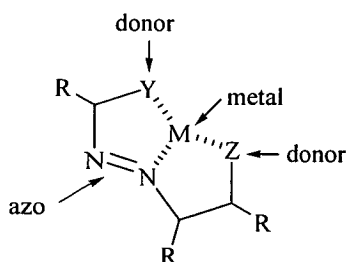


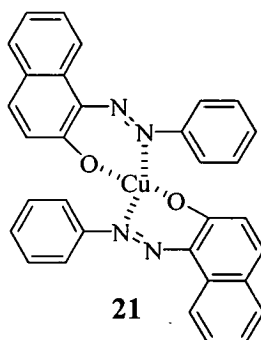
Figure 7 An example of a metallised complex.

1.22.1 Coordination

With the exception of copper phthalocyanines, metal complexes of azo compounds are by far the most important and widely used dyes and pigments.²⁵

They can be divided into two classes: those where the azo group forms part of the metallisable system (by far the most important), and those in which the azo group is

independent of the metal. In the former class, a metallisable substituent (heteroatom with a lone pair) must be present in at least one ortho position relative to the azo group *e.g.* OH or NH₂.²⁵ Azo groups themselves have relatively weak donor properties. X-Ray structures have proved that only one of the nitrogen lone pairs of the azo group participates in complexation, an example of which is shown below for the 2:1 copper complex **21**.^{9,25}



The presence of a heterocycle, frequently containing a nitrogen atom in an appropriate position relative to the azo group for chelation, is now commonplace.²⁵ Large numbers of patents involving heterocycles have appeared in which the azo molecule functions as a tridentate ligand.⁹

The other possibility where coordination does not involve the azo group is currently of little use in ink jet applications. These dyes are generally brighter but show no enhancement in light fastness. The increased brightness is a result of conjugation of the azo group to the metallisable system, which is not possible in ink jet dyes due to coordination.⁹

1.22.2 Complexation

Upon complexation, the properties of the dye change from those shown by the free ligand. Generally, a bathochromic shift is observed, the light fastness and resistance to oxidation is increased, but they also become duller and of lower solubility.^{9,19}

The change in colour is caused by chelation of the metal to the major donor/acceptor groups such as azo or hydroxy, and not from d-d transitions from the metal itself, which are not formally allowed. Chelation causes a perturbation of the π electron distribution *e.g.* coordination of the metal with a hydroxyl group increases the ease

of donation of the lone pair into the conjugated system, leading to an intense $\pi\text{-}\pi^*$ transition (ligand to metal charge transfer), not present in the free ligand.⁹ The more electropositive the metal, the greater the effect. This however, is a problem in itself, as predicting the shade then becomes more difficult. The formation of an ideal complex would cause no change in the λ_{max} value from the free ligand, but still result in the desired increase in absorption, producing a narrower curve in the process.

The improvement in light fastness is also due to the perturbation of the π electron system. The electron deficient metal attracts electrons from the ionised hydroxyl group, and also from the azo group, so that electron density at the latter groups is reduced. The metallised complex can also reduce photochemical oxidation, by acting as a barrier, resulting in less surface area of the dye molecule being available to attack by singlet oxygen. Metallised complexes may also form sheet like aggregates and thus reduce solubility.⁹

1.22.3 Stability

There are several important factors that have an influence on the metallised complex stability. The size of the chelate ring is one important element, and it has been shown that five or six membered rings are the most stable, as they show the least ring strain, whereas 7, 8 and 9 membered rings are non-planar and form less stable complexes.^{9,25} The greater the number of annelated chelate rings, then the more stable the complex that is generated. Metallised bidentate ligands exhibit inadequate stability, whereas tridentate ligands show good stability, as the metal is held between two rings. The most basic ligands are said to form the most stable complexes.^{9,25} The metal itself is also vitally important, as different metals tend to have different donor-atom preference. Nickel, cobalt and cadmium show relative donor stabilities in the order nitrogen > sulfur > oxygen, whereas zinc shows nitrogen > oxygen > sulphur and copper shows nitrogen = sulfur > oxygen.^{9,25}

1.22.4 Other stability trends

Dye combinations can exhibit less stability when mixed together in a print area, by comparison with isolated print areas. Excited dyes can catalyse the production of singlet oxygen resulting in oxidative fading, or they can transfer absorbed energy to

another dye, which is at lower energy, resulting in fading of either dye. Such transfers occur when the dyes are less than 5 nm apart. Organic molecules called spacers, *e.g.* fatty acids, can hinder energy transfer and promote light fastness.⁷

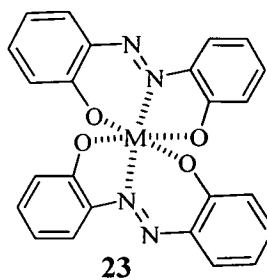
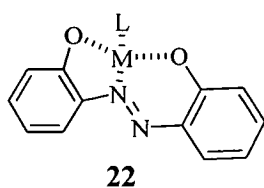
Aggregates are found to be more resistant to fading than dyes in a monomolecular state. Although these processes are not fully understood, highly aggregated dyes are thought to dissipate the energy from the excited state of the dye before it can react (effectively reducing the lifetime of the excited state). There is also a much smaller surface area available for attack by the reactive species such as singlet oxygen, radicals and hydrogen peroxide. Arguments such as these are used to explain the higher fastness of pigments over dyes.^{7,9,22}

Aggregation can be induced by reducing the solubility. This can be achieved by the addition of a co-solvent with less solvating power, or lowering the pH to suppress ionisation. However, aggregation tends to give broader absorption curves and hence a decrease in brightness.²²

Another approach currently being investigated is the use of additives, *e.g.* singlet oxygen quenchers, free radical inhibitors and antioxidants (guards against the accelerating effect of moisture and high humidity).⁷

1.22.5 Stereochemistry

The stoichiometry of the complex formed depends on the structure of the starting dye, proportion of metal compound used and the metallisation conditions. 1:1 or 1:2 complexes are formed from tridentate ligands, where the preferred ring sizes are 5,5, 6,6 or 5,6.¹⁸ Below are examples of typical 1:1 **22** and 1:2 **23** complexes, with 5,6 ring systems formed. 1:1 complexes contain further ligands (L), *e.g.* water, hydroxyl, halogen or acid group depending upon the method of synthesis.¹⁸



1.23 Conclusions

All the chemical aspects of dye technology which are used in ink jet printing systems, have been considered above. This technology is still a rapidly developing field, especially the constitution of the dyes themselves. Many factors contribute to the success of a dye, and the major problem of stability to light and ozone still exists, particularly for magenta dyes. One of the current ways to counter this is the synthesis of metallised complexes.

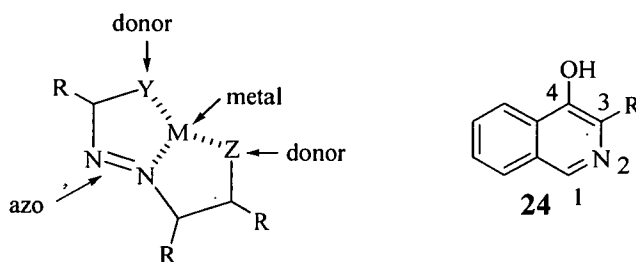
2. DISCUSSION

3-Substituted Isoquinolin-4-ols

Systems based on 3-substituted isoquinolin-4-ols **24** are of great interest, as their azo coupled products have potential for coordination to a metal, *via* the heterocyclic nitrogen atom and the oxygen atom of the hydroxyl group, as shown below in a typical generic structure.

The following Sections (2.1 to 2.5) are a detailed literature review of the synthesis and reactions of 3-substituted isoquinolin-4-ols **24**. The applications of metallised isoquinolin-4-ol compounds are discussed in Section 2.6. New research is discussed in Sections 2.7 to 2.14.

It was found that routes to isoquinolin-4-ols **24** are often low yielding, or involve multi-step routes. There are surprisingly few examples of such compounds, and no general method for their synthesis exists. However, certain trends have emerged on close examination of the literature, with two common methods being apparent.

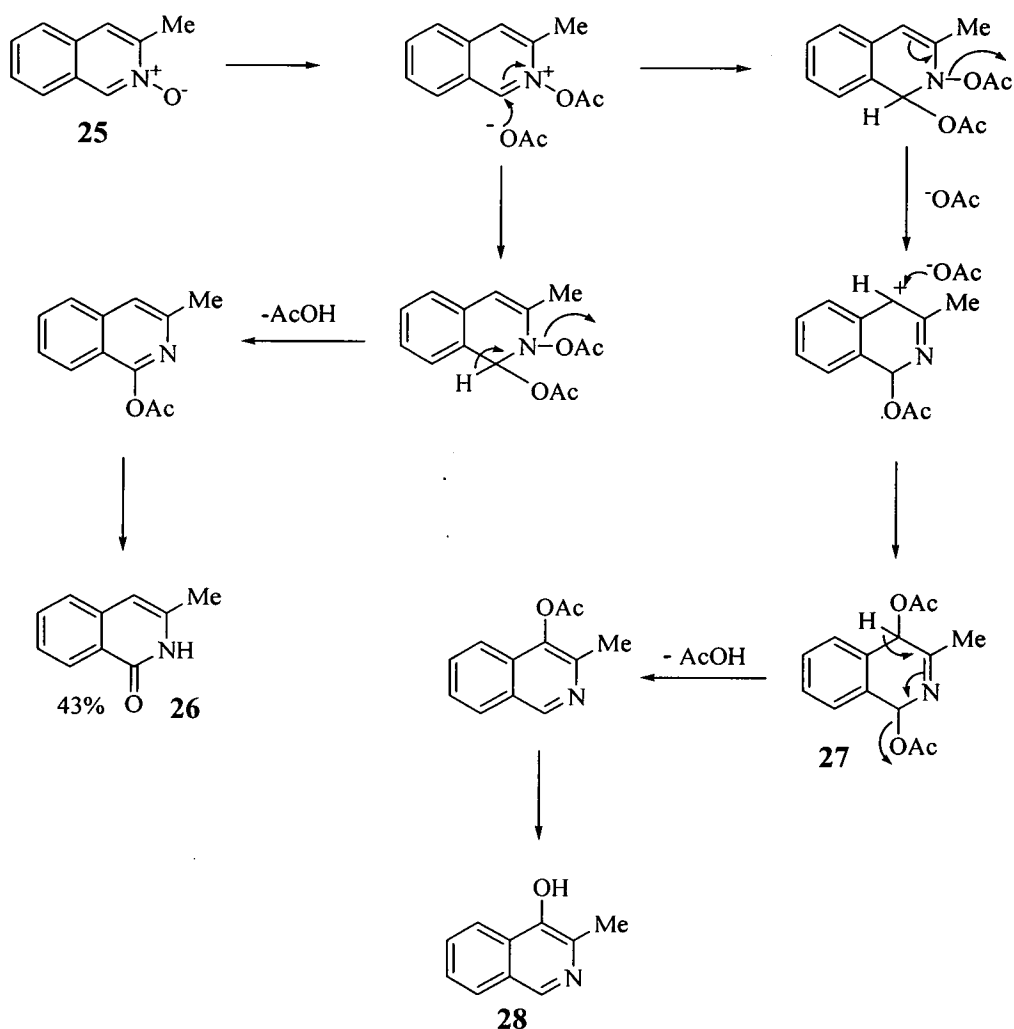


2.1 Synthesis of 3-substituted isoquinolin-4-ols from isoquinoline *N*-oxides.

Heterocyclic *N*-oxides, in general, are much more reactive to electrophilic and nucleophilic substitution reactions than their parent compounds, and can also undergo reactions at the oxygen atom. Isoquinoline *N*-oxides are created by the reaction of isoquinoline with hydrogen peroxide, and rearrangement reactions of these *N*-oxides with acetic anhydride and *p*-toluenesulfonyl chloride has initiated much research.

One such rearrangement occurred when 3-methylisoquinoline *N*-oxide **25** was heated under reflux in acetic anhydride. Two competing pathways exist, which are highlighted in Scheme 7. The predominant product that resulted was 3-methylisocarbostyryl **26**, along with a small amount of the target 3-methylisoquinolin-4-ol **28**.²⁷ Similar results were found involving rearrangements with 3-phenylisoquinoline *N*-oxide,²⁸ and from isoquinoline *N*-oxide itself **29**.²⁷

In total contrast to the regioselectivity of these acetic anhydride rearrangements, was the reaction of isoquinoline *N*-oxide **29** with *p*-toluenesulfonyl chloride, as this rearrangement goes preferentially to the 4-position. The one standard method for the synthesis of isoquinolin-4-ol utilises this reaction (Scheme 8).^{29,30}



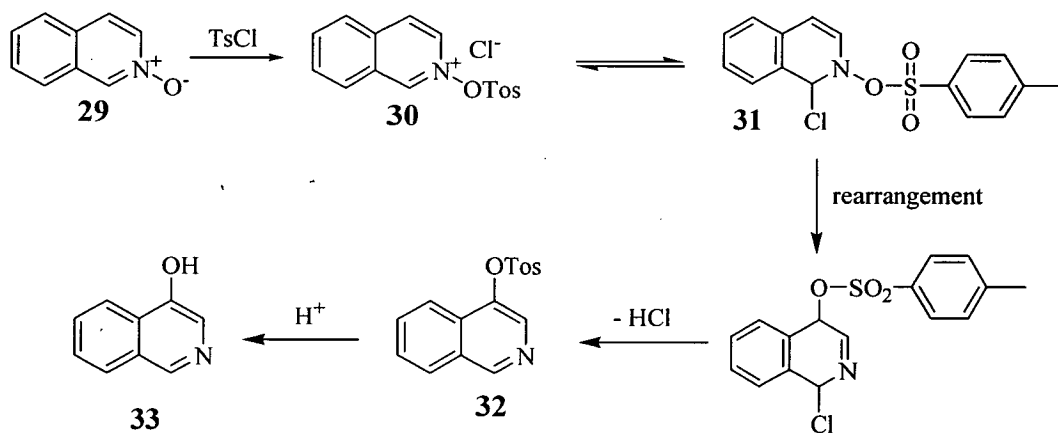
Scheme 7

This reaction with tosyl chloride has initiated great interest mechanistically in the literature, and offered below is a discussion of the results found. Isoquinoline *N*-oxide **29** was prepared in the usual way, and was then reacted with *p*-toluenesulfonyl chloride. The first step is the formation of *N*-tosyloxyisoquinolinium chloride **30**,

which can be isolated as a perchlorate salt.³¹ Addition of chloride at the 1-position, followed by 1,3 rearrangement of the tosyl group to the 4-position, and elimination of hydrochloric acid, then gives **32**, as shown in Scheme 8. The final step in the synthesis is a simple acid hydrolysis, to give isoquinolin-4-ol **33**.

The rearrangement can be simulated by addition of chloride anion when the perchlorate salt of **30** was formed, thus providing support for the addition of the chloride at the 1-position.³² Addition of excess chloride anion also been seen to increase the rate of the reaction.³¹

The regioselectivity of this rearrangement is somewhat surprising, as the most active site for nucleophilic attack is at the 1-position, as seen in the rearrangement with acetic anhydride. This difference in regioselectivity has been rationalised by the addition of the chloride anion at the 1-position, thus blocking this site for any subsequent addition. In the case of the acetic anhydride rearrangement in Scheme 7, the leaving groups are the same in **27**, whereas below in Scheme 8, the chloro and tosyl groups are present, which have different electronic properties. In Scheme 7 however, it is unclear why one acetate is cleaved in preference to the other, it may simply be down to a difference in acidity of the protons at the 1- and 4-positions.



Scheme 8

The actual mode of migration of the tosyl group, has generated a lot of interest in the literature, and it can proceed by three possible pathways;³² a tight ion-pair or sliding

mechanism **34**, an intramolecular [3,3] sigmatropic shift **35**, or an intermolecular solvent-separated ion-pair mechanism **36**, all shown below in Figure 8.

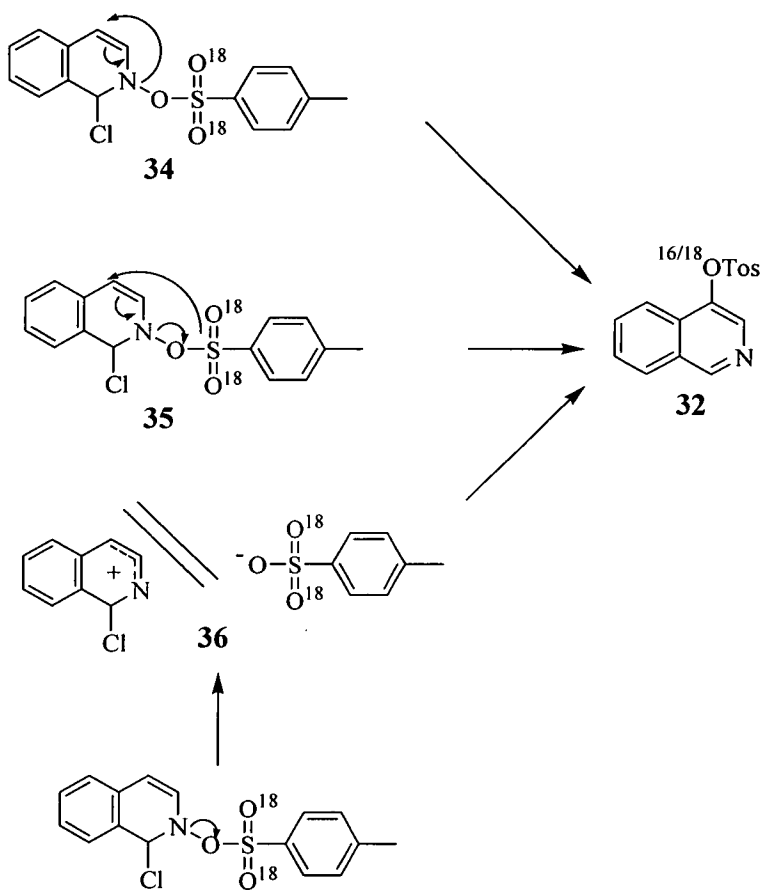


Figure 8

To investigate this mechanism, a standard rearrangement reaction was carried out in chloroform, as in Scheme 8, with oxygen-18 (^{18}O) labelled tosyl chloride. The quaternary carbon at the 4-position of **32** was identified at ~ 142 ppm, and the intensity of the signals corresponding to the 4-position in the ^{13}C NMR spectrum, were used to estimate the ratio of ^{18}O incorporation in the rearranged product. A 73:27 ratio of $^{16}\text{O}/^{18}\text{O}$ was found in the tosylate **32**; an isotopic shift of 3 Hz was seen between the respective isotope signals. Negative-ion mass spectrometry provided support for the NMR result, as two key fragments were produced by cleavage of the sulfur/oxygen bond. Analysis of m/z 144/146 afforded an $^{16}\text{O}/^{18}\text{O}$ ratio of 69:31 at the 4-position, which was a similar ratio to that seen in the ^{13}C spectrum.

For mechanism **34** to operate, a 100% ^{16}O retention is required, for mechanism **35**, a 0% ^{16}O retention is required, and for mechanism **36**, a 33% ^{16}O retention (67% ^{18}O incorporation) is required. Furthermore, the rearrangement was studied in different solvents, with a small increase in the ^{18}O incorporation found with increasing polarity of solvent (chloroform 31% *c.f.* acetonitrile/water 45% ^{18}O incorporation). Polar solvents would be expected to greatly increase the contribution of mechanism **36**; therefore, **36** was deemed insignificant due to this small increase in ^{18}O incorporation.³²

Previous experiments showed negligible oxygen isotope scrambling in a doping experiment where unlabelled tosyl chloride was added to a mixture of the *N*-oxide and ^{18}O labelled tosyl chloride, which rules out intermolecular exchange (mechanism **36**).

A combination of mechanisms **34** and **35** seems more likely, with a 70% contribution from mechanism **34**, and a 30% contribution from mechanism **35** estimated, whereas previously it was thought that mechanism **34** operated exclusively.^{29,32}

The rate-determining step of the reaction was found to be the cleavage of the nitrogen-oxygen bond. This was identified by the secondary kinetic isotope effect, with $k_{\text{H}}/k_{\text{D}} = 1.16$ for the 1-deuteriated derivative of the *N*-oxide, and $k_{\text{H}}/k_{\text{D}} = 1.22$ for the 1,3,4-trideuteriated derivative, indicating that a carbon-hydrogen bond was not broken in the rate-determining step. Other possibilities such as the nucleophilic attack of the chloride ion at the 1-position or the attack of the tosyl group at the 4-position would require $k_{\text{H}}/k_{\text{D}} < 1$. If the elimination of hydrochloric acid was the rate determining step, it would require $k_{\text{H}}/k_{\text{D}} > 2$.³¹

If heterolysis of the nitrogen-oxygen bond was the rate-determining step, then the rate should be enhanced by a better leaving arylsulfonate. A straight line was observed in the Hammett plot when substituents in the arylsulfonyl chloride were varied. The rate increased with increasingly good leaving groups, with the fastest reactions observed for the *p*-chloro and bromo substituted sulfonates, and the slowest rate observed was for the *p*-methyl substituted, out of the compounds studied. Large positive ρ values of +2 were observed, indicating that a high negative charge in the transition state was present.³¹

It should be pointed out again that this rearrangement is in stark contrast to that with acetic anhydride, which rearranges to give isocarbostyryl as the predominant product. Despite all the mechanistic work discussed above, it remains unclear as to why these reactions take such different courses, although it seems that the presence of the chloride anion, and subsequent addition at the 1-position, is playing a vital role.

No indication was given as to what effect the variation of conditions and reagents in these experiments has on the yield of the rearranged product.

A further contrast to the above *N*-oxide rearrangements, was the reaction of 3-chloroisoquinoline *N*-oxide with acetic anhydride. Rearrangement went exclusively to the 4-position and 3-chloroisoquinolin-4-ol was successfully synthesised in 77% yield.³³ Clearly the introduction of this chloro substituent has a remarkable effect on the course of these reactions. Electronic effects are playing a part in this rearrangement, the exact nature of which remains unclear.

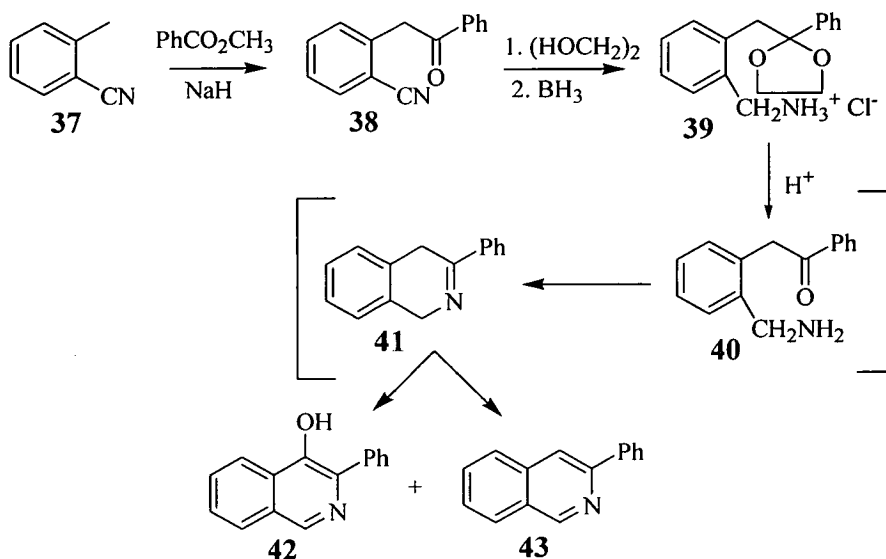
2.2 Synthesis of 3-substituted isoquinolin-4-ols via autoxidation of 1,2 and 1,4-dihydro intermediates.

In many of the literature reports, 3-substituted 1,2- and 1,4-dihydro isoquinolines are common intermediates, yielding isoquinolin-4-ols upon spontaneous oxidation.

3-Phenylisoquinolin-4-ol **42** was generated this way, as an unexpected side-product in a reported synthesis of 3-phenylisoquinoline **43** (Scheme 9).³⁴ The starting point of this synthesis was the reaction between *o*-toluonitrile **37** and methyl benzoate in the presence of sodium hydride, which resulted in benzylation of the methyl group. The resulting ketone **38** was protected using ethylene glycol, and then the nitrile group was reduced to the amine hydrochloride salt **39**, using borane. Deketalisation and cyclisation were carried out *in situ* under acidic conditions, to give the 1,4-dihydro intermediate **41** via **40**.

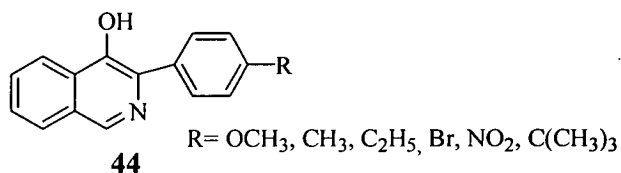
Iodine was added to promote dehydrogenation to 3-phenylisoquinoline **43** which was obtained in 52% yield, along with 3-phenylisoquinolin-4-ol **42** in 21% yield, formed by allylic oxidation of the 1,4-dihydro intermediate **41**; this intermediate **41** has also been seen in the formation of **42** from triazole **45**, as shown in Scheme 10. To improve the yield of **42** relative to **43** (Scheme 9), the treatment with iodine was excluded, giving the isoquinolin-4-ol **42** as the major product (50%). Due to the

absence of iodine, oxygen was not being excluded, and spontaneous air oxidation of intermediate **41** occurred to give **42**. This air oxidation appears in several of the forthcoming reactions. The dehydrogenation product **43** was also obtained in 28% yield. To test this hypothesis further, the crude reaction mixture was degassed, and then treated with a degassed solution of base, resulting in **43** as the major product.



Scheme 9

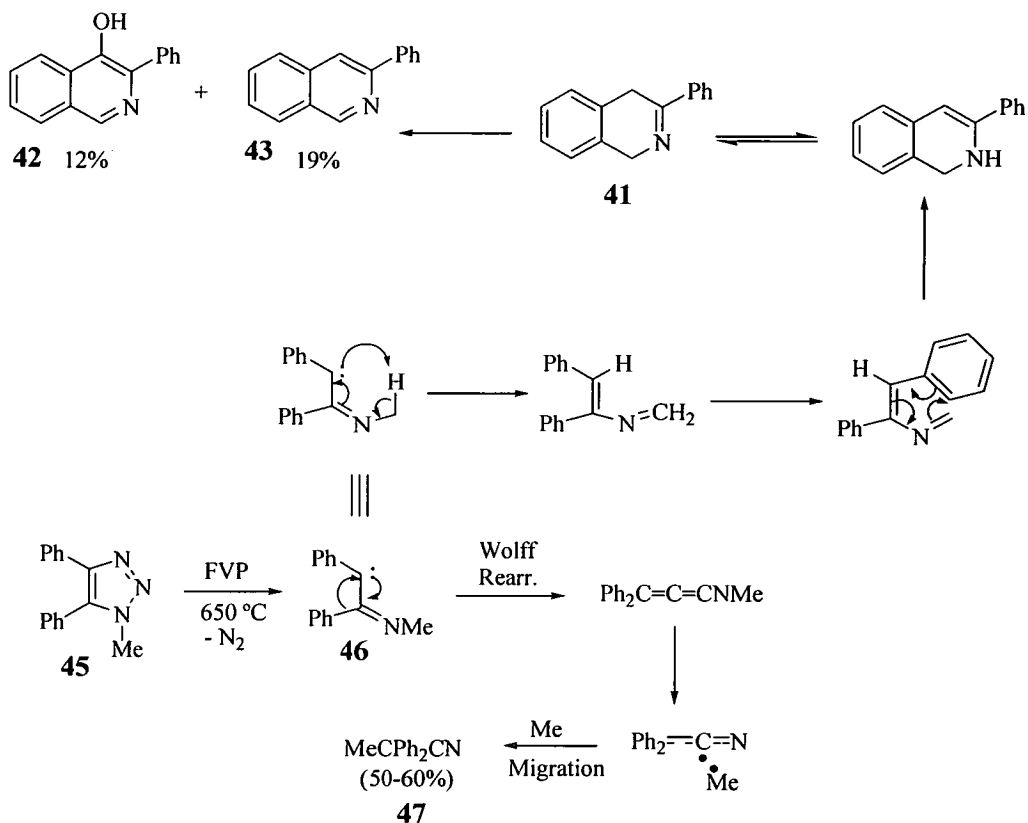
Several other 3-arylisquinolin-4-ol derivatives **44** have also been synthesised.³⁵ However, these compounds appeared in a mass spectroscopy journal, in which only detailed analysis of their mass spectra was reported. No other information on their synthesis *etc.* is available at present.



Flash Vacuum Pyrolysis (FVP) (see Section 3.3 for a fuller explanation of the technique) has been used in the synthesis of 3-phenylisoquinolin-4-ol **42**, once again *via* the same 1,4-dihydro intermediate **41** as in Scheme 9.²⁸ The isoquinolin-4-ol **42**

and 3-phenylisoquinoline **43**, however, are formed in low yield as side products. Nitrogen was eliminated under the FVP conditions, from 1-methyl-4,5-diphenyl-1,2,3-triazole **45**, to give a carbene intermediate **46**. A Wolff rearrangement and methyl migration gave the major product **47**.

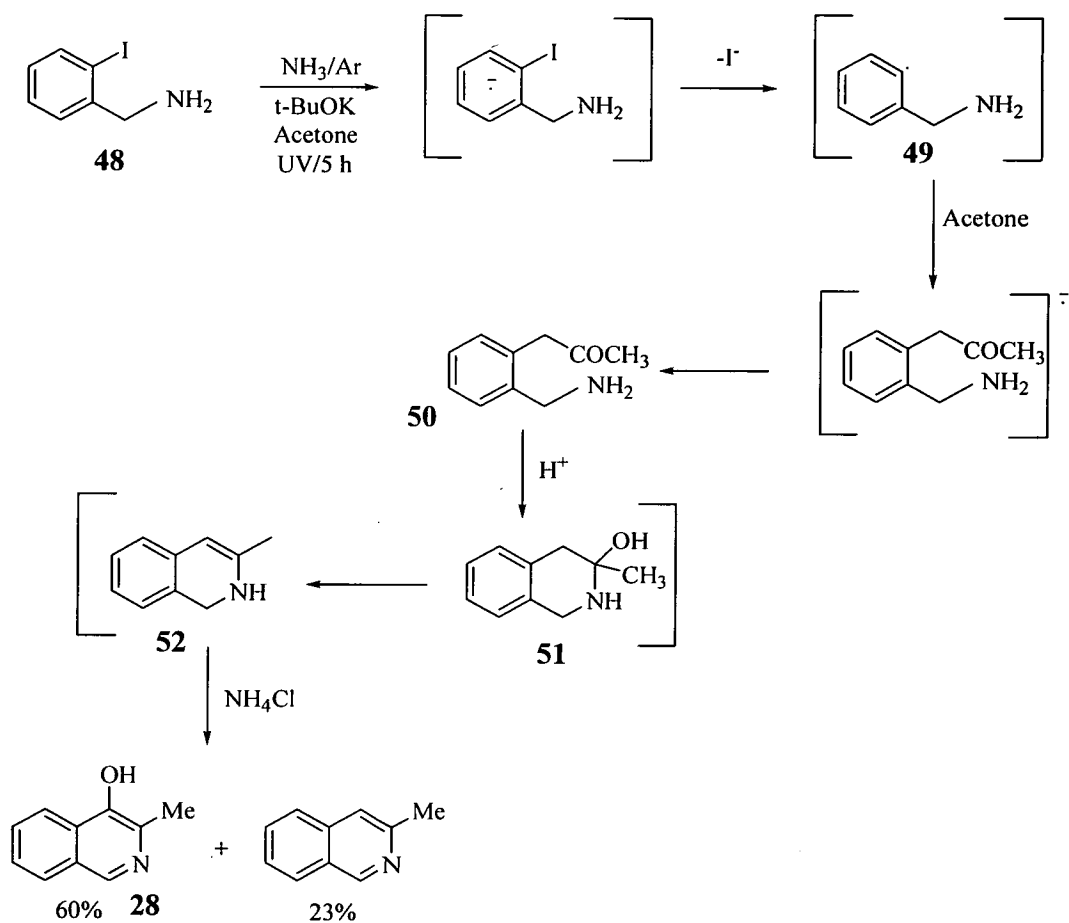
The minor products **42** and **43** were formed due to a rare 1,4-hydrogen shift from the carbene **46**. Cyclisation to the 1,4-dihydro intermediate **41** then followed, and autoxidation, as seen above, gave the products shown. In a similar experiment as to that described above in Scheme 9, in which oxygen was excluded, no isoquinolin-4-ol **42** product was obtained.



Scheme 10

A 1,2-dihydro intermediate **52** has been accessed *via* an S_{RN}1 reaction, and similar to the reactions with the 1,4-dihydro intermediates, isoquinolin-4-ol **28** is yielded upon spontaneous oxidation.³⁶ The S_{RN}1 mechanism is a radical reaction, in which the carbon-halogen bond in **48** is cleaved to generate the arylradical **49**. These radicals

can then react with enolates to produce the $S_{RN}1$ primary product **50**. The commercially available iodobenzylamine **48**, and the other reactants shown, were irradiated for 5 hours with a 100 W Mercury lamp. The 1,2-dihydroisoquinoline intermediate **52** was formed *via* the α -amino alcohol **51**, which resulted from cyclisation of the $S_{RN}1$ primary product **50** (Scheme 10). Spontaneous oxidation of **52** then yielded 3-methylisoquinolin-4-ol **28** as the major product. A 3-*t*-butyl substituted compound (60%) and a 3-isopropyl substituted compound were also both reported, synthesised in a similar manner.



Scheme 11

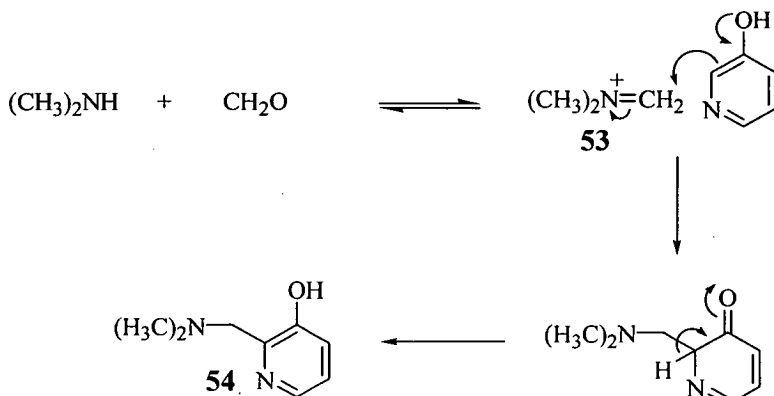
2.3 Synthesis of 3-substituted isoquinolin-4-ols from isoquinolin-4-ol.

The 3-position of isoquinolin-4-ol has been shown to be very reactive to substitution, with various reactions reported in the literature. Activation of the 3-position is enhanced by electron donation from the hydroxyl group, and is the preferred site for substitution.

2.3.1 The Mannich Reaction

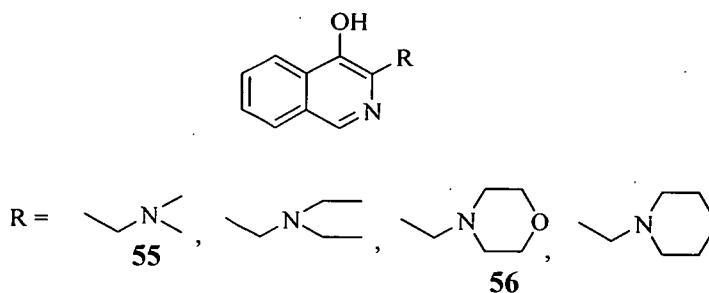
Several 3-substituted isoquinolin-4-ol derivatives have been synthesised *via* Mannich reactions from isoquinolin-4-ol.

In general, the Mannich reaction involves the reaction of an active methylene compound or an activated aromatic with formaldehyde and an amine, to give a β -aminocarbonyl compound, known as the Mannich base **54**. The amine is introduced as its hydrochloride, and the formaldehyde as its dimer or trimer, in a slightly acidic medium. Secondary amines are normally used to avoid side reactions between the Mannich base and additional formaldehyde, that primary amines or ammonia may undergo. An iminium salt **53** is first obtained from the amine and formaldehyde, which then undergoes electrophilic attack on the enol form of the active methylene. The position *ortho* to the hydroxyl group and the nitrogen atom in isoquinoline systems is highly activated, despite the presence of the adjacent pyridine type nitrogen, and is available for substitution reactions.³⁷



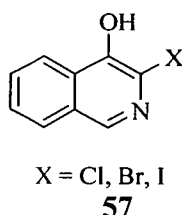
Scheme 12

A number of isoquinolin-4-ol derivatives, shown below, substituted at the 3-position with the following groups, have been synthesised using this method.³⁸



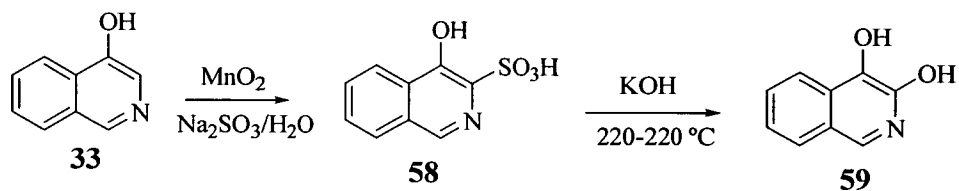
An example of a typical Mannich synthesis involved reacting isoquinolin-4-ol with dimethylamine and formaldehyde at 0 °C in methanol, giving 3-dimethylaminomethyl isoquinolin-4-ol **55** (82%). Similarly, when isoquinolin-4-ol was treated with formalin and piperidine, 3-piperidinomethyl isoquinolin-4-ol **56** was obtained in 71% yield.³⁹ Mannich bases can be hydrogenated to provide 3-methylisoquinolin-4-ol **28**. For example, **55** was hydrogenated for 10 hours to give **28** in 69% yield.

2.3.2 Other substitution reactions.



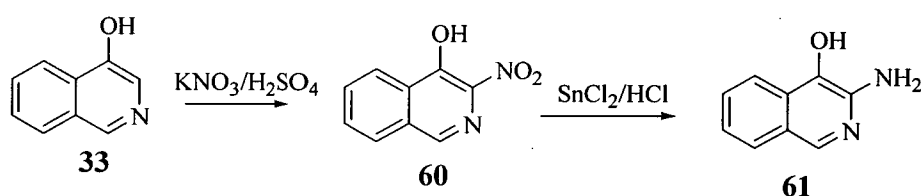
Exclusive halogenation at the 3-position **57** has been successfully achieved; the bromo and iodo derivatives have been prepared in 76% and 88% yields respectively from alkaline solutions of isoquinolin-4-ol and bromine or iodine.³⁸

Furthermore, sulfonation has been successfully accomplished. Compound **58** was synthesised in 60% yield by a rather unusual oxidative sulfonation reaction carried out in weakly alkaline conditions at 90 °C.⁴⁰ It has been shown that if a standard sulfonation is carried out in strongly acidic medium, then substitution is directed to the benzene ring due to the formation of a positively charged isoquinolinium ion, which reduces the reactivity of the isoquinolin-4-ol ring. No such ions are formed in alkaline conditions. Compound **59** was then prepared from **58** in 51% yield, by heating for 3 hours with potassium hydroxide.⁴¹



Scheme 13

Nitration at the 3-position has been successfully achieved in 49% yield, as shown in Scheme 14, by the reaction of sulfuric acid and potassium nitrate.³⁰ Reduction of 3-nitroisoquinolin-4-ol **60** to give the amine **61** in 75% yield, could be carried out using stannous chloride and hydrochloric acid.⁴¹

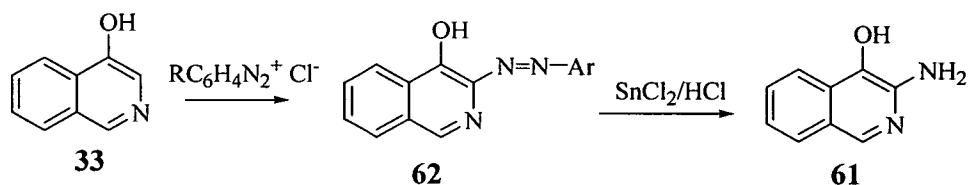


Scheme 14

2.3.3 Azo coupling and subsequent reactions.

Azo coupling is another reaction that readily takes place at the highly reactive 3-position. There are many examples of such compounds made by Andranova *et al.*⁴¹ Diazonium salts derived from *p*-toluidine, *p*-bromoaniline, *p*-nitroaniline, *p*-sulfanilic acid and *p*-anisidine, **62**, have been successfully coupled to isoquinolin-4-ol, in yields ranging from 70-90%. 1,3-Disubstituted derivatives can also be prepared, by using two equivalents of the appropriate diazonium salt.

These azo coupled products have been used to generate the corresponding 3-amino substituted compound **61** by reduction of the azo group using stannous chloride and hydrochloric acid, in 80% yield.

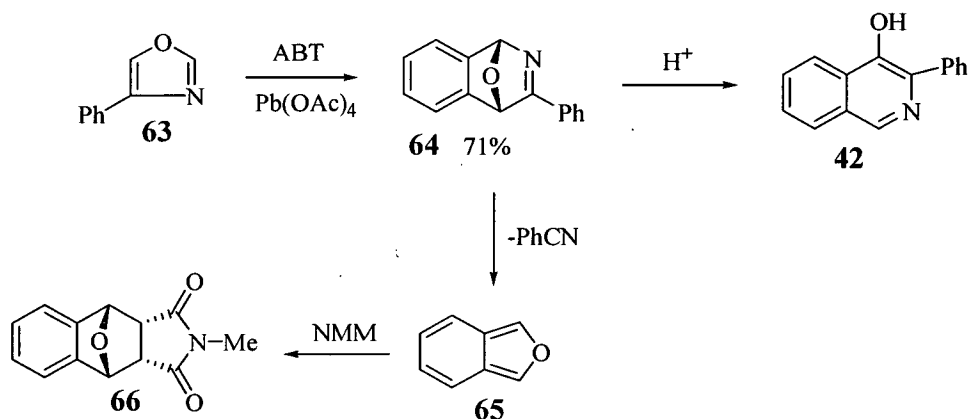


Scheme 15

2.4 Other Methods

2.4.1 An acid catalysed rearrangement reaction.

An acid catalysed rearrangement reaction has been shown to yield 3-phenylisoquinolin-4-ol **42** as an unexpected product.⁴² This report was concerned with the *in situ* generation of benzyne, from 1-aminobenzotriazole (ABT) and lead tetra-acetate, and its cycloaddition reaction with 4-phenyloxazole **63** as a possible route to isobenzofuran **65**. The thermally stable cycloadduct **64** was obtained, which underwent a retro-Diels-Alder reaction, with the elimination of benzonitrile, generating isobenzofuran **65** as a reactive intermediate. This was trapped as its cycloadduct **66** with *N*-methylmaleimide (NMM), in 78% yield.



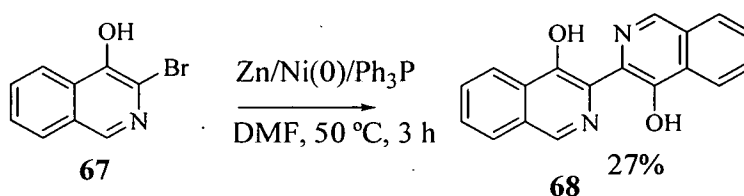
Scheme 16

However, in an attempt to purify **64** by column chromatography, rearrangement to the isoquinolin-4-ol **42** occurred. The same rearrangement occurred if the addition of trifluoroacetic or acetic acid was made to the reaction mixture. This is another

example of a rearrangement to the isoquinoline compounds, this time the acid is catalysing the rearrangement.

2.4.2 Organometallic Reagents

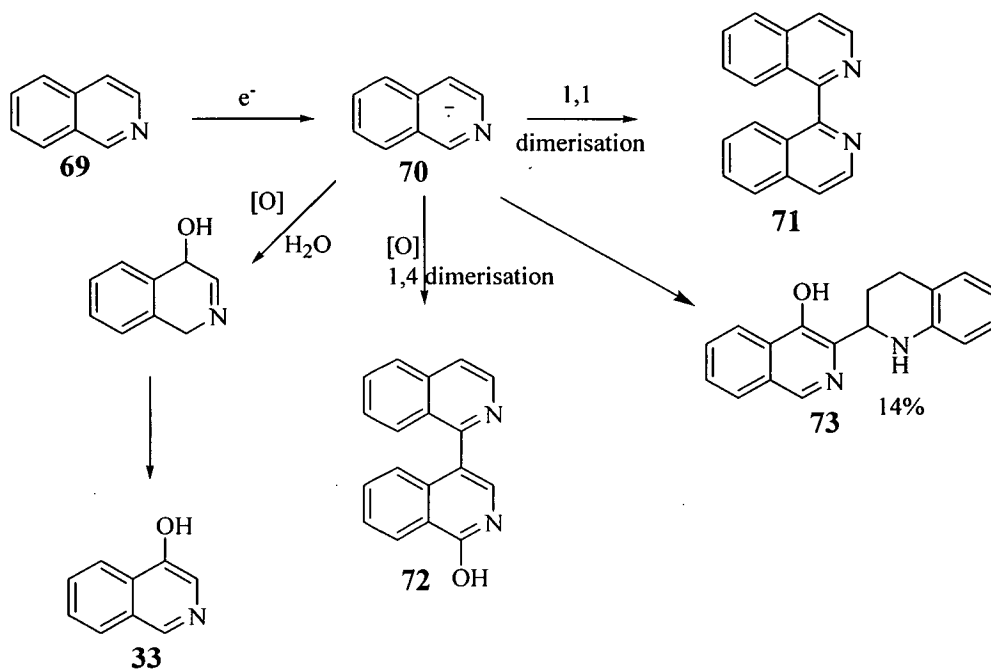
The bisisoquinoline **68** was produced in 27% yield from 3-bromoisoquinolin-4-ol **67**, in a reductive organometallic coupling reaction.⁴³ This type of reaction normally requires protection, as the acidity of the phenolic hydroxy group inhibits organometallic reagents. However, zinc in DMF was found to give access to aryl coupling, even in the presence of phenolic groups. Metal complexation increases yields by inhibiting reduction of the dihydroxy compound **68**, *e.g.* nickel(0) with triphenylphosphine, protects this compound from further reaction. This simplifies the procedure and ensures constant activation of the zinc surface for aryl coupling is maintained. The nickel complex of **68** also precipitates, thus simplifying work-up.



Scheme 17

2.4.3 Single Electron Transfer Reagents.

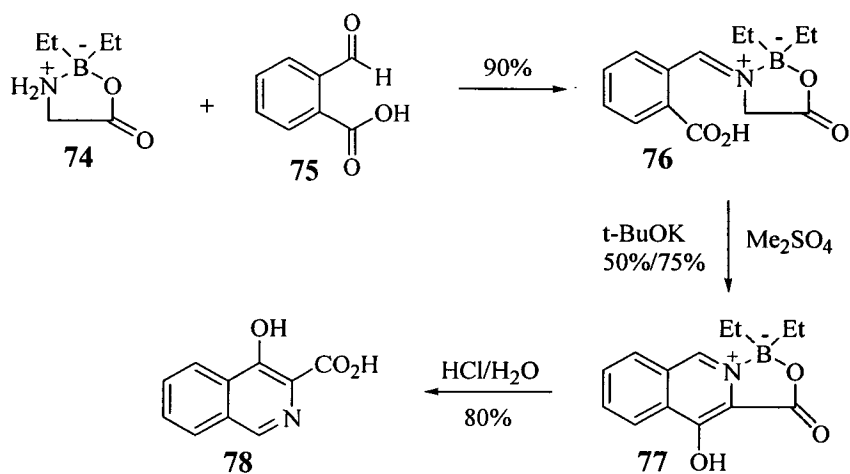
Sodium naphthalenide is a single electron transfer reagent. In the absence of proton donors in the medium, it has been used to donate an electron to isoquinoline **69** and thus generate an isoquinoline anion radical **70**. When these reagents are reacted together in anhydrous monoglyme, three dimerisation products **71**, **72** and **33** are produced, as shown in Scheme 18.⁴⁴ 1,1 Dimerisation of **70** gave **71** in 20% yield, 1,4 coupling and oxidation gave **72** in 26% yield, and by quenching the reaction after fifteen minutes, **33** was obtained in 12% yield. The isoquinolin-4-ol **73** was also obtained from this reaction in 14% yield, but the mechanism of its formation is unclear.



Scheme 18

2.4.4 Synthesis from a boroxazolidone.

The boroxazolidone 74 can be prepared from glycine and triethylborane, and has been used in a synthesis of 4-hydroxyisoquinoline-3-carboxylic acid 78, as shown in Scheme 19.⁴⁵ Such boroxazolidones exhibit a strong intramolecular coordination between the boron and the amino group, but despite this, the nitrogen atom still has nucleophilic properties. Nucleophilic attack by the nitrogen occurs at the aldehyde carbonyl of aromatic aldehydes, such as 75, to give the imine 76. Esterification, followed by addition of base, initiates an intramolecular condensation giving 77. Deboration to the isoquinolin-4-ol 78 was easily achieved by hydrochloric acid and water.



Scheme 19

2.5 Conclusions

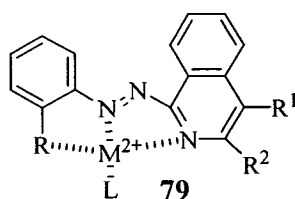
It has been shown that literature routes to 3-substituted isoquinolin-4-ols are rather limited. Only the *N*-oxide rearrangement with *p*-toluenesulfonyl chloride has any synthetic potential, as none of the other routes offer a good balance between the number of steps and yield. This rearrangement has sparked much mechanistic investigation, as the regioselectivity to the 4-position, is in contrast to the rearrangement with acetic anhydride. Furthermore, there are many substitution reactions known at the highly reactive 3-position of isoquinolin-4-ol, which offers great potential for functionalisation; the isoquinolin-4-ol itself being made by a rearrangement reaction. The Mannich reaction, sulfonation and halogenation are the most attractive propositions.

2.6 Metallised Isoquinolin-4-ol dyes

The isoquinolin-4-ol project arose from information found in several patents.^{46,47,48} Although these patents were not a direct reference to ink jet dyes, the isoquinolin-4-ol compounds synthesised, nonetheless, displayed very interesting and useful properties. It was thought that such compounds could have potential use as dyes in ink jet systems.

Described in these patents were various metallised 1-arylaizoquinolin-4-ol dyes, which fit the generic structure 79, giving good cyan dyes. A metal chelating group or salt of (R) (any group which donates electrons to the metal) in the *ortho* position of the arylazo moiety, and a hydroxy group or salt of (R¹) must be present; (R²) would preferentially be an alkyl substituent. When chelated to a metal, the UV-Vis spectra generally showed good curves with a cyan hue, with minimal unwanted absorptions. The metals used must have a stable oxidation state, form a tightly coordinated complex with the ligand giving the desired hue, and give a complex which is stable to heat, light and chemical reagents. Good results were achieved using various polyvalent metal ions such as zinc (II), nickel (II), platinum (II), palladium (II) and cobalt (II).

The structure of the metallised complex with the tridentate ligand is believed to be that shown below, where M²⁺ is the metal and L is a number of ligands depending upon the coordination number of the metal. A cyan dye would ideally have a λ_{\max} value of around 650 nm.



Many of the dyes tested showed excellent λ_{\max} values around this mark, and particularly good results were obtained when coordinated to nickel (II). The half band width values in the UV-Vis spectra were around 100 nm which is also desirable. Stability to light was tested, when the samples were subjected to three weeks of a simulated average northern skylight fading test. Again, these dyes

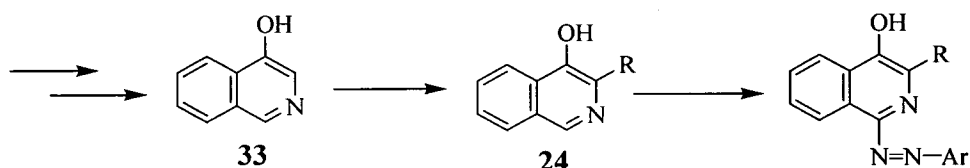
performed well, and therefore, isoquinolin-4-ols were aimed at as potential couplers in the synthesis of ink jet dyes.

2.7 New Routes to 3-substituted isoquinolin-4-ols.

As has been previously discussed in Section 2.1, literature methods to 3-substituted isoquinolin-4-ols are rather limited. The aim of this project was to find new, shorter and higher yielding routes to such compounds, for subsequent azo coupling reactions at the 1-position.

Due to the expertise within the group in FVP methods, and therefore the possibility of a quick, clean and high yielding synthesis, much of the discussion which begins in Section 2.12, involves such methodology.

It was also thought that routes to azo cyan dyes could be accessible from isoquinolin-4-ol **33**. As has been previously discussed, the best literature route to **33** involves a rearrangement reaction from isoquinoline *N*-oxide **29**. The 3-position of **33** is known to be highly reactive towards various substitution reactions (see Section 2.13), and by carrying out an appropriate reaction, this position could be blocked, and coupling could take place at the 1-position.



Scheme 20

2.8 Characterisation of Isoquinoline Derivatives

The chemical shifts observed in the ^1H and ^{13}C NMR spectra of the various isoquinoline derivatives discussed below, are very important for analysis of the products. These derivatives show similar chemical shifts to those of isoquinoline, which are well documented.⁴⁹

The chemical shifts shown in Figure 9 for isoquinoline, are recorded in $[\text{}^2\text{H}]_6\text{DMSO}$, for direct comparison with the NMR spectra discussed below. The proton at the 1-position consistently appears at a higher frequency than all the other protons in the NMR spectra, due to the adjacent electron withdrawing nitrogen atom and the

aromatic ring. This high frequency singlet is used primarily to characterise the various compounds discussed below.

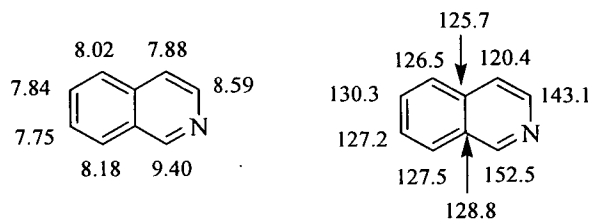
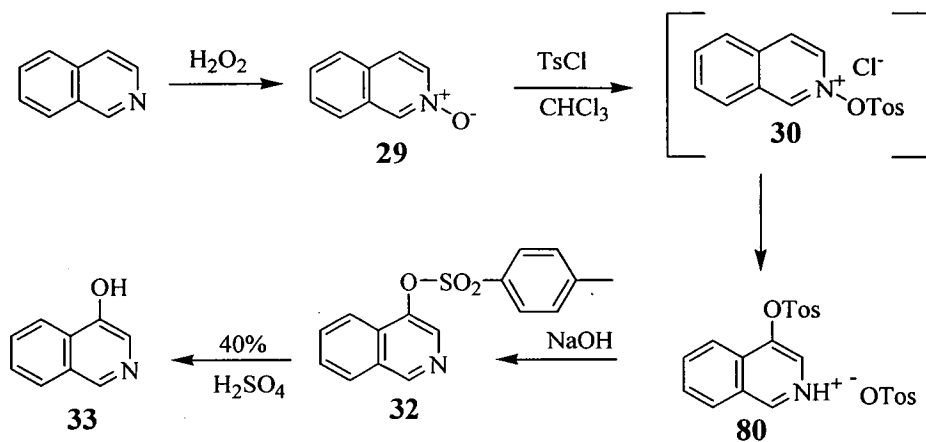


Figure 9 ¹H and ¹³C NMR data for isoquinoline in [²H]₆DMSO.⁴⁹

2.9 Synthesis of Isoquinolin-4-ol 33

The first step in the standard literature route to isoquinolin-4-ol **33**, involves the synthesis of isoquinoline *N*-oxide **29** from isoquinoline, using hydrogen peroxide, which was carried out in 60% yield. This compound had a wide ranging melting point, starting at about 50 °C. This was consistent with the literature, which stated that the product is a dihydrate of the *N*-oxide **29**, and the authors also found that it melted over a wide range, whereas a thoroughly dried sample melted at 98 °C.^{27,31} The next stage in the synthesis required that the *N*-oxide was dried with magnesium sulfate in a chloroform solution overnight; the desiccant was removed before the next step, the rearrangement, was attempted. It should be noted that the rearrangement occurs spontaneously after the addition of tosyl chloride, no other reagents were added, and **32** is synthesised in a one-pot reaction.



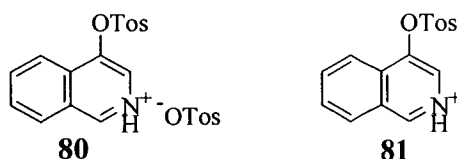
Scheme 21

One equivalent of tosyl chloride is added to the *N*-oxide **29** in chloroform at 0 °C, which results in **30**, after nucleophilic displacement of the chloride. This compound was isolated in the literature as the perchlorate salt.³¹ Two different literature methods were followed, which differed slightly at this point. After the addition of the tosyl chloride, one method described a two hour heating step,²⁹ whereas the other did not.⁵⁰ After repetition of these steps, it was found that the heating was unnecessary, and had no effect on the final tosylate yield. A dilute sodium carbonate solution (10%) was then added to the solution, which was stirred overnight,⁵⁰ but this also proved unnecessary after inspection of the ¹H NMR spectra. It was unclear what the purpose of this step was, and similar spectra could be obtained without this addition. The work-up simply involved separating the organic layer, drying this layer with magnesium sulfate, and removing the solvent to afford a thick yellow oil, which eventually solidified upon exposure to air.

The crude ¹H NMR spectra obtained for these reactions were all very messy. Product peaks could be identified, accounting for ~30-40% of the material, but the majority of the spectra showed unidentified aromatic material. The literature stated that a simple crystallisation of the crude residue with methanol would afford **32** at this point.⁵⁰

Crystallisation readily occurred giving a highly crystalline solid, but this was found not to be the target tosylate **32**, as the ¹³C NMR spectrum displayed too many CH peaks, and the ¹H NMR spectrum had too many aromatic protons. The solid obtained

was identified as the tosylate salt **80**; four large CH signals in the ^{13}C spectrum corresponding to two sets of tosyl CH resonances, and a high frequency CH corresponding to the isoquinoline 1-position at δ_{H} 146 ppm, were identified. The correct total mass m/z 472 $[(\text{MH}^+, 22\%)]$ was obtained by FAB mass spectroscopy, which also revealed the base peak of m/z 300 $[(\text{MH}^+, 100\%)]$, corresponding to **81**. Further evidence from the FAB mass spectrum came from m/z 599 $[(\text{MH}^+, 46\%)]$, corresponding to two units of **81** joined together by a hydrogen bond, and from m/z 771 $[(\text{MH}^+, 43\%)]$, corresponding to two units of **81** and one anionic tosyloxy unit.



The unwanted salt was neutralised by several washes with dilute sodium hydroxide solution (20%), but there was no mention of this salt in any of the literature procedures. However, a solid has been isolated at this stage previously, which was also washed with sodium hydroxide solution. This solid was probably the same salt as found above, but it was not identified.²⁹ The tosylate **32** was obtained in high purity after these basic washes, but only in about 30% yield.

The unusual feature of this synthesis was the incorporation of two moles of tosylate in **80**, when only one equivalent of tosyl chloride was used, and how **80** was formed remains unclear. The addition of two moles of tosyl chloride only resulted in the recovery of a large amount of unreacted tosyl chloride. *p*-Toluenesulfonic acid is being formed, as an extra oxygen atom and an extra hydrogen atom is present in the salt. Where these atoms come from is unclear, although the hydrogen may come from the solvent, and the oxygen from any water present. There may be some water present from the starting dihydrate, as it is speculated in the literature that a trace of water is essential for the rearrangement to occur.²⁹

The synthesis however, was now robust and reproducible; good quality material could be obtained quickly and on a large scale (10 g). A run of a typical experiment involves drying isoquinoline *N*-oxide dihydrate overnight with magnesium sulfate, removal of the desiccant, followed by the addition of one equivalent of tosyl

chloride, at 0 °C. The solution is then warmed to room temperature, and stirred for approximately 30 minutes, after which, it is washed several times with dilute sodium hydroxide solution to neutralise the tosylate salt. The organic layer is then separated, dried with MgSO₄, and evaporated to afford the tosylate **32**, which requires no further purification.

The regioselectivity of the rearrangement to the 4-position rather than the 1-position was established by comparison with literature ¹³C NMR spectrum.³² The presence of a singlet at δ_{H} 9.05 ppm was also good evidence, as no singlet would be expected if the rearrangement went to the 1-position. Furthermore, an X-ray crystal structure of the rearranged product has been obtained, clearly showing the tosyl group in the 4-position as required. This crystal structure is, in fact, the first of a 4-substituted hydroxyisoquinoline derivative.

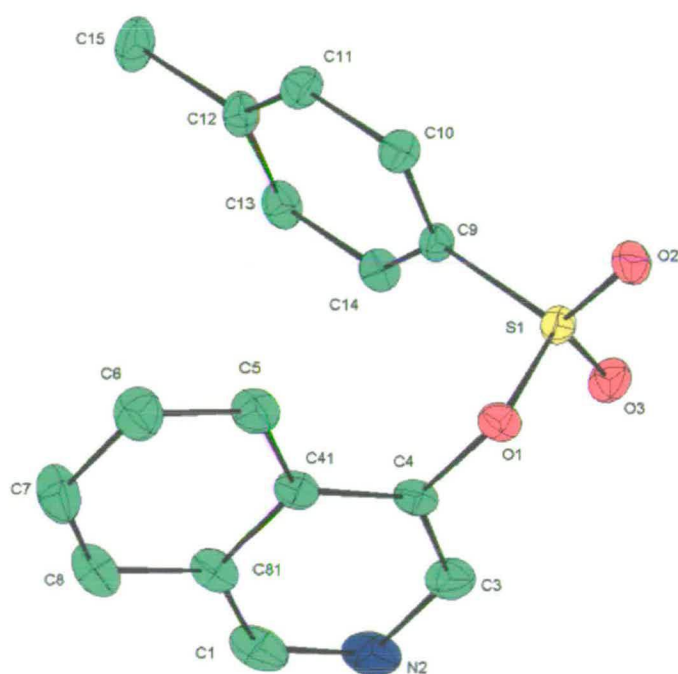


Figure 10 X-ray structure of the rearranged tosylate **32**

The bond lengths of **32** are shown below in Figure 11, along with those of isoquinoline⁵¹ and a 4-substituted analogue **32a**.⁵² The bond lengths of the two 4-substituted analogues **32** and **32a** are very similar. The addition of the groups at the 4-position has however given shorter C(1)-N(2) bond lengths of [1.316(3) Å] in **32**

and [1.313(4) Å] in **32a**, compared with [1.3631(16) Å] in isoquinoline. The N(2)-C(3) bond lengths of [1.363(2) Å] in **32** and [1.358(4) Å] in **32a** of are also shorter than the 1.3919 Å (17) witnessed in isoquinoline. The C(3)-C(4) and C(4)-C(41) bond lengths of **32** and **32a** are comparable with those in isoquinoline.

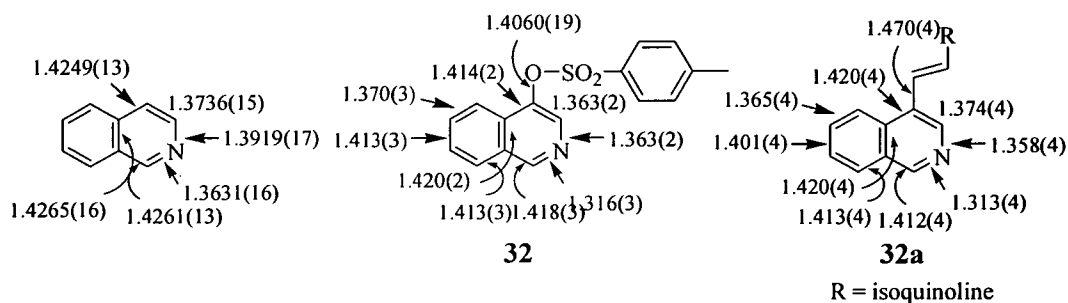


Figure 11 Comparison of bond lengths for isoquinoline, **32** and a 4-substituted analogue **32a**.

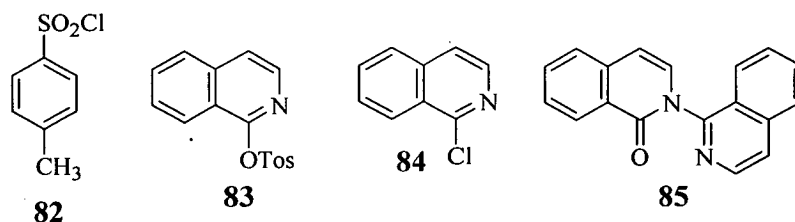
The disappointing aspect of this rearrangement was the low to moderate yield, the reasons for which were not fully understood. Clearly, significant amounts of material was lost during the reaction, resulting in poor yields. In an attempt to try to account for the low yield, and to identify what other products might be formed during this reaction, the crude material obtained after the tosyl chloride addition was purified by dry-flash column chromatography. No additions of sodium hydroxide were made to remove the salt **80**. The very surprising result from this experiment was that the tosylate **32** was isolated in 76% yield, and in a very pure state.

As the column proceeded, the yield of product obtained was initially consistent with the previous experiments (0.47g, 30%). TLC showed that all the product had eluted from the column, and that only baseline material remained. The column was then washed with methanol to remove, and to hopefully identify, the baseline material, which was significant in its quantity. However, an unexpected second batch of tosylate **32** was isolated, and therefore, the methanol wash had effectively more than doubled the yield of tosylate (1.2g, 76%). The majority of the material was accounted for, but other fractions were also obtained. A small amount of the starting *p*-toluenesulfonyl chloride **82** (73 mg, 9%) was identified, and its NMR spectra

closely matched that reported.⁵³ Two large doublets were observed in the ¹H NMR spectrum, as expected for this structure. The tosyloxyisocarbostyryl compound **83** (rearrangement to the 1-position) was found in a small amount (61 mg, 4%). The ¹H NMR spectrum did not reveal the high frequency singlet around δ_H 9 ppm, which would correspond to the proton at the 1-position. The electron impact mass spectrum showed the correct mass at *m/z* 299 [(M⁺, 58%)].

The other isolated fraction (70 mg) was a mixture of products, thought to be perhaps 1-chloroisoquinoline **84** or 4-chloroisoquinoline, as the mass spectrum suggests, *m/z* 165 (M⁺, 83%), 163 (M⁺, 100%), and 128 (90) (loss of ³⁵Cl), and also some isocarbostyryl *N*-isoquinoline **85**, also seen in the mass spectrum, *m/z* 271 (M⁺, 1%) and 145 (88) (loss of isoquinoline). The ¹H NMR spectrum clearly showed a mixture of products, and was more consistent with 4-chloroisoquinoline, due to the presence of two singlets at δ_H 9.31 ppm and 8.59 ppm.

Compounds **83**, **84** and **85** were very tentatively identified, but they are known in the literature, and were previously identified by ¹H NMR spectroscopy from a similar reaction.³²



The mass of crude material before the column was now comparable with that obtained from the combined fractions after the column. It can be concluded that most of the material lost during the reaction is therefore unidentified material, that seems to have potential to be turned into product.

Clearly the difference between this work-up and the standard synthesis, is the presence of methanol and of silica from the column. It was thought that either the silica or methanol or a combination of both, were somehow converting the baseline material into product. Experiments were then conducted which involved refluxing the crude material in methanol, stirring in the presence of silica and a combination of the two, but complex ¹H NMR spectra were obtained.

Further experiments were carried out, by absorbing the crude product on a dry-flash column, and then washing it through with methanol after the material has been on the column for about 30 minutes. After evaporation of the methanol, a respectable yield of 55% of pure tosylate **32** was obtained. A similar yield was obtained in the literature when **32** was obtained from a column.³² The same procedure was repeated again, but this time leaving the crude product on the column for 24 hours, and then washing it off again with methanol. The yield this time was about 46%, which was still an improvement on the standard method used, but not as good as the previous attempt.

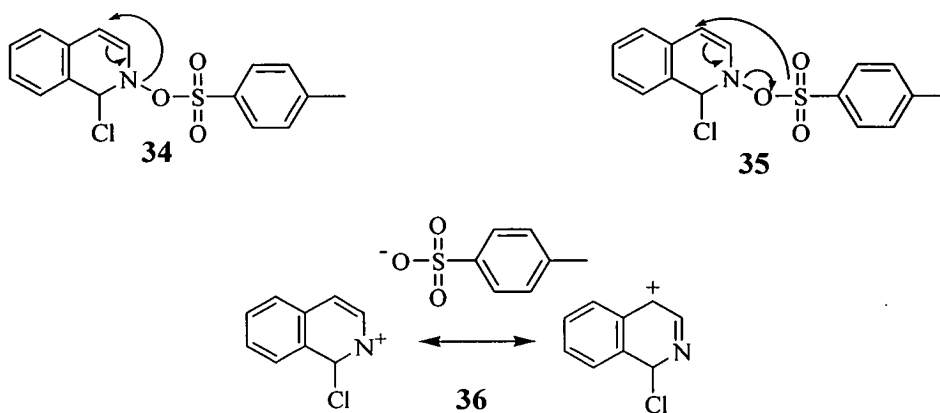
It was thought that perhaps some of the product was being lost to the aqueous layer during work-up, but attempts to isolate any more material by means of a liquid-liquid continuous extraction with dichloromethane, proved unsuccessful. Further tosylate **32** was isolated after this work-up, but only an increase of 3% was obtained. Other unidentified material was also isolated, but not in any significant quantities.

2.9.1 Rearrangement Mechanism

The mechanism of this rearrangement reaction has generated much research in the literature, and has been discussed in Section 2.1.

To summarise, the regioselectivity of this rearrangement is surprising, as the most active site for nucleophilic attack is at the 1-position, as seen in the rearrangement with acetic anhydride (see Section 2.1). This difference in regioselectivity has been rationalised by the addition of the chloride anion at the 1-position, thus blocking this site for any subsequent rearrangement.

The actual mode of migration of the tosyl group can proceed by three possible pathways;³² a tight ion-pair or sliding mechanism **34**, an intramolecular [3,3] sigmatropic shift **35** or an intermolecular solvent-separated ion-pair mechanism **36**, all shown below. A combination of mechanisms **34** and **35** were postulated based on the isotopic labelling results.



2.9.2 Hydrolysis

The final part of the synthesis was the hydrolysis of the tosylate **32** to isoquinolin-4-ol **33**. By refluxing the tosylate **32** for eight hours in 40% sulfuric acid, the tosyl group can be removed as *p*-toluenesulfonic acid (cleaving the sulfur-oxygen bond), to give **33** in 70% yield.^{29,31,32,50}

No basic hydrolysis conditions of the tosylate **32** are known in the literature, although attempts were made using sodium hydroxide,⁵⁴ resulting in a mixture of the tosylate **32** and isoquinolin-4-ol **33**. Further hydrolysis of this mixture was attempted under the same conditions, but only resulted in a similar mixture of the two products. Full characterisation of isoquinolin-4-ol has been achieved by NOESY and HSQC spectroscopy, and the data are listed below in Table 2. The signals in the ¹H and ¹³C NMR spectra corresponding to the 1-position, appear at higher frequency than the signals for all the others in **33**, δ_{H} 8.81 ppm and δ_{C} 143.76, due to the adjacent electron withdrawing nitrogen atom, and the aromatic ring. The 1-position singlet at δ_{H} 8.81 ppm correlated to the doublet at δ_{H} 8.07 ppm, which corresponded to the 8-position, in the NOESY spectrum. Similar correlations allowed full assignment of **33**.

Position	¹ H chemical shift (ppm)	¹³ C chemical shift (ppm)
1	8.81	143.76
3	8.10	127.79
5	8.15	121.83
6	7.75	130.61
7	7.68	128.39
8	8.07	127.75

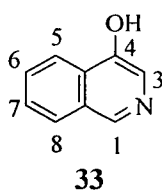


Table 2 ¹H and ¹³C NMR data for isoquinolin-4-ol **33**.

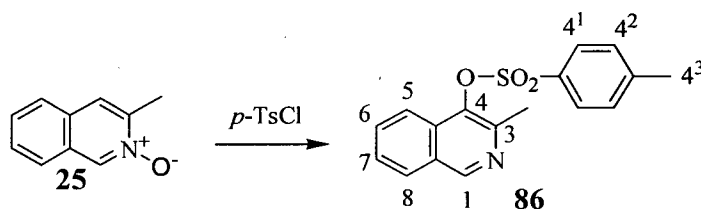
2.10 Other Rearrangements

It seemed surprising that no rearrangement had been done with the readily available 3-methylisoquinoline *N*-oxide **25** and *p*-toluenesulfonyl chloride, to access 3-substituted isoquinolin-4-ols, especially as the corresponding reaction with acetic anhydride had been carried out.²⁷ One drawback of this synthesis however is the extra cost of the starting 3-methylisoquinoline compared with isoquinoline (approximately ten times more expensive).

The *N*-oxide **25** was first synthesised in the same manner as that for the parent isoquinoline, using hydrogen peroxide, and was then reacted with one equivalent of *p*-toluenesulfonyl chloride, in chloroform. After stirring at room temperature for 1 hour and then at 45 °C for 1 hour, the crude material was washed with sodium hydroxide solution to neutralise the tosylate salt. The tosylate **86** was obtained after removal of the solvent, and it was found that the group migrated to the 4-position exclusively, again in 30% yield; a similar result to the rearrangement discussed above with isoquinoline *N*-oxide **29**. No attempts have been made to optimise this particular rearrangement.

The regioselectivity of this rearrangement was confirmed by ^1H NMR spectroscopy, which showed the characteristic singlet at δ_{H} 9.62 ppm, due to the proton at the 1-position. No such signal would be present if the rearrangement proceeded to the 1-position. The NOESY spectrum showed correlation between the singlet at δ_{H} 9.62 ppm, and the doublet at δ_{H} 8.41 ppm, which corresponded to the proton at the 8-position. Further correlations allowed assignment of the remaining protons.

In addition, no correlation to the methyl group at the 3-position was seen in the spectrum. Correlation would be expected between the proton at the 4-position and the methyl group if the tosyl group migrated to the 1-position.



Scheme 22

Position	^1H Chemical Shift (ppm)
1	9.62
8	8.41
6	7.93
4 (1)	7.92
7	7.86
5	7.82
4 (2)	7.55
3	2.47
4 (3)	2.45

Table 3 ^1H NMR data for 3-methyl-4-(*p*-toluenesulfonyloxy)isoquinoline **86**.

Hydrolysis to **28** from **86** was successful under the same acidic conditions as described previously for **33**. The expected precipitate did not form, but 3-methylisoquinolin-4-ol **28** was isolated after the aqueous layer was continuously

liquid-liquid extracted with dichloromethane for six hours. Conditions would have to be optimised to make this a viable route, as it should be possible to improve upon the 42% yield for the hydrolysis. Due to the poor characterisation of **28** in the literature, and the small amounts of material obtained, NOESY and HSQC spectra were obtained, which allowed full assignment of **28**, as shown in Table 3. From the NOESY spectrum, the singlet at δ_{H} 8.74, corresponding to the proton at the 1-position, correlated to the proton at δ_{H} 7.97, and therefore this proton could be assigned as the 8-position. Similar correlations were made around the aromatic ring, which allowed assignment of all the protons, and subsequently the ^{13}C signals from the HSQC spectrum.

Position	^1H chemical shift (ppm)	^{13}C chemical shift (ppm)
1	8.74	142.52
5	8.14	120.91
8	7.97	127.11
6	7.64	129.19
7	7.55	126.34

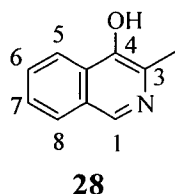
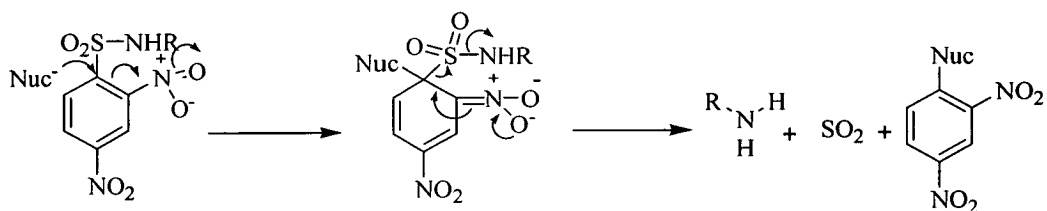


Table 4 ^1H and ^{13}C NMR data for 3-methylisoquinolin-4-ol **28**.

It has been shown in the literature that rearrangements involving isoquinoline *N*-oxide **29** and several substituted benzenesulfonyl chlorides, namely *p*-bromo, chloro and methyl substituted, give a straight line in a Hammett plot.³¹ It was thought that such rearrangements may proceed faster and therefore cleaner than those observed with tosyl chloride, hopefully improving the yield of rearranged product. With this in mind, the rearrangement with isoquinoline *N*-oxide **29** and *p*-nitrobenzenesulfonyl

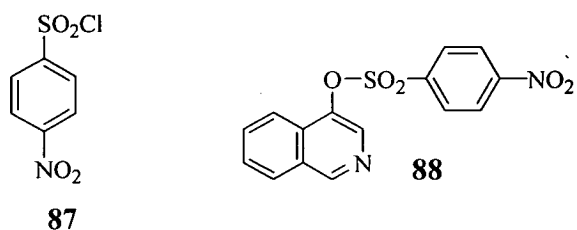
chloride was attempted to see if this trend would continue for derivatives with a more powerful electron withdrawing group.

In addition, milder hydrolysis conditions have been reported in the literature than those described above with 40% sulfuric acid.⁵⁵ It has been shown that carbon-sulfur bonds can be cleaved to remove arylsulfonyl groups which are dinitro substituted, as shown below in Scheme 23. The facile deprotection of these compounds can be carried out by treatment with propylamine at room temperature for ten minutes, or with thiophenol and triethylamine at room temperature for five minutes. It should be noted that this reaction involves a different mechanism to the standard acid hydrolysis. Nucleophilic attack occurs at the 4-position, due to the directing effects of the two nitro groups, which is followed by elimination of sulfur dioxide, to give an amine and a substituted aromatic compound as the products. This potential for milder hydrolysis conditions was another reason for attempting the rearrangement with *p*-nitrobenzenesulfonyl chloride.



Scheme 23

The rearrangement between isoquinoline *N*-oxide and *p*-nitrobenzenesulfonyl chloride **87** was carried out in chloroform, as with the other rearrangements described above. The solution obtained after the addition of one equivalent of *p*-nitrobenzenesulfonyl chloride to the *N*-oxide, was heated to reflux for 1 hour, with a precipitate forming after about thirty minutes. After washing this solid with sodium hydroxide solution, the rearranged product **88** was obtained in 22% yield. This product was identified by ¹H NMR spectroscopy, as the characteristic singlet at 9.36 ppm, corresponding to the proton at the 1-position, was present.

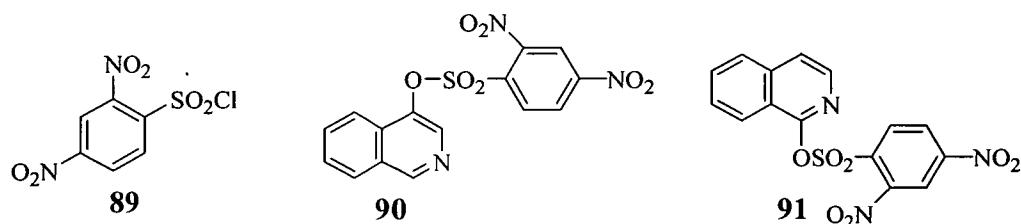


After removal of the solvent from the filtrate, a solid was obtained, which contained the starting *p*-nitrobenzenesulfonyl chloride **87** [from the mass spectrum, m/z 223 (M^+ , 9%) and 221 (M^+ , 24%), revealing an ~3:1 chlorine isotope pattern]. The ^1H NMR spectrum showed two large doublets, which fits the structure, but extra signals were also present corresponding to unidentified material.

In an attempt to try to convert this starting material to product, another experiment was carried out, which involved heating the reactant solution to reflux for three hours instead of one. The ^1H NMR spectrum of the precipitate formed this time however, revealed a lot more signals corresponding to unidentified material, and after work-up, did not increase the yield of **88**.

A preliminary experiment has been carried out to try to utilise milder hydrolysis conditions than the 40% sulfuric acid used for the tosyloxy derivatives. The reaction mixture was heated to reflux in 10% aqueous sulfuric acid, and a 3:1 mixture of isoquinolin-4-ol **33** to **88** was found. This result was encouraging, showing that the arylsulfonate group in **88** was easier to cleave than the tosyl group in Scheme 21. Clearly further work would have to be done on this route, and perhaps basic hydrolysis could be possible as suggested in the literature with the dinitro derivatives discussed above.

To extend these rearrangements further, the reaction between isoquinoline *N*-oxide **29** and 2,4-dinitrobenzenesulfonyl chloride **89** was investigated, in an attempt to synthesise **90**.



The starting arylsulfonyl chloride **89** was not particularly soluble in chloroform, and after the mixture was heated to reflux for three hours, the solid that was present was filtered off. The ^1H NMR spectrum showed that the target compound **90**, was not formed. Rearrangement to the 1-position rather than the 4-position had occurred, to give **91**, identified by the absence of the high frequency singlet at δ_{H} ~9 ppm.

Prominent signals in the ^1H NMR spectrum corresponding to the 2,4-dinitrobenzene moiety in **91** were apparent at δ_{H} 8.56 (1H, d), 8.41 (1H, dd) and 8.11 (1H, d) ppm. Overlapping peaks occurred in the ^1H NMR spectrum, that were resolved in the HSQC spectrum, which showed the presence of four doublets and two triplets corresponding to the aromatic ring of the isoquinoline moiety. The integrals in the ^1H NMR spectrum were consistent with the structure of **91**. Signals corresponding to the CH's of the 2,4-dinitrobenzene moiety were observed in the ^{13}C spectrum at δ_{H} 130.61, 125.54 and 118.20 ppm; six other CH signals were also seen, which is again consistent with **91**. The COSY spectrum provided good evidence for this structure, which showed correlation between the protons of the dinitro substituted moiety, correlation between the protons at the 3- and 4-positions of the isoquinoline moiety, and correlation between the protons of the isoquinoline aromatic ring.

The solvent was removed from the filtrate to give a yellow solid, which was isolated in greater quantity than the precipitate described above. The spectra obtained were very similar to those obtained for the precipitate, but the material was not as pure.

To overcome the solubility problem, the reaction was repeated in acetonitrile, but gave similar results. Similar work-ups to those described previously were attempted, such as the basic washes, but this did not improve the NMR spectra.

It was concluded that this rearrangement was perhaps too ambitious, departing too much electronically from the compounds in the Hammett plot, although it has provided a very interesting result. This was the only rearrangement where migration to the 1-position rather than the 4-position occurred, and has raised doubts over the mechanism discussed in Sections 2.1 and 2.9.1.

The addition of the chloride anion at the 1-position of **30** was deemed to be the controlling factor of the regioselectivity observed in the reaction between isoquinoline *N*-oxide and *p*-toluenesulfonyl chloride (rearrangement to the 4-position). In this case however, the chloride anion is present again, but the regioselectivity favours the 1-position rather than the 4-position. The addition of the extra nitro group has had a major effect, as the rearrangement was in contrast to the reaction between isoquinoline *N*-oxide and *p*-nitrobenzenesulfonyl chloride, which gave the 4-substituted product. Perhaps the electronic effects of the *ortho* nitro

group, or steric reasons, are playing a vital role. No further work has been carried out to investigate this mechanism further.

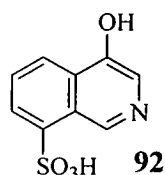
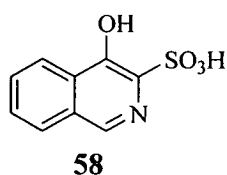
In conclusion, the rearrangement reaction of isoquinoline *N*-oxide and *p*-toluenesulfonyl chloride, and subsequent hydrolysis of **32**, has provided a reliable route to isoquinolin-4-ol **33**. A similar rearrangement from 3-methylisoquinoline *N*-oxide **25** has given 3-methylisoquinolin-4-ol **28**, which could be reacted with a diazonium salt to give azo dyes without further derivatisation. Isoquinolin-4-ol **33** on the other hand, requires reaction at the 3-position before any azo coupling can take place.

2.11 Reactions of Isoquinolin-4-ol

2.11.1 Sulfonation

As has been discussed previously, the 3-position is the most reactive site of isoquinolin-4-ol **33**, due to the electron donating effect of the hydroxyl group, and must be blocked to stop any unwanted coupling reactions. Water solubility is also eventually required in the final dye, and the introduction of a sulfonic acid group would improve this. Sulfonation at the 3-position would assist both these requirements, although it was unclear how the presence of this electron withdrawing group would then affect azo coupling.

Standard sulfonation reactions involve the use of 20% oleum, but this has been reported in the literature not to take place at the 3-position of **33**, but rather to give 4-hydroxyisoquinoline-8-sulfonic acid **92**.⁴⁰ The authors believed that this was caused by the formation of a positively charged isoquinolinium ion, causing deactivation of the heterocyclic ring, and directing the substitution to the aromatic ring.



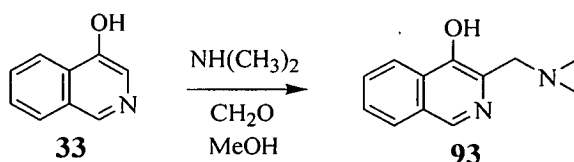
The same authors then successfully sulfonated the 3-position under weakly alkaline conditions, to give **58** (see Section 2.3.2). Following this recipe, two attempts were

made to repeat this synthesis but were not successful. Complex NMR spectra were obtained and no molecular ion peaks corresponding to the sulfonated product **58** were obtained in the mass spectra.

A reaction that was not carried out, but may prove useful, is to try to sulfonate isoquinolin-4-ol **33** with oleum, but under harsher conditions. This may sulfonate the compound at additional sites to the 8-position on the aromatic ring, perhaps even sulfonating the required 3-position.

2.11.2 The Mannich Reaction

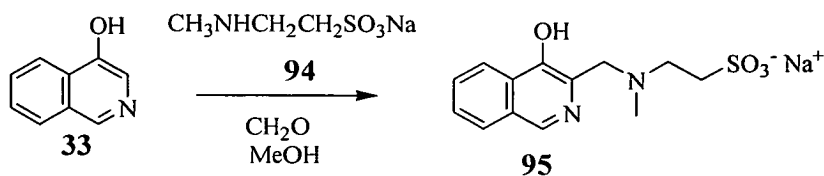
Aminomethylation of isoquinolin-4-ol at the 3-position is a well known reaction in the literature, and several examples are reported.^{38,39} The reaction between dimethylamine, formaldehyde and isoquinolin-4-ol was repeated, to give **93** in 52% yield (see Section 2.3.1 for general Mannich mechanism).



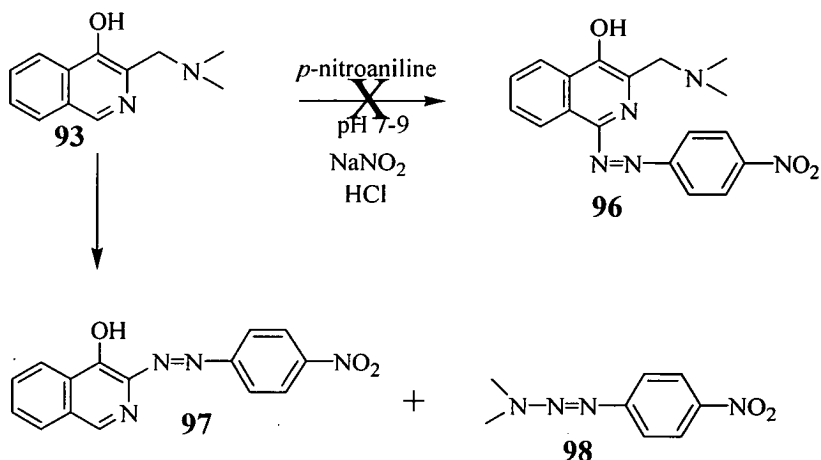
Scheme 24

The product was identified by ¹H and ¹³C NMR spectroscopy, with the signal at δ_H 8.10 ppm, (corresponding to the 3-position of isoquinolin-4-ol) now absent. The characteristic high frequency singlet at δ_H 9.36 ppm was present, corresponding to the proton at the 1-position.

This Mannich product **93**, has the 3-position blocked as required for forthcoming coupling reactions, none of which had been attempted on such derivatives in the literature. It was thought that a sulfonated amine could be used to impart water solubility as a Mannich product. Accordingly, aqueous *N*-methyltaurine sodium salt **94** was reacted with formaldehyde and isoquinolin-4-ol **33** as above, and the water soluble Mannich product **95** was successfully synthesised. Again, the ¹H NMR spectrum revealed the absence of the singlet at the 3-position of isoquinolin-4-ol at δ_H 8.10, and the presence of the singlet at δ_H 9.17 was apparent.



Scheme 25

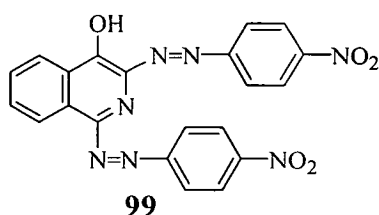


Scheme 26

The next step was to investigate the reactivity of the derivatives towards azo coupling, and this was first attempted with **93** and *p*-nitrobenzenediazonium chloride (derived from the reaction between *p*-nitroaniline and sodium nitrite), at pH 8-9. A deep red coloured solution was observed instantly upon addition of the diazonium salt to the basic solution containing the isoquinolin-4-ol **33**. The precipitate that formed was shown to be a mixture of products by ^1H NMR spectroscopy. However, the spectrum showed no signals corresponding to the CH_2 and CH_3 groups, and the singlet at high frequency, δ_{H} 8.92 ppm, was still present, immediately indicating that coupling at the 1-position was not successful. After column chromatography, the two products obtained were identified as the triazene **98**, and the azo compound **97**, as shown in Scheme 26. The target compound **96** was not obtained. This experiment was repeated at pH 7.5, but a similar result was obtained. The Mannich product **93** was apparently not stable to the coupling conditions; a retro-Mannich reaction was occurring, to provide **97** and **98**.

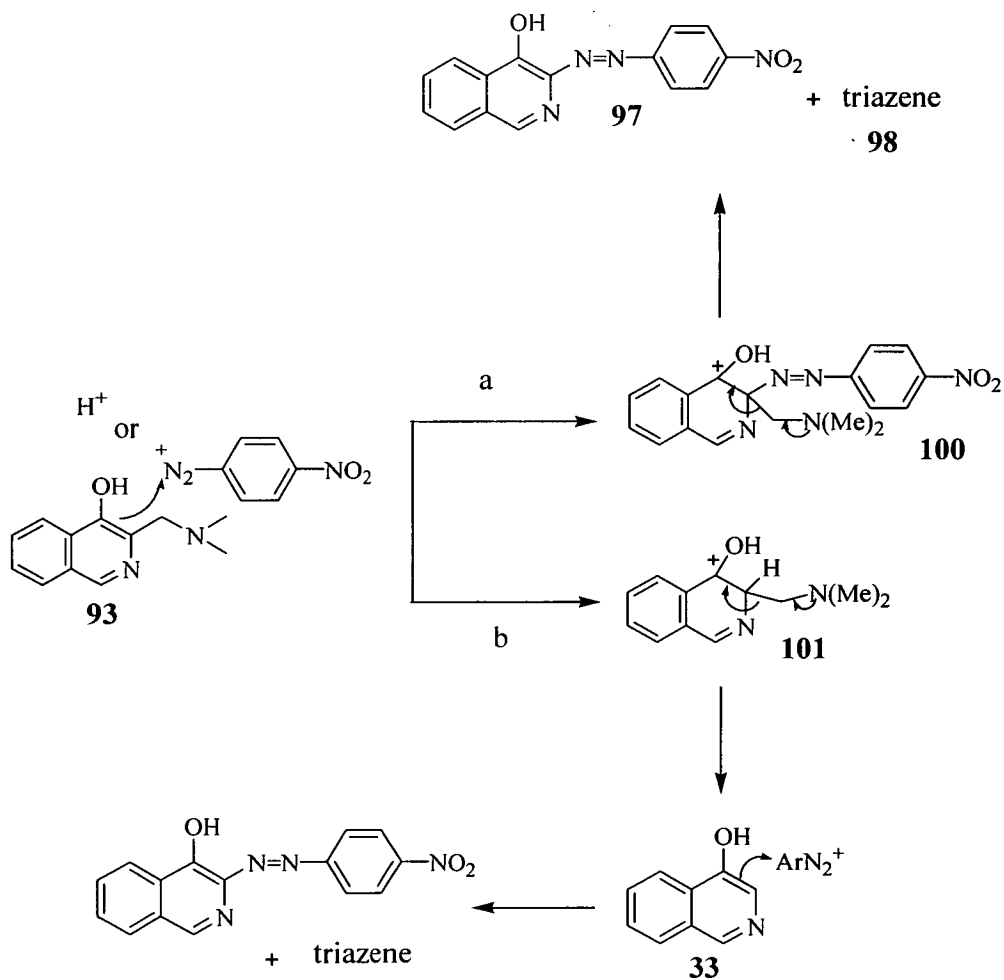
The triazene **98** is a literature compound, and its NMR spectra and melting point matched the literature well.⁵⁶ The azo compound **97** is also known in the literature, but no NMR data have been reported.⁴¹ The ¹H NMR spectrum revealed the characteristic high frequency singlet at δ_{H} 8.92 ppm, and the ¹³C spectrum revealed two large peaks corresponding to the CHs on the aromatic ring at the 3-position of **97**, and four other CH signals corresponding to the isoquinoline aromatic ring. Again, the high frequency CH signal at δ_{H} 154 ppm was present. The electron impact mass spectrum revealed the molecular ion peak at 294, with a breakdown peak at 249 corresponding to the loss of the nitro group, and a signal at 144 corresponding to the loss of the *p*-nitroazo moiety. The NMR spectra however, were not entirely clean, and the azo compound **97** was synthesised for comparison, by the reaction of isoquinolin-4-ol **33** and *p*-nitrobenzenediazonium chloride, generated under standard diazo coupling conditions. The NMR and mass spectra of this compound matched these of the azo compound **97** isolated above from the dry-flash column.

Very small amounts of one other component was isolated from the above dry-flash column but remains unidentified. No singlet was seen in the ¹H NMR spectrum, and it was therefore thought to be the disubstituted derivative **99**. Two triplets were observed which would fit the proposed structure (corresponding to the isoquinoline aromatic ring), with the rest of the spectrum made up of doublets. However, no molecular ion peak corresponding to the disubstituted derivative **99** was found in the mass spectrum.

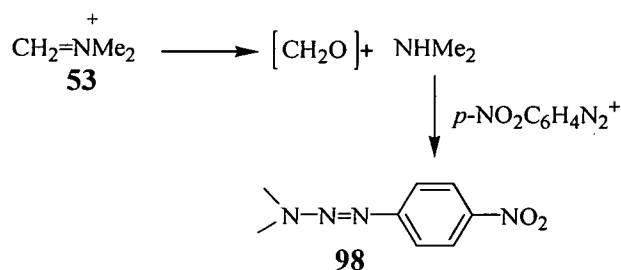


The coupling reaction with *p*-nitrobenzenediazonium chloride was repeated for the taurine derivative **95**, but again a retro-Mannich process was occurring, with the azo compound **97** identified as the only product. A triazene was assumed to have formed again, but was lost in the aqueous work-up due to the sulfonic acid group now present.

The retro-Mannich process could occur either by electrophilic attack by the diazonium salt (path a) or the hydrogen ion at the 3-position (path b), forming the intermediates **100** and **101**, shown in Scheme 27. From intermediate **100**, the azo compound **97** is formed after the aminoalkyl group is eliminated as an iminium species **53**, which collapses to formaldehyde and the secondary amine. The amine then reacts with the diazonium salt to produce the triazene **98**, (Scheme 28). From intermediate **101**, the aminoalkyl group is eliminated in a similar manner, forming isoquinolin-4-ol **33** as an intermediate, which can then react with the diazonium salt at the 3-position to form **97**, along with the triazene **98**.



Scheme 27



Scheme 28

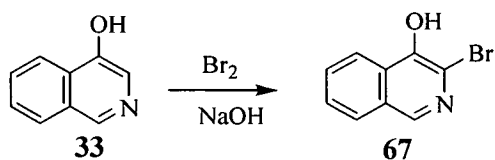
The mechanism could be clarified by subjecting one of the Mannich derivatives to the conditions of the azo coupling reaction, but without adding the diazonium salt. If isoquinolin-4-ol **33** is recovered, then the mechanism must follow path b.

Due to these results, this route was pursued no further, and another substitution reaction was then investigated. However, the Mannich derivatives can be used to provide another route to 3-methylisoquinolin-4-ol **28**. This has been successfully achieved by hydrogenation of **55** and **56**, see Section 2.3.1.

2.11.3 Bromination

Selective halogenation is another reaction known to take place at the 3-position of isoquinolin-4-ol **33** (see Section 2.3.2). It was thought that by brominating this position, then a Suzuki coupling reaction could be carried out, potentially introducing a variety of aromatic substituents at the 3-position.

No products were obtained when the reaction was carried out at room temperature, using the conditions of Andranova *et al.*⁵⁷ However, use of an alkaline solution of bromine with careful control of temperature, during the reaction (< 0 °C) and at the isolation stage (-10 °C). 3-Bromoisoquinolin-4-ol **67** was eventually obtained in 37% yield, after a continuous liquid-liquid extraction with dichloromethane for seven hours.⁵⁸ The mass spectrum showed the two bromine isotope peaks in a 1:1 ratio at *m/z* 223 and 225, and the NMR data matched those expected for this structure.

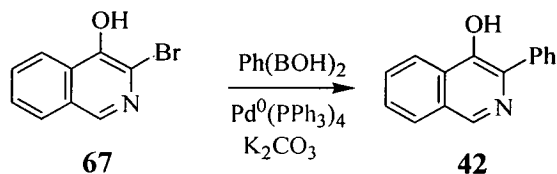


Scheme 29

2.11.4 Suzuki Coupling

No Suzuki coupling conditions could be found in the literature for compounds of this type, which is not surprising, as most of the work done with these systems was in the 1960s and 1970s. Conditions have however, been developed and used within the group for Suzuki coupling reactions on heterocyclic systems.⁵⁹

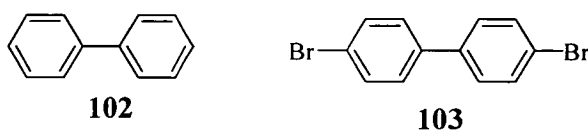
It was decided to attempt the coupling of 3-bromoisoquinolin-4-ol 67 with phenylboronic acid, to provide 3-phenylisoquinolin-4-ol 42 as the product. As good quality spectra had been obtained for 42 (Section 2.2), then it would be easy to compare the spectra to see if the reaction was successful. Clearly this method could provide much diversity at the 3-position if successful, as coupling to various boronic acids could then be carried out.



Scheme 30

The conditions used involved heating a mixture of 3-bromoisoquinolin-4-ol 67, tetrakis(triphenylphosphonium)palladium, phenylboronic acid and potassium carbonate to reflux for four hours under nitrogen, in a 3:1 dioxane:water solution. After work-up, no 3-phenylisoquinolin-4-ol 42 was apparent in either the ¹H NMR spectrum or the mass spectrum of the reaction mixture. The ¹H NMR spectrum clearly showed the splitting pattern previously seen for the bromo compound 67, and was confirmed by mass spectroscopy with the 1:1 bromine isotope pattern apparent. The mass spectrum also showed a peak at *m/z* 154 corresponding to biphenyl 102, which suggests that self-coupling of the boronic acid was occurring. The identification of 102 could not be corroborated by the ¹H NMR spectrum due to

overlapping signals. Self-coupling of boronic acids in Suzuki type coupling reactions is known.⁶⁰ For example, **103** is obtained from the self-coupling of *p*-bromobenzene boronic acid, in the presence of either Pd(II) acetate or tetrakis(triphenylphosphine)Pd(II) catalysts.

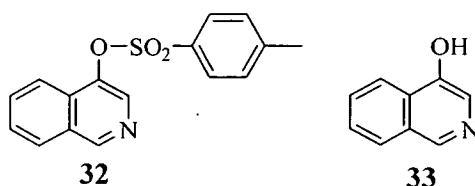


As a result of this experiment, and the presence of starting material, a pilot experiment using a microwave was attempted. This involved heating a mixture of 3-bromoisoquinolin-4-ol **67**, phenylboronic acid, cesium carbonate and tetrakis(triphenylphosponium)palladium, in a 3:1 THF:water mixture, at 120 °C (power 150 W) in a microwave for ten minutes. The ¹H NMR spectrum was again very messy, and any signals corresponding to 3-phenylisoquinolin-4-ol **42** were very difficult to identify.

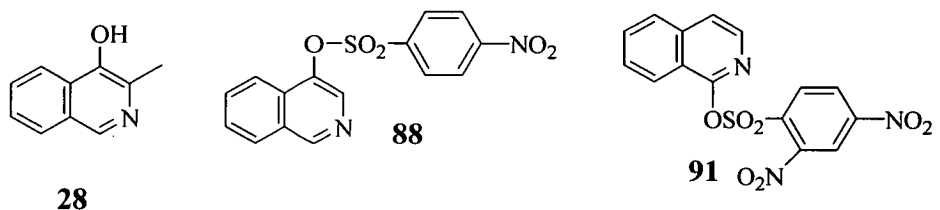
Such coupling reactions with electron rich halides are known to be slow, and under the basic conditions of the experiment, the phenoxide ion will cause the reaction to be even slower. Low yielding aryl coupling to 3-bromoisoquinolin-4-ol **67** is known in the literature, but not under these conditions (see Section 2.4.2).⁴³ This report suggests that problems may arise from the acidity of the hydroxyl group, which can inhibit organometallic reactions, and that protective groups may be required.

These Suzuki coupling reactions were not successful, but it is possible that conditions could be found where the desired product is successfully synthesised, such as by changing the catalyst. Recent research has shown that Suzuki coupling reactions involving very unreactive aryl halides, can be successfully carried out using catalysts containing a tri(*t*-butyl)phosphine ligand.⁶¹

In conclusion, the rearrangement reaction of isoquinoline *N*-oxide and *p*-toluenesulfonyl chloride, has provided a quick, robust and reproducible route to **32**. The low to moderate yield of this rearrangement remains the biggest problem associated with the synthesis of **33**, the reasons for which are unclear.



Optimisation of this step would have to be achieved to make this route synthetically useful. Further rearrangements have been successfully carried out to provide **28** and **88**, in contrast to the rearrangement with 2,4-dinitrobenzenesulfonyl chloride, which gave **91**. Functionalisation at the 3-position has also been achieved *via* Mannich and bromination reactions. Despite the disappointing coupling reactions with the Mannich products, these products can nevertheless, provide another route to **28**, *via* hydrogenation.



The initial problem of finding a high yielding route to the isoquinolin-4-ols was still not rectified. A very different methodology has also been looked at, with the aim to accomplish this feat. This route utilised flash vacuum pyrolysis, and ultimately provided a novel 3-arylsubstituted isoquinolin-4-ol synthesis, and a novel target azo cyan dye.

2.12 FVP Methods

2.12.1 FVP Overview

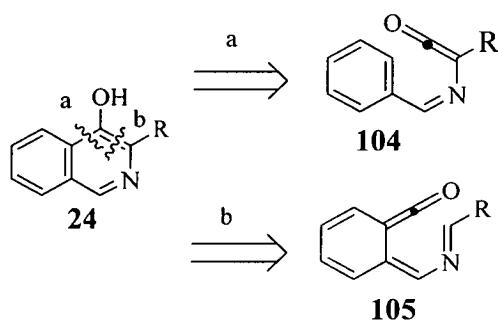
Flash Vacuum Pyrolysis (FVP) simply involves vacuum distillation of a substrate through a hot tube. Reaction occurs in the gas-phase, and can provide products that are unattainable by solution-phase methods. The advantage of FVP is that the individual molecules are isolated from solvent, precursor and products, when the pyrolysis takes place. Therefore, FVP is excellent for intramolecular reactions, *e.g.* eliminations and cyclisations. One drawback of FVP, is the requirement that the substrate must be volatile at low pressures. Decomposition of poorly volatile precursors in the FVP inlet tube, is a problem encountered in several of the reactions discussed below.^{62,63} A more detailed description of the technique, along with the apparatus used, is offered in Section 3.3.

2.12.2 Ketene Intermediates

Unsaturated ketene intermediates are commonly generated under FVP conditions by elimination reactions from suitable precursors; once generated, ketenes are highly reactive and can undergo spontaneous cyclisation.⁶⁴

Much of the forthcoming discussion focuses on the generation of ketene intermediates from various precursors. There have been many literature reports in the synthesis of iminoketene intermediates by FVP methods.⁶⁴

Two different iminoketene intermediates **104** and **105** can be obtained retrosynthetically from **24**, and routes to these will be discussed in the forthcoming Sections. The most obvious disconnection is labelled a in Scheme 31, and FVP routes to **104** from imine precursors have been investigated.

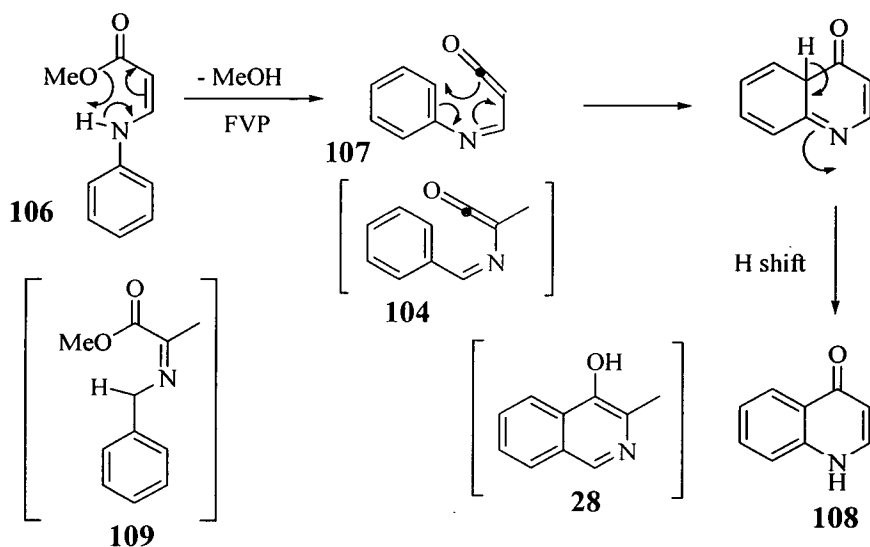


Scheme 31

2.12.3 Imine precursor **109** derived from benzylamine.

The very well known Conrad-Limpach synthesis of quinolones, such as **108** from **106**, is very successfully carried out by FVP methods.⁶⁴ Scheme 32 shows this part of the synthesis, and under FVP conditions, an elimination of methanol occurs from the precursor, generating the ketene intermediate **107**. This reaction proceeds in high yield through to the quinolone **108** after cyclisation.

By simply moving the nitrogen atom from the 1-position in the quinolone structure, to the 2-position in the isoquinolin-4-ol, a close analogy is evident. The compounds in brackets in Scheme 32 are the target analogous precursor **109**, ketene **104** and isoquinolin-4-ol **28**. Therefore, precursor **109**, in theory, should readily generate ketene **104**, by a similar mechanism to that for the quinolones.

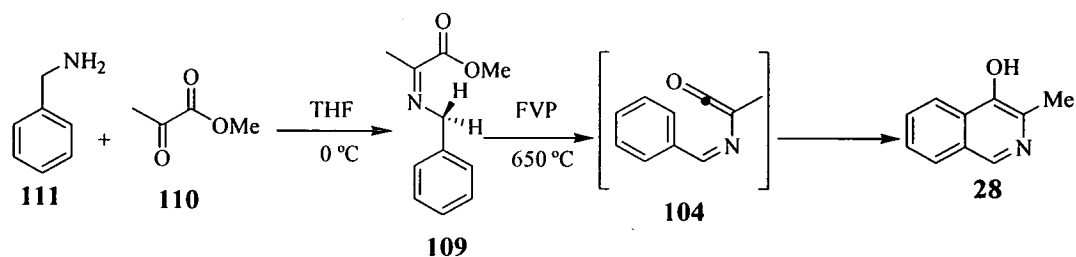


Scheme 32

Imine **109** was synthesised in 70% yield from the reaction between methyl pyruvate **110** and benzylamine, **111** but was found to contain impurities.⁶⁵ Signals in the ^1H NMR spectrum corresponding to **109**, were present at δ_{H} 2.2 ppm (CH_3), 3.8 ppm (OMe), 4.6 ppm (CH_2) and 7.3 ppm. The electron impact mass spectrum showed the correct mass m/z 191, and breakdown peaks of m/z 131 ($\text{M}-\text{CH}_3$)⁺ and m/z 91 PhCH_2^+ .

Reaction conditions were varied in an attempt to remove the impurities (~50% in crude material), including the use of activated molecular sieves, performing the reaction under nitrogen, and in different solvents. Each time however, an impure imine resulted. Prominent features of the impurity in the ^1H NMR spectra, included singlets at δ_{H} 3.8 ppm and 5 ppm, and a triplet at 4.2 ppm. Several recrystallisations reduced these peaks, but could not remove them completely (~15% impurity remained). Nevertheless, despite the impurities, several small scale pyrolyses were carried out. It was found that 3-methylisoquinolin-4-ol **28** was forming, but the NMR spectra were complex. The major problem associated with this synthesis was the poor volatility of the imine **109**; approximately half of **109** decomposed in the FVP inlet. The optimum temperature was found to be 650 °C, signals corresponding to the isoquinolin-4-ol **28** in the ^1H NMR spectrum were apparent, with the high frequency

singlet at δ_{H} 8.8 ppm (1-position), and doublets at δ_{H} 8.1 and 7.8 ppm. A preparative pyrolysis of 0.5 g of **109** was then carried out, resulting in complex NMR spectra, but signals due to **28** were clearly evident in the ^1H spectrum.

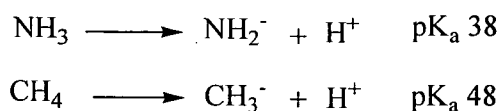


Scheme 33

The pyrolysate obtained after FVP gave a very messy ^1H NMR spectrum, and was (Kugelrohr) distilled to leave ~90 mg of material containing **28**. This mixture was then purified by dry-flash chromatography, from which 3-methylisoquinolin-4-ol **28** was obtained, with the ^1H NMR spectrum matching that in the literature, but in very low yield (3%).⁶⁶ No other products were identified, and the presence of bibenzyl which may be expected as a sideproduct, was not apparent, due to the lack of any signal in the ^1H NMR spectrum at δ_{H} 2.8 ppm. This gave proof that the strategy does work, to a certain extent, but is much less efficient than was expected compared with the corresponding reaction in Scheme 32 above.

The elimination of methanol from the precursor **106** requires the abstraction of a hydrogen atom from the nitrogen in the quinolone synthesis in Scheme 32, whereas abstraction of a hydrogen from a carbon is required in **109**. The difference in bond strengths is not a factor, as the CH bond strength in methane (105 kcal mol⁻¹) is less than the NH bond strength (108 kcal mol⁻¹) in ammonia,⁶⁷ which is the opposite of what would be expected if bond strength was playing a role.

A factor that is important is the difference in acidity between the C-H and N-H hydrogens, and is clearly having a major effect on the efficiency of ketene formation. This difference in acidity, shown in Scheme 34, is an order of magnitude of 10 greater for NH compared with CH, which may account for the difference in yield between the respective reactions, due to a more efficient generation of the ketene **107**.¹¹



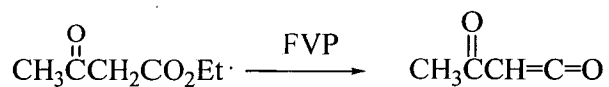
Scheme 34

Despite the low yield, it was clear that the synthesis of the isoquinolin-4-ol **33** was possible, using this strategy. The instability of the imine **109**, its impure nature, and the low acidity of the abstracted proton, all contributed to the low yields found. This route was therefore not pursued any further, and another more stable imine precursor was then sought to generate the same ketene **104**.

2.12.4 Imine precursor derived from benzaldehyde.

Scheme 35 shows work carried out on a β -keto ester under FVP conditions, which generates a ketene by the 1,2- elimination of ethanol.⁶⁴

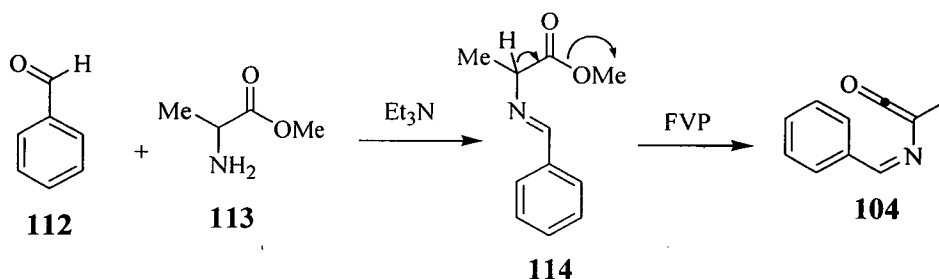
By analogy to the ester precursor in Scheme 35, another imine was obtained. The imine precursor **114** was synthesised as a yellow oil in 55% yield, from the reaction between benzaldehyde **112** and methyl alanate hydrochloride **113** with triethylamine in water.⁶⁸



Scheme 35

This imine, like that described above in Section 2.12.3, was not pure (~50% impurity was present containing some unreacted benzaldehyde), and was (Kugelrohr) distilled (~30% impurity remained). The imine **114** was identified by ¹H NMR spectroscopy on comparison with the literature.⁶⁹ A doublet at δ_{H} 1.50 ppm corresponding to the methyl group, a quartet at δ_{H} 4.1 ppm corresponding to the CH, a singlet at δ_{H} 3.6 ppm corresponding to CO₂Me, and a singlet at δ_{H} 8.1 ppm corresponding to CH=N, were all identified. The electron impact mass spectrum showed the correct mass, m/z 191 and a breakdown peak, m/z 91, corresponding to PhCH₂⁺. A 1,2-elimination of

methanol under FVP conditions should occur in principle to generate the ketene **104**, similarly to the elimination of ethanol in Scheme 35.



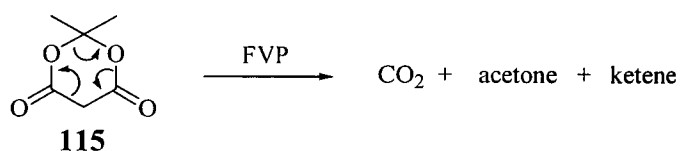
Scheme 36

Despite the impure nature of **114**, several small scale pyrolysis experiments were carried out, where the optimum temperature was found to be 600 °C. The ^1H NMR spectrum revealed a mixture of starting material, and very small amounts of the target isoquinolin-4-ol **28**.

At higher furnace temperatures the amount of starting material decreased, but the isoquinolin-4-ol peaks became even smaller in the ^1H spectrum, than those at 600 °C. For this reason, this route was not pursued any further. As with the result of the previous imine pyrolysis, this was greatly disappointing; this procedure is attractive in principle, since the benzene ring of the product would be derived in two steps from benzaldehyde, thus enabling easy derivatisation.

2.12.5 Methyl Meldrum's Acid Derivatives

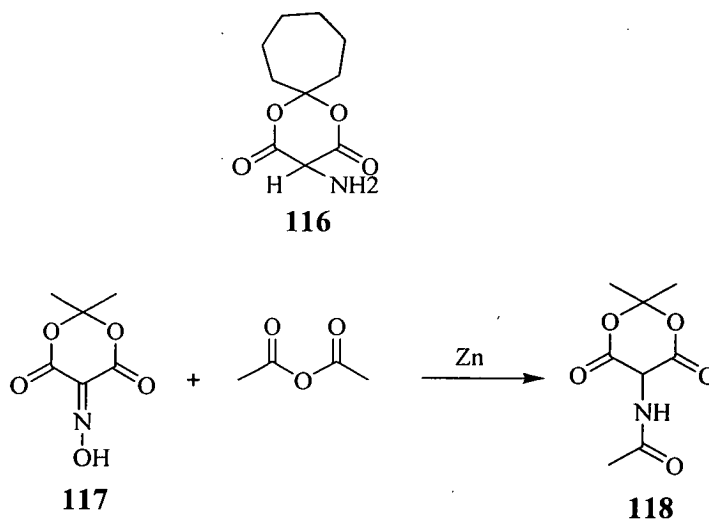
A well documented proven ketene generator, is the pyrolysis of Meldrum's acid **115** derivatives which was pioneered by R.F.C. Brown and F.W. Eastwood in the 1970s.⁷⁰ Such pyrolysis takes place by loss of acetone and carbon dioxide, to provide ketenes (Scheme 37).^{70,71}



Scheme 37

2.12.6 Synthesis of azo precursors.

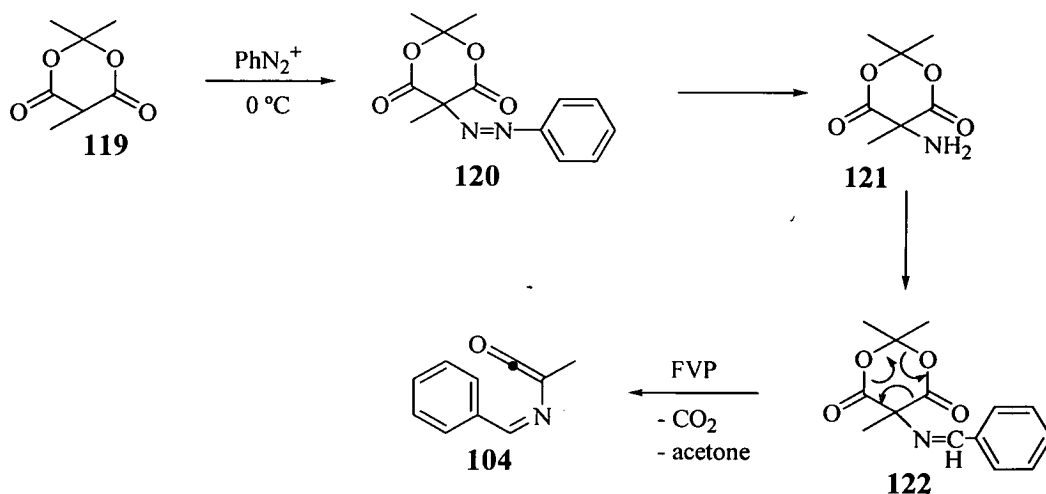
On inspection of the literature not many saturated 5-*N*-substituted Meldrum's acid derivatives are known. No 5-*N*-substituted methyl Meldrum's acid derivatives are known at all. Compound **116** on the other hand, has been reported in the literature, as has **118**, obtained from the reaction between the oxime **117** and acetic anhydride, in the presence of zinc.⁷²



Scheme 38

Due to the lack of literature routes to these derivatives, it was clear that a new methodology was required, which is outlined below in Scheme 39.

This new strategy to generate ketene **104**, utilised methyl Meldrum's acid **119** as the starting material; the methyl group is necessary to provide the 3-substituent of the isoquinolin-4-ol.



Scheme 39

This synthesis firstly involves a diazo coupling reaction of a benzenediazonium salt with methyl Meldrum's acid **119** to yield compound **120**.⁷² Reduction of the azo group in **120** would then give the amine **121**, which could condense with benzaldehyde to give **122**, and this compound would, in principle, generate the ketene **104**, under FVP conditions.

The first step in this sequence was the reaction of a diazonium salt, prepared by the standard textbook method, with a solution of methyl Meldrum's acid **119** in dilute sodium carbonate.⁷² This part of the reaction scheme worked very well, and compound **120** precipitated quickly in 76% yield. Further examples of azo methyl Meldrum's acid derivatives have been synthesised in high yield (see Figure 12).⁷³

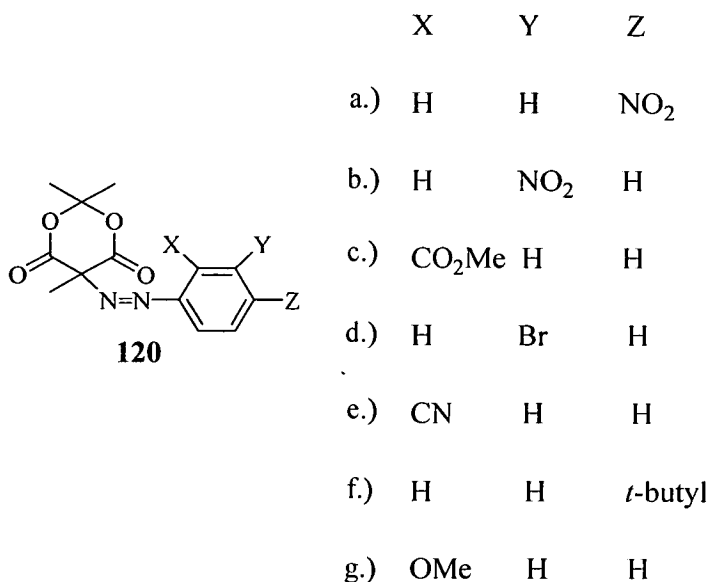


Figure 12 Methyl Meldrum's acid azo derivatives synthesised.

A crystal structure of **120g** was obtained and is shown below in Figure 14. Interesting features of this structure are the boat type conformation that the Meldrum's acid part of the molecule adopts, and the *syn* relationship between the azo and methyl group.

Not many examples of X-ray structures of compounds such as **120g** are known (generic structure: aliphatic-N=N-aromatic). One relevant example is **120h**, but was a poorly refined structure as shown by the e.s.d. values, and is therefore not used for comparison.⁷⁴

It can be seen from Figure 13 that the bond lengths of the Meldrum's acid moiety in **120g**, compare similarly to the bond lengths found in Meldrum's acid.⁷⁵

The C(9)-N(8) bond length [1.425(2) Å] in **120g** is significantly shorter than the C(5)-N(7) bond length [1.505(2) Å], probably due to the electron donating effect of the methoxy group, giving the C(9)-N(8) bond some double bond character. The C(9)-N(8) bond is also shorter than the C-N bond in azobenzene [1.452(3) Å].⁷⁶ The N=N bond length in **120g** [1.2259(19) Å] is shorter than that seen in azobenzene [1.243(3) Å].

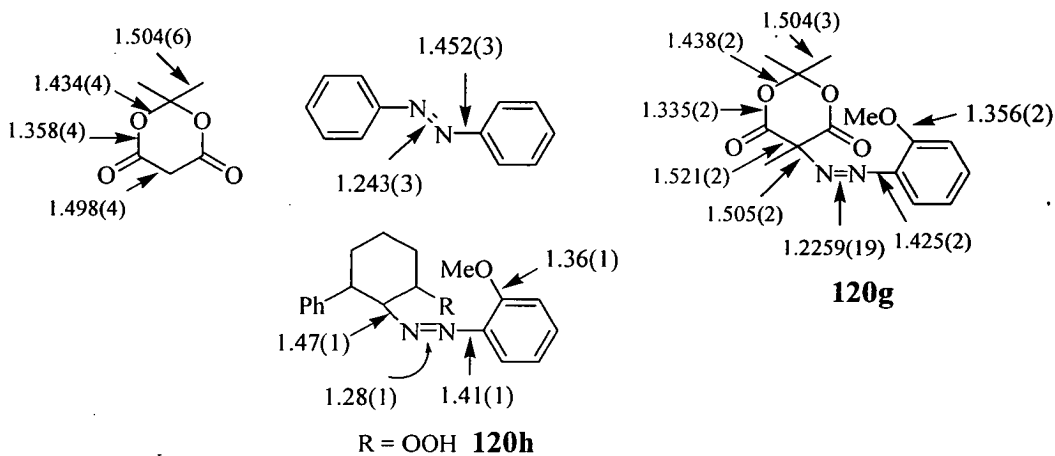


Figure 13 Comparison of bond lengths, in Å, between 120g, Meldrum's acid, azobenzene and 120h.

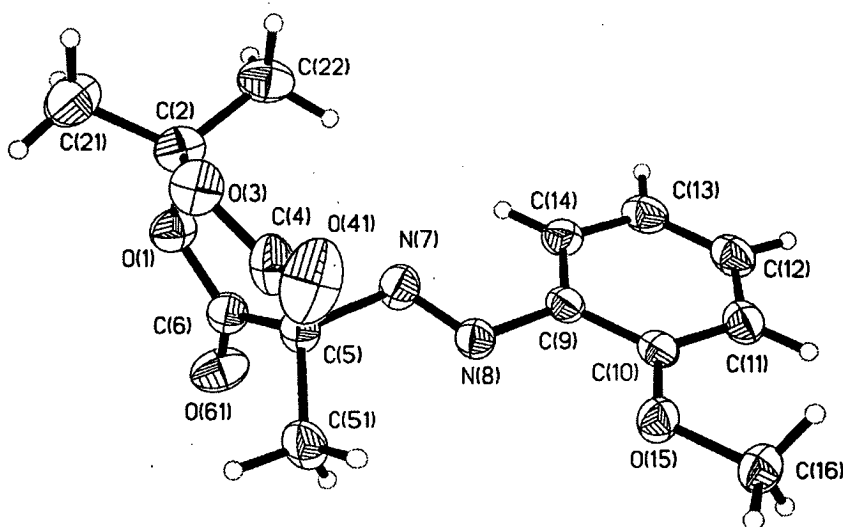


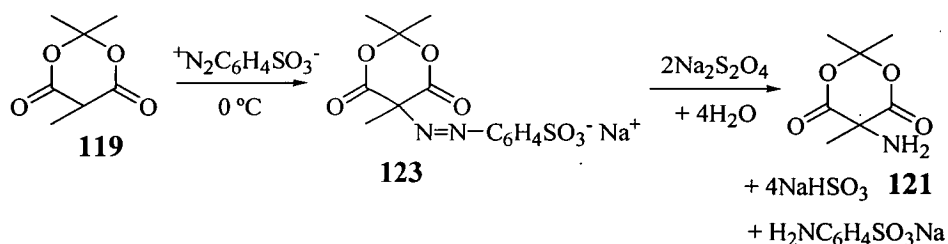
Figure 14 X-ray crystal structure of the azo Meldrum's acid derivative 120g.

2.12.7 Attempted reduction of azo group

The problematic part of this reaction sequence was the reduction of 120 to 121. The most appropriate conditions for this transformation appeared to be the catalytic hydrogenation of 120 using PtO₂ (Adam's catalyst), in toluene.⁷⁷ This was attempted at a pressure of 3 atmospheres and at atmospheric pressure, both at room temperature. Mostly starting material was found by ¹H NMR spectroscopy, in both

cases, although very small changes in the IR and ^1H NMR spectra could be seen for the experiment at 3 atmospheres. Perhaps higher pressures would be more successful, but at the time, no such apparatus was available. It was also unclear if the Meldrum's acid part of the molecule would be stable to hydrogenation at higher pressures.

Another attempt was made at this reduction using sodium hydrosulfite (Scheme 40), which is a standard literature method for the reduction of aromatic azo compounds.⁷⁸ Diazotisation was firstly carried out forming *p*-benzenediazonium sulfonate from sulfanilic acid, which was then coupled with methyl Meldrum's acid to give **123**. The expected precipitate did not form at this stage, but this was maybe due to the sulfonic acid group making the product too water soluble. Nevertheless, reduction was then attempted *in situ* using sodium hydrosulfite. Once again no precipitate formed, but the solution did change colour from a deep red to pale yellow, suggesting the reduction did take place, it may be that the amine product is too water soluble for precipitation to occur. Unfortunately, the amine was also not readily extractable into any organic solvents. The use of a less water soluble phenyl substituted compound may prove more successful.

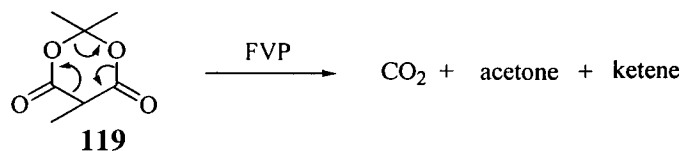


Scheme 40

Clearly more work will have to be carried out on this reaction to try to find suitable conditions for reduction to take place. Varying the conditions of the method above, or other methods maybe considered, such as using stannous chloride and hydrochloric acid, which has been reported previously in the reduction of azo compounds to amines.^{27,77,78} If a method to compound **121** could be found, then in principle, the rest of Scheme 40 should be straightforward for the generation of ketene **104**.

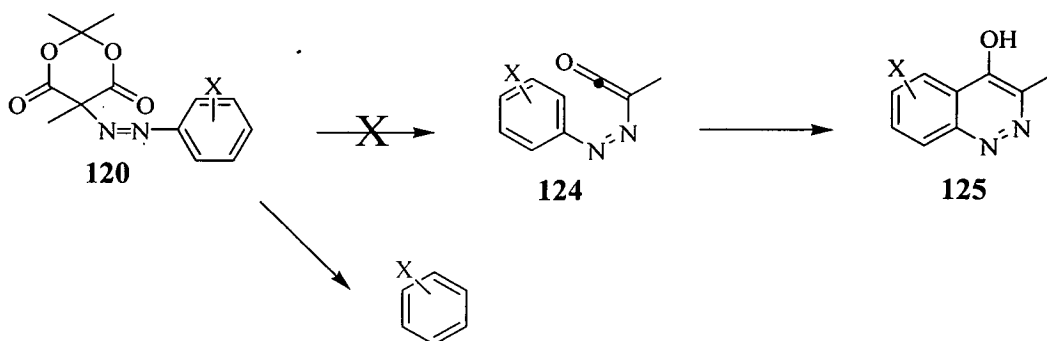
2.12.8 Pyrolysis of methyl Meldrum's acid derivatives.

As was briefly discussed in Section 2.12.5, the pyrolysis of Meldrum's acid derivatives are known to be highly efficient ketene generators. Scheme 41 shows a similar result from pyrolysis of methyl Meldrums acid derivatives.



Scheme 41

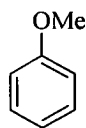
No pyrolyses of compounds such as those shown in Figure 12, have ever been carried out. An investigation into these reactions has been undertaken, where it was initially thought that ketene **124** would be generated, and therefore **125** would result as the product. Several small scale pyrolyses were first carried out on the parent compound **120**, with the temperature range studied from 450-900 °C.⁷³



Scheme 42

No starting material was found at any temperature, even at temperatures as low as 450 °C, which are considered to be very mild in FVP experiments. The expected product **125**, however, was not formed at all. Only very weak ¹H NMR signals were obtained, suggesting a volatile product. A less volatile product with substituents on the aromatic ring, was therefore sought after, in an attempt to identify the FVP products.

Pyrolysis of **120g** was then carried out, and again, no starting material was observed. A less volatile product was obtained than that observed from the above FVP experiment, and has been identified as anisole **126**.

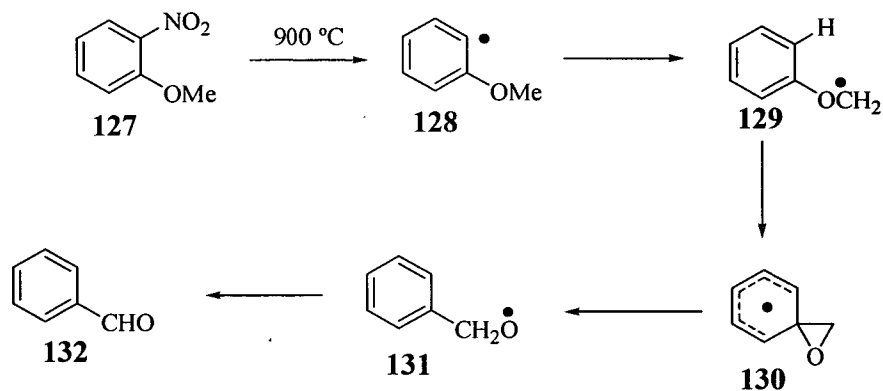


126

Pyrolyses of all the compounds shown in Figure 12 have been carried out at various temperatures, and every reaction gave only the reduced aromatic product. These products have all been characterised by $^1\text{H}/^{13}\text{C}$ NMR spectroscopy,⁵³ and mass spectroscopy. The azo compounds, however, were not particularly volatile, and all the FVP experiments were accompanied by a lot of decomposition of the starting material in the inlet tube (38-89%). As a result, yields are very low, and therefore, this is not a suitable general method for such reductions.

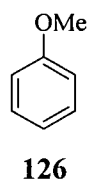
2.12.9 Mechanistic Studies

It was initially thought that phenyl radicals were being generated during this process. Scheme 43 shows a well known reaction in which *o*-methoxyphenyl radicals are generated under FVP conditions.⁷⁹ This Scheme involves the formation of a phenyl radical **128**, generated by the homolytic cleavage of the nitro group from **127**. A hydrogen shift then occurs to generate the β -radical **129**. This radical then attacks the benzene ring causing a rearrangement to give the spiro-intermediate **130**. The formation of the spiro-intermediate and subsequent re-opening to **131**, is known as the neophyl rearrangement, which in this case gave benzaldehyde **132** as the sole product.

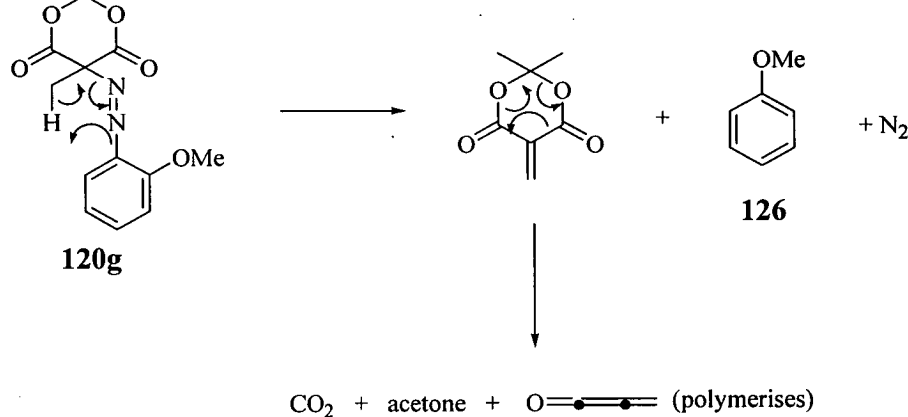


Scheme 43

As was discussed above, pyrolysis of the *o*-methoxy derivative **120g** gave anisole **126** as the major product. Only traces of benzaldehyde **132** were identified from the ^1H NMR spectra, with a very small singlet at δ_{H} 10 ppm apparent.



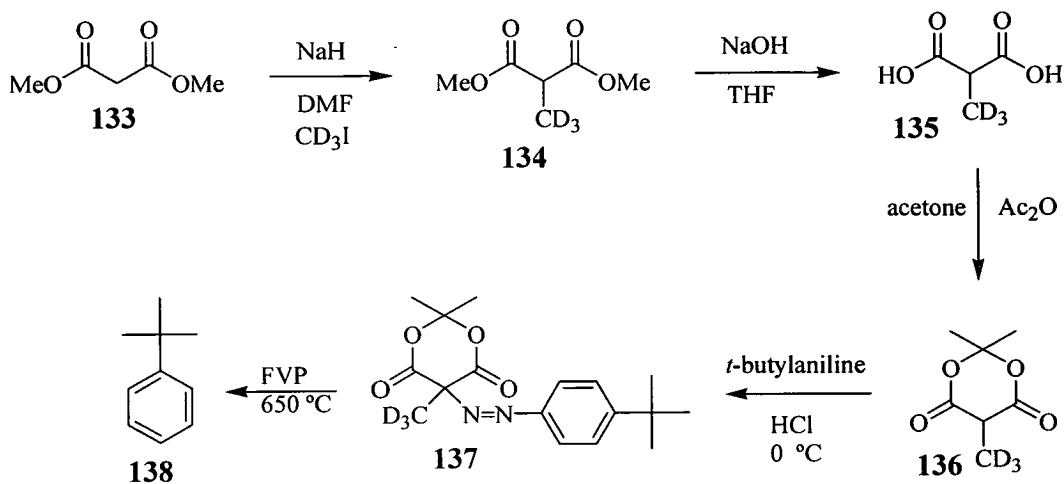
This suggests that phenyl radical intermediates are not being formed in this novel reduction of an azo group, (methods in the solution-phase for the reduction of diazonium salts are known *e.g.* hypophosphorous acid). Some other mechanism must be operating, and Scheme 44 shows a proposal based on the observations made during the experiment. There was a large pressure increase from 1×10^{-2} Torr to 1×10^0 Torr, which is consistent with the loss of nitrogen, and an insoluble polymer and acetone was formed in the U-tube. The mechanism in Scheme 44 involves the extraction of a hydrogen atom from the methyl group of the Meldrum's derivative **120g**, giving the products shown.



Scheme 44

2.12.10 Isotopic Labelling studies

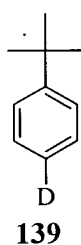
To investigate this reduction further, a study was carried out using a deuteriated azo derivative **137**, to try to provide support for the mechanism in Scheme 44. By replacing the protons in the methyl group at the 5-position of **120g**, with deuterium atoms, then if the mechanism above in Scheme 44 is operating, deuterium must be incorporated in the reduced product. The deuteriated derivative **137** was obtained by utilising the standard synthesis of Meldrum's acid, which firstly involved the reaction of dimethyl malonate **133** with deuteriated methyl iodide, to give **134**. This was then converted to **135** by sodium hydroxide, and the deuteriated methyl Meldrum's acid derivative **136** was obtained by reacting **135** with acetone and acetic anhydride. Compound **136** was synthesised and kindly provided by Miss Beeta Balali-Mood.⁸⁰ A standard diazo coupling reaction then followed between **136** and *t*-butylbenzene diazonium chloride, giving the azo compound **137**. *p*-*t*-Butylaniline was chosen as the reactant for the diazo component, due to the dispersed and easily identifiable signals in the ¹H NMR spectrum, obtained in the azo product. Therefore, if *t*-butylbenzene **138** was formed, then two triplets and a doublet would be observed.



Scheme 45

The deuteriated azo derivative **137** was pyrolysed at 650 °C, and similarly to the pyrolysis of the non-deuteriated derivative, the sole product obtained was *t*-butylbenzene **138**.

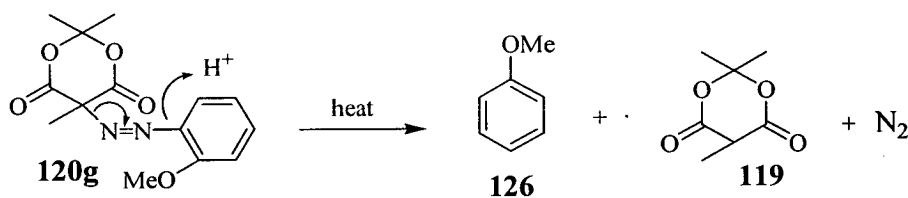
The ^1H NMR spectrum of the product from the pyrolysis was identical with that of an authentic sample of *t*-butylbenzene **138**. No incorporation of deuterium was found in the product, as the splitting pattern of a doublet at δ_{H} 7.44 ppm (2H), a triplet at δ_{H} 7.34 ppm (2H) and a triplet at δ_{H} 7.21 ppm (1H) was clearly seen in the ^1H NMR spectrum, which would have been very different if deuterium was present in the product.



The obvious place for deuterium to be incorporated, would be the *para* position, to give **139**, which would give two doublets in the ^1H NMR spectrum. Any small incorporation of deuterium at this position would result in a change in the triplet observed at δ_{H} 7.34 ppm. The appearance of a small doublet would be expected directly between the signals of the triplet. Very small signals corresponding to this doublet were observed, and from the integral, the level of incorporation of deuterium

could be estimated at less than 5%. The integral of the triplet observed at δ_{H} 7.21 ppm, would also be expected to decrease if deuterium was present, although it was not clear from the spectrum of this was the case, due to impurities present.

Finally, it was thought that perhaps this reduction was not in fact the product of an FVP reaction, but was taking place in the solid state inside the Kugelrohr oven. Another experiment was then carried out on the *o*-methoxy derivative **120g** to test this theory. This involved a slight modification of the standard FVP apparatus, where the U-tube trap was connected directly to the inlet Kugelrohr oven and not *via* the furnace. The substrate was simply heated in the inlet tube, and the product was collected as normal in the U-tube.



Scheme 46

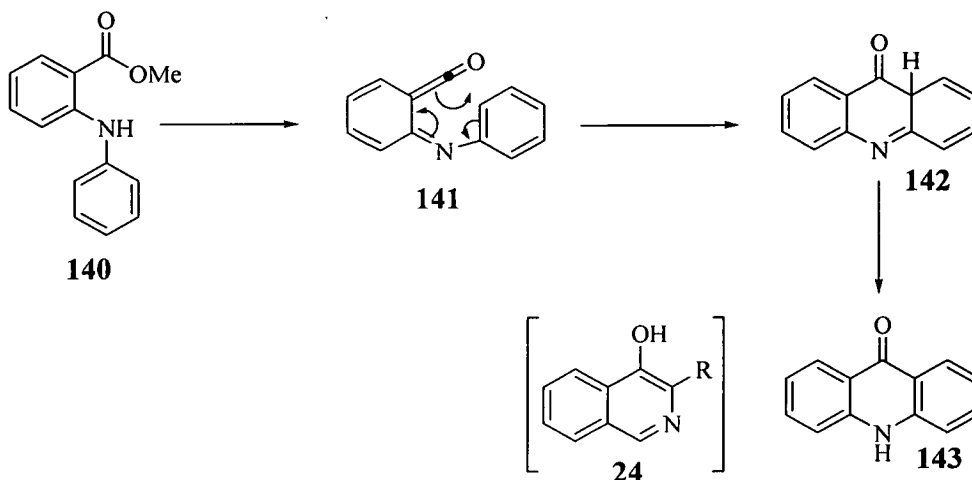
Two products were obtained from this reaction; the first was anisole **126** as before, and the second was methyl Meldrum's acid **119**. Both of the obtained products had ^1H and ^{13}C NMR spectra which closely matched those in the literature.⁵³ This showed that the reaction was in fact happening in the solid state (in the inlet tube) and not in the gas phase as previously thought (in the furnace). Methyl Meldrum's acid **119** survived due to the absence of the high furnace temperatures. Quite simply, the molecule upon exposure to heat is losing nitrogen and picking up a hydrogen atom from elsewhere. The source of the hydrogen atom is unclear. It has been shown above that it cannot be due to a radical process, or from the 5-methyl substituent. It may come from any water present in the sample, or possibly from one of the methyl groups at the 2-position. These results also explain the very mild pyrolysis conditions, and the low pyrolysis yields obtained.

The above route and those described in Sections 2.12.3 and 2.12.4, did not provide a high yielding synthesis of the target isoquinolin-4-ols, *via* ketene **104**. Generation of **104** was not efficient enough from the above precursors, and focus was therefore

switched to find a route to a different ketene **144**. Disconnection at b, as outlined in Scheme 31 above, would provide **144**.

2.12.11 Synthesis and pyrolysis of isoindolone precursors.

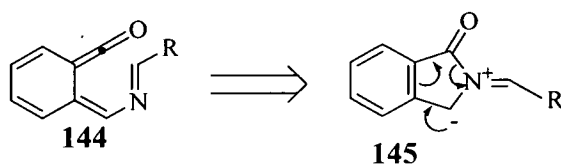
As has been discussed in Section 2.12.2, there are many literature reports on the generation of iminoketenes, as in the formation of acridones in Scheme 47.⁶⁴



Scheme 47

The iminoketene intermediate **141** was formed *via* the elimination of methanol from the precursor **140**, and after cyclisation, resulted in **142** which tautomerised to **143**.

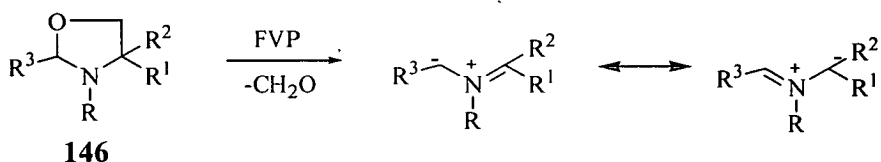
The acridone **143** is analogous to the desired isoquinolin-4-ol compounds, and initial work was therefore aimed at generating precursors which could generate the related iminoketene **144**, thus providing a potential route to the isoquinolin-4-ols.



Scheme 48

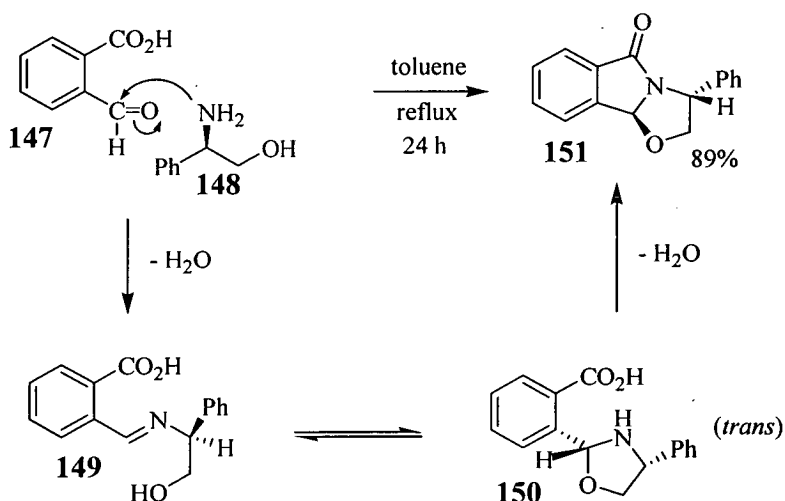
The ketene **144** is analogous to **141** (Scheme 48), and could be obtained from the azomethine ylide **145**. The synthesis of an appropriate precursor that would generate this intermediate was therefore desirable.

Joucla and co-workers have studied the generation of azomethine ylide intermediates from the pyrolysis of oxazolidines **146**, shown in Scheme 49.⁸¹ A precursor based on the oxazolidine structure was then synthesised, in an attempt to generate ketene **144**.



Scheme 49

The isoindolone **151** was synthesised in one high yielding step from 2-carboxybenzaldehyde **147** and *R*-phenylglycinol **148**.⁸² The initial reaction is attack at the aldehyde of **147** by the amine, forming a hydroxyimine **149**. Reversible cyclisation can then occur, by attack at either face of **149**, but only the *trans* isomer **150** (shown below in Scheme 50) is formed. Ring closure of **150** with loss of water, yields the more thermodynamically stable product **151**. The authors have proved the stereochemistry of the **151** by X-ray crystallography, and concluded that the functional groups in **149** are deemed to be too far apart for the *cis* isomer to form. Furthermore, no interconversion from the *trans* to the *cis* isomer occurred over a period of seven days. The product was identified by comparison with the literature NMR data.⁸³

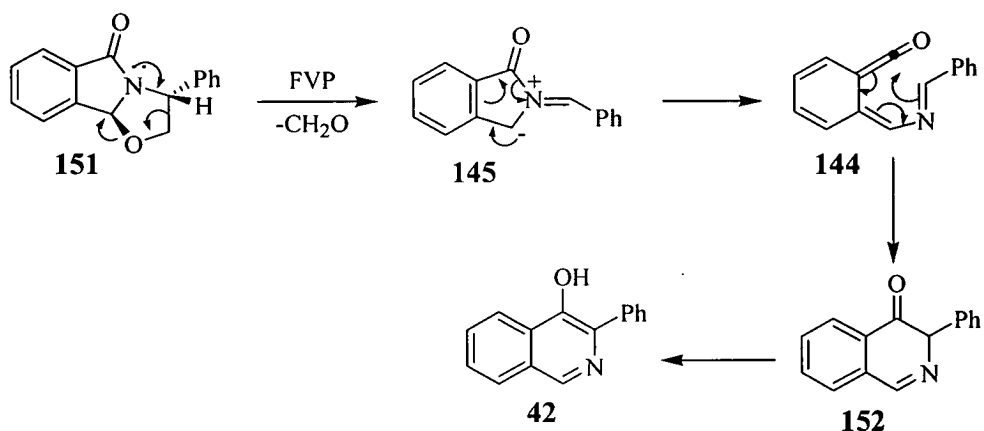


Scheme 50

The reactivity of **151** was then studied under FVP conditions at 650 °C, and the crude pyrolysate revealed peaks in the ¹H NMR spectrum corresponding to 3-phenylisoquinolin-4-ol **42**; the characteristic singlet at δ_{H} 8.81 ppm and a doublet at δ_{H} 8.20 ppm were evident. This proved that the synthesis of **42** was possible using this strategy, and several small scale pyrolyses (50 mg) were then carried out at 50 °C intervals (650-800 °C), to identify the optimum conditions for a preparative scale reaction.

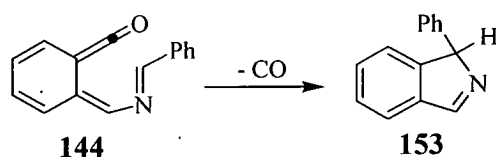
As well as the formation of **42** at 650 °C, the starting isoindolone **151**, was also present. It is commonplace in FVP to increase the furnace temperature if starting material is present, to convert this to product. By increasing the temperature, the starting material **151** gradually disappeared as expected, but this was also at the expense of the 3-phenylisoquinolin-4-ol **42**, with unidentified aromatic products being formed. At 800 °C, neither **151** nor the isoquinolin-4-ol **42** were present. The optimum temperature was identified as 650 °C, and a preparative pyrolysis of 0.5 g at this temperature was carried out. After dry-flash chromatography, isoquinolin-4-ol **42** was obtained in 20% yield (24% based on recovery of unreacted starting material), along with **151** in 21% yield. Much of the rest of the material was lost due to decomposition of the precursor in the FVP inlet (15-20%).

The initial step in this FVP reaction is a retro-1,3-dipolar cycloaddition of formaldehyde from **151** to generate the azomethine ylide intermediate **145**, similarly to that seen in Scheme 49 above. From this intermediate, the iminoketene **144** is formed, and cyclisation then affords the target isoquinolin-4-ol **42** from its tautomer **152**, as shown in Scheme 51.



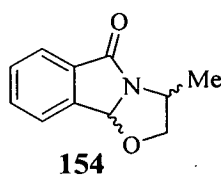
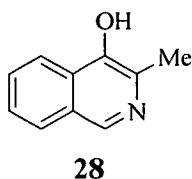
Scheme 51

As no isoquinolin-4-ol **42** was obtained at high temperatures, it was first thought that **42** itself was thermally unstable. However, pyrolysis of **42** at 650-850 °C showed that it was stable up to 850 °C, at which temperature it decomposed. The formation of such small quantities of **42** at temperatures greater than 650 °C, therefore may be accounted for by other possible pathways that intermediates **144**, **145** and **152** could take, leading to unidentified products. For example, ketene **144** may decarbonylate to give an unstable isoindole nucleus **153**.



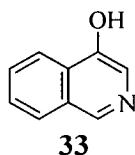
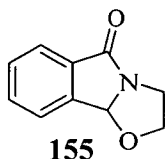
Scheme 52

Using the same strategy, the synthesis of 3-methylisoquinolin-4-ol **28** was attempted. The corresponding methyl substituted isoindolone **154** was firstly obtained by the same method as for the phenyl compound above, using *R,S*-2-aminopropanol as the starting material.

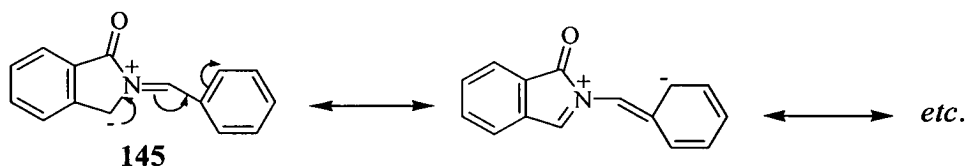


The ^{13}C and ^1H NMR spectra revealed a mixture of diastereomers of **154** in ~7:1 ratio, which was then subjected to FVP conditions as for the phenyl compound above. Unfortunately, only a small amount of isoquinolin-4-ol **28** could be detected in the ^1H NMR spectra of the crude pyrolysates. A singlet at δ_{H} 8.7 ppm was observed, corresponding to the 1-position, and a singlet at δ_{H} 2.5 ppm was observed, corresponding to the methyl group. A higher furnace temperature of 700 °C was required to form the ketene **144** than previously with the phenyl compound. This might be expected, since there is not the same stabilisation of the dipolar intermediate **145** by the methyl substituent compared with the phenyl group. However, the isoquinolin-4-ol **28** was not formed in sufficient amounts to warrant a preparative scale reaction.

To investigate the scope of this synthesis further, 2-carboxybenzaldehyde and ethanolamine were reacted as above to give an oil, and after dry-flash chromatography, gave **155** in 11% yield. After small scale pyrolysis (25 mg) experiments, 700 °C was found to be the optimum temperature, where starting material **155** was obtained along with very small amounts of isoquinolin-4-ol **33**.



From this experiment, and the attempted synthesis of **28**, it is clear that aryl substituents are required for a more efficient synthesis. As was said above, the aryl group can stabilise the dipolar intermediate **145**, as shown below in Scheme 53, which is not possible with the alkyl derivatives.

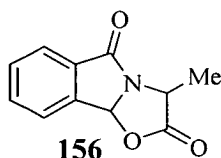


Scheme 53

The introduction of electron withdrawing groups to the aryl substituent such as nitro or nitrile, may help further. However, pyrolysis of **151** was accompanied by a significant amount of decomposition in the FVP inlet, and introduction of electron withdrawing groups may reduce the volatility of the precursors even further.

2.12.12 Other isoindolone precursors.

The above two-step synthesis of 3-substituted isoquinolin-4-ols from isoindolone precursors looked a very attractive route, as the isoquinolin-4-ol compounds were forming in only two steps. Precursors **151**, **154** and **155** all utilised formaldehyde as the thermal leaving group. It would be advantageous if a precursor, such as **156** could be obtained that had a better thermal leaving group, such as carbon dioxide. This may improve the efficiency of ketene formation, and subsequently improve the isoquinolin-4-ol yield.



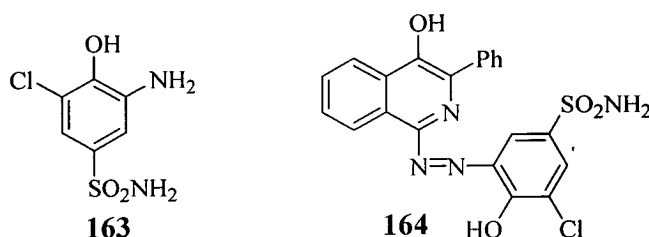
2.13 Synthesis of azo dye **164**.

Having devised a novel two step synthesis of 3-phenylisoquinolin-4-ol **42** (Section 2.12.11), the methodology developed was then used in the synthesis of a target azo cyan dye **164**. This involved a diazo coupling reaction of the sulfonamide **163** (see Section 2.13.1 for synthesis), which forms the diazonium component, and **42**.

3-Phenylisoquinolin-4-ol **42** is suitably activated to azo coupling at the 1-position by the OH group, with the phenyl group blocking any unwanted coupling at the 3-position. The sulfonamide **163** was reported in a patent as the diazo component of the 3-methyl substituted metallised analogue of **164**, which gave a desirable cyan hue.⁴⁷

Although this patent was not in reference to ink jet dyes, due to the good properties displayed by this dye, **164** was a novel and interesting synthetic target.

The ligand **164** would be reacted with nickel (II) acetate tetrahydrate, to produce a novel metallised cyan dye. The metallisation process can be followed by UV-Vis spectroscopy, as an increase in absorption intensity and shade (λ_{\max}) is expected in going from the ligand to the metallised material.



2.13.1 Preparation of 3-phenylisoquinolin-4-ol **42**

Using the FVP method from Section 2.13.1, the first stage in the synthesis of the azo dye, was to produce 0.5 g of 3-phenylisoquinolin-4-ol **42**. As this method proceeded only in 20% yield, several repeats of the initial reaction to synthesise the isoindolone precursor **151** were required. This was followed by ten preparative pyrolyses (0.5 g) of **151**, producing 3.4 g of crude pyrolysate, which was purified by two dry-flash columns, providing over 0.5 g of 3-phenylisoquinolin-4-ol **42**.

2.13.2 Synthesis of 2-Amino-6-chloro-4-sulfamidophenol **163**

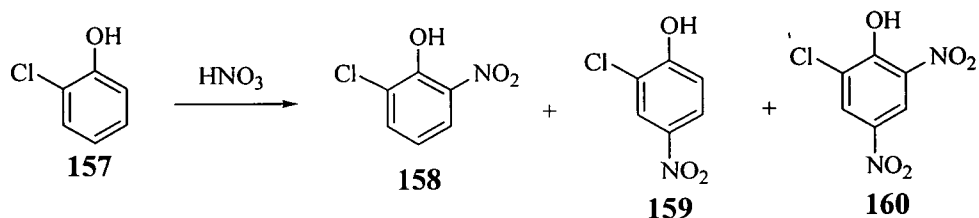
An unpublished route provided by Avecia was followed for the synthesis of the sulfonamide **163**.⁸⁴

2.13.2.1 6-Chloro-2-nitrophenol **158**

The first step in this synthesis was the nitration of 2-chlorophenol **157**, by reaction with nitric acid on a 250 g scale. A very dark solid resulted which was a mixture of the nitration products **158**, **159** and **160** shown in Scheme 54, which were identified by ¹H NMR spectroscopy. An approximate 2:4:1 ratio of **158** to **159** to **160** was found from the crude ¹H NMR spectrum. A nitration pattern such as this is to be

expected due to the strong *o/p* directing effect of the OH group. Compound **159** is the major isomer due to the lack of any steric interactions.

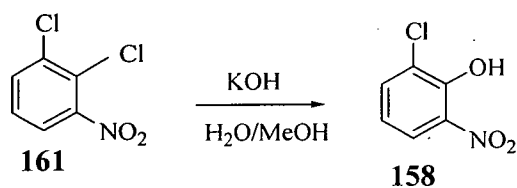
When this mixture was steam distilled for four days, **158** crystallised out of the cold distillate as a yellow solid, leaving behind 133 g of the mixture of the two other nitration products **159** and **160**. Attempts were made to separate **159** and **160** by crystallisation, but without success.



Scheme 54

The steam distillation step worked very well, giving 83 g of **158** in high purity (25% yield) for subsequent reactions. This compound has been reported in the literature, and the ¹H NMR spectrum obtained matched this well.⁸⁵ The same authors reported a different method for the synthesis of **158**, which was claimed to be quicker and higher yielding, avoiding the time consuming steam distillation step, and is shown in Scheme 55. A yield of 58% was reported, by refluxing the readily available 1,2-dichloro-3-nitrobenzene **161**, in a mixture of two equivalents of potassium hydroxide and 1:1 methanol/ water mixture, for 43 hours.

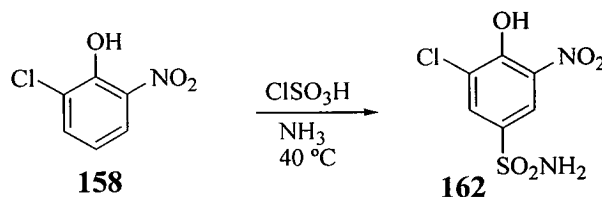
It was also said that the unreacted starting material obtained from this reaction, can be easily separated from the product, and taking this into account, the yield is almost quantitative.



Scheme 55

2.13.2.2 6-Chloro-2-nitro-4-sulfonamidophenol 162

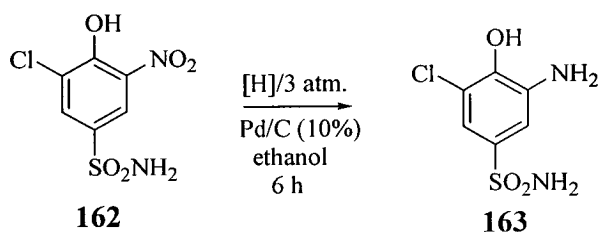
6-Chloro-2-nitrophenol **158** was reacted with chlorosulfonic acid to yield a sulfonyl chloride intermediate, which was quenched with ammonia to give the sulfonamide **162** as a dark solid. Once again the directing effects (OH strongly *para* directing in this case) are such that this is the only expected product. ^1H NMR spectroscopy revealed a very simple spectrum, with a doublet (4J 2.2 Hz) for each of the two aromatic ring protons.



Scheme 56

2.13.3.3 2-Amino-6-chloro-4-sulfonamidophenol 163

The final step in the synthesis was the reduction of the nitro group. This was done by a simple catalytic hydrogenation of **162** (10% Pd/C) at a pressure of 3 atmospheres, at room temperature, for 6 hours.⁸⁶ A dark solid **163** resulted which contained some impurities, giving a different melting point to that in the Avecia procedure. This product was then purified by dry-flash chromatography, giving a dark brown solid in 87% yield, and the melting point matched that previously quoted.⁸⁴



Scheme 57

The ^1H NMR spectrum of the reduced compound **163** showed two doublets still present but shifted to lower frequency. A broad singlet was also apparent at 7.15 ppm, corresponding to the amino group. This procedure differed and improved upon

that in the Avecia procedure, which used sodium sulfide as the reducing agent at 100-105 °C, giving a 62% yield.⁸⁴

2.13.4 Coupling reactions of 3-phenylisoquinolin-4-ol **42**.

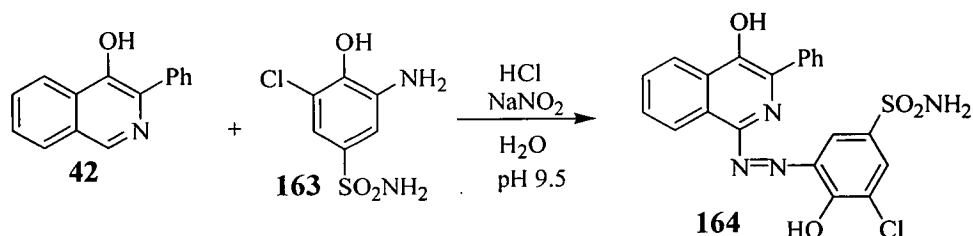
A pilot reaction under standard azo coupling conditions, was done on a small scale (0.2 mmol), following an Avecia procedure, in which the diazonium salt of sulphonamide **163** was reacted with a basic solution of 3-phenylisoquinolin-4-ol **42**.⁸⁷ A dark blue precipitate resulted, and FAB mass spectroscopy revealed a small peak due to the expected product m/z 455 [(MH⁺, 4.5%), and no peak corresponding to the starting isoquinolin-4-ol **42** was seen. The ¹H NMR spectrum showed the characteristic singlet at 8.81 ppm corresponding to the proton at the 1-position, indicating that coupling was incomplete. This solid was identified as a 3:2 mixture of isoquinolin-4-ol **42** to the azo **164** by HPLC.

A similar result was obtained from the reaction between 3-phenylisoquinolin-4-ol **42**, and the diazonium salt derived from *p*-toluidine, indicating that coupling to 3-phenylisoquinolin-4-ol **42** required optimisation. This optimisation was successfully achieved at Avecia where better control of the conditions, particularly pH, and monitoring of the reaction was available. Under standard coupling conditions, it is normally unnecessary to closely monitor the pH.

It was not clear from the trial experiment above, whether it was the diazotisation of **163**, the diazo coupling reaction, or both, that was the problem in this synthesis. However, diazotisation of **163** was observed to occur quickly and readily by HPLC monitoring.

The diazonium salt was added dropwise over 1 hour to a solution of the isoquinolin-4-ol **42** solution at pH 7.5, but HPLC indicated that no reaction was occurring. The pH was raised to 9.5, and the solution became blue in colour; HPLC showed that slow conversion to the product was occurring. This solution was left to stir overnight at room temperature, and a high conversion to **164** was found (92% by HPLC) the next morning. Due to the dilute conditions, only a small amount of precipitate had formed, and some of the solvent had to be evaporated; after dropping the pH to 3 a precipitate was obtained. This reaction was done on a 0.75 mmol scale, which would ideally require about 1-2 cm³ of solvent for highly concentrated conditions, but such

a small amount of solvent is not practical, especially when removing samples for HPLC analysis *etc.* To monitor the pH of the solution, and the reaction by HPLC, an amount of solvent which is greater than ideal is added, which made the conditions far too dilute by a factor of 10. These dilute conditions also contributed to the slow rate of coupling, and make the isolation of any product more difficult, especially when a water soluble species is being formed. This type of problem has occurred several times (see Section 2.25.6 and 2.28).



Scheme 58

2.13.5 Metallisation of 164

As has been discussed in Section 1.23, one way to counteract poor light fastness properties is by the formation of metallised complexes. The azo compound **164** gives cyan shades in solution, and was metallised using nickel (II) acetate tetrahydrate, which was used for all the forthcoming metallisations. Nickel is the metal most commonly used in ink jet dye synthesis, and was also used in the patent described above, although other metals such as copper and cobalt have been used. The metallisation process was followed on a very small scale (2 mg of **164** in 100 cm³ water) by UV-Vis spectroscopy. The ligand **164** gave a broad symmetrical curve of low intensity, (Figure 15), and a λ_{max} value of 619 nm and a half-band width of 137 nm was observed. One equivalent of nickel (II) was added to the ligand solution, and the UV-Vis spectrum was recorded immediately. The solution became more blue in colour and a different shaped curve was observed. The curve now had a double peak of greater intensity than that of the ligand, and at a higher wavelength. The more intense peak was at the higher wavelength of 637 nm, which showed the characteristic increase in λ_{max} in transforming the free ligand into the metallised complex. This increase in wavelength was only 18 nm, which is quite small in

comparison to those observed later in the indazole/naphthol series, where shifts of up to 80 nm were observed. This smaller increase in λ_{max} is considered to be advantageous, as too large an increase makes predicting the dye shade very difficult. The intensity of the absorption also increased; the extinction coefficient of the ligand was $15\,700\text{ l mol}^{-1}\text{ cm}^{-1}$, compared with the metallised complex at $25\,600\text{ l mol}^{-1}\text{ cm}^{-1}$. An increase in intensity is normally accompanied by a narrower sharper curve, and the metallised complex gave a half-band width of 100 nm, which is considered to be a good figure. Other points to note were that the relatively steep high wavelength end of the curve showed no secondary absorptions, which are undesirable, as they tend to give duller shades. This observed λ_{max} was perhaps too low, as an ideal cyan would be around 650 nm, and the data in the patent for the analogous 3-methyl substituted dye was around this figure.

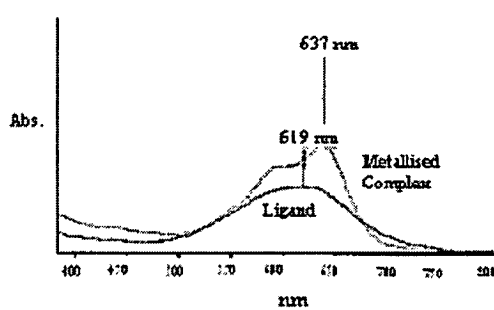


Figure 15 UV-Vis curves obtained for ligand **164** and metallised complex.

An industrial standard metallised azo cyan dye was then studied by UV-Vis spectroscopy for comparison. The spectrum obtained for **164** and its metallised complex compared favourably with the spectrum obtained for the industrial compound. The standard cyan dye also gave a double peak, but with the lower wavelength peak the more intense at 616 nm. The less intense peak at higher wavelength was absorbing well over the 650 nm mark, and a balance of the two peaks gave the desired cyan colour. The half-band widths were 100 nm and 106 nm for **164** and the industrial compound respectively.

Due to the success of this trial metallisation, the remaining ligand **164** (180 mg) was then metallised. The ligand was dissolved in deionised water, and the pH was adjusted to 7. A solution of nickel (II) acetate tetrahydrate (1 eq.) was then added, resulting in a dark blue solution. The pH had to be readjusted to 7, and the solution was stirred for 45 minutes. The UV-Vis spectrum was recorded again at this point, to see if it matched that previously obtained. This showed the metallisation to be successful and the solution was then heated in an oven at 40 °C until all the solvent had evaporated (~2 days), which is the industrial method for isolating the complexes, resulting in 180 mg of the metallised complex.

This material (180 mg) was then sent to Avecia for high through-put testing, but unfortunately, it has proven to be too insoluble for this purpose. Unsurprisingly, this complex is not significantly water soluble, as there are no sulfonic acid groups present. It was a synthetic target however, due to the excellent properties that the analogous 3-methyl substituted compound displayed in the patent described above. Further derivatisation to improve the water solubility would be necessary for dyes derived from **164** to be useful for ink jet applications.

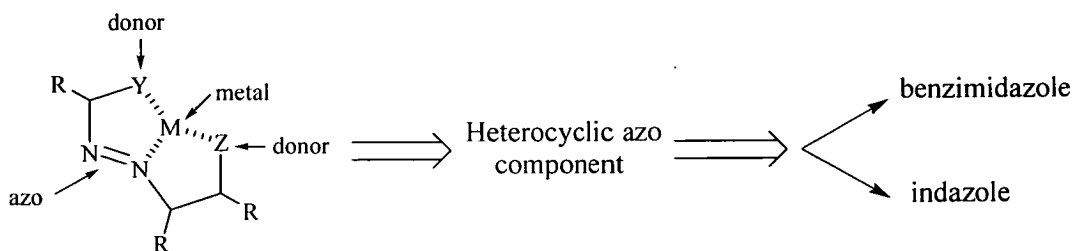
2.14 Conclusions

Two different methods have been used to synthesise 3-substituted isoquinolin-4-ols. By close inspection of the literature, a route was found to 3-substituted isoquinolin-4-ols by means of a rearrangement of isoquinoline *N*-oxide **29** with *p*-toluenesulfonyl chloride. Subsequent hydrolysis of the tosylate **32** afforded isoquinolin-4-ol **33** which was functionalised at the 3-position by means of the Mannich reaction and bromination. A similar rearrangement and hydrolysis from 3-methylisoquinoline provided a functionalised isoquinolin-4-ol **28** in only three steps. FVP methods have also been used providing a novel two step synthesis of 3-phenylisoquinolin-4-ol **42**, and although the yield of 20% was disappointing, the route was as good as anything previously in the literature, considering that the first step proceeds in 90% yield. Several other precursors were synthesised in an a similar effort to provide a high yielding route to the isoquinolin-4-ols, with the methyl Meldrum's acid derivatives **120** providing an unexpected novel reduction of the azo group.

The FVP methodology was successfully applied to provide the 3-phenylisoquinolin-4-ol **42** as the coupler component used in the azo coupling reaction, which gave the novel azo compound **164**. The synthesis of a metallised complex of this novel azo compound was also successfully carried out.

2.15 3-Diazo-3*H*-indazole derivatives and reactions

As has been discussed earlier in Section 1.21, many heterocycles are now used in ink jet dye synthesis. This part of the project was focused on the production of new classes of heterocyclic azo dyes, while keeping the typical generic structure shown below in mind, as the possibility of coordination to a metal is essential.



Inspection of the literature revealed that dyes derived from indazole and benzimidazole structures are not common; both of which fit the criteria above.

A detailed review of the literature is offered below (Sections 2.15 to 2.20), where the synthesis and reactivity of diazoindazole **170** is discussed. Sections 2.21 to 2.22 briefly outlines the literature syntheses of benzimidazole azo systems. The remainder of the Section (2.23 to 2.33) discusses the new research carried out.

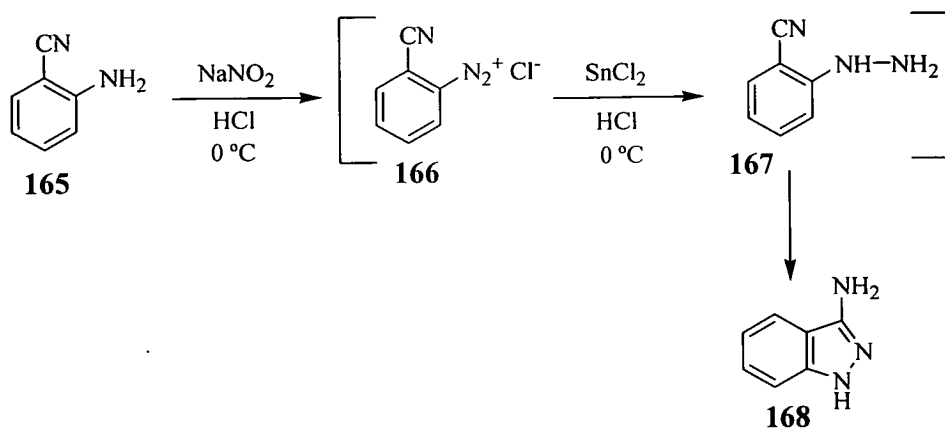
2.16 3-Diazo-3*H*-indazole

3-Diazo-3*H*-indazole **170** has long been known in the literature,⁸⁸ and was in fact the very first heterocyclic diazo compound reported.⁸⁹ Diazoindazole **170** itself has been used as a starting point for many syntheses, including the formation of azo compounds. The synthesis and reactivity of diazoindazole and several of its analogues are discussed below.

2.16.1 Synthesis of 3-Diazo-3*H*-indazole

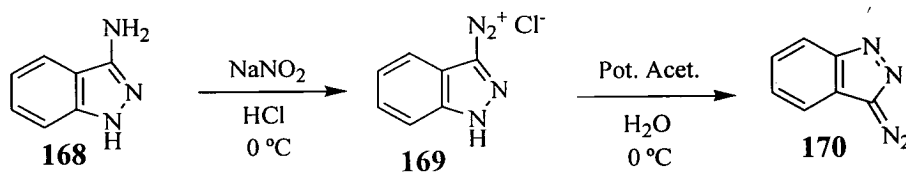
The preparation of 3-diazoindazole **170** firstly requires the synthesis of 3-aminoindazole **168**, which has been known in the literature since 1899.⁹⁰ Diazotisation of *o*-aminobenzonitrile **165**, under standard aqueous conditions is first carried out, and the diazonium salt **166** formed is reduced to the hydrazine **167** by

either zinc or tin chloride, to give 3-aminoindazole **168** after *in situ* cyclisation. The best literature yield found was 43%.⁸⁹

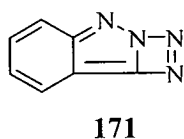


Scheme 59

3-Aminoindazole **168** readily forms its diazonium salt **169** under standard aqueous conditions, and after treatment with base, yields diazoindazole **170** as a stable solid. This reaction proceeds typically in around 90% yield.⁸⁸



Scheme 60



The original author in 1899, Bamberger, proposed the structure as that of indazolotriazolene **171**, but the diazo structure **170** was postulated a few years later.⁸⁹

Since then, the structure has been partly identified by IR spectroscopy, with a typical N=N absorption band observed at 2119 cm^{-1} , characteristic of diazo compounds. Further evidence for the diazo structure **170** was obtained by firstly reacting it in non-aqueous coupling reactions to give azo compounds, and also replacing the diazo group with halogens, both of which are not possible with **171**.⁸⁹ A crystal structure has since been obtained for diazoindazole **170**, which was a target for the authors due to the lack of data on such compounds in the literature.⁹¹

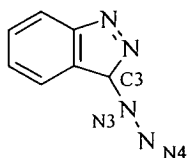
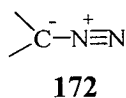


Figure 15 The numbering system used in the X-Ray analysis of diazoindazole.

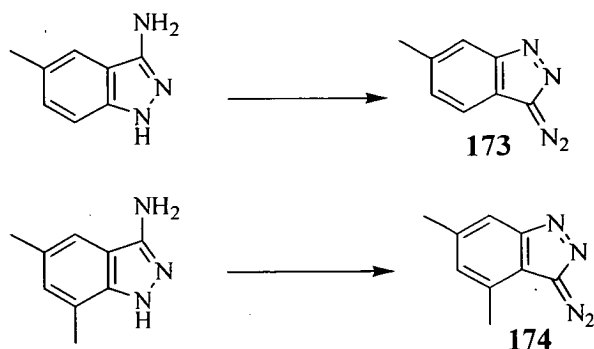
The indazole part of the molecule was found to be planar, and bond distances of C(3)-N(3) [$1.338(3)\text{ \AA}$] and N(3)-N(4) [$1.110(3)\text{ \AA}$] were found. The short C(3)-N(3) (*c.f.* average C-N bond length of 1.40 \AA in diazo compounds) and N(3)-N(4) bond lengths, suggests substantial carbanionic dipolar character of the azo group, as shown in **172**.



The other bond lengths were found to be intermediate between double and single bonds, indicating the presence of considerable conjugation in the molecule.

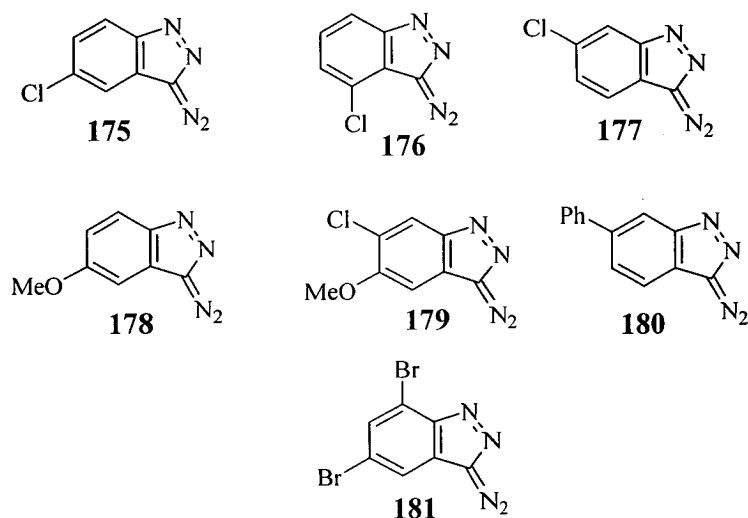
2.17 Standard synthesis of diazoindazole derivatives

Various derivatives of diazoindazole **170** have been synthesised using the same standard method as for the parent compound above, from the appropriately substituted amine. Bamberger first demonstrated this with the synthesis of the two alkyl derivatives **173** and **174** below. However, no further reactions have been carried out with these compounds.



Scheme 61

Further derivatives have since been made in a similar fashion, with electron withdrawing/donating groups and a phenyl group introduced at positions 4, 5 and 6.^{92,93} Again, the reactivity of these compounds has not been studied.



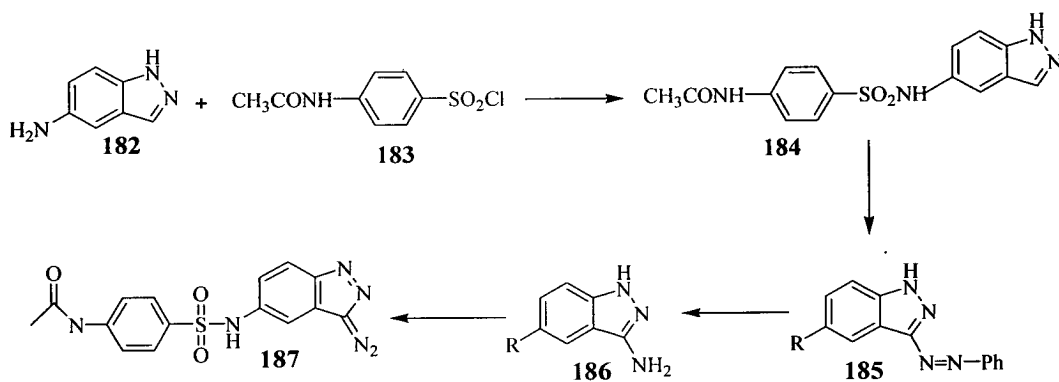
The N=N infra-red absorptions characteristically range from 2120 cm^{-1} to 2140 cm^{-1} for these diazo compounds. UV-Vis spectra have also been recorded, with the λ_{max} values ranging from 352 to 364 nm and the extinction coefficient values ranging from 6400 to 8000.

The use of stabilised diazonium salts is well known in photocopying; compounds **180** and **181**, have found use in this area as lithographic sensitisers.⁹³ The photodecomposition products of the light sensitive diazo compounds are highly

water resistant and ink receptive.⁹⁴ Diazo compounds are now used in some cases in place of diazonium salts in the manufacture of photographic material.⁹⁵

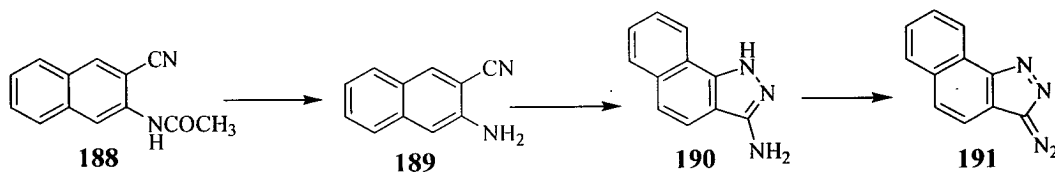
2.18 Other syntheses of diazoindazole derivatives

The synthesis of derivative **187** involved a six step synthesis from indazole, which was first nitrated at the 5-position, and then reduced to 5-aminoindazole **182**.⁹³ The resulting amine was reacted with *p*-acetamidebenzenesulfonyl chloride **183** to give **184**, which underwent diazo coupling at the 3-position with benzenediazonium chloride to give **185**. The azo group was then reduced to the amine **186** with sodium dithionite, which was subsequently diazotised and treated with base, to afford the diazo compound **187**.



Scheme 62

An indazole derivative **191** with a further fused aromatic ring has been synthesised.⁹⁴ The first step in the synthesis of 3-diazo-3*H*-benzo[*g*]indazole **191**, was the deacetylation of 2-acetamido-1-naphthonitrile **188**, with sodium hydroxide in aqueous isopropyl alcohol, to 2-amino-1-naphthonitrile **189**.



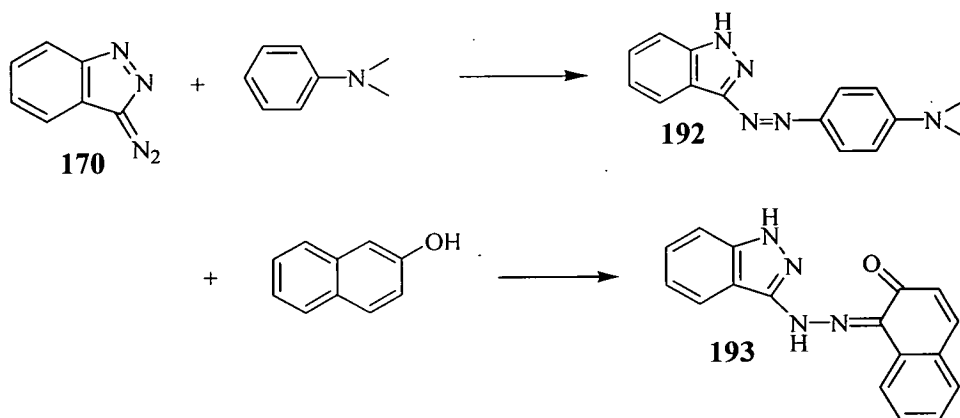
Scheme 63

Diazotisation of **189**, followed by reductive cyclisation with tin (II) chloride, gave 1*H*-benzo[*g*]indazol-3-ylamine **190**. The target diazo compound **191** was then obtained by further diazotisation and addition of base.⁹³

2.19 Reactions of diazoindazole and derivatives

2.19.1 Azo Coupling

Diazoindazole **170** readily undergoes non-aqueous coupling reactions to form azo compounds. Bamberger was the first to demonstrate this reaction by coupling to dimethylaniline and β -naphthol, to give **192** and **193**.⁸⁸

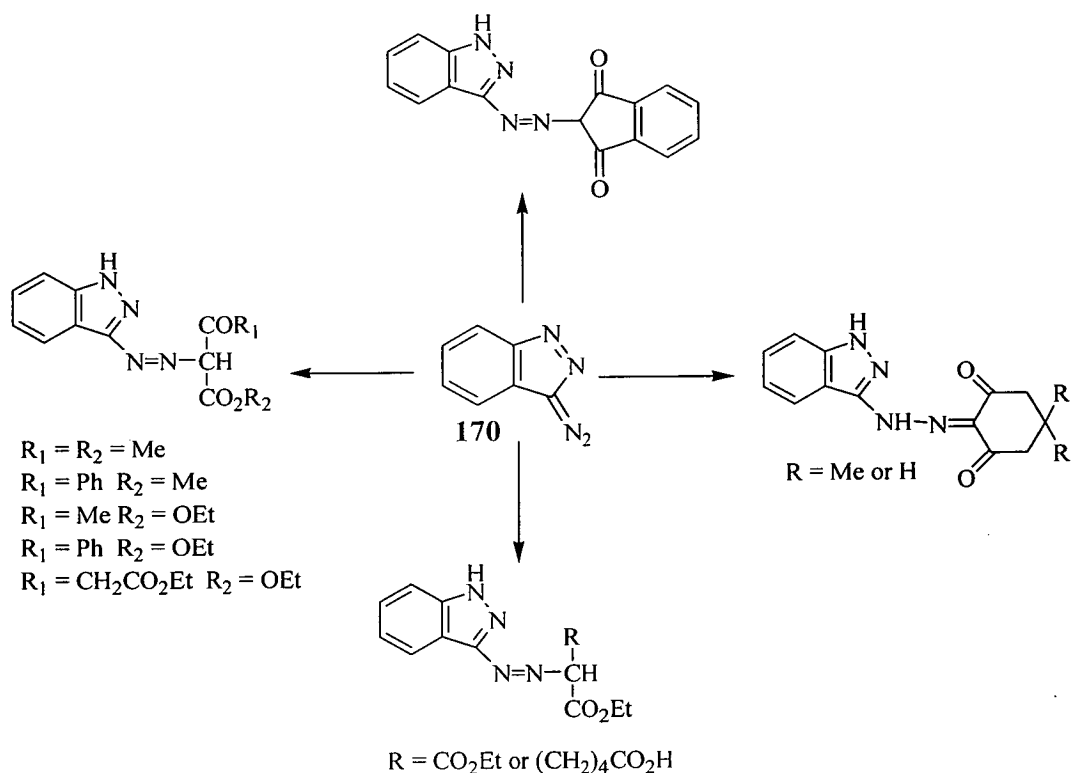


Scheme 64

Despite this high reactivity and ability to form azo compounds, not much work has been done in this area since. One publication however, has reported several other similar reactions, as shown below in Scheme 65, where diazoindazole was coupled to 1,3-diketones, β -ketoesters, cyclic β -diketones and diethyl malonate.⁸⁹ This reaction involved an ethanolic solution of diazoindazole being treated with the appropriate coupling component at room temperature, then filtering off and crystallising the resulting precipitate, with yields ranging from 55-90%.

The structures drawn below in Scheme 65 are as reported, but there is always the possibility that such structures can be drawn in either the azo or hydrazone form, and the carbonyl group can be written in the keto or enol form. No attempt was made

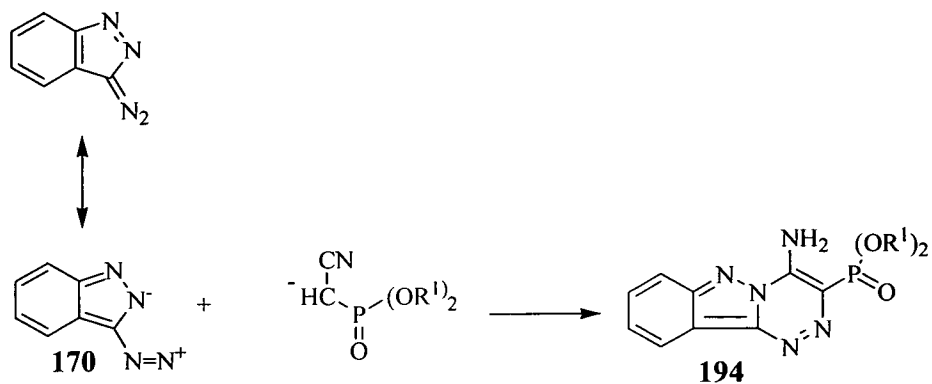
however, to examine the structures of these products in detail, but it was postulated that the hydrazone form dominates when coupling takes place at a methyl or methylene carbon, (as in Scheme 65), based on previous reports.



Scheme 65

2.19.2 Cyclisation reactions

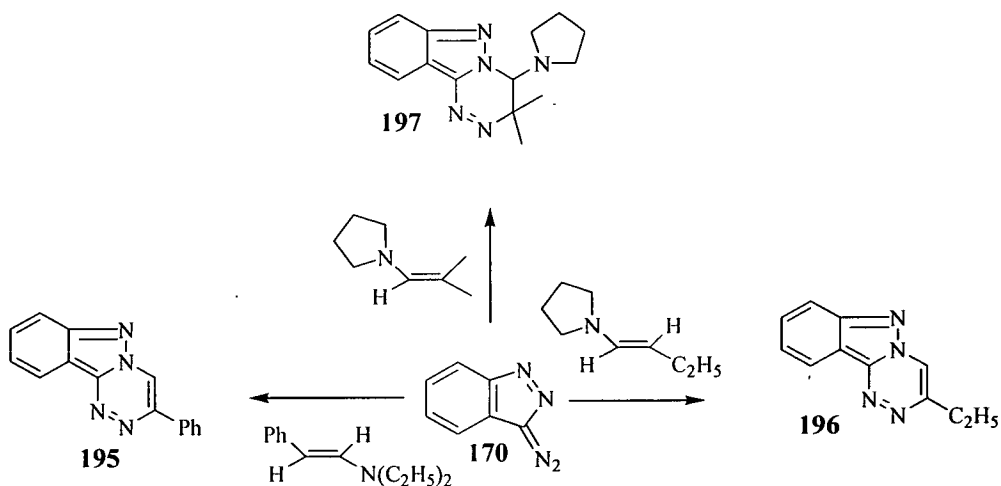
Organic phosphorus compounds, like phosphono derivatives, are active against osteoporosis and can function as antibiotics.⁹⁶ Phosphonato substituents have been introduced to the 3-position in simple cyclisation reactions, using diazoindazole and phosphonoacetic acid derivatives, an example of which, **194**, is shown in Scheme 66. Other phosphonoacetic acid derivatives have been used, where aromatic ketones and esters replaced the nitrile group that is shown in Scheme 66.



Scheme 66

2.19.3 Cycloaddition reactions

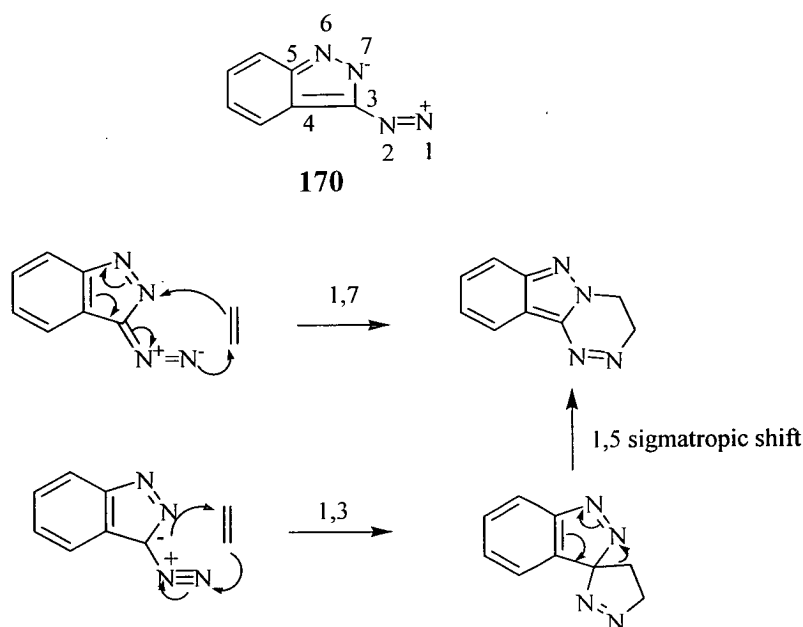
Diazoindazole has been shown to undergo cycloaddition reactions with electron rich olefins in excellent yields, giving triazinoindazoles.^{97,98} These products arise from cycloaddition on to the nitrogen atom immediately flanking the diazoalkane moiety. In **195** and **196**, the final products have been formed due to elimination of the tertiary amine moiety, whereas in **197**, the presence of the methyl substituents have prevented any elimination occurring.



Scheme 67

Such products could arise from two different pathways, one being a 1,7 union ($8+2$) π e^- of the dipole and dipolarophile, but equally as likely is an initial 1,3 cycloaddition followed by a 1,5 sigmatropic shift. The 1,7 and 1,3 nomenclature of these cycloadditions, refers to **170** acting as either a 1,7 or 1,3 dipole, taking part in either [7+2] and [3+2] processes, referring to the number of atoms involved.

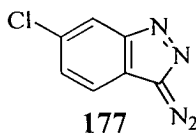
The high regioselectivity found could also be from either mechanism. Scheme 68 illustrates these mechanisms. The numbering below in **170** shows the number of atoms that are potentially involved in the cycloadditions.



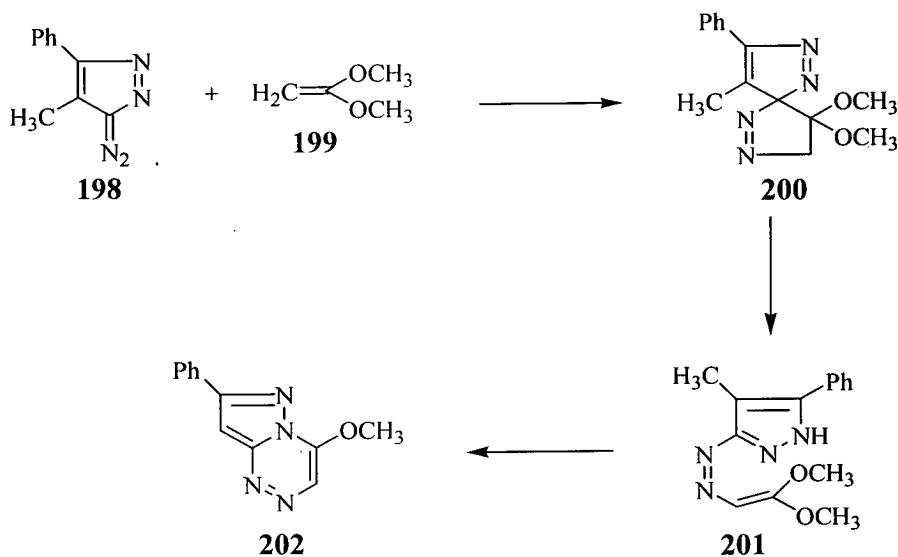
Scheme 68

The detection of two discrete, sequential intermediates in the reaction of 1,1-dimethoxyethylene **199** and diazopyrazole **198** shown below in Scheme 69 was clearly inconsistent with a 1,7 cycloaddition. Intermediate **200** isomerises to **201**, which slowly rearranges to the product **202** shown. These intermediates **200** and **201** were isolated and identified by NMR spectroscopy, and therefore, the initial 1,3 cycloaddition seems the more likely mechanism. The reactions with diazoindazole **170** were found to be very similar to those of diazopyrazole, and the mechanisms were assumed to be similar.

Further cycloaddition reactions have been carried out with the 6-chloro derivative **177** and electron rich alkynes, although the yields are less in comparison to the above olefin reactions.⁹⁸

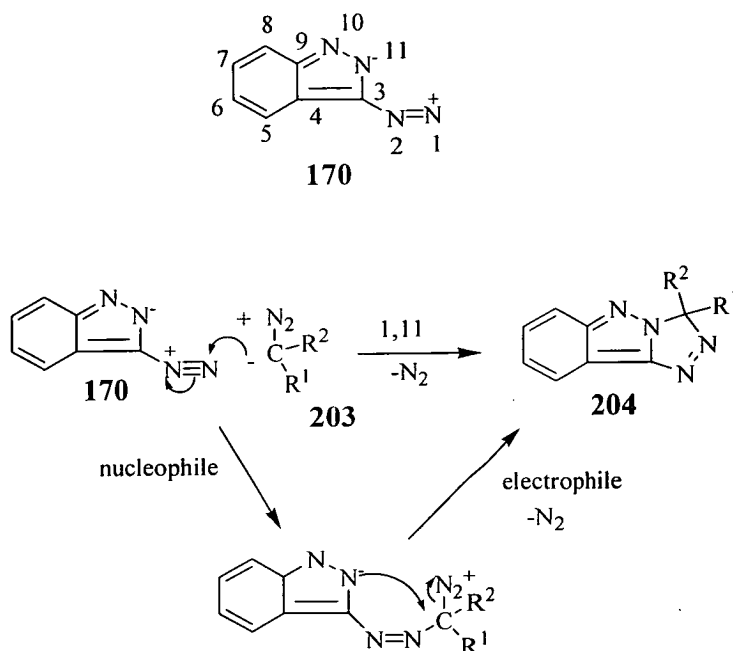


These cycloaddition products typically exhibit λ_{max} values in the range 510-550 nm and relatively weak ϵ values of 7000-8000.



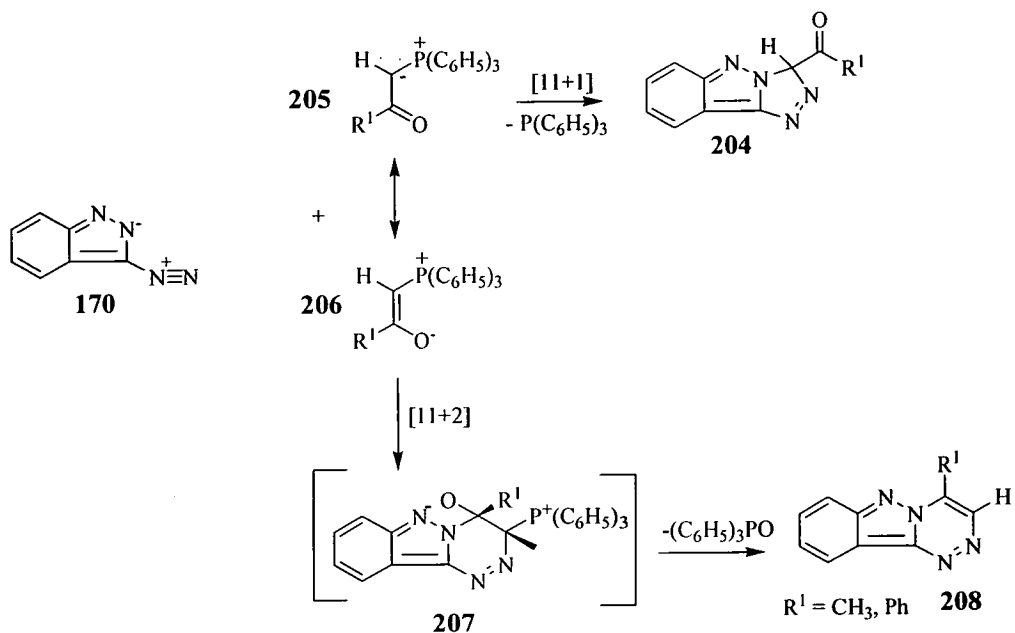
Scheme 69

Diazoazoles are known to react as 1,7 or 1,11 dipoles with a variety of ylides, such as diazoalkanes, phosphonium and sulfonium ylides, in [7+1] or [11+1] cycloadditions forming azolotriazoles **204**.⁹⁹ The [7+1] and [11+1] nomenclature again refers to the number of atoms involved in the cycloadditions.¹⁰⁰ An example is shown in Scheme 70 where diazoindazole **170** acts as a 1,11 dipole, and reacts with a diazoalkane ylide **203**, acting as a 1-nucleophile-1-electrophile, shown in Scheme 70.¹⁰⁰



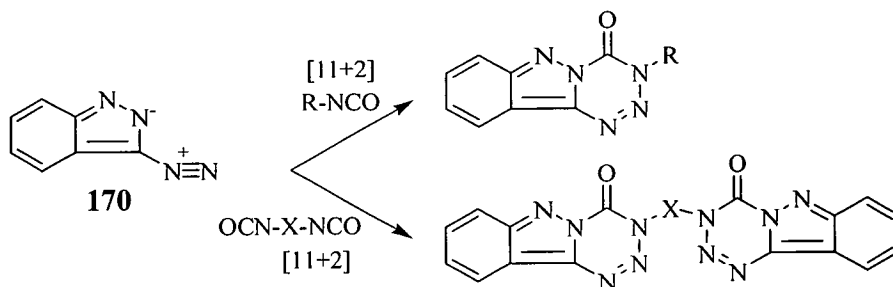
Scheme 70

Acyl-substituted phosphonium ylides were reacted with diazoazoles, and expected to form triazoles **204** by acting as a 1-nucleophile-1-electrophile.⁹⁹ This was seen for the reaction between diazoindazole **170** and **205**, where an [11+1] cycloaddition took place. However, acylphosphonium ylides can also behave as 1-nucleophile-2-electrophiles, as they have been shown to exist largely as phosphonium enolates **206** by ¹H NMR spectroscopy. This form explains the observed product **208**, where an [11+2] cycloaddition occurred, forming the betaine **207**, which gave **208** after the elimination of triphenylphosphine oxide. No carbonyl group was found in the IR spectrum, and yields were 71% for the methyl substituted compound and 73% for the phenyl substituted compound.



Scheme 71

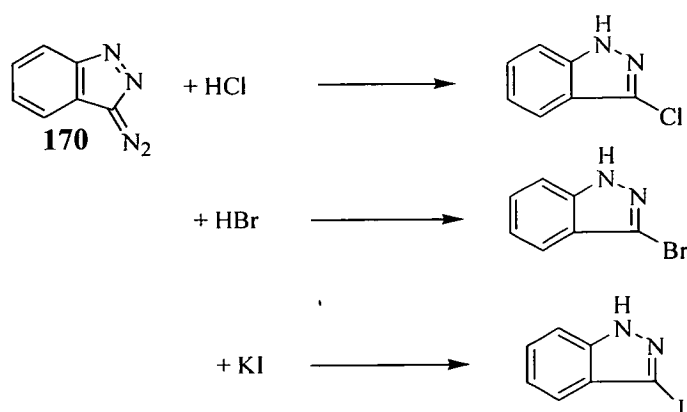
Diazoindazole 170 has also been reacted with mono and diisocyanates.¹⁰¹ An [11+2] cycloaddition was observed for these reactions, occurring twice in the reaction with the diisocyanates. The carbonyl group occurred in the IR spectra at 1750 cm^{-1} .



Scheme 72

2.19.5 Substitution reactions

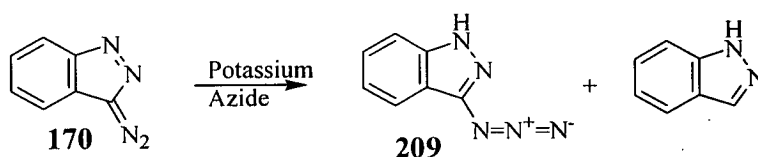
The diazo group can readily be replaced in substitution reactions, as shown below in Scheme 73.⁸⁸



Scheme 73

Nitrogen is clearly being eliminated during these reactions, and the formation of the halogen derivatives is consistent with nucleophilic substitution reactions. It is likely that these reactions are of that of the indazole carbene, after the elimination of nitrogen, with a nucleophile. Under harsher conditions further substitution can take place in the aromatic ring.

The azide derivative **209** has also been synthesised in a similar nucleophilic substitution reaction to those in Scheme 73.¹⁰²

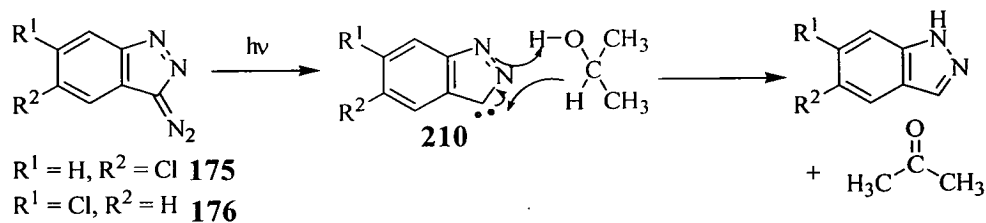


Scheme 74

2.19.5.1 Photolysis

Photolysis of compounds **175** and **176** has been studied in detail in various solvents.⁹² The reactions were first studied in ethanol and in isopropyl alcohol, with acetaldehyde and acetone formed as the respective byproducts, along with the

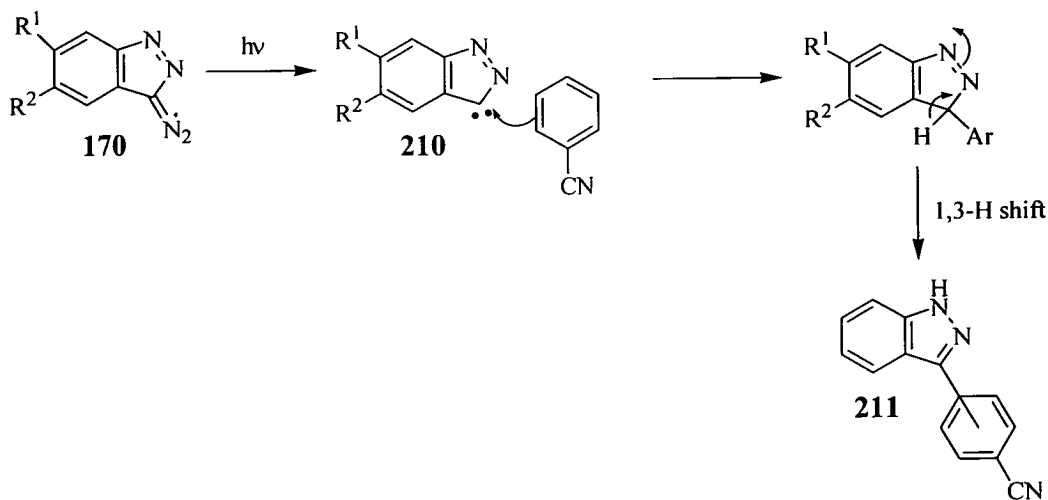
substituted indazole. Scheme 75 demonstrates the reactions of **175** and **176** with isopropyl alcohol. Photolysis of the diazo compounds results in the generation of a carbene **210** after the elimination of nitrogen. Insertion of a hydrogen atom from the alcohol into the carbene, and abstraction of a hydrogen from the hydroxyl group, then yields the products, with an NH observed in the ^1H NMR spectra.



Scheme 75

No insertion of any OR groups from the alcohols was found. Product yields varied from 17% for the parent compound **170** to 85% for the 5-chloro substituted derivative **175**.

Similar studies have been carried out in aromatic solvents; benzene, benzonitrile, 1,2-dimethoxybenzene, methyl benzoate and *p*-chlorotoluene. The carbene **210** was first generated, with subsequent insertion of the aromatic molecule, resulting in a substituted indazole **211**, as shown in Scheme 76 for benzonitrile. Yields varied greatly from 5% in dimethoxybenzene to 72% in benzene.⁹² No indication was given in the literature of the regiochemistry of the products.

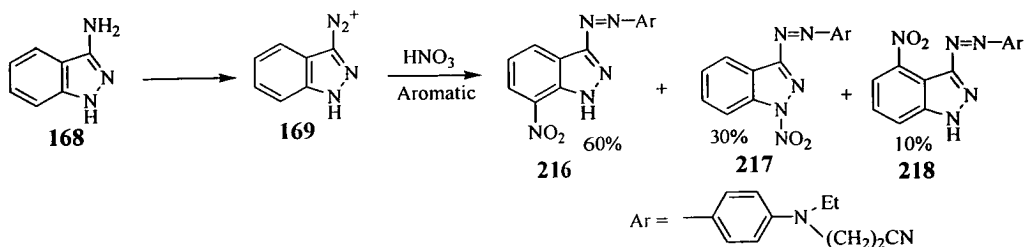


Scheme 76

Photolysis of the 6-chloro substituted compound **176** has been carried out in the heterocyclic solvents, pyridine and thiophene. These reactions proceeded similarly to that shown in Scheme 76, with substitution of the appropriate heterocycle for the diazo moiety, providing further 3-substituted indazoles. The pyridine substitution resulted in a 36% yield and the appearance of an NH signal at 8.65 ppm in the ^1H NMR spectrum, whereas a 26% yield was found for the thiophene compound.⁹² The 6-chloro derivative **176** was also reacted in cyclohexane, giving **213** shown below, as the product, and not the substituted indazole.⁹⁸ The carbene rearranges to a nitrene **212**, as observed in the thermolysis reactions below in Scheme 78, giving the same product **213**.

2.19.5.2 Nitration

3-Aminoindazole **168** was first diazotised under unusual conditions using nitrosonium hydrogensulfate, which was followed by *in situ* nitration with nitric acid in concentrated sulfuric acid.¹⁰³ The 7-nitro- **216**, 4-nitro- **218** and 1-nitroindazole **217** diazonium ions were formed, with the 7-nitro derivative dominating.



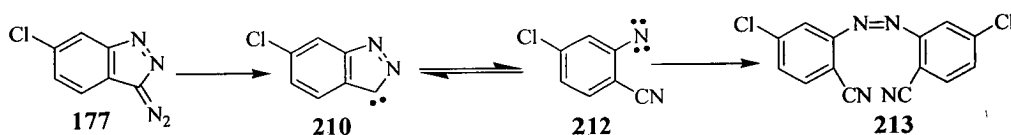
Scheme 77

These compounds were isolated as azo coupled products, and identified by NMR spectroscopy.¹⁰³ Scheme 77 shows these coupled nitration products.

In contrast, nitration of 3-aminoindazole, followed by diazotisation and coupling gave the 5-nitro derivative as the predominant isomer (68%), although the 7-nitro **216** (22%), 1-nitro **217**(6%) and the 5,7 dinitro (4%) were also formed.

2.19.6 Thermolysis

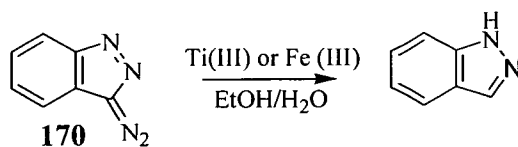
Compound **177** has been the study of thermolysis reactions at a temperature of 380 °C and a pressure of 0.5 Torr.⁹⁸ As with Scheme 75 above, nitrogen is firstly eliminated resulting in the generation of a carbene **210**, which is believed to rearrange *via* the nitrene **212**, to yield the azo compound **213**. An absorption frequency of 2235 cm⁻¹ was found in the IR spectrum corresponding to the nitrile group.



Scheme 78

2.19.7 Reduction

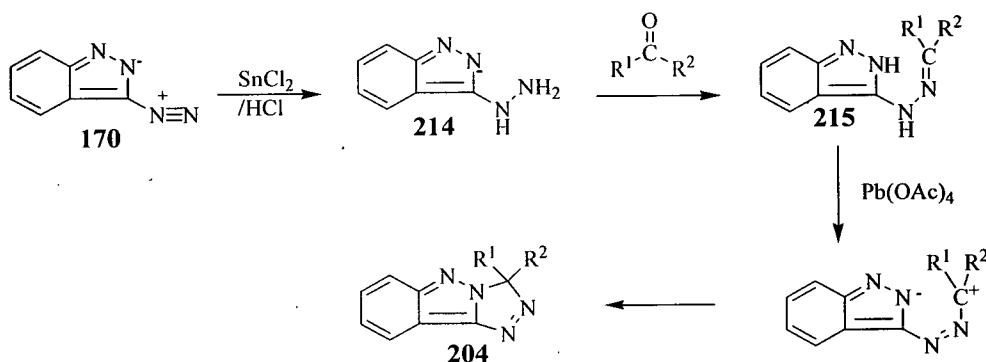
The reduction of diazo compounds in general, where the diazo or diazonium group is replaced by hydrogen, has been well documented, with a variety of reducing agents such as zinc, copper or sodium stannite used. Titanium (III) chloride or iron (II) sulfate can be employed for the reduction of diazo heterocycles.¹⁰⁴



Scheme 79

An exothermic reaction occurs, with a vigorous evolution of nitrogen taking place at room temperature. The reactions are relatively quick, taking approximately 30 minutes, and the reduced products are the only products observed. Yields are 65% for titanium salts and 53% for iron salts, due to difficulties when separating the organic product from the inorganic byproducts. This method however, was limited to heterocycles, as aromatic diazonium salts were not reduced in this manner, although no details of such reactions were reported.

Diazoindazole **170** can be reduced to the hydrazine **214** by stannous chloride, providing a route to azolotriazoles **204**¹⁰⁵ The hydrazine **214** was condensed with a carbonyl compound to give the hydrazone **215**, and the product **204** was formed as the result of a cyclising dehydrogenation, after treatment of **215** with lead tetraacetate.



Scheme 80

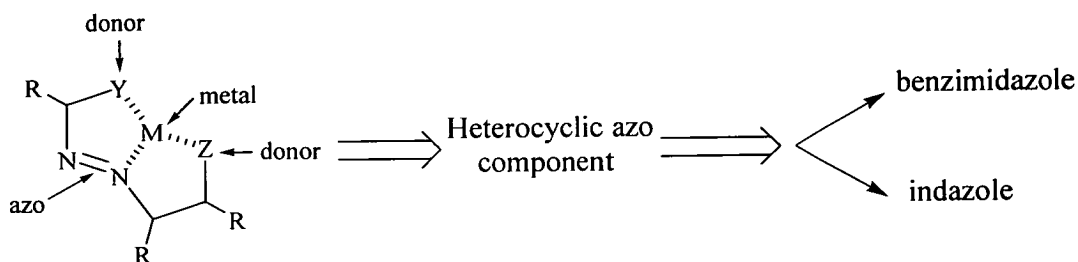
2.20 Conclusions

It has been shown that diazoindazole is easy to synthesise, and readily undergoes further reaction. The reactivity has been investigated under a variety of conditions, with azo coupling, cycloadditions and substitution reactions all successful, providing much synthetic potential. A number of derivatives has also been made, most of

which utilise the standard synthesis, and have found some use in the printing industry.

2.21 Benzimidazole Derivatives

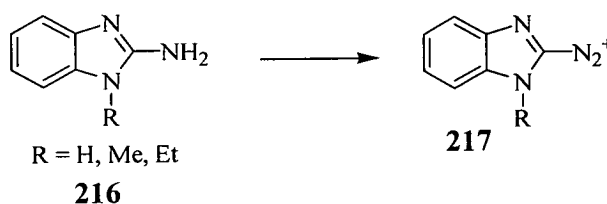
As has been discussed in Section 2.15, dyes derived from benzimidazole and indazole structures both fit the generic structure in Scheme 81. A review of the literature on the synthesis of azo benzimidazole derivatives, is presented below.



Scheme 81

2.22 Synthesis of Benzimidazole Derivatives

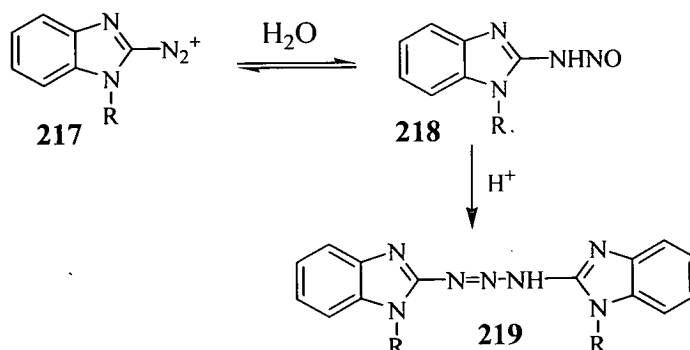
2-Aminobenzimidazole (R=H) **216** is a readily available and inexpensive starting material. However, on inspection of the literature it was found that diazotisation and coupling were not trivial, and did not proceed under standard conditions. Diazotisation of 2-aminobenzimidazole (R = H) itself is not known, only that of the *N*-alkylated derivatives **216** (R = Me, Et) are reported.^{106,107,108,109,110} The 1-alkylated derivatives were not considered for this project, as the nitrogen atom at this position is required for any potential coordination to a metal.



Scheme 82

The diazonium salts **217** of the alkylated derivatives are not formed under standard acidic conditions, but are formed as phosphate salts in strongly acidic media.¹⁰⁶ A mixture of nitrosylsulfuric acid and concentrated sulfuric acid has also been used to form 1-alkylated benzimidazole diazonium salts **217**. Once formed however, these diazonium salts are very unstable but highly reactive.¹⁰⁸ The addition of water to the

diazonium solution shifts the equilibrium to the right, forming stable *N*-nitrosoamines **218**, which are converted to symmetrical triazenes **219**. The addition of acid causes partial denitrosation of **218** to give the starting amine **216**, which can then condense with any remaining **218**, resulting in the formation of **219**.¹⁰⁷



Scheme 83

The coupling reactions of these diazonium salts with phenols, are known to give a mixture of products, making the isolation of the desired product very difficult. Long reaction times of eighteen hours were required for coupling to *p*-substituted phenols.¹⁰⁶ The amount of side products formed were reduced by dilution of the reaction mixture with water, but too great a dilution causes competition between coupling and triazene formation. Further complications are found due to dealkylation at the nitrogen, which has been seen for 1-substituted methoxy derivatives.¹⁰⁶ Coupling has also taken place with naphthols, and various aromatic compounds under the same conditions. This resulted in a mixture of products which were separated by the usual methods, *e.g.* chromatography, crystallisation.^{109,110}

Though, no diazotisation conditions were found for 2-aminobenzimidazole itself, preliminary attempts were made to diazotise 2-aminobenzimidazole under standard conditions, then under the conditions described above, in attempts to couple first with β -naphthol, and then dimedone. These reactions however did not give any identifiable products. It was therefore concluded that this system was of little synthetic use, under the conditions studied.

2.23 Indazole Derivatives

Although there is not much literature data on indazole derived azo compounds (see Section 2.19.1), several examples are known, and their synthesis seemed relatively straightforward. This route was then pursued, and ultimately proved to be highly successful.

2.24 Synthesis of 3-diazo-3*H*-indazole 170

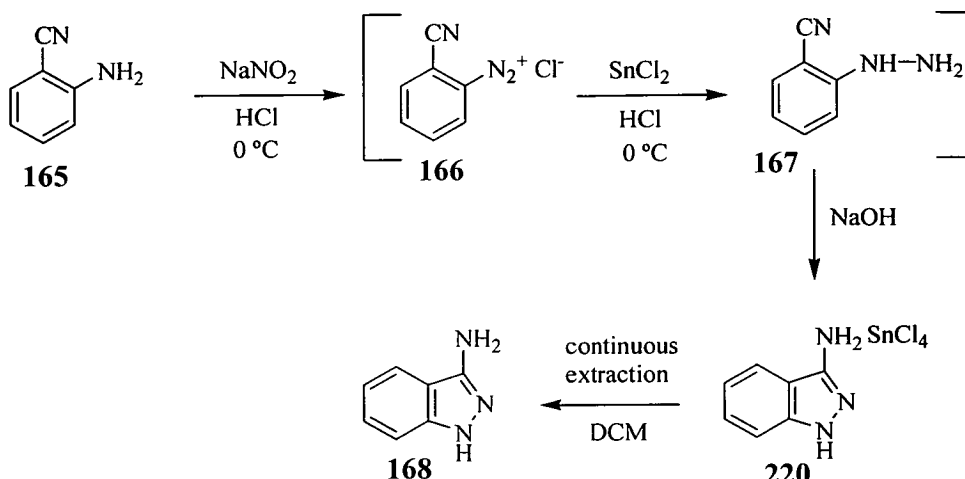
Clearly for an azo coupling reaction to take place, a primary amine is required. 3-Aminoindazole **168** is well known in the literature, and was the starting point for the dye synthesis.⁹⁰ The best literature yield found was only 42%, but after repetition of the procedure, poor yields of around 15% were obtained, which included purification by dry-flash chromatography. This procedure had also been followed previously within our group, and similar low yields were obtained.¹¹¹

The synthesis involved the diazotisation of *o*-aminobenzonitrile **165**, reduction of **166** to the hydrazine **167** with tin (II) chloride, and *in situ* cyclisation to the product **168**. To isolate **168**, sodium hydroxide was added, resulting in a white precipitate which was initially thought to be 3-aminoindazole **168**; NMR spectra were obtained that would be expected for this structure. This solid however, was very insoluble in chloroform, and after elemental analysis, was found to be a tin salt of 3-aminoindazole **220** (see Section 3.17 for values). During this reduction, tin (II) is oxidised to tin (IV), but the exact nature of the salt has not been identified, as tin (IV) is known to exist in tetrahedral, trigonal bipyramidal and octahedral geometries.¹¹²

This salt **220** was dissolved in water, the resulting solution was boiled, and then made strongly alkaline in an attempt to remove the tin salt. The resulting precipitate however, still contained the tin salt, and the solid was redissolved in water. The yield was dramatically improved by an overnight continuous liquid-liquid extraction of the aqueous solution with dichloromethane, removing the tin salt, and giving 3-aminoindazole **168** as a white solid in 66% yield, requiring no further purification.

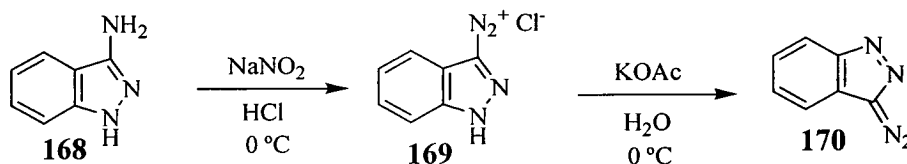
The four aromatic protons of **168** showed chemical shifts of δ_{H} 7.71 ppm (1H, d) 7.20-7.29 ppm (2H, m) and 6.95 ppm (1H, m), in the ¹H NMR spectrum. The ¹³C spectrum showed four CH signals at δ_{C} ~123, 117, 115 and 107 ppm. Such chemical shifts were also characteristic for the azo compounds discussed below. This reaction

has been repeated many times on large scales (20 g), providing multi-gram quantities of material for use as a starting point for forthcoming reactions.



Scheme 84

The synthesis of the stable diazoindazole 170, which was also known in the literature, proceeded without any problems and in high yield (90%).⁸⁸ 3-Aminoindazole 168 was diazotised under standard conditions, and after the addition of base, the water insoluble diazoindazole was obtained.



Scheme 85

A crystal structure has been obtained for diazoindazole 170, which has already been reported in the literature (see Section 2.16).⁹¹ The most noticeable feature of this structure was the short nitrogen (3)-nitrogen (4) bond in the diazo group [1.118(6) Å], compared with the nitrogen (1)-nitrogen (2) bond [1.305(6) Å], and the short carbon (3)-nitrogen (3) bond [1.335(7) Å], compared with the average C-N bond length of 1.40 Å in diazo compounds. As was discussed in Section 2.16, these short bonds suggest great carbanionic character in the azo group 172.

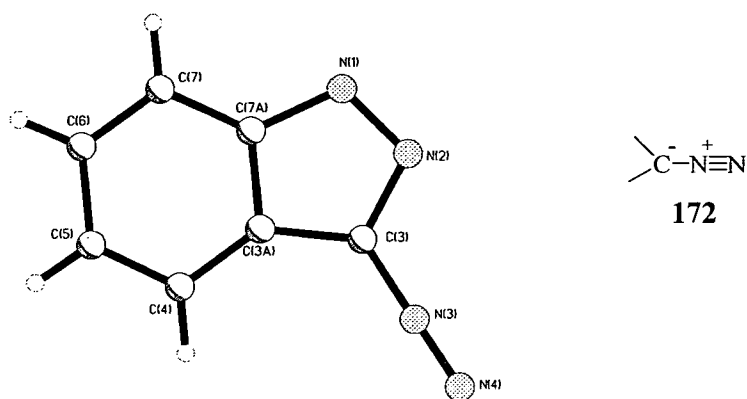
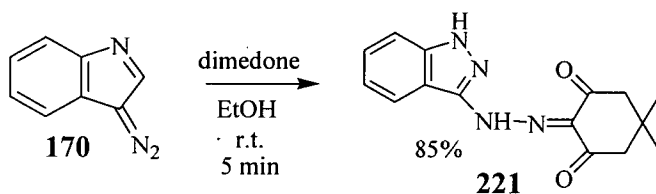


Figure 16 X-ray crystal structure of diazoindazole **170**

2.25 Yellow Dyes

2.25.1 Non-Aqueous Coupling Reactions

Two non-aqueous coupling reactions of diazoindazole **170** were reported in the initial paper (see Section 2.19.1), and this reaction was the basis for much of the forthcoming discussion.⁸⁸ The coupling reaction was carried out by dissolving diazoindazole **170** in ethanol at room temperature, adding one equivalent of the appropriate coupler, resulting in rapid precipitation of the azo compound. This procedure was used many times in the synthesis of various yellow and magenta dyes. A solvent soluble yellow coloured azo compound **221** was obtained in high yield and purity, from repetition of the reaction between diazoindazole **170** and dimedone.⁸⁹



Scheme 86

These non-aqueous coupling reactions have several advantages over standard aqueous conditions. The azo products under these non-aqueous conditions are very easy to isolate, and this was particularly useful when water soluble products were obtained. Furthermore, the yields are all quantitative in theory, as only the two

reactants and the solvent are added; only the azo compound should be formed, and no side products have to be separated. Another advantage of the non-aqueous procedure, was that no salts were added. Under aqueous conditions, salt is often added to promote precipitation of a highly water soluble compound, in a procedure known as salting out. Excesses of salt would have to be removed if the compound was to have any commercial applications, due to problems associated with clogging of the printer nozzles. This is carried out by a procedure known as dialysis, which is time consuming and adds extra expense to the dye synthesis. Material also tends to be lost during this process.

A disadvantage of the non-aqueous procedure however, is that it is not used in industry, where standard aqueous conditions are utilised. The dyes synthesised in this research are intended for an industrial application (ink jet printing), and therefore aqueous conditions would be preferred.

2.25.2 Model coupling reactions of diazoindazole 170

A series of model compounds has been synthesised utilising the non-aqueous method described above, by reaction of 170 with active methylene compounds or with active aromatics, see Scheme 87. All compounds were formed in high yield and purity, and compounds 222, 223 and 224 were yellow in colour.

Due to the insoluble nature of these azo compounds, the NMR spectra were recorded in DMSO. The ^1H NMR spectra of the compounds below, showed similar patterns in the aromatic region to that observed for 3-aminoindazole 168, (discussed above), as did the ^{13}C spectra, showing CH signals at $\delta_{\text{C}} \sim 125$, 120 ($\times 2$) and 108 ppm. In addition, quaternary peaks were observed at $\delta_{\text{C}} \sim 140$ ($\times 2$) [C7a and C3] and 110 ppm [C3a].

Another interesting feature of all these indazole derived azo compounds were the signals at very high frequencies corresponding to the NH's, typically around 13 ppm; signals as high as 15 ppm have been observed, *e.g.* in the ^1H NMR spectrum of 221 two signals at 15.45 and 13.20 ppm were found. As Figure 17 shows, this could be ascribed to intramolecular hydrogen bonding, and also hydrogen bonding to the solvent.

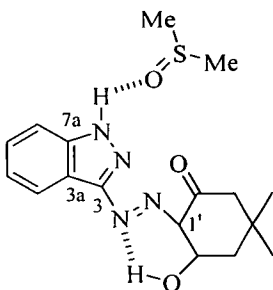
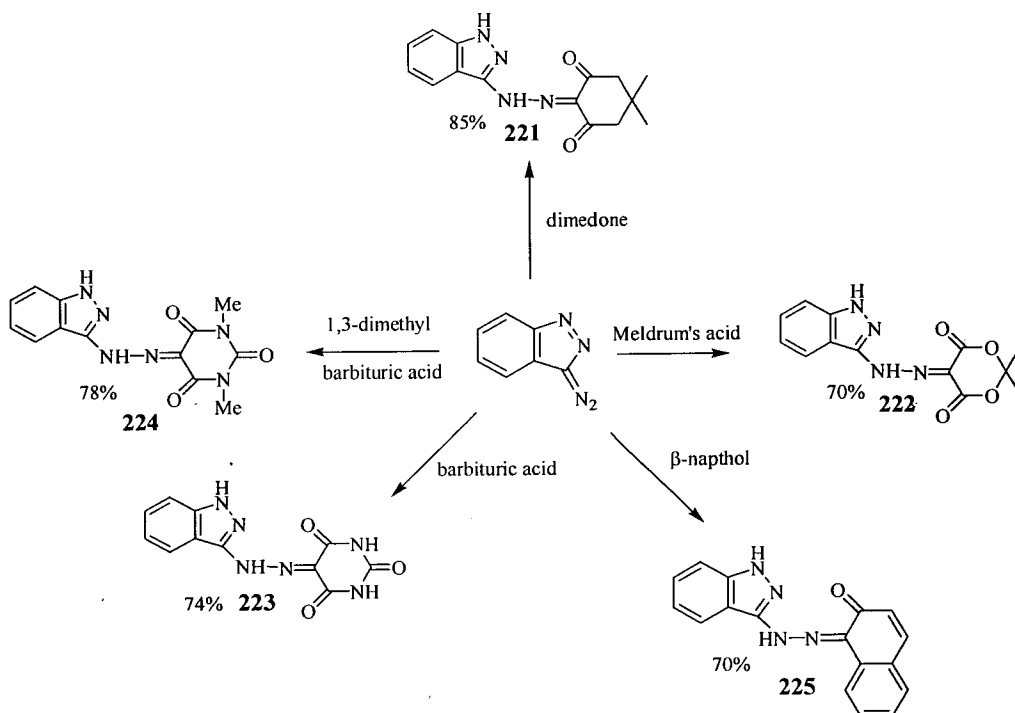


Figure 17 Hydrogen bonding in **221**, responsible for the high chemical shifts observed.



Scheme 87

The β -naphthol derivative **225** was more orange in colour than the others above, (which was reflected in the higher λ_{max} value), and also gave very broad signals in the ^1H NMR spectrum. It was unclear why these broad peaks were observed; this phenomenon was seen again for the R-acid derivative **249** in Scheme 95.

These compounds were inappropriate dyes for ink jet systems as they were all insoluble in water. The barbituric acid **223**, 1,3-dimethylbarbituric acid **224** and β -naphthol **225** derivatives were indeed very insoluble in most solvents, and proved very difficult to purify for analysis.

2.25.3 UV-Vis analysis

Yellow dyes ideally absorb around 430-440 nm, with extinction coefficients in excess of $30\,000\text{ l mol}^{-1}\text{ cm}^{-1}$. The UV-Vis spectra obtained for compounds **221**, **222**, **223** and **224** were excellent, giving symmetrical and sharp curves, with half-band width values of less than 100 nm and extinction coefficients of around $20\,000\text{ l mol}^{-1}\text{ cm}^{-1}$. There was some variation in the λ_{max} value; compound **221** gave a λ_{max} value of 422 nm, and the introduction of two oxygen atoms in **222** caused a hypsochromic shift to 398 nm. The addition of the two methyl groups in **224** made no difference to the curve and data obtained, compared to that of **223**.

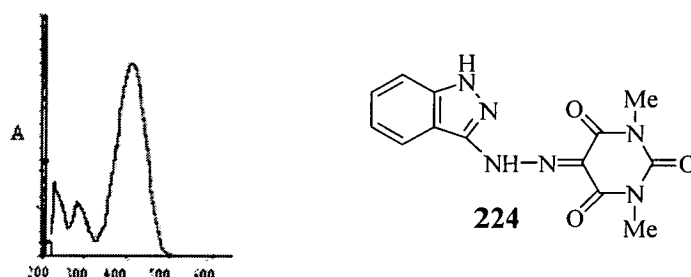


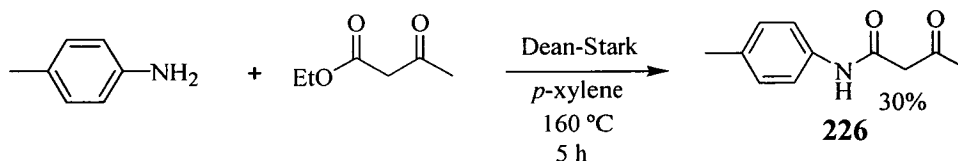
Figure 18 The UV-Vis curve obtained for the 1,3-dimethylbarbituric acid derivative **224**. This spectrum is also typical of **221**, **222** and **223**.

The β -naphthol derivative **225**, gave a curve which was not as symmetrical and sharp as the other three, but had a double peak beginning to appear instead of the single peak observed for those above. This type of curve shape with double peaks became very common with the other naphthol derivatives discussed in Section 2.26. The half-band width was also greater at 113 nm. The extinction coefficient of $21\,000\text{ l mol}^{-1}\text{ cm}^{-1}$ was similar to those above, but the most significant change was the increase in the λ_{max} value to 457 nm. This increase could be expected due to the presence of the extra unsaturated unit, and therefore an extended chromophore system compared with the others in Scheme 87.

The next part of the strategy was to synthesise yellow dyes that had similar properties to those used commercially. β -Ketoamide structures, such as **226** below, offer more flexibility than the couplers that are shown in Scheme 87; they have also been used previously in the synthesis of yellow dyes.⁹ As has been discussed in Section 1.17, aqueous solubility is essential, and this could be introduced *via* the β -ketoamide moiety.

2.25.4 β -Ketoamide Dyes

The β -ketoamide derivative **226** was synthesised in a condensation reaction between *p*-toluidine and ethyl acetoacetate, under Dean-Stark conditions.⁸⁶



Scheme 88

Diazoindazole **170** was then reacted with this coupler **226** in the same manner as those in Scheme 87 above, resulting in a yellow precipitate. The ^1H and ^{13}C NMR spectra showed the absence of the CH_2 signal at δ_{H} 3.49 ppm, and δ_{C} \sim 50 ppm. Again, the characteristic signals in the NMR spectra were obtained for the indazole aromatic ring, and two doublets were observed for the other aromatic ring, in the ^1H NMR spectrum.

UV-Vis spectroscopy gave an excellent sharp and symmetrical curve with an excellent half-band width of 75 nm, and a λ_{max} value of 390 nm. The extinction coefficient of $25\,000\text{ l mol}^{-1}\text{ cm}^{-1}$ was also an improvement on those observed for the compounds in Scheme 87. Although this compound had a closer resemblance to a commercial dye, it still was insoluble in water due to the lack of sulfonic acid groups.

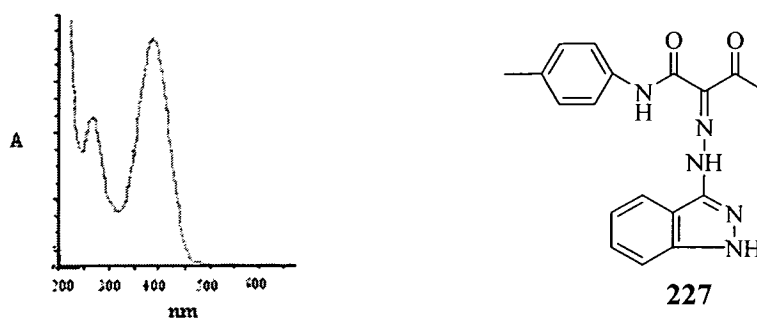
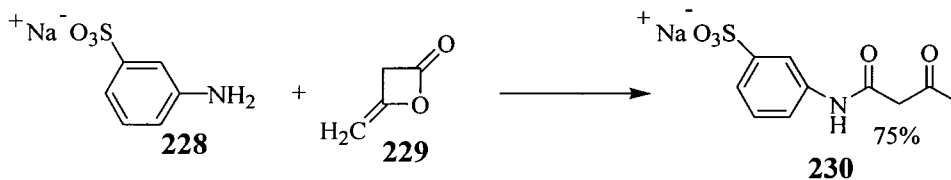


Figure 19 UV-Vis curve for **227**

The obvious way forward to improve the aqueous solubility was to introduce sulfonic acid groups. Using similar conditions as those above, the synthesis of the β -ketoamide derivative **230** was attempted, from metanilic acid **228** and ethyl acetoacetate. Only starting material was obtained; the metanilic acid **228** was very insoluble in organic solvents. Another procedure was then followed involving the reaction between metanilic acid **228** and diketene **229**, under aqueous conditions, producing the sulfonic acid derivative **230**.¹¹³



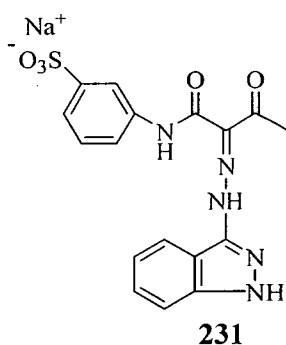
Scheme 89

This coupler **230** was now water soluble, and therefore a slight modification of the standard coupling conditions was required. Diazoindazole **170** was dissolved in ethanol as usual, but the sulfonic acid coupler **230** had to be dissolved in the minimum amount of water, before being added to the diazoindazole solution. The coupler **230** remained in solution even when added to the ethanolic reaction mixture.

After this addition, the reaction proceeded as before, and **231** was obtained as a yellow precipitate in 79% yield.

The azo derivative **231** is the first compound discussed containing a sulfonic acid group. It is important to highlight the characterisation procedure involved, as nearly all of the forthcoming azo compounds that are discussed contain sulfonic acid salts.

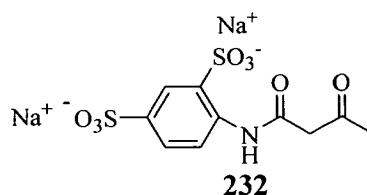
NMR spectra were obtained, but were recorded in $[\text{}^2\text{H}]_6\text{DMSO}$ due to the poor solubility of the azo compounds. FAB mass spectrometry was used due to the presence of the salts, and melting points were mostly recorded as decomposition points. UV-Vis spectroscopy has been carried out, and is discussed in detail. Due to the highly hygroscopic nature of these salts, addition of a number of water molecules had to be made to these compounds to give values that were in an acceptable range, for elemental analysis. No purification of these water soluble salts was attempted either, but NMR spectra showed very low levels of impurities.



The NMR spectra showed the absence of the CH_2 signals. The UV-Vis spectra of **230** and **231** were very similar, with the λ_{max} , ϵ and half-band width values all closely matching (in methanol). When the UV-Vis spectrum of **231** was recorded in water, a λ_{max} of 380 nm was observed, compared with 390 nm in methanol, and an increase in the half-band width was also found. A yellow colour was observed in aqueous solution, but the solubility ($\sim 1\%$ w/v) was still considerably less than that required for an ink jet dye (5-10% w/v), and therefore, another sulfonic acid group was required.

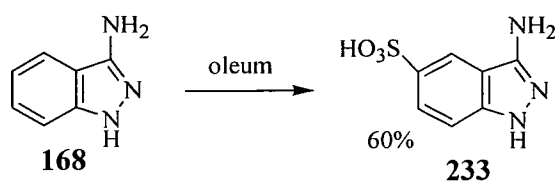
In an attempt to add a second sulfonic acid group and synthesise **232**, aniline-2,4-disulfonic acid was reacted with diketene **229** as above, but unfortunately only an unidentified solid was obtained. This route was taken no further, and the second

sulfonic acid group was instead introduced *via* the aromatic ring in the indazole moiety, thus making the non-aqueous coupling reaction inapplicable.



2.25.5 Sulfonation of 3-aminoindazole

Substitution reactions with 3-aminoindazole **168** are known in the literature at various positions, see Section 2.19.5. Sulfonation has been reported but the site of electrophilic attack was not established.¹¹⁴



Scheme 90

3-Aminoindazole **168** was successfully sulfonated with oleum at room temperature, (the absence of one of the aromatic protons was immediately obvious from the NMR spectra), and the 5-position was established as the site of substitution (also the preferred site for nitration, see Section 2.19.5.2), to give **233**. This regioselectivity was identified by inspection of a fully coupled proton-carbon NMR spectrum.

Important minor couplings in aromatic systems are 3-bond, in the range 4-12 Hz.¹¹⁵ The interpretation of the ¹H-coupled ¹³C spectrum involved identifying all the quaternary carbons, and then establishing the multiplicity of each. Carbon 3 was identified (δ_C 145 ppm) as it was the only singlet present, and was at the highest frequency due to the two adjacent electron withdrawing nitrogen atoms. The important signals were those corresponding to carbons 3a and 7a, and their 3-bond couplings were used to determine the regioselectivity of the sulfonic acid group. Carbon 7a (δ_C 142 ppm, ³J 6.9) was observed at higher frequency than 3a (δ_C 110 ppm, ³J 11.7) due to the adjacent electron withdrawing nitrogen atom. As shown in

Figure 20, a doublet of doublets was observed for carbon 7a, and a doublet for carbon 3a. The only other possible site of substitution could be the 6-position, in which case the observed splitting pattern for 3a and 7a would have been reversed.

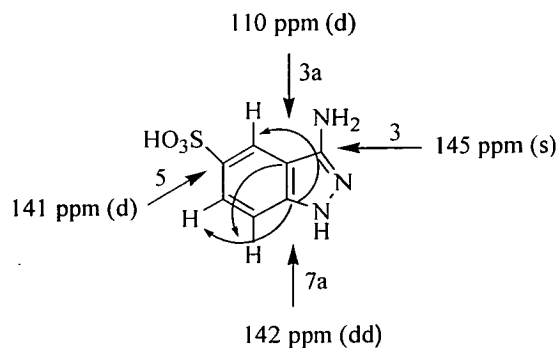


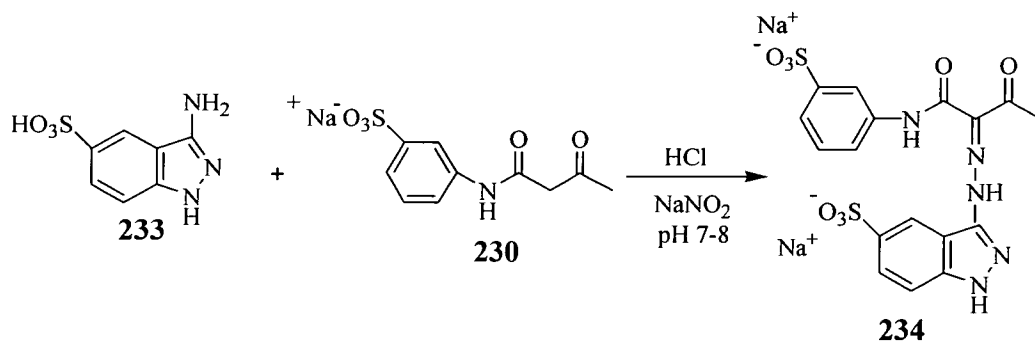
Figure 20 Identification of the quaternary carbon signals, and their coupling patterns.

2.25.6 Coupling Reaction of 3-Aminoindazole-5-sulfonic acid **233**

3-Aminoindazole-5-sulfonic acid **233** could now be coupled *via* a standard aqueous coupling reaction to β -ketoamide **230**; to give an azo compound with two sulfonic acid groups. This particular coupling proved difficult, as the product was now much more water soluble than the previous compounds, and proved troublesome to isolate. Several small scale attempts were made at this reaction, and a yellow coloured solution was observed upon addition of the diazonium solution to the β -ketoamide solution, but no solid material was obtained. When the reaction was monitored by HPLC, and more sophisticated pH monitoring equipment, the yellow dye **234** was obtained (see also Section 2.13.4).

The pH was carefully monitored, and maintained at 7-8 for the coupling to take place. As has been discussed previously in Section 2.13.4, such great care in pH control is not normally required for standard azo coupling reactions, which tend to work almost instantaneously. Despite these measures, the product was still not readily isolable; conditions were far too dilute ($\sim 10\times$) for such a water soluble compound to precipitate. The pH was lowered to 1, and the addition of $\sim 15\%$ w/v of sodium chloride was made to promote precipitation. The water soluble target

yellow dye **234** was obtained, and the NMR spectra were consistent with the structure of **234**; the CH₂ again was absent.



Scheme 91

No dialysis was carried out on this novel yellow dye due to the small amount of **234** obtained. Material tends to be lost during this process, and it was thought that it would be more beneficial to use it in crude form for the testing process, see Section 1.15.

The UV-Vis spectrum in Figure 21, was not as good as those obtained above; the curve had more of a tail and was not as steep, at the high wavelength side (see Figure 21). A hypsochromic shift was again witnessed after the addition of the second sulfonic acid group, with a λ_{max} of 361 nm observed.

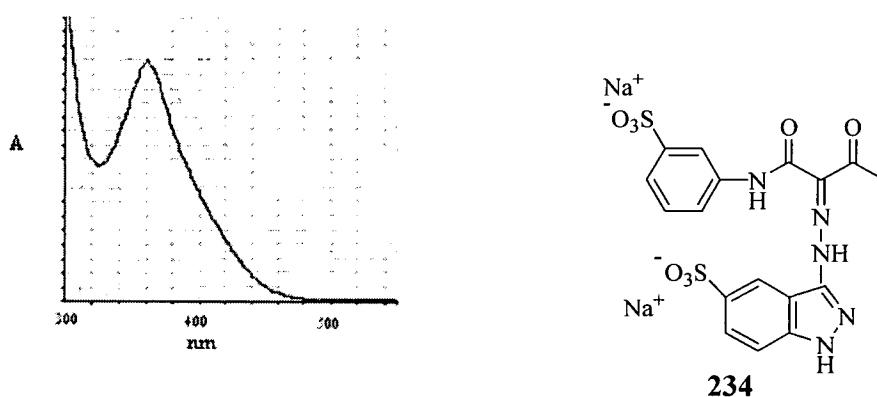


Figure 21 UV-Vis curve for **234**

2.25.7 Metallisation of 231

As has been discussed in Section 1.23, metallised dyes are more stable to light exposure. The possibility of coordination to a metal was then investigated on a UV-Vis scale, for ligand **231**, in different solvents (methanol and water). A few milligrams of **231** was dissolved in methanol, the UV-Vis spectrum was recorded, and a λ_{\max} of 388 nm was observed. An excess of nickel (II) acetate tetrahydrate was added, giving a more intensely yellow coloured solution, and an increase in the λ_{\max} to 449 nm. The colour change and subsequent increase in λ_{\max} is a trend that occurs with metallised complexes, see Section 1.23.2.

An unusual feature of this UV-Vis spectrum was that the intensity of the curve decreased upon metallisation. The complex however, showed good stability, as a curve of similar shape and intensity was observed after eight days, with the λ_{\max} reaching an equilibrium value of 454 nm.

Another experiment was then carried out in methanol to examine the kinetics of the metallisation process, and to see if any intermediate was involved, which could be detected by the presence of isobestic points. The UV-Vis curve was recorded immediately after the addition of nickel (II), then at one minute intervals up to 30 minutes, and then after selected periods of time.

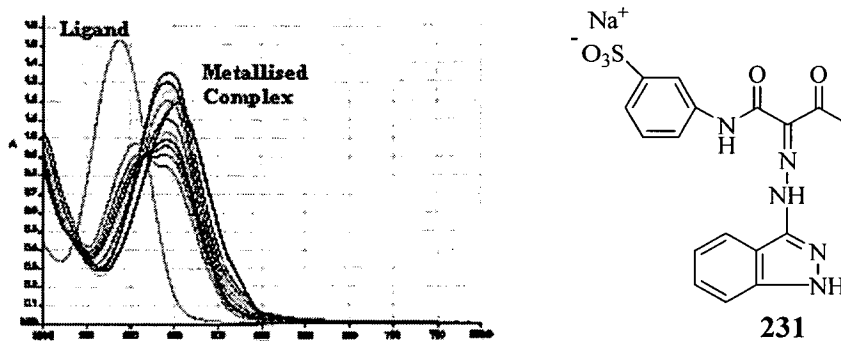


Figure 22 UV-Vis curves for ligand **231** and its metallised complex, recorded in methanol over various periods of time

The UV-Vis curve recorded immediately after the addition of nickel (II), showed a peak corresponding to the ligand **231**, and the appearance of a small peak corresponding to the metallised complex, at higher wavelength. No curve corresponding to the ligand was present after five minutes. An isobestic point at about 415 nm was observed for the first few readings, but after about three minutes, no more were observed. The curve corresponding to the metallised complex, reached a maximum intensity after a few hours, and then began to decrease in intensity, eventually settling at an equilibrium value. Due to this compound's enhanced water solubility over the model compounds above, the same experiments were carried out in water.

An excess of nickel (II) acetate tetrahydrate was added to the ligand solution as above, and a bathochromic shift to 434 nm from 380 nm was observed. The UV-Vis spectra were recorded every minute, but no isobestic points or the presence of ligand were observed this time, and the process could be deemed to be instantaneous. This is a trend that was observed for all the metallisation studies in aqueous solution.

The intensity of the curve of the metallised complex was much less than that of the ligand (ϵ 14 000 l mol⁻¹ cm⁻¹ compared with 27 000 l mol⁻¹ cm⁻¹), which began to decay much quicker than in methanol, and a noticeable difference was observed in the spectra after ninety minutes. After several days the solution had lost its yellow colour and the curve had reverted back to that of the ligand, indicating that a very weak coordination was taking place.

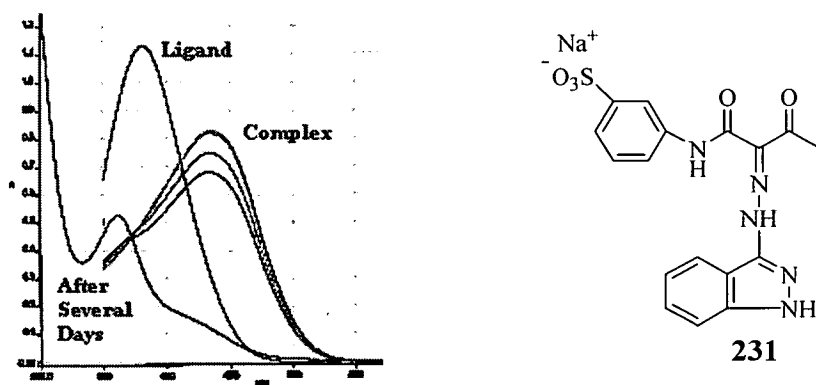


Figure 23 UV-Vis curves obtained for **231** and metallised complex, recorded in water over various periods of time.

The donors in this type of molecule are not ideally set up for coordination. Stable complexes require the formation of two rings, which is probably not possible in this case; two structures of many that may be formed are shown below.

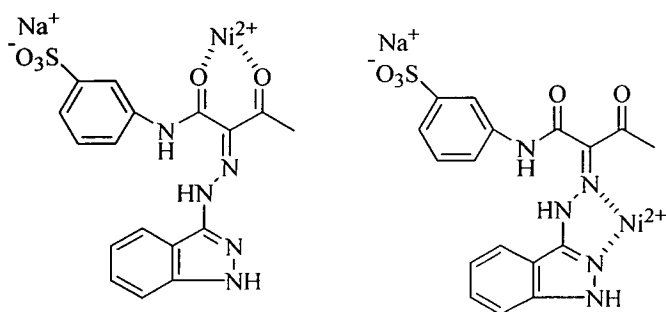
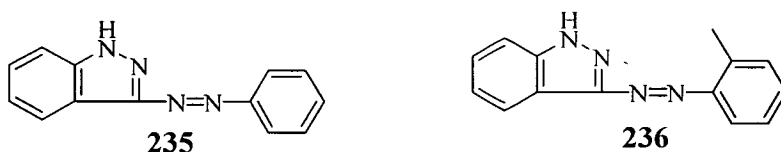


Figure 24 Two possible ways that nickel may coordinate to the ligand

The geometry of the molecule will allow coordination to either the two carbonyl groups or to the azo group and one of the indazole nitrogen atoms, but not to both. Therefore, an unstable complex is formed, as reflected in the UV-Vis studies.

2.25.8 Standard aqueous coupling reactions of indazole

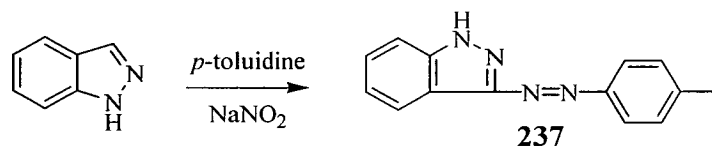
Indazole can be used as the coupling component, as well as the azo component, and indeed some standard aqueous coupling reactions from indazole are known in the literature.⁸⁸ The two compounds **235** and **236** shown below were reported; synthesised from the reactions between indazole and the diazonium salts of aniline and *o*-toluidine, respectively. Syntheses such as these appeared to be very useful, as azo dyes could be obtained in only one step.



The reaction of indazole with *p*-toluidine was then investigated. A 1:1 ratio of indazole and the diazonium salt derived from *p*-toluidine were reacted together in acidic media, following the standard coupling procedures outlined in the literature.¹⁰

An orange precipitate was formed after the addition of sodium hydroxide, which was identified from the ^1H NMR spectrum as a 1:1 mixture of indazole and the azo compound **237**. A singlet at δ_{H} 8.10 ppm was observed, corresponding to the 3-position of indazole, along with two NH signals at δ_{H} ~11 and 12 ppm, corresponding to indazole and **237**. After dry-flash chromatography, a mixture of indazole and **237** was obtained, as the two components co-eluted, proving very difficult to separate. Even after variation of the solvent systems, the mixture was still difficult to separate by TLC.

Another experiment was then carried out in which three equivalents of the *p*-methylbenzene diazonium chloride were sequentially added, to minimise the amount of unreacted indazole, and improve purification. After the addition of the first equivalent of the diazonium salt, sodium hydroxide was again added as above, to yield a precipitate which was assumed to be a similar mixture of indazole and the azo product **237**. The precipitate was not isolated, but redissolved by the addition of concentrated hydrochloric acid. A second equivalent of the diazonium salt was then added, and a precipitate again formed after the addition of sodium hydroxide. The steps described above were then repeated one more time for a third equivalent of the diazonium salt. After this final addition, the precipitate was filtered off, and from TLC, no starting material was present. The singlet at δ_{H} 8.10 ppm was not present in the ^1H NMR spectrum of the crude product. This solid was purified by dry-flash chromatography, and the NMR spectra showed the now familiar aromatic pattern for the four aromatic protons of indazole, and the ^{13}C spectrum showed two large CH ($\times 2$) signals at δ_{C} 130 and 123 ppm. However, a yield of only 25% was obtained, and when compared to the non-aqueous route described above, was not nearly as useful synthetically.



Scheme 92

This azo compound **237** was not water soluble, as was expected, due to the lack of sulfonic acid groups. A yellow colour was observed in solution, giving a λ_{max} of 357 nm and an extinction coefficient of $22\,700\text{ l mol}^{-1}\text{ cm}^{-1}$. The curve shape in the UV-Vis spectrum was similar to those obtained in the model indazole reactions above, and a very narrow half-band width of 61 nm was observed.

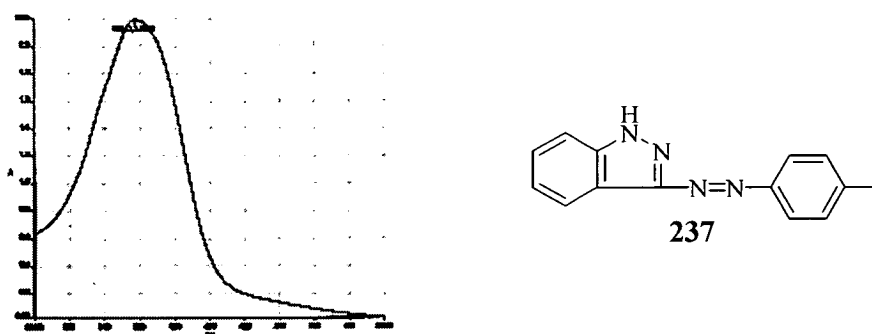
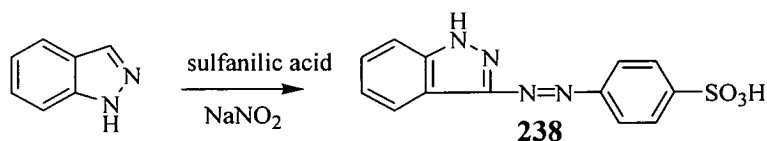


Figure 25 UV-Vis curve for **237**.

Compound **238** is known in the literature, and a mechanistic study has been carried out on the coupling reaction between indazole and the diazonium salt derived from sulfanilic acid. The results showed that the reaction involves only a small amount of the required anion in equilibrium with the neutral indazole molecule.¹¹⁶ The indazole anion must be present for coupling to the diazonium salt to take place. With only a small amount of the anion present, the equilibrium is largely in favour of the neutral indazole molecule, and explains the recovery of indazole in the experiment described above.



Scheme 93

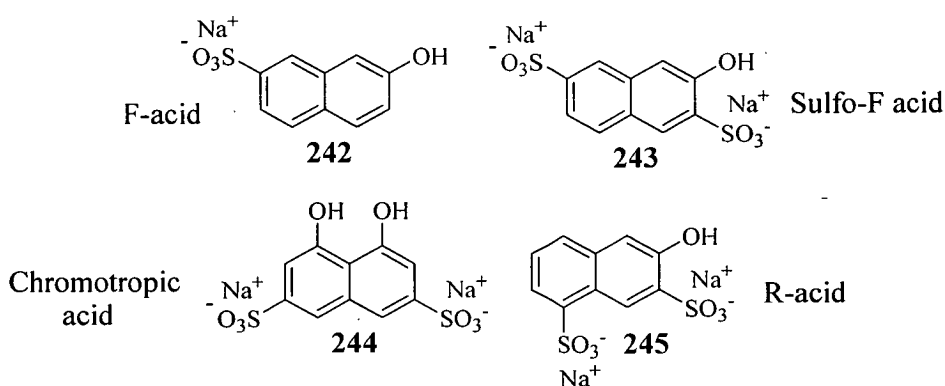
This coupling reaction was attempted under standard conditions to try to introduce water solubility into the system, but proved unsuccessful.

Due to the low yields and the difficulty in isolating the products, this route to azo dyes was not pursued any further, particularly when compared to the success of the non-aqueous reactions.

Yellow dyes which are used in ink jet printers are not causing the same stability problems when in print as magenta dyes, which are the quickest to fade (see Section 1.21.2). By inspection of the λ_{max} values in the model yellow compounds above, in particular the β -naphthol derivative **225** where a λ_{max} of 457 was observed, it was thought that magenta dyes would be obtainable by reacting diazoindazole with commercial coupling components. In commercial magenta dye synthesis, couplers based on sulfonic acid derivatives of α and β -naphthols are used, of which a vast range is available, and coupling to these was investigated. In addition, magenta dyes require metallisation to improve their fastness properties, and this would also help increase the λ_{max} into the magenta range.

2.26 Magenta azo dyes

The sulfonated naphthol compounds: F-acid **242**, sulfo-F acid **243**, chromotropic acid **244** and R-acid **245**, (these trivial names will be used throughout, see Abbreviations Section 3.1 for systematic names) are all typical couplers that are used in commercial magenta dye synthesis. These couplers tend to give dyes with hue in the correct region when coupled to a heterocycle, and also the oxygen atom of the hydroxyl group is essential for complexation to a metal.

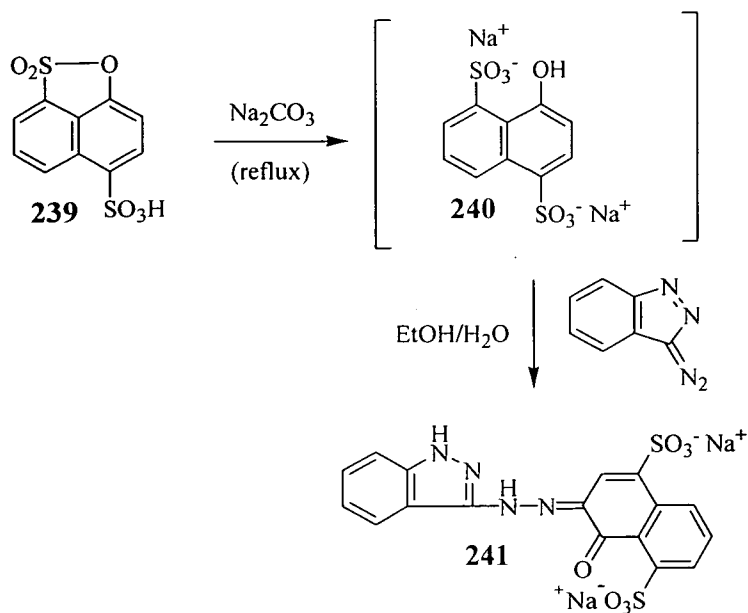


Diazoindazole **170** was coupled to all these naphthol compounds in the same way as described above in Section 2.25.4, *via* the modified non-aqueous coupling reaction. The azo compounds were synthesised in high yield and purity, giving red/purple coloured precipitates, the structures of which are shown below in Scheme 95. All the compounds in Scheme 95 were characterised in the way described in Section 2.25.4. The aromatic signals corresponding to the indazole part of the molecules were evident again in the ^1H and ^{13}C spectra.

One interesting feature of the R-acid derivative **249** was the very broad signals obtained in the ^1H NMR spectrum, which was also witnessed earlier when diazoindazole was coupled to β -naphthol. The spectrum was recorded at higher temperatures, and an addition of trifluoroacetic acid was made (protonates all sites, stopping zwitterion formation), in attempts to improve the spectrum, but the broad peaks remained.

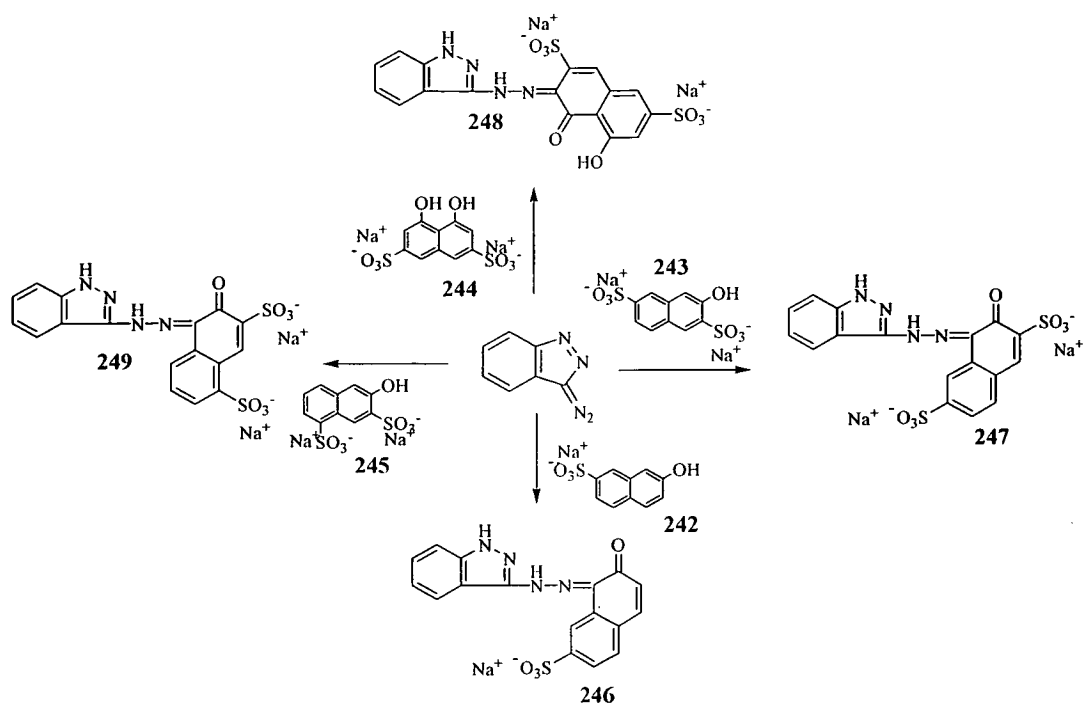
The F-acid derivative **246** only has the one sulfonic acid group, and therefore much lower water solubility than the others, which was not good enough for industrial standards, as was seen before with the monosulfonated yellow dye; for ink jet printing systems, a dye must have an aqueous solubility of 5-10% *w/v*.

The α -naphthol derivative **241** has also been synthesised, as outlined below in Scheme 94. Sodium 1,8-naphthosultone-4-sulfonic acid **239** was first ring-opened by heating to reflux in a basic aqueous solution, generating **240** *in situ*. The resulting red solution was then added to an ethanolic solution of diazoindazole **170**, resulting in a red/purple coloured precipitate **241**.



Scheme 94

The UV-Vis data has been recorded for ligands **241**, **246**, **247**, **248** and **249** and are reported in Table 5. All the ligands gave broad absorption curves, which is not uncommon; the half-height width of the ligand curves are not as important as those of the metallised complex curves. The α -naphthol derivatives **241** and **248** gave higher λ_{max} values than the β -naphthol derivatives **246**, **247** and **249**, and the addition of a second sulfonic acid group caused a bathochromic shift of around 20 nm, (F-acid derivative **246** 447 nm compared with Sulfo F-acid derivative **247** 467 nm). The one unusual result obtained, was for the chromotropic acid derivative **248**, and this will be discussed further in Section 2.26.1.2.



Scheme 95

Coupler	Ligand	$\lambda_{\text{max}}/\text{nm}$	$\epsilon/\text{l mol}^{-1}\text{cm}^{-1}$	$w_{1/2}/\text{nm}$
F-Acid	246	447	15 800	127
Sulfo F-Acid	247	467	15 600	178
R-Acid	249	467	9 300	160
Chromotropic Acid	248	530	27 900	102
α -naphthol	241	507	14 600	131

Table 5 UV-Vis data for the naphthol derivatives in Schemes 94 and 95.

As has been discussed before, many magenta dyes designed for ink jet printing systems require metallisation in an effort to improve their fastness to light. A full metallisation study for the naphthol derivatives above, was carried out.

2.26.1 Metallisation Studies

2.26.1.1 Preliminary Studies using methanol solution

A preliminary experiment was carried out to see if metallisation occurred at all. This process was followed by UV-Vis spectroscopy; initial studies were carried out in methanol solution. A few milligrams of the ligand was dissolved in methanol and a ten-fold excess of solid nickel (II) acetate tetrahydrate was added to the solution. The F-acid derivative **246** gave an orange colour in solution with a λ_{\max} of 443 nm, and a weak extinction coefficient of $13\,100\text{ l mol}^{-1}\text{ cm}^{-1}$. The addition of nickel (II) caused a large shift of the λ_{\max} to 547 nm and a small increase in the extinction coefficient to $16\,800\text{ l mol}^{-1}\text{ cm}^{-1}$. As has been discussed above, characteristic signs of a successful metallisation process are an increase in the λ_{\max} , an increase in absorbance (ϵ) and a colour change. Similar to the observations made for the yellow dye **231** in Section 2.25.4, the intensity of absorption for this complex fell with time, indicating that it was not stable, although the λ_{\max} did settle at an equilibrium value of 547 nm.

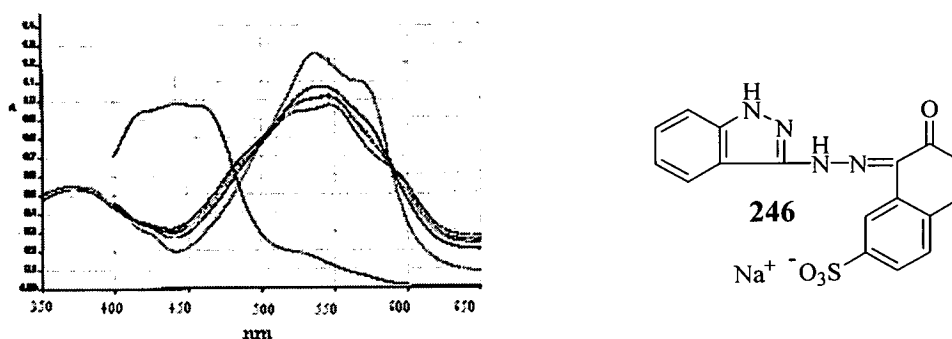


Figure 26 UV-Vis curves obtained for ligand and metallised complex of **246**, recorded in methanol.

The sulfo F-acid derivative **247** showed similar characteristics, in that a λ_{\max} shift occurred upon addition of nickel (II), from 467 nm to 544 nm, and the intensity also increased. This time however, the complex was much more stable and the curve did not decrease in intensity with time (UV-Vis spectrum recorded again after 8 days).

Both these experiments showed that metallisation was occurring; furthermore, with these compounds being water soluble and water being the solvent used in ink jet systems, all the remaining UV-Vis spectra of the magenta dyes were recorded in aqueous solution.

2.26.1.2 Preliminary studies at pH 6 and 9

The metallisation process of the magenta ligands was studied by UV-Vis spectroscopy at pH 6, and then at pH 9.

The appropriate ligand was dissolved in deionised water (pH of ~6 resulted), and a ten-fold excess of nickel (II) acetate tetrahydrate was added. The UV-Vis spectrum for each experiment was recorded immediately after the addition of nickel (II), then after every minute, and then at various intervals. In the experiments carried out for compounds **241**, **247**, **248** and **249**, metallisation was concluded to be instantaneous, and the complexes formed were very stable, as the curve shapes, λ_{\max} and absorption intensities remained constant after eight days. None of the starting ligands were observed in the UV-Vis spectra, after the addition of nickel (II).

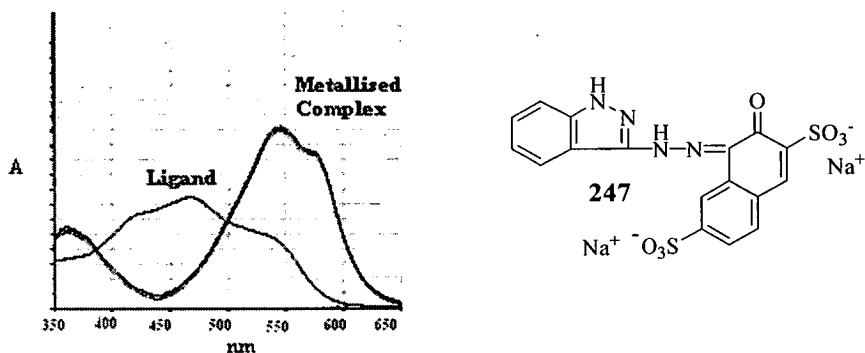


Figure 27 The UV-Vis curves obtained for the sulfo F-acid ligand **247** and metallised complex, at pH 6, which is typical of the compounds in Schemes 94 and 95.

It should be noted that all the curves displayed double peaks, and that the λ_{\max} values quoted are those of the more intense peak. By calculating the mid-point of the absorption at half the maximum intensity, it was thought that a more representative

picture of the absorption would be obtained, but in most cases, the values did not differ by any significant amount, e.g. the sulfo F-acid derivative **247** gave 545 nm (as in Table 6), compared with the recalculated value of 549 nm.

Coupler	Compound	λ_{\max}/nm	$\epsilon/\text{l mol}^{-1}\text{ cm}^{-1}$	$w_{1/2}/\text{nm}$
F-Acid	246	532	23 600	97
Sulfo F-Acid	247	545	21 900	90
R-Acid	249	541	15 500	107
Chromotropic Acid	248	544	29 400	112
α -naphthol	241	566	20 200	112

Table 6 UV-Vis data of metallised complexes at pH 6

The F-acid derivative **246** also gave a complex that was instantaneously formed; there was a large increase in intensity (ϵ 15 800 $\text{l mol}^{-1}\text{ cm}^{-1}$ to 23 600 $\text{l mol}^{-1}\text{ cm}^{-1}$), and a reduction in the half-band width ($w_{1/2}$ 127 nm to 97 nm). However, this complex was not as stable as the others, as the intensity of the curve began to fall after only a few minutes. This was also observed when the spectrum was recorded in methanol (see above), but the instability was much more noticeable in this case, as the solution lost its purple colour and the UV-Vis absorption eventually fell in intensity by a factor of five.

During this process a precipitate was formed, which was thought to be the metallised complex (see below). Due to the presence of only one sulfonic acid group, it was thought that the complex was only sparingly soluble in water.

The metallisation process was then studied again at pH 9, in the same way as was carried out at pH 6. The pH was maintained at 9 for each reaction, by using phosphate buffer solutions.

The same trends were observed for the F-acid derivative **246**, as observed at pH 6. The precipitate formed even quicker at pH 9, and the intensity of the curve fell rapidly.

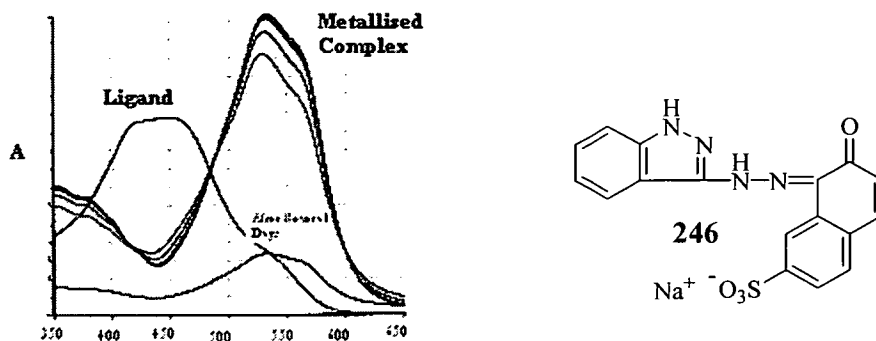


Figure 28 UV-Vis curve obtained for ligand **246** and the metallised complex at pH 6.

In an attempt to identify this precipitate, a larger scale metallisation was carried out so enough of the precipitate could be obtained for analysis. One equivalent of nickel (II) solution (dissolved in the minimum amount of water) was added to the ligand solution (dissolved in 100 cm³ water), and 50 mg of the precipitate was eventually obtained. The best method for analysing this was by elemental analysis, as FAB mass spectroscopy proved inconclusive; no mass corresponding to either 1:1 or 1:2 stoichiometries of the metallised complexes were found. The elemental analysis results were shown to fit that of a 1:1 complex better than that of a 1:2 complex. Additions of water were made, and removal of hydrogen atoms from the molecular formulae had to be taken into account for this analysis, as it was assumed that one hydrogen atom would be lost upon coordination to form a 1:1 complex, and two hydrogen atoms would be lost upon coordination to form a 2:1 complex. The results shown appear very similar, but 7 water molecules had to be added to the 1:2 complex molecular formula to give any numbers that matched the results obtained: 1:1 complex (-1H) (Found: C, 42.2; H, 2.9; N, 11.6. C₁₇H₁₀N₄NaNiO₄S.2H₂O requires C, 42.1; H, 3.1; N, 11.5%); 1:2 complex (-2H) (Found: C, 42.4; H, 3.5; N, 11.6).

$C_{34}H_{16}N_8Na_2NiO_8S_2 \cdot 7H_2O$ requires C, 42.4; H, 3.3; N, 11.5%). No further evidence was found in favour of either complex, and perhaps a mixture of complexes was formed.

The solvent has also influenced the λ_{max} values observed, with the metallised complex of **246** giving a λ_{max} of 532 nm in water, compared with 547 nm in methanol. The curve shapes are greatly changed too, with a vastly increased extinction coefficient of 24 000 l mol⁻¹ cm⁻¹ in water, compared with 7 500 l mol⁻¹ cm⁻¹ in methanol, and a reduced half-band width of 97 nm, compared with 137 nm in methanol. No further work was done with the F-acid derivative **246** due to its insoluble nature.

The UV-Vis spectra obtained for the sulfo F-acid derivative **247** showed a λ_{max} increase from 467 nm to 545 nm upon metallisation, an increase in the ϵ value from 15 600 l mol⁻¹ cm⁻¹ to 21 900 l mol⁻¹ cm⁻¹, and a vastly reduced half-band width of 178 nm to 90 nm.

At pH 9, an increase in the λ_{max} to 568 nm was observed compared with 545 nm at pH 6. This increase in λ_{max} at higher pH was not unexpected, as more ionisation occurs, and the increase in electron density can easily be donated into the conjugated system causing a bathochromic shift.¹⁹

The solvent had no effect on the spectrum, in contrast to the F-acid derivative **246**, with all the values obtained being very similar in both water and methanol.

The R-acid derivative **249** is an isomer of the sulfo F-acid derivative **247**, and both had similar UV-Vis spectra; λ_{max} values of 467 nm and 541 nm, and ϵ values of 9 300 l mol⁻¹ cm⁻¹ and ϵ 15 500 l mol⁻¹ cm⁻¹ were observed for the ligand and complex respectively, at pH 6. A lower extinction coefficient was the only real difference, compared with the sulfo F-acid derivative **247**. This ligand **249** and metallised complex, also behaved similarly to the sulfo F-acid derivative **247** at pH 9, with increases in the λ_{max} of the ligand and metallised complexes observed at 471 nm and 559 nm respectively.

The chromotropic acid derivative **248** gave very unusual curves at pH 6. The ligand displayed a very high λ_{max} of 530 nm, and a very high extinction coefficient of 27 900 l mol⁻¹ cm⁻¹. The curve was much sharper and more symmetrical than the typical curves observed for the other ligands above; the half-band width of 102 nm was very

narrow for a ligand. Upon metallisation, the λ_{\max} only increased marginally to 544 nm, and the extinction coefficient increased slightly to 29 700 l mol⁻¹ cm⁻¹. Another unusual feature was that the curve became broader upon complexation, with the half-band width increasing from 102 nm to 112 nm, which is the opposite of what is expected. At pH 9 the behaviour was more recognisable, where the ligand gave a λ_{\max} of 447 nm and a very broad curve of 150 nm. The addition of the nickel (II) then caused a λ_{\max} increase to 553 nm. The curve also became narrower (half-band width of 102 nm) and gave a more intense absorption of 28 600 l mol⁻¹ cm⁻¹ (increased from 12 000 l mol⁻¹ cm⁻¹).

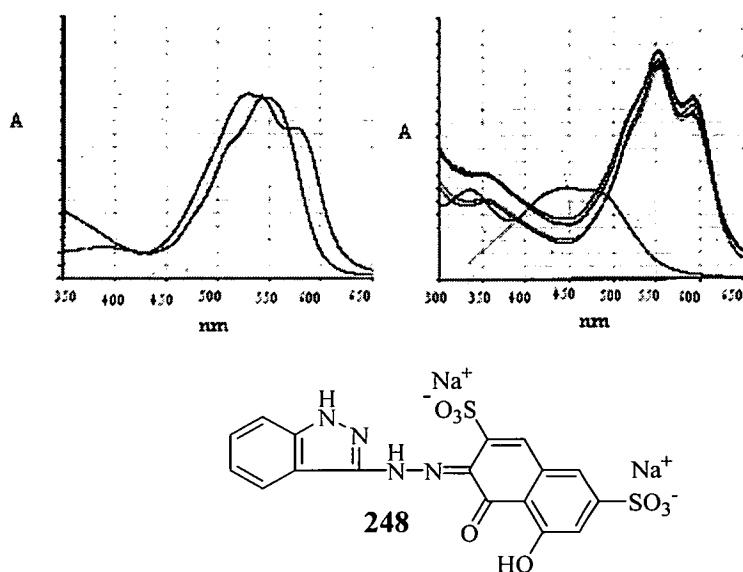


Figure 29 UV-Vis curves obtained for **248** and metallised complex at pH 6 and 9.

The α -naphthol derived ligand **241** showed a high λ_{\max} of 507 nm in comparison to the β -naphthols, and upon metallisation it increased to 566 nm; the extinction coefficient increased to 20 000 l mol⁻¹ cm⁻¹ from 14 600 l mol⁻¹ cm⁻¹, and the half-band width did reduce as expected, although at 112 nm it was broader than the β -naphthols. The two α -naphthol derivatives **241** and **248**, both gave higher λ_{\max} values for the ligand and complex, and broader curves than the β -naphthols. This is characteristic of β -naphthols versus α -naphthols.¹¹⁷

2.26.1.3 Effect of varying pH upon metallised complexes

As was seen above, the UV-Vis curves can vary upon changes in pH. An experiment (on the UV-Vis scale) was carried out in aqueous solution, to test the stability of the sulfo F-acid derivative **247** to changes in pH. The pH was altered with very dilute sodium hydroxide and hydrochloric acid solutions, and the UV-Vis spectra were recorded at the following pH's: 2.75, 4.0, 4.76, 5.65, 6.60, 8.0, 9.9, 11.0 and 12.0.

At pH 3, the curve represented that of the ligand and the solution was orange in colour. It was not unexpected that the ligand curve was obtained at this pH, as preparative scale metallisations take place at a pH of around 7.

At pH 4.6, a significant change occurred with a peak appearing that was product like at around 545 nm, and the ligand peak decreased in intensity. From pH 3 to 5.3, isobestic points were observed. The intensity continued to increase as the pH was increased, and the λ_{\max} value remained constant up to pH 8, where the isobestic points were no longer apparent.

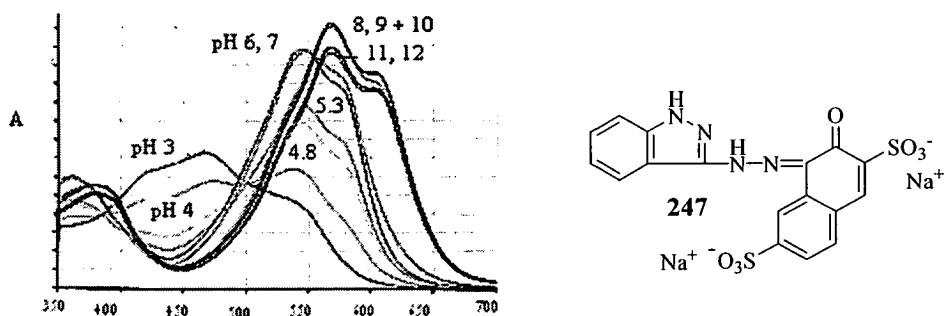


Figure 30 UV-Vis spectra obtained at various pH for **247**

From pH 8-10, the λ_{\max} value increased further to 567 nm, as did the intensity. The λ_{\max} value did not increase any further at pH 11-12, but the intensity decreased slightly. Noticeable colour changes were observed from orange at pH 3, to pink at pH 4.8, to dark red at pH 5.65 and magenta/purple at higher pH. It can be clearly seen from Figure 30 that the complex is definitely not insensitive to pH. At higher pH values, deprotonation at the 1-position in **247** will occur, enabling delocalisation of electrons into the conjugated system, and thus a bathochromic shift is observed.

2.26.1.4 Industry Standard Magenta Dyes

Two metallised magenta ink jet dyes of undisclosed structure, were obtained for comparison of UV-Vis data, with the dyes discussed above.

An aqueous solution of dye A was studied at pH 6.7 initially, and gave a double peaked curve as witnessed for the magenta compounds above. Several differences however, were noted. The higher wavelength peak was more pronounced than the lower wavelength peak, giving a λ_{max} of 532 nm which appears low for an ideal magenta, but the curve's high wavelength side extended above 555 nm. A balance between the high and low wavelength parts of the curve give the complex the desired magenta colour.

The curve is narrow with a half-band width of around 80 nm, and the high wavelength end of the spectrum is very steep by comparison with the indazole dyes, with no high wavelength tails (see Section 1.8). High wavelength tails in UV-Vis spectra provide unwanted absorption, and have a significant effect on the colour obtained.

The same complex was studied at pH 9, with both the peaks now becoming more equal in intensity. Under these more basic conditions, the higher wavelength peak was shifted to 540 nm, the half-band width remained the same, and the lower wavelength peak was at 513 nm. A fuller pH dependency study was then carried out. At pH 3, a curve that was very broad, and of low intensity corresponding to the free ligand was obtained, similarly to the sulfo F-acid derivative **247** above. As the pH was increased to 5 and above, the ligand curve disappeared, and the double peaked curve corresponding to the metallised complex began to form. The only shift in wavelength was observed between pH 7-9, (λ_{max} increased from 532 nm to 540 nm) and even at pH 11, the curve remained similar to those at lower pH. No further change in λ_{max} occurred above pH 9, which is in contrast to the sulfo F-acid derivative **247**.

The UV-Vis spectrum of another commercial magenta ink jet dye B was then recorded at pH 7. The curve obtained was similar in shape to the sulfo F-acid derivative **247**, with the familiar double hump. The higher wavelength peak was observed at 546 nm, and again there was some absorption at wavelengths greater

than 550 nm, and a considerable amount below 530 nm. A half-band width of 90 nm was observed and no high wavelength tails were observed (see Section 1.8).

2.26.1.5 Analysis of Metallisation Processes

The effect upon complexation of varying the amount of nickel (II) added to the ligand solutions, was analysed in detail for **247** and **241**. This was done at Avecia, Grangemouth, where monitoring of the conditions, as discussed previously, was more controlled.

Generally, this procedure involved dissolving 100 mg of the ligand in deionised water at pH 7. Small aliquots (0.1 eq) of nickel (II) solution were then added to the ligand solution, and the UV-Vis spectra were recorded. HPLC monitoring of this process was attempted, but only the ligands were apparent on the trace; the metallised complexes were not seen, and therefore, UV-Vis spectroscopy was used to monitor the process (all UV-Vis spectra were recorded in pH 5 acetate buffer solution). The results obtained for the two derivatives **247** and **241** were very similar. For the sulfo F-acid derivative **247**, a change in the UV-Vis spectrum was seen after addition of only 0.1 equivalents of nickel (II), with a small bump appearing that corresponded to the metallised complex. Gradually, as the concentration of nickel (II) was increased, the ligand curve disappeared (after ~0.4-0.5 eq) and the curve corresponding to the metallised complex increased in intensity. After the addition of 1.2 equivalents of nickel (II), a precipitate began to form, and no further additions of nickel (II) were made. The L, a, b coordinates (see Section 1.11.2) were also a good way to estimate the end point of this process, as the changes in these values became less after a while, and the coordinate eventually became constant. The changes in the b value in particular were significant, and Figure 31 shows a plot of b against the number of equivalents of nickel (II) added. This graph shows a decrease in b, as the amount of nickel (II) added is increased. The decrease in b is rapid at first, and begins to slow down after ~0.5 equivalents, but continues to decrease slowly up to ~1 equivalent. On inspection of the UV-Vis curves, and the b coordinate, it was estimated that the process was complete after the addition of approximately 0.85 equivalents of nickel (II).

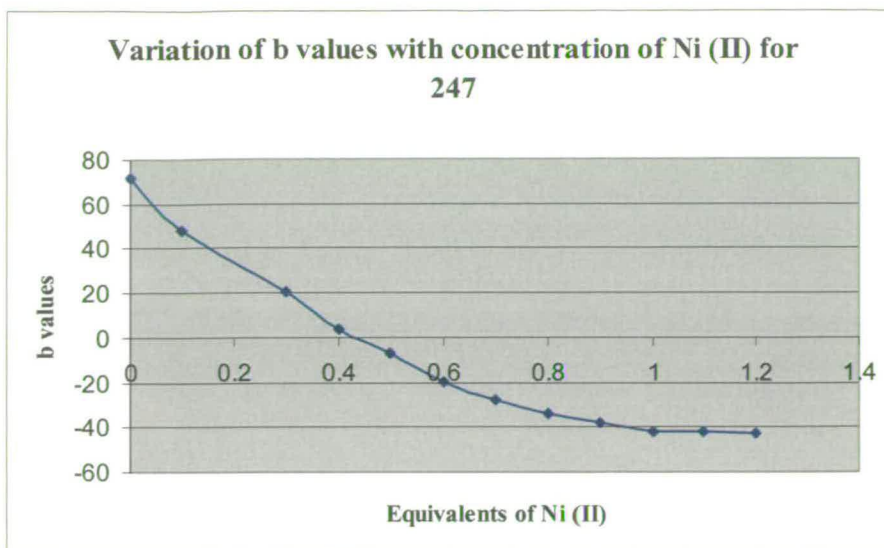


Figure 31 Graph of b values versus equivalents of nickel (II) added for **247**.

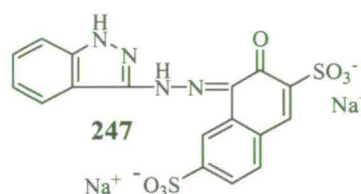
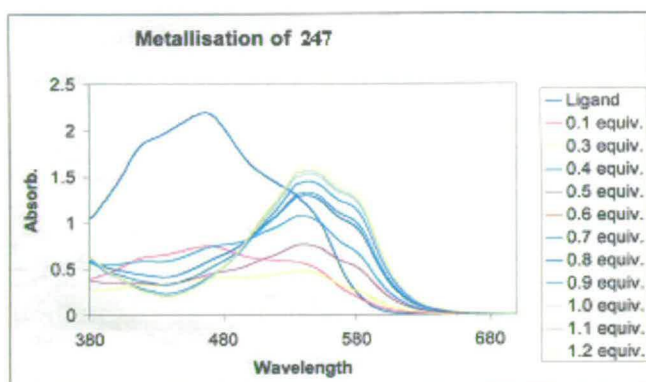


Figure 32 UV-Vis curves obtained for quantitative additions of nickel (II) to **247**.

The α -naphthol derivative **241**, behaved in very similar fashion to the sulfo F-acid derivative **247**, during this process. It took around 0.5 equivalents of nickel (II) for the ligand curve to disappear completely, and a precipitate was also observed when greater than 1 equivalent of nickel (II) was added. A plot of b against the number of equivalents of nickel (II) added is shown in Figure 33, and is very similar to that in Figure 31. From inspection of Figures 33 and 34, it was again estimated that the end point of the reaction was after ~ 0.85 equivalents of nickel (II).

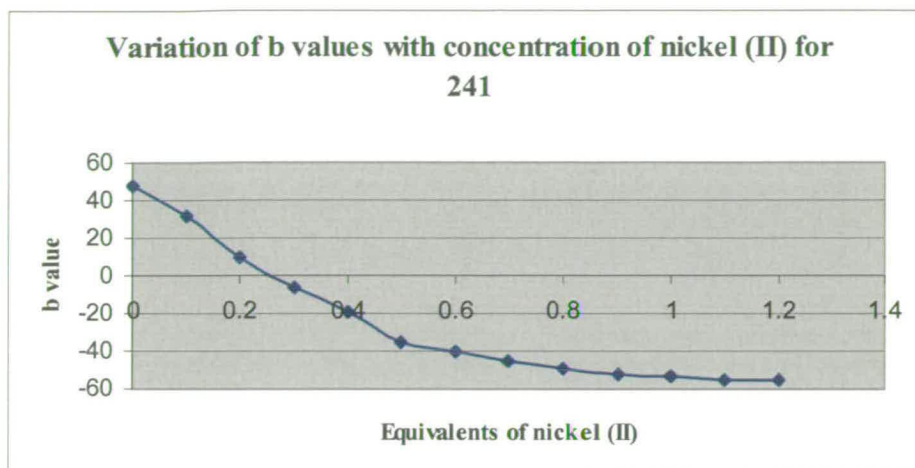


Figure 33 Graph of b values versus equivalents of nickel (II) added for 241.

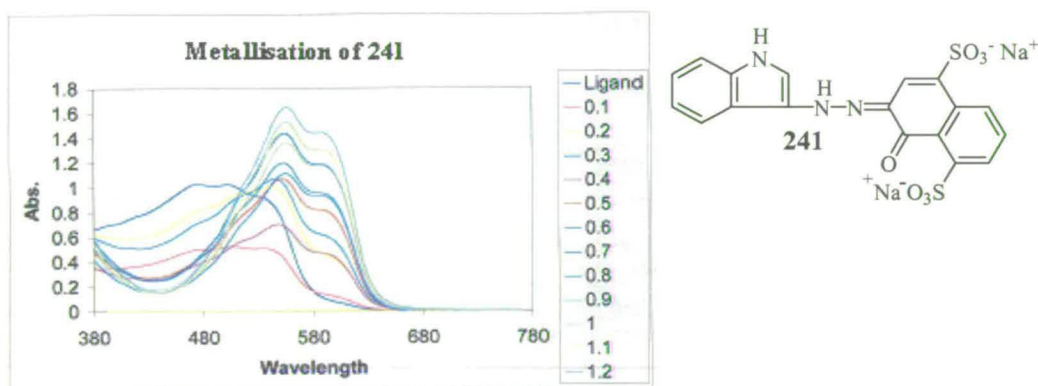


Figure 34 UV-Vis curves obtained for different amounts of nickel (II) added to 241.

2.26.1.6 Metallised Complex Stability

Several small scale experiments were conducted to test the stabilities of the sulfo F-acid derivative 247 and α -naphthol derivative 241, towards metallisation. These experiments were designed to probe how strongly the indazole complexes were bound to the nickel, when in the presence of a ligand that is competing for the nickel. Both the sulfo F-acid and α -naphthol derivatives 247 and 241 were tested in this manner, giving very similar results.

The ligand was dissolved in deionised water at pH 7, and 0.85 equivalents of nickel (II) were added. After stirring the solution for 30 minutes, samples of the resulting metallised complexes were taken for HPLC analysis and UV-Vis spectroscopy. A ligand (C) used in the synthesis of magenta ink jet dyes, was then added to the dark purple coloured solution containing the indazole derived metallised complex. The dark solution quickly became lighter in colour, with more of a magenta shade. Samples of this solution were taken for HPLC and UV-Vis spectroscopy, with HPLC indicating a mixture of products. Ligand C was not observed on the HPLC, but its metallised complex was apparent at 3 minutes. Again, the metallised complexes of **247** and **241** were not observed on the HPLC traces, in the appropriate experiments, but the ligands **247** and **241** were apparent at 8 minutes and 10 minutes respectively. The final UV-Vis curve obtained was not exclusively either of the metallised complexes, and it was concluded that a mixture of products was obtained.

The reversal of this experiment was also carried out, where one equivalent of the α -naphthol derivative **241** was added to a metallised ink jet dye (D). This was to see if the ligand **241** had the strength to coordinate to the already strongly coordinated nickel, as from the results of the previous experiment, it was thought that perhaps the metal was not coordinating strongly enough to the indazole derived ligands. Also, the fact that the complexes were not seen on the HPLC traces suggested weak coordination.

Dye D, gave a magenta colour in solution, which became darker when **241** was added. As above with the previous experiment, a mixture of products was obtained on the HPLC trace, and the curve obtained in the UV-Vis spectrum was not exclusively that of either metallised complex.

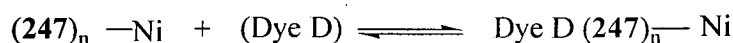
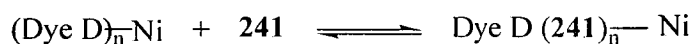


Figure 35 The equilibria that exists in the processes discussed above.

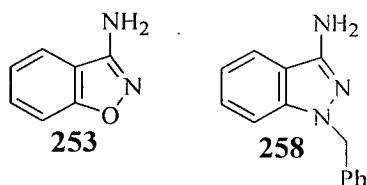
The results did not conclusively prove whether the ligands **241/247**, and dye D, were strongly coordinating or not. It was however, a positive result that **241** had the ability to coordinate to the nickel when in the presence of a competitor. An equilibrium clearly exists, as shown in Figure 35, where a mixture of products is being formed.

2.26.1.7 Isolation of Metallised Complexes

The next step was to isolate the metallised complexes. This was done first on a small scale, by dissolving the ligand in deionised water at pH 7, adding 0.85 equivalents of the nickel (II) solution, and then stirring the solution for 30 minutes. A small sample was then taken to record the UV-Vis spectrum, to ensure the reaction was complete, by comparison with the spectra obtained previously. Once this was successfully achieved, the dye solutions were heated in an oven at 40 °C until all the solvent had evaporated, leaving a dark solid. To find out if the complexes were stable to these isolation conditions, the solids obtained were then reconstituted in water and the UV-Vis spectra were recorded again, with both complexes giving spectra that matched those obtained previously. It was concluded that they were stable to the isolation conditions, and the same experiments were successfully repeated on larger scales to give enough material required for testing (> 1 g).

Despite the success of the above metallisations, very little information has been obtained on how the nickel coordinates with the ligands, and the stoichiometries of the resulting complexes.

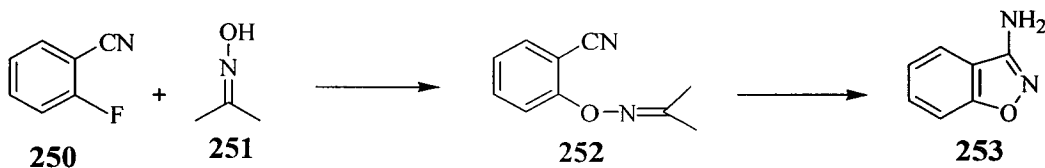
To explore this further, azo analogues have been made where the NH moiety has been replaced, firstly with an oxygen atom (**253**), and then with an *N*-benzyl group (**258**). These compounds were then coupled to sulfo F-acid for a comparison of the metallisation process with the indazole analogue **247**



2.27 Benzisoxazole dyes

An analogous series was synthesised for comparison with the indazole derived compounds above, where the NH at the 1-position in 3-aminoindazole, was replaced by an oxygen atom. As well as discovering how this structural change would influence the the metallisation process, changes in the UV-Vis spectra may be expected. This would reveal if the NH was essential for coordination to take place, and perhaps which nitrogen atoms the nickel coordinates to.

3-Amino-1,2-benzisoxazole **253** is known in the literature and was synthesised from *o*-fluorobenzonitrile **250** and acetone oxime **251**, which was acting as a protected derivative of hydroxylamine, ensuring that the oxygen was acting as the nucleophile and not the nitrogen.¹¹⁸ Compound **252** was first isolated as an oil in 70% yield, and then the oxime **252** was deprotected under acidic conditions, to give the hydroxylamine, which cyclised to the amine **253**, in 72% yield. 3-Aminobenzisoxazole **253** was identified by comparison to the literature NMR data.¹¹⁸



Scheme 96

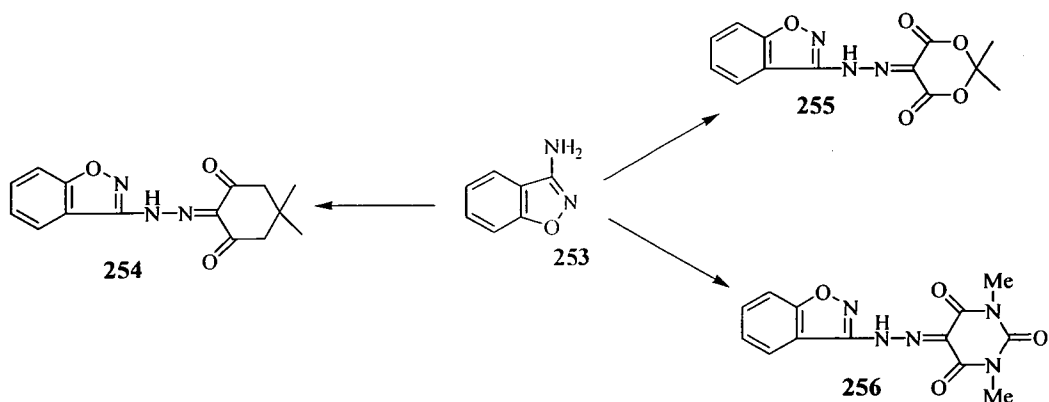
The ^1H and ^{13}C NMR chemical shifts of **253** were similar to those observed for 3-aminoindazole derivatives, now with the absence of the NH signal. The data reported in Table 7 is a list of NMR signals for **168** and **253**. No further work was carried out to establish full characterisation of these compounds.

3-Aminoindazole 168		3-Aminobenzisoxazole 253	
$\delta_{\text{H}}/\text{ppm}$	$\delta_{\text{C}}/\text{ppm}$	$\delta_{\text{H}}/\text{ppm}$	$\delta_{\text{C}}/\text{ppm}$
11.40 (1H, s)	124 (CH)		129 (CH)
7.71 (1H, d)	118 (CH)	7.86 (1H, d)	122 (CH)
7.2-7.3 (2H, m)	115 (CH)	7.44-7.56 (2H, d)	121 (CH)
6.95 (1H, m)	111 (q)	7.26 (1H, d)	116 (q)
5.29 (2H, s)	107 (CH)	6.44 (2H, s)	109 (CH)

Table 7 Comparison of the important ^1H and ^{13}C NMR chemical shifts for **168** and **253**.

The benzisoxazole derived series below in Scheme 97 was synthesised utilising standard azo coupling reactions, with the various couplers which have been used before in Scheme 87 above, so a comparison of the UV-Vis data could be made. The dimedone **254**, Meldrum's acid **255** and 1,3-dimethylbarbituric acid **256** derivatives were all obtained as yellow solids, and were very insoluble in water as expected.

The insoluble nature of these compounds meant that ^{13}C NMR spectra were difficult to obtain, and when they were run, quaternary peaks were difficult to identify. Table 8 shows a comparison of NMR data for **221** and **254**. The signals in the ^1H NMR and ^{13}C spectra for **254** are at a slightly higher frequency than those observed for **221**. The yields for this series were less, (**254** 82%, **255** 52% and **256** 50%), and the reactions were not as clean as the non-aqueous diazoindazole couplings.



Scheme 97

Benzisoxazole 254		Indazole 221	
$\delta_{\text{H}}/\text{ppm}$	$\delta_{\text{C}}/\text{ppm}$	$\delta_{\text{H}}/\text{ppm}$	$\delta_{\text{C}}/\text{ppm}$
14.53 (NH)	131.49	15.45 (NH)	125.48
8.28	124.49	13.20 (NH)	119.36
7.68	124.00	8.28	119.22
7.43	110.03	7.43	108.31
2.66 (CH ₂)	51.70 (CH ₂)	7.23	49.25 (CH ₂)
0.98 (CH ₃)	27.78 (CH ₃)	2.62 (CH ₂)	25.55 (CH ₃)
		1.05 (CH ₃)	

Table 8 Comparison of NMR data for benzisoxazole derivative **254** and indazole derivative **221**

2.27.1 UV-Vis Data

The UV-Vis spectra were first recorded in methanol, as were these of the model indazole series above, but very low extinction coefficients and unsymmetrical curves were obtained. It was thought that perhaps the ligands were not soluble enough in methanol, and therefore, the spectra were recorded in DMF solution, the results of which are shown in Tables 9 and 11. The UV-Vis curve shapes in DMF were symmetrical with a steep high wavelength side, and a bathochromic shift was

observed when changing the solvent from methanol to DMF. The ϵ value also increased, and the half-band width values are by far the narrowest curves seen for any of the compounds discussed in this thesis. It is known that solvent effects are more pronounced in polar solvents than in non-polar solvents. It is also believed that in many coloured compounds, the ground state is less polar than the excited state, and therefore a more polar solvent will stabilise the excited state more than the ground state, causing a bathochromic shift.¹⁹

Benzisoxazole Derivatives

Coupler	Compound	DMF	
		$\lambda_{\text{max}}/\text{nm}$	$\epsilon/\text{l mol}^{-1}\text{cm}^{-1}$
Dimedone	254	383	38 000
Meldrum's Acid	255	369/467	33 000
1,3-Dimethyl Barbituric Acid	256	371	47 000

Table 9 Comparison of UV-Vis data for the benzisoxazole derivatives in DMF.

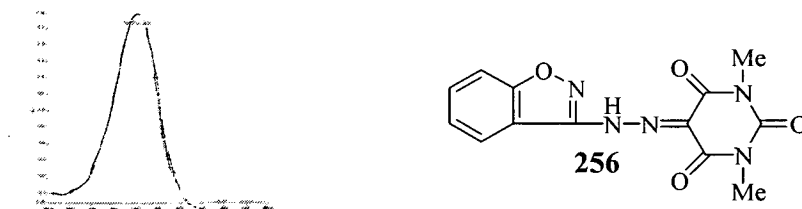


Figure 33 UV-Vis curve in DMF, for **256**, which is typical for the compounds in Scheme 97.

Indazole Derivatives

Coupler	Compound	Methanol	
		λ_{\max}/nm	$\epsilon/\text{l mol}^{-1} \text{cm}^{-1}$
Dimedone	221	422	19 400
Meldrum's Acid	222	398	21 600
1,3-Dimethyl Barbituric Acid	224	411	20 000

Table 10 Comparison of UV-Vis data for indazole derivatives in methanol.

Coupler	Compound	Benzisoxazole	Indazole
		DMF	Methanol
		$w_{1/2}/\text{nm}$	$w_{1/2}/\text{nm}$
Dimedone	254, 221	46	90
Meldrum's acid	255, 222	41	85
1,3-Dimethyl Barbituric Acid	256, 224	43	80

Table 11 Comparison of half-band widths for indazole and benzisoxazole derivatives.

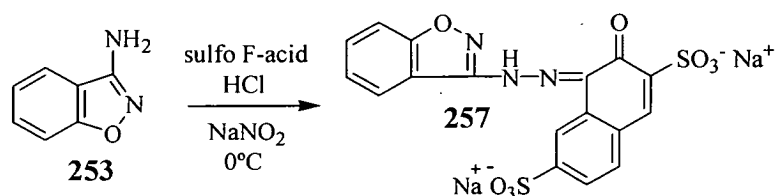
The UV-Vis spectra of the indazole derivatives were also recorded in DMF, but were very unpredictable. The curve shapes were not as symmetrical as those recorded in methanol, with shoulders appearing at the high wavelength side of the spectra; λ_{\max} and ϵ values varied greatly and are therefore not reported.

2.27.2 Synthesis and Metallisation of 257

To examine the effect of replacing an oxygen atom for the NH moiety in the indazole derivatives on the metallisation, 3-aminobenzisoxazole **253** was coupled to sulfo F-acid, as shown above in Scheme 98. Compound **257** was surprisingly easy to isolate

from water (formed as a precipitate), despite the presence of the two sulfonic acid groups.

The metallisation process was firstly examined on a small scale by UV-Vis spectroscopy, as with the previous studies.



Scheme 98

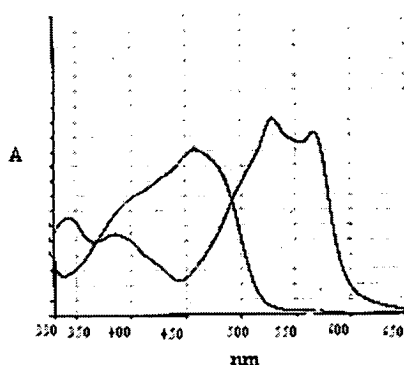


Figure 36 UV-Vis curves obtained for ligand **257** and metallised complex.

The ligand **257** was dissolved in deionised water giving a λ_{max} of 459 nm and a weak extinction coefficient of $9\,000\text{ l mol}^{-1}\text{ cm}^{-1}$. An approximate ten fold excess of nickel (II) acetate tetrahydrate was added to the orange coloured solution, causing an instantaneous colour change to purple, with a λ_{max} of 530 nm and a weak extinction coefficient of $11\,000\text{ l mol}^{-1}\text{ cm}^{-1}$. The metallised UV-Vis spectrum showed the familiar double maxima, with the second peak absorbing at around 570 nm. The curve again has become narrower with a half-band width of 98 nm, compared with the 122 nm observed for the ligand.

The oxygen atom has had an effect on the spectra obtained, with the ligand **257** and its complex differing from that of the indazole analogue **247**. The ligand λ_{max} values

were 460 nm for **257** *cf.* 470 nm for **247**, whereas the metallised complexes were 530 nm for **257** *cf.* 545 nm for **247**. The half-band width of the benzisoxazole complex is greater than that obtained for the indazole analogue (98 nm *cf.* 90 nm), and the extinction coefficient is reduced significantly (11 000 l mol⁻¹ cm⁻¹ *cf.* 22 000 l mol⁻¹ cm⁻¹). Again, similar to the model derivatives above, **257** was much less soluble than the corresponding indazole analogue **247**, and may account for the low extinction coefficient. The synthesis of **257** was then scaled up to give enough material for a potential metallised dye that could be tested, which was achieved without any problem, giving 6 g of product.

Small scale metallisation studies were then carried out to determine the end point of this process. Small aliquots of nickel (II) (0.1 eq.) were added to the ligand **257** solution at pH 7, and the UV-Vis spectra were recorded. This however, did not match the behaviour of the corresponding indazole analogue **247**.

HPLC did not prove a good method for following this process, as again similar to the above discussion, the complex was not apparent on the trace. Only the starting ligand **257** was present after the addition of one equivalent of nickel (II). Further additions were made, and more than two equivalents were eventually added, but still the UV-Vis spectrum consisted of mainly ligand **257**; less than 50% conversion to the metallised complex had occurred.

Another experiment was carried out, where after the addition of 1 equivalent of nickel (II), the metallised solution was stirred for 24 hours. The UV-Vis curve obtained immediately after the addition of nickel (II) was identical to that obtained after 24 hours. The metallisation was still occurring instantaneously, but **257** was a poorer ligand than the corresponding indazole ligand **247**, and requires greater quantities of nickel to force the equilibrium towards the metallised complex.

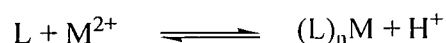
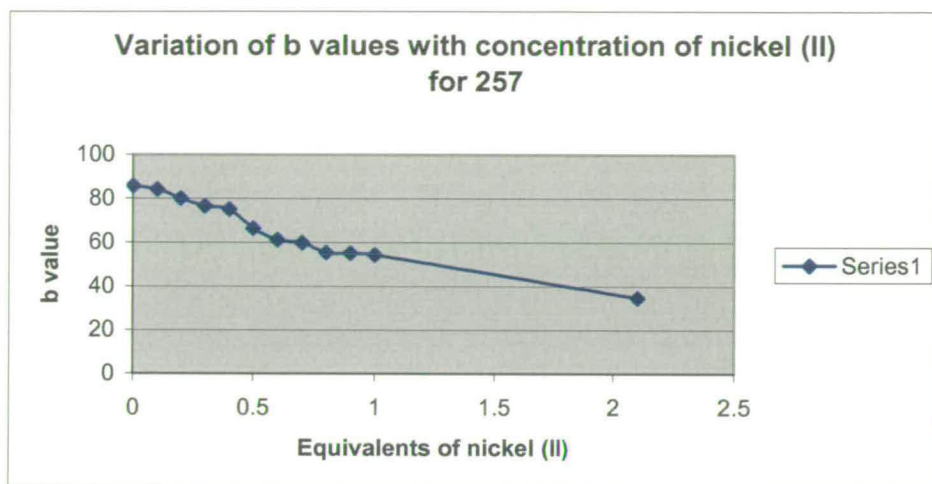


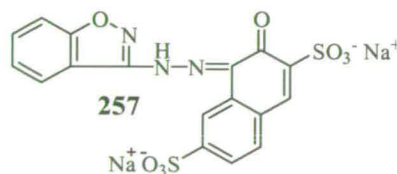
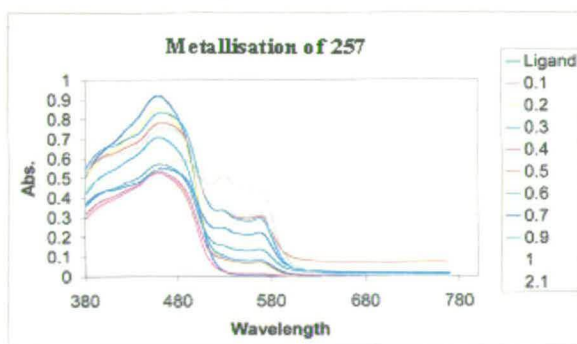
Figure 37 The equilibrium that exists in the metallisation process.

The plot of the various *b* values at different concentrations of nickel (II) in Figure 38, shows that the *b* value is still decreasing, and has not become constant as in Figures 31 and 33, indicating that the metallisation process is not complete.

At this stage, it was concluded that this compound was unsuitable as a potential ink jet dye due to the vast excess of nickel that would be required to form the complex, and therefore it would not be tested.



a.)



b.)

Figure 38 a.) Graph of *b* value against equivalents of nickel (II) added and b.) UV-Vis curves for quantitative addition of nickel (II) to **257**.

The only difference between **257** and the corresponding indazole analogue **247**, is the replacement of the NH for an oxygen atom, which is clearly having a significant effect upon complexation. Due to the more electronegative nature of oxygen compared with nitrogen (3.50 versus 3.07, Allred-Rochow formula), the electron density is pulled towards the oxygen in **257**, thus weakening the donor effect of the nitrogen at the 2-position.¹¹²

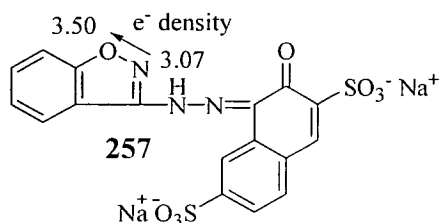


Figure 39 The electron density being attracted towards the oxygen atom in **257**

Furthermore, comparison of the pK_a data of indazole (1.2) with benzisoxazole (-4.2), shows that benzisoxazole is the much weaker base; for this reason, benzisoxazole derivatives are known to have very low reactivity as nitrogen donors, which is consistent with the results shown in Figure 38.^{119,120}

Derivative **259**, where the NH was replaced by a benzyl group, was then synthesised for further comparison.

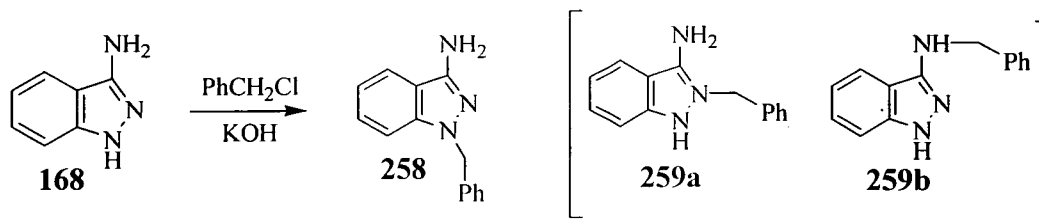
2.28 Synthesis of 1-Benzyl-3-aminoindazole **168** and reactions

To investigate the effect of structure on complexation further, 1-benylation of 3-aminoindazole **168**, and then coupling to sulfo F-acid to give **259**, was successfully carried out. Attempts to methylate the 1-nitrogen were unsuccessful, using an *N*-alkylation synthesis based on work previously done within the group. Methyl iodide was reacted with a basic solution of 3-aminoindazole,¹²¹ but only complex NMR spectra were obtained, and this method was not pursued any further.

The benzylation derivative **258** however is known in the literature, and was synthesised from the reaction between 3-aminoindazole **168** and benzyl chloride, under basic conditions, in 54% yield after column chromatography.¹²² The ¹H NMR

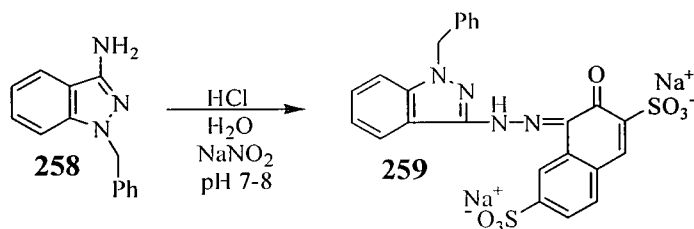
spectrum obtained matched that in the literature, with the CH₂ signal appearing at δ_{H} 5.30 ppm and δ_{C} 52 ppm.

It was thought that perhaps benzylation was also possible at the 2-position **259a** or 3-position **259b**, but the presence of the amine group at δ_{H} 4.01 ppm ruled out any of **259b**.



Scheme 99

The absence of the NH signal at δ_{H} 11.40 ppm in the ¹H NMR spectrum indicated which nitrogen (1- or 2-position) had been benzylated. The NOESY spectrum confirmed this further, as the benzyl CH₂ correlated to the two *ortho* protons on the phenyl ring and to the proton at the 7-position of the indazole aromatic ring. Only correlation between the CH₂ and the phenyl protons would be expected if benzylation had occurred at the 2-nitrogen.



Scheme 100

Compound **258** was then coupled to sulfo F-acid to give **259**, to give a comparison of the UV-Vis data and metallisation characteristics of **259**, with analogues **247** and **257**. The azo coupling proved difficult, and despite one initial success, was not easily reproduced. For reasons described above in Sections 2.13.4 and 2.25.6, careful monitoring of pH proved the key to the success of this reaction. The amine **258** was not soluble in aqueous, acidic or basic conditions alone, so acetonitrile was used as

the solvent, a slight modification on normal azo coupling reactions. The reaction was carried out at pH 7.5, and isolation of the product involved adjusting the pH to 3-4, resulting in the the azo compound precipitating.

The UV-Vis spectrum of **259** gave the usual broad curve of low intensity, with a λ_{\max} of 475 nm, and a ϵ value of 11 500 l mol⁻¹ cm⁻¹. One equivalent of nickel (II) was added to the solution and metallisation occurred quickly, with the expected colour change observed. This process was comparable with the indazole analogue **247**, and in contrast to the benzisoxazole **257** above, as no vast excess of nickel (II) was required to form the complex. This experiment showed that the NH was not essential for complexation to occur.

The curve obtained for the metallised complex was very good (see Figure 40), as there were no secondary absorptions or tails at high wavelengths. The λ_{\max} value of 558 nm was too high for an ideal magenta, with the second peak absorbing at just below 600 nm, and the ϵ value had increased to 16 800 l mol⁻¹ cm⁻¹ from 10 000 l mol⁻¹ cm⁻¹. As was discussed above for **257**, the ϵ value may be lower than that calculated for **247**, due to problems with solubility.

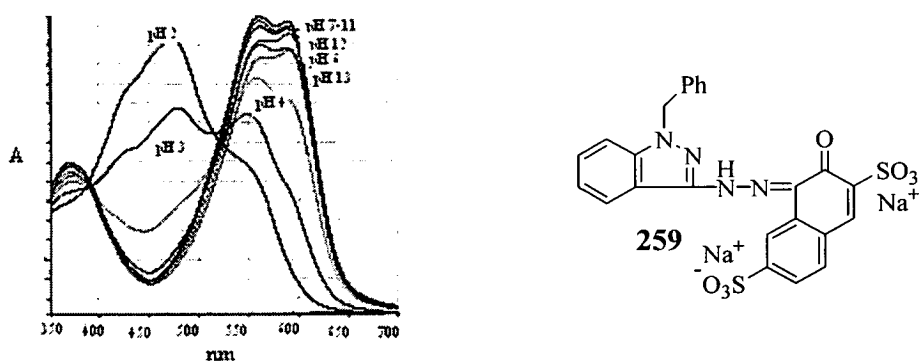


Figure 40 Variation of UV-Vis curves with pH for **259**.

The pH dependency of the metallisation process was also analysed by UV-Vis spectroscopy for this compound. At pH 2, only the free ligand **259** was observed, and

the solution was orange in colour. Two peaks then began to appear at pH 3, one corresponding to **259** and the other to the metallised complex of **259**. As the pH was increased further, the solution became the familiar purple colour associated with the metallised complex. From pH 4 onwards, the curves all resembled that of the metallised complex, with the only change being the increasing intensity of the curves, where it reached its maximum around pH 7-11. No further variation on the wavelength occurred, in contrast to the indazole derivative **247**, discussed in Section 2.26.1.3. The difference between **247** and **259** is obviously the addition of the benzyl group, and therefore no deprotonation can occur at high pH, resulting in a more stable complex. In **247**, loss of the NH proton at high pH may account for the variation in the spectra observed, which is not possible in **259**.

A similar study to those previously described in Section 2.26.1.5 was carried out, by adding small aliquots (0.1 eq.) of nickel (II) solution to the ligand, in order to determine the end-point of the process. The process was again followed by UV-Vis spectroscopy, but for the first time HPLC could also be used, as a peak corresponding to the metallised complex was apparent. Perhaps the increased molecular weight and bulkier benzyl group made this compound more stable. The ligand **259** appeared at 13.47 minutes on the HPLC trace, and a small peak appeared at 12.93 minutes after the addition of 0.1 equivalents of nickel (II). This peak at 12.93 minutes, which was assumed to be that of the metallised complex, increased in intensity as the number of equivalents was increased, whereas the ligand peak at 13.47 minutes decreased in intensity. The metallisation process appeared to occur readily for this compound, as after only 0.1 equivalents of nickel (II) were added, the UV-Vis curve corresponding to the metallised complex began to form, and no ligand was seen to remain after 0.3 equivalents. This process was followed up to 0.6 equivalents, where unfortunately, extra peaks began to appear on the HPLC trace. This was thought to be due to contamination, and the UV-Vis curves did not correspond to those obtained previously. The end-point of this process could not be predicted, so it was assumed to be ~0.85 equivalents, as with the indazole analogues discussed above.

The appearance of the metallised complex on the HPLC trace, and the stability at high pH, showed the increased stability of **259** compared with the other naphthol derived compounds discussed above.

2.29 Comparison of UV-Vis data for various sulfo F-acid derivatives

Compound	Ligand			Metallised Complex		
	λ_{\max}/nm	$\epsilon/\text{l mol}^{-1}\text{cm}^{-1}$	$w_{1/2}/\text{nm}$	λ_{\max}/nm	$\epsilon/\text{l mol}^{-1}\text{cm}^{-1}$	$w_{1/2}/\text{nm}$
247	467	12 400	178	545	21 900	90
257	459	9 200	122	530	10 800	98
259	475	10 000	182	557	16 800	110

Table 12 Comparison of UV-Vis data for the various sulfo F-acid derivatives and complexes

Table 12 shows the UV-Vis data for the three sulfo F-acid derivatives **247**, **257** and **259**. The addition of the benzyl group has caused an increase in the λ_{\max} values for ligand and complex. Derivative **257**, with the more electronegative oxygen atom, has the lowest values for λ_{\max} and ϵ , although as was discussed above, the less soluble nature of this derivative may account for the low ϵ value.

2.30 Metallised Complex Geometry

Several coordination possibilities exist for nickel (II) d^8 complexes, which can be either 4 (square planar, tetrahedral), 5 (trigonal bipyrimidal) or 6 (octahedral) coordinate, and it is difficult to predict which will predominate for these systems. The ligands are however, set up for square planar coordination to the metal, with three heterocyclic atoms available to coordinate. Due to the successful metallisation of **259**, it has been shown that the NH of the indazole is not essential for complexation to occur. It can therefore be concluded that coordination is not occurring at this site, and that it must take place at one of the nitrogen atoms in the

azo group, the nitrogen at the 2-position in the indazole moiety, and with the oxygen of the naphthol.

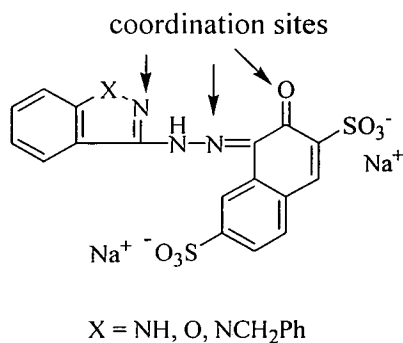
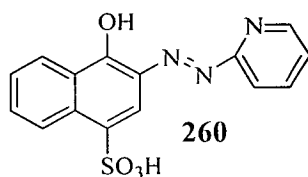


Figure 41 Coordination sites available in the various sulfo F-acid derivatives.

The stoichiometry of the complexes is also difficult to determine. It has been assumed that by adding 0.85 equivalents of nickel to the ligands discussed in Section 2.26.1.5, that 1:1 complexes are formed, but no evidence exists to support this assumption. Analysis of these complexes by mass spectrometry has proved unsuccessful; FAB and ESI methods have been used, but no molecular ion peaks corresponding to either a 1:1 or 1:2 complex have been found. Elemental analysis has also been generally unsuccessful, with the F-acid derivative **246** giving the only meaningful results; the metallised complex precipitated out of solution, and the elemental analysis results obtained were more consistent with a 1:1 complex than a 2:1 (ligand:metal), see Section 3.27. It seems likely however, that in general, a mixture of complexes is formed in these systems. Previous work has shown that various complexes are formed for the analogous 1-naphthol derivative **260** below, and also the corresponding 2-naphthol derivative, upon coordination to nickel.¹²³ A 1:1 complex was formed when large excesses of nickel were used, and a 2:1 (ligand:metal) complex was obtained when a moderate excess was used.



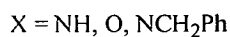
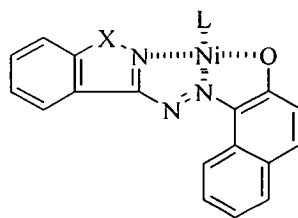


Figure 42 A 1:1 square planar metallised complex.

Figure 42 shows the d⁸ nickel coordinating to the ligand, forming a square planar 1:1 complex, and generating a stable 5,5 ring system. The remainder of the coordination sphere (L) would be made up from water or acetate molecules. If the complex formed was 2:1 (ligand:metal), then the nickel would be octahedral and 6 coordinate.

2.31 Dye testing

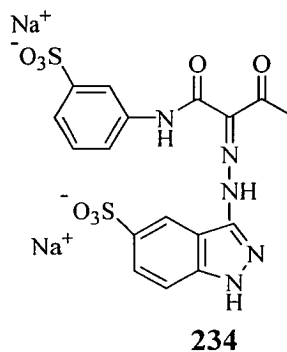
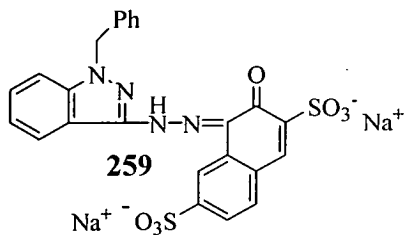
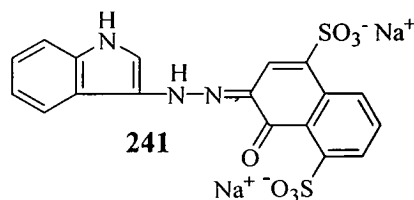
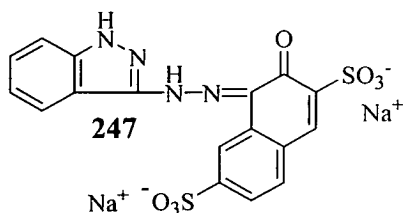
Due to their good UV-Vis results, the novel metallised magenta dyes **241**, **247**, and **259**, and the novel yellow dye **234**, were selected to be tested at Avecia, Blackley. The dyes fastness properties on exposure to light and ozone were tested, which is the main problem encountered for magenta dyes, and the colour properties were also established.

There are many different types of ink vehicles that could have been chosen for the dyes, with the dye making up 3-6% of the overall ink. A generic ink vehicle was used where the dye (0.3 g) made up 3% w/v of the ink. This was added to a 5:5:1 mixture of 2-pyrrolidone, diethylene glycol and Surfynol 465. 2-Pyrrolidone and diethylene glycol are humectants; high boiling water-miscible co-solvents that stop evaporation of the water when the printer is not in use; 2-pyrrolidone may also help overcome any small solubility problems. Surfynol 465 is a surfactant, which lowers the surface tension effecting rapid penetration of the ink into the medium (see Section 1.6). One unforeseen problem encountered with this procedure, was that the nickel complexes of **247**, and **259** in particular, were not sufficiently water soluble, and this had an effect on the results obtained (see below).

The pH of the three mixtures was adjusted to 8.5, and all were sonicated to aid solution. The α -naphthol derivative **241** was soluble enough for use after this, but the

other two **247** and **259** still had solid present, as was seen under the microscope, and had to be filtered. The benzylated derivative **259** was particularly troublesome, forming large crystal aggregates. By carrying out these filtrations the strength of the dyes was reduced, which affected the results obtained.

The yellow dye **234** proved to be the most soluble after sonification, and did not require filtration, but it was also weak due to the addition of salt during isolation, thus making the accuracy of estimation of the dye strength difficult. It was estimated at ~60% strength from the elemental analysis results.



Each of the four inks was then injected *via* a syringe into the ink cartridge, which was then loaded into an HP 5550 printer, and prints of the four dyes were obtained on seven different types of paper. The various papers would have a great effect on the dyes in print. Three plain papers were used; Xerox Acid (Xerox), HP Printing Paper and HP Multipurpose. Three microporous papers were used; Canon HG 201 (alumina humidity microporous), Canon PR101 (PR101) (alumina microporous) and SEC Premium (SEC) (silica microporous). One swellable paper was used; HP Premium (see Section 1.13). All the various tests below were performed for each of the four inks on all seven of the above papers.

2.31.1 Colour Measurements

The colour properties of a dye in print may vary from those of the dye on its own, due to pH changes, paper properties *etc.*, and can be measured using a colorimeter. Measurements are taken, by simply holding the instrument directly over the prints, to measure the reflectance, which was converted to the reflectance optical density (ROD) using equation 1, see Section 1.11.3. It is desirable to have a high ROD value, as more dense colour will then appear on the paper, and less white paper will show through. The L, a, b, c and h values were also calculated using this instrument.

Due to the insoluble nature of the magenta dyes, and the weak strength of the yellow dye, the ROD values were all quite low. Dyes **247** (~0.57), **259** (~0.25) and **234** (~0.28) were all very weak, and an ideal ROD value would be approaching 1, especially for the yellow dye **234**. Dye **241**, gave the highest ROD values (ranging from 0.67-1.07), which was not unexpected, as it was also the most soluble of the magentas. These values do vary greatly, as do the L, a, b, C and h values, depending on the paper used. Higher ROD values are obtained for the coated papers, where more of the ink is held at the surface, compared with a plain paper where there are voids for the ink to flow into.

The h value (hue) is measured as an angle, and a magenta would ideally be around 340°. The three magenta dyes gave values ranging from 293° to 320°; they all gave values that were too low, (or too blue), a trend also reflected in the high λ_{\max} values. These dyes were also too dull, reflected in the C values, (a measure of brightness), which were all too low. **247** gave values ranging from 25-53, **241** from 39-69, and **259** from 17-24. A good indication for all the dyes, is that a c value of 60 is required on the Xerox Acid plain paper, whereas values of only 20-38 were obtained.

The yellow dye **234** was very weak due to the unknown strength, caused by the addition of the salt upon isolation. The c value was very low (20-30) and the L value was far too high, or too white. This L value however, was probably due to the low loading of the sample, as the less sample on the paper, then the more white will show through, and the lighter the image that is formed. An ideal yellow would have an h value of about 90°; a value of about 115° was observed for the yellow **234**, which is venturing into the green area.

It should also be noted that the L, a, b, C and h values observed for the dyes in print, differed from those measured for the dye itself in aqueous solution. The values in Table 13 were recorded during the synthesis of each of the dyes.

Dye	L	a	b	C	h/°
247	58	62	-28	68	336
241	55	54	-50	74	317
259	51	36	-45	58	308
234	100	-7	10	12	118

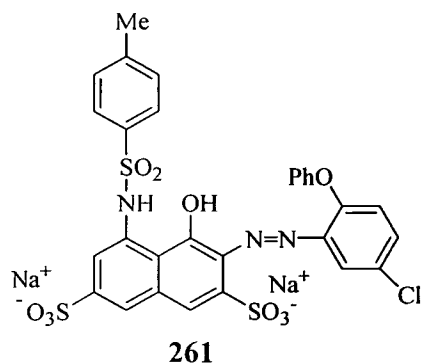
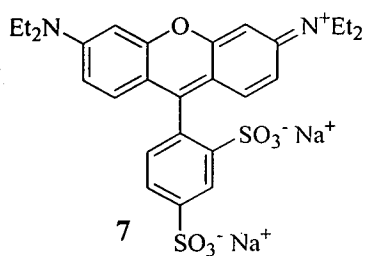
Table 13 Colour properties of the dyes in water.

The a and h values of the magentas have all decreased in print, whereas the L values have all increased, except in the case of **241** where a slight decrease was seen. The increase in the L values in print, is due to the poor solubility of the compounds, whereas **241**, the most soluble magenta, was fairly constant. The change in the other values may be due to interactions with the paper; the data in Table 14 is an example of the values obtained on a typical plain paper.

Dye	L	a	b	C	h/°
247	61	39	-31	50	321
241	53	13	-36	38	290
259	79	10	-17	20	302
234	93	-8	21	22	111

Table 14 Colour properties of the dyes in print on the plain paper Xerox Acid.

For comparison with the colour properties, in print, of the four dyes above, the colour data for the two magenta dyes Acid Red 52 7 and Acid Red 249 **261** are listed below in Tables 15 and 16. The inks were formulated in the same way as for those described above, and were tested on three of the same papers.



Acid Red 52 7

Paper	L	a	b	C	h/°
SEC	40	89	-43	99	334
Xerox	43	66	-31	73	355
PR101	39	86	-37	93	337

Table 15 Colour properties for magenta dye Acid Red 52 7, on several papers.

The first thing to notice is that the values vary with the different papers, largely due to the different structures or coatings of each paper. Lower L values are observed than those for the magenta dyes above, indicating a higher loading of the sample, with not as much of the paper showing through. Acid Red 52 7 is known to give brilliant bright magenta shades, reflected in the h values which are in the correct range (~340°). The C values in Table 15 are much higher than those for the dyes above, indicating that 7 is brighter, especially on the coated papers. Furthermore, an excellent value of 73 was observed on the plain paper, where 60 is deemed to be a good result.

Acid Red 249 261

Paper	L	a	b	C	h/°
SEC	49	84	4	84	363
Xerox	53	64	1	64	361
PR101	50	83	9	83	366

Table 16 Colour properties for magenta dye Acid Red 249, on several papers.

The results for Acid Red 249 261 in Table 16 show a similar comparison. The dye is brighter, more concentrated, and the h values are closer to the 340° mark, than those observed for 241, 247 and 259. The h values at greater than 360° were however, not as close to 340° as those observed for 7.

2.32.2 Fastness Properties

Three different tests were carried out on these dyes; light fastness, ozone fastness and water fastness. The ozone test was an accelerated test lasting 24 hours at a constant ozone concentration of 1 ppm that simulated 100 days in an office, and light fastness tests lasted 100 hours at a relative humidity of 40%. The dyes fastness properties are easily and best seen from the ROD percentage loss column in the appendix, where the lower the value recorded, then the better the dye has performed. Upon fading, the L, a, b, C and h values change, which is not surprising, as the dye is becoming less dense.

In general, the light and water fastness properties were good, but the magenta dyes would fail on some media due to their poor ozone fastness.

All three magenta dyes showed reasonable light fastness, giving best results on the swellable and silica microporous papers (ROD losses of 3-7%), with 247 giving the best results. It was advised that plain papers could be discounted for the light fastness results, as results are always poor on these papers; losses of up to 32% were observed (after 100 hours).

Ozone fastness is known to vary with paper in the following order, porous < plain < swellable (swellable being best); HP Premium (swellable paper) generally gave the

best results. The ozone molecules cannot get in to attack the dye, as the ink is held and protected beneath the swellable coating (see Section 1.13).¹⁷

The sulfo F **247** and α -naphthol **241** derivatives, both showed poor fastness to ozone, particularly on the porous papers (losses of ~90%). Ozone molecules are absorbed into the pores of a print, and attack the dyes. A catalytic effect is believed to occur, with for example silica porous papers, which increases the rate of incorporation of ozone into the paper.¹⁷

Better results were obtained for the plain papers (6-11%), and excellent results were obtained for the swellable paper, as expected (3-4%). The best ozone results came from the benzylated derived dye **259**, and the values reported would be acceptable. Very low ROD losses were obtained for **259** on the plain and swellable papers (3-7%), whereas the loss on the porous papers was still high (64-70%), but less than for the other magenta dyes. It was thought that perhaps the absence of the NH may be having an effect, and that the molecule has some π stacking occurring due to the extra aromatic ring, or aggregates may be forming at this level of concentration, hindering attack by the ozone molecules.

To see if this derivative was forming sheet like aggregates, (this compound was also the least soluble), an experiment was conducted to see if it obeyed the Beer-Lambert law. The UV-Vis spectra were recorded at various concentrations, and then a plot of absorbance versus concentration was made. This plot gave an excellent straight line which passed through the origin, and therefore, obeyed the Beer-Lambert law. It was concluded that aggregation was not occurring in solution, the dye displayed good resistance to ozone, and that it was just less soluble than the others; the addition of the extra aromatic ring would not have helped the solubility. This increased stability was also observed from the HPLC results, as this complex was the only one to appear on the traces.

Plot of absorbance versus concentration for metallised complex of derivative 259.

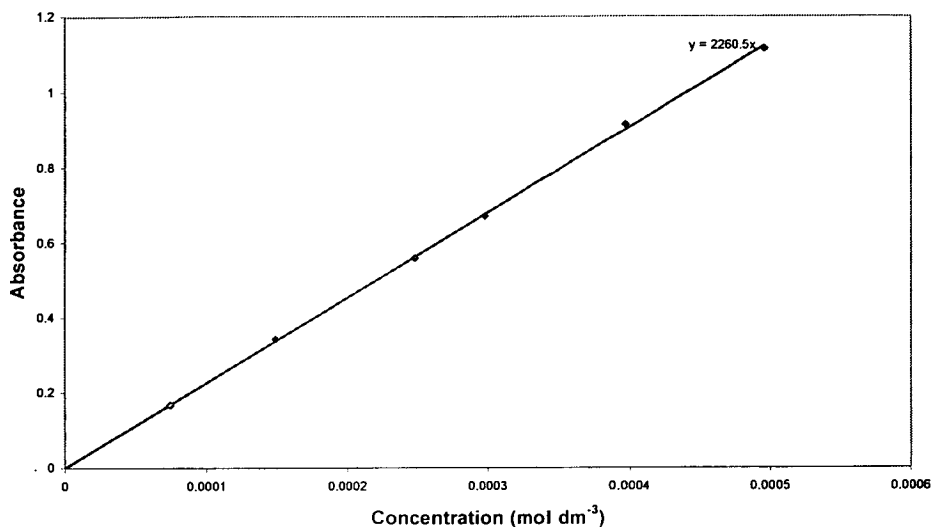


Figure 43 Beer-Lambert plot for derivative 259.

The yellow dye **234** also displayed reasonable ozone fastness, showing similar trends on the different papers to the magenta dyes, with best results on the swellable paper (5%) and poorest on the porous paper (46%). On the other papers, moderate losses of around 15% were observed.

The two dyes below in Tables 17 and 18 are known not to be particularly photostable, and their results for lightfastness percentage loss (LF) and ozone fastness percentage loss (OF) are listed. Acid Red 52 7 was one of the first magenta dyes used (see Section 1.19.2), and was not chosen for its light fastness, but its brilliant magenta shades.

Acid Red 249 261

Paper	LF (% Loss)	OF (% Loss)
SEC	52	7
Xerox	83	2
PR101	72	44

Table 17 Light and ozone fastness results for Acid Red 249 261.

The light fastness results were very poor for this dye, and the three magenta dyes above were far better, which demonstrates how much more photostable metallised complexes are. The ozone results were however, very good, displaying the usual trend described above for each of the papers, and were better than the magenta dyes above.

Acid Red 52 7

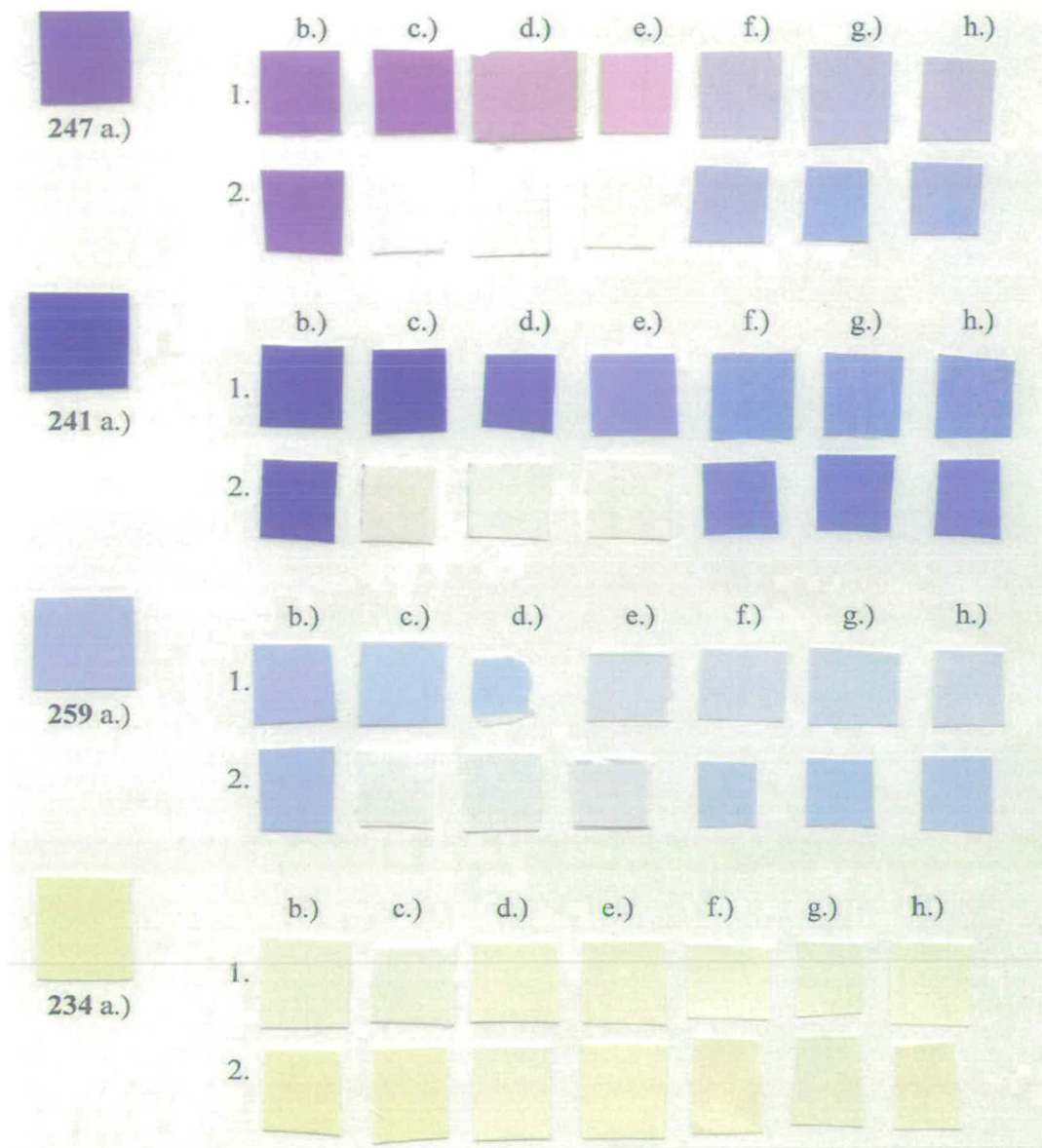
Paper	LF (% Loss)	OF (% Loss)
SEC	97	76
Xerox	78	1
PR101	98	48

Table 18 Light and ozone fastness results for Acid Red 52 7

The light fastness and ozone results were very poor for this early magenta dye, although on the plain paper excellent ozone results were obtained.

2.32.3 Water Fastness

Several horizontal bars or strips were made from each of the prints, and were held at 45°. Water was then dripped across these strips, at various time intervals. The ROD values were then measured between the horizontal strips, to see how much colour had accumulated there. The ROD values of the papers themselves were also recorded, and subtracted from the ROD values obtained. The more colour that was between the bars, then the less water fast the dye was, as the greater the amount of colour that had run. These results proved to be very good, and all dyes would be acceptable on this account. The α -naphthol derived dye 241 displayed the poorest wet fastness results, which was also the most water soluble magenta dye.



a.) Dye prints before testing on HP Premium Paper, b.) after testing on HP Premium
 c.) after testing on Epson Premium, d.) after testing on Canon PR101, e.) after testing
 on Canon HG201, f.) after testing on HP Multi-Purpose, g.) after testing on HP
 Printing, h.) after testing on Xerox Acid.

1. Dye prints after light fastness tests, 2. Dye prints after ozone fastness tests.

2.32.4 Dye Testing Conclusions

The main problem identified for these dyes, was the colour properties. The magenta dyes were all too blue, as shown by the low h values. The UV-Vis curves also showed this, with their higher than ideal λ_{max} values. The yellow dye also had a problem with its colour, as the UV-Vis curve gave a λ_{max} value that was too low, and high h values were obtained. The low loading of the samples, made results difficult to interpret, and this was partly responsible for the low ROD values and high L value. Experiments could be carried out with higher loading of the samples to give more meaningful results, but the solubility of **247** and **259** would have to be improved, by adding yet another sulfonic acid group. The salts present in the yellow sample could be removed to give a more accurate indication of the dye strength, which would improve the loading.

However, the main problem of the dyes being the incorrect shade of magenta would not be so easily solved, and would require the addition of electron donating or withdrawing groups (see Section 1.17) to alter the hue.

2.33 Conclusions

Three new classes of azo dye derivatives have been successfully synthesised *via* high yielding non aqueous and aqueous coupling reactions. A high yielding route to 3-aminoindazole **168** was developed, from which diazoindazole **170** was obtained. Model yellow compounds and water soluble yellow dyes were synthesised utilising high yielding coupling reactions.

Diazoindazole **170** was coupled to several sulfonated naphthol derivatives, giving a series of novel water soluble magenta compounds. Extensive UV-Vis work was done to analyse the colour properties of these compounds, stability, and also to monitor the various metallisation processes, which were all successful when the ligands were reacted with Ni (II) solutions.

The effect of structural change upon metallisation was investigated by synthesising the benzisoxazole derivative **257**, and the benzylated derivative **259**, using standard aqueous coupling reactions, and then monitoring the metallisation processes. The results of metallisation of **247**, **257** and **259** showed that the NH moiety was

favourable over the oxygen atom, but not essential as successful metallisation of **259** proved.

Several dyes were selected for applications testing, where their colour properties were investigated, along with examining their stability upon exposure to ozone and light.

3. EXPERIMENTAL

3.1 ABBREVIATIONS

^1H NMR	proton nuclear magnetic resonance
^{13}C NMR	carbon-13 nuclear magnetic resonance
$\delta_{\text{H}}, \delta_{\text{C}}$	chemical shift
CDCl_3	deuteriated chloroform
$[\text{}^2\text{H}]_6\text{DMSO}$	deuteriated dimethyl sulfoxide
DMSO	dimethyl sulfoxide
DMF	dimethyl formamide
THF	tetrahydrofuran
DCM	dichloromethane
F-Acid	sodium 2-naphthol-7-sulfonic acid
Sulfo F-Acid	disodium 2-naphthol-3,7-disulfonic acid
Chromotropic Acid	disodium 1,8-dihydroxynaphthalene-3,6-disulfonic acid
R-Acid	disodium 2-naphthol-3,5-disulfonic acid
HPLC	high performance liquid chromatography
TLC	thin layer chromatography

mmol	millimoles
mol	moles
s	singlet
d	doublet
dd	doublet of doublets
t	triplet
q	quartet
m	multiplet
br	broad
quat	quaternary
<i>J</i>	coupling constant
Hz	Hertz
MHz	megaHertz
FAB	fast atom bombardment
EI	electron impact
<i>m/z</i>	mass to charge ratio

λ_{\max}	peak wavelength
ϵ	molar extinction co-efficient
$w_{1/2}$	width of UV-Vis curve at half the maximum absorbance
M^+	molecular ion mass (EI)
MH^+	molecular ion mass (FAB)
UV-Vis	Ultraviolet-Visible spectroscopy
h	hours
min	minutes
cm³	cubic centimetres
w/v	weight/volume
g	grams
°C	degrees Celcius
mp	melting point
bp	boiling point
lit.	literature value
eq.	equivalents

ROD	reflectance optical density
HOMO	highest occupied molecular orbital
LUMO	lowest unoccupied molecular orbital

3.1.1 FVP Abbreviations

FVP Flash Vacuum Pyrolysis

T_f furnace temperature

T_i inlet temperature

P pressure

m_a mass of substrate used

3.2 INSTRUMENTATION

a.) Nuclear Magnetic Resonance Spectroscopy.

¹H NMR spectra were recorded on DPX360 (360 MHz), Bruker ARX250 (250 MHz), and a Varian Gemini 200 (200 MHz). ¹³C NMR spectra were recorded on DPX360 (90 MHz), Bruker ARX250 (63 MHz) and Bruker AC200 (50 MHz) spectrometers.

The DPX360 was operated by Mr S.I. Wharton and the Bruker ARX250 was operated by Mr J.R.A. Millar.

¹H and ¹³C spectra were recorded in [²H]chloroform solution, unless otherwise stated. Chemical shifts are quoted in parts per million relative to tetramethylsilane ($\delta = 0.0$) and all coupling constants are given in Hertz.

b.) Mass Spectrometry

Low resolution electron impact mass spectra were recorded on a Finnigan 4600 instrument by Mr A.W.Taylor and Mr H.G. McKenzie. FAB mass spectra were recorded by Mr A.W.Taylor on a Kratos MS50 TC instrument.

c.) Elemental Analysis

Microanalyses were carried out on a Perkin Elmer 240 CHN Elemental Analyser by Mr T. Calder and Mrs. S. Djurdjevic.

d.) Structure Determination

X-ray crystal structure data were obtained and solved by Miss F. P. A. Fabbiana, Mr I. Oswald and Dr. S. Parsons and on a Stoe STADI-4 four circle diffractometer with graphite monochronator.

e.) UV-Vis Spectroscopy

All UV-vis spectra were recorded by Mr K. J. Boyle on a Perkin-Elmer 900 Lambda spectrometer instrument and a Shimadzu UV-1601 UV-visible Spectrophotometer at Avecia, Grangemouth.

f.) Melting Points

Melting points were measured on a Gallenkamp capillary tube apparatus and are uncorrected.

g.) Chromatography

Thin-layer chromatography was carried out on Merck aluminium-backed plates coated with Kieselgel GF254 (0.2 mm), impregnated with an ultra violet indicator.

Dry-flash column chromatography was carried out on Kieselgel GF254 silica. The crude materials were pre-absorbed onto silica gel using dichloromethane, and then loaded onto the column. Elution was carried out under a vacuum supplied by a water pump or a diaphragm pump.

h.) HPLC

High Performance Liquid Chromatography was carried out on a Chemstation HP1100 Series at Avecia, Grangemouth.

i.) Solvents and reagents

All reagents were standard laboratory grade and were used as supplied, unless specifically stated in the text. Solvents for general use were standard laboratory grade and were used as supplied, unless specifically stated in the text.

j.) Light Fastness

Light fastness tests were conducted on an Atlas Ci 5000 Xenon Weather-Ometer at Avecia, Blackely, using a water cooled Xenon Argon lamp as a light source, for 100 h. The relative humidity was 40%, back panel temperature was 63 °C and wet bulb temperature was 16 °C.

k.) Ozone Fastness

Ozone fastness tests were conducted on a 903 Hampden Ozone Test Chamber, at Avecia, Blackely. The relative humidity was 50% and the temperature was 40 °C. A constant ozone concentration (1 ppm) was maintained for 24 h on a rotating carousel.

1.) Colour Measurements

The ROD values were recorded using a Spectrolino Gretag Macbeth instrument, at Avecia, Blackely. The illumination source was D65, the observer angle was 2° and the density standard was ANSI A.

3.3 Flash Vacuum Pyrolysis

The apparatus used in flash vacuum pyrolysis (FVP) is outlined in Figure 44, and is based on the design of W.D. Crow of the Australian National University.

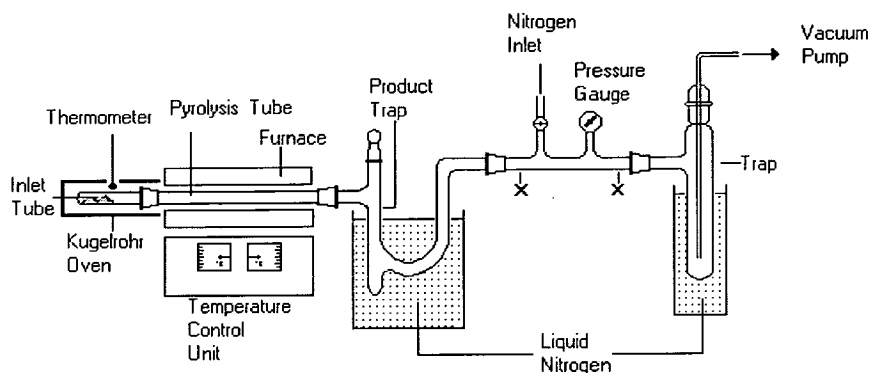
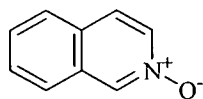


Figure 44 The apparatus used in a typical flash vacuum pyrolysis experiment.

The substrate is placed in the inlet tube which is heated by a Kugelrohr oven, causing the substrate to vaporise in the furnace tube; silica (30 cm \times 2.5 cm). The pyrolysis tube is held at the desired temperature, typically 400-1000 $^{\circ}$ C, by the electronically controlled furnace Model No MTF 12/338/250. The apparatus is maintained at a vacuum of 10^{-2} - 10^{-3} Torr by an Edwards Model ED100 high capacity oil pump. Reaction products are collected in a U-shaped trap, cooled in liquid nitrogen, at the exit of the furnace. The apparatus ensures that the substrate is in the hot zone for a very short contact time (\sim milliseconds). The low pressure ensures that intramolecular reactions are more likely than intermolecular reactions. This results in cyclisations, rearrangements and eliminations, in preference to bimolecular coupling reactions. Once the reaction is complete, the pump is isolated and the trap is allowed to warm to room temperature under an atmosphere of nitrogen. The product is then removed from the trap in [2 H]chloroform, from which crude 1 H and 13 C NMR spectra were recorded, or in dichloromethane for further work-up.

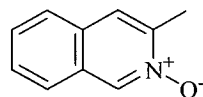
Pyrolysis parameters are quoted as follows: furnace temperature (T_f), inlet temperature (T_i), pressure (P) and quantity of substrate (m_a).

3.4 General synthesis of isoquinoline *N*-Oxides



Isoquinoline (12.9 g, 0.1 moles) was dissolved in glacial acetic acid (30 cm³), and was treated with dilute hydrogen peroxide solution (30%, 10 cm³).²⁷ The solution was heated at 60-70 °C for 3 h, after which, further hydrogen peroxide (8 cm³) was added, and the reaction mixture was heated at 60-70 °C for 9 h. The solution was then allowed to cool and concentrated to about 20 cm³, by careful rotary evaporation. Water (20 cm³) was added and the solution was concentrated further to about 15 cm³. Chloroform (30 cm³) was then added to the concentrate, the solution was poured onto a paste of potassium carbonate (5 g) and water, shaken, and left overnight. The organic layer was separated, dried with MgSO₄ and evaporated to give a white solid which was identified as isoquinoline *N*-oxide dihydrate **29** (8.82 g, 61%) mp > 50 °C [lit.,²⁷ > 40 °C]; δ_H (250 MHz) 8.50 (1H, s), 8.08 (1H, dd, ³J 7.1, ⁴J 1.8) and 7.29-7.65 (5H, m); δ_C (63 MHz) 136.57 (CH), 135.93 (CH), 129.32 (CH), 128.86 (CH), 128.58 (2 × quat), 126.46 (CH), 124.78 (CH) and 124.07 (CH); *m/z* 145 (M⁺, 100%), 117 (61), 90 (85), 63 (43) and 43 (35). A wide ranging melting point was observed due to the hygroscopic nature of this material.

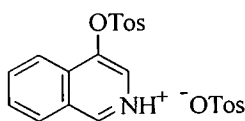
3-Methylisoquinoline *N*-Oxide **25**



3-Methylisoquinoline (1 g, 7 mmol) in glacial acetic acid (5 cm³), was treated with dilute hydrogen peroxide solution (30%, 0.71 cm³), and heated at 70 °C for 3 h, after which a further addition of hydrogen peroxide (0.57 cm³) was made. The work-up procedure was as above, and a white solid was obtained, which was identified as 3-methylisoquinoline *N*-oxide **25** (0.97 g, 81%) mp 135-136 °C [lit.,¹²⁵ 136-138 °C]; δ_H (250 MHz) 8.84 (1H, s), 7.68-7.72 (2H, m), 7.62 (1H, s), 7.50-7.54 (2H, m) and 2.64 (3H, s); δ_C (63 MHz) 145.76 (quat), 136.15 (CH), 128.98 (quat), 128.33 (quat), 128.54 (CH), 128.10 (CH), 125.68 (CH), 124.31 (CH), 122.94 (CH) and 17.56 (CH₃); *m/z* 159 (M⁺, 77%), 143 (51), 142 (100) and 115 (68).²

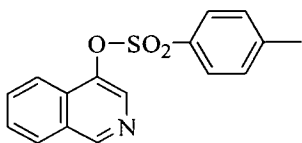
3.5 Rearrangement reactions

2-(*p*-Toluenesulfonyl)-4-(*p*-toluenesulfonyloxy) isoquinolinium 80



Isoquinoline *N*-oxide dihydrate **29** (1 g, 5.5 mmol) was dissolved in chloroform (30 cm³), and stirred in the presence of MgSO₄ overnight. The MgSO₄ was then filtered off and the solution was concentrated to about 20 cm³. The concentrate was cooled to 0 °C, and a solution of *p*-toluenesulfonyl chloride (1.1 g, 5.7 mmol) in chloroform (10 cm³) was added dropwise. A cloudy solution resulted which was heated on a water bath at 70 °C for 2 h, yielding a golden coloured solution. Dilute sodium carbonate solution (10%, 10 cm³) was added after the solution was allowed to warm to room temperature, and this solution was then stirred overnight.³ The organic layer was separated off, dried with MgSO₄ and evaporated. After removal of the solvent a yellow coloured oil was obtained, which soon solidified upon exposure to air. After recrystallisation 2-(*p*-toluenesulfonyl)-4-(*p*-toluenesulfonyloxy) isoquinolinium **80** was obtained as a yellow solid (1 g, 40%) mp 169-171 °C (from methanol) (Found: C, 58.6; H, 4.45; N, 3.0 C₂₃H₂₁NO₆ requires C, 58.7 H, 4.7, N, 2.9%); (Found: MH⁺ (FAB) 472.0891. C₂₃H₂₂NO₆S₂ requires *M* 472.0889); δ_H (250 MHz) 9.82 (1H, s), 8.58 (1H, d, ³*J* 8.4), 8.23 (1H, s), 8.12 (1H, d, ³*J* 8.4), 8.01 (1H, t, ³*J* 7.2), 7.90 (1H, t, ³*J* 7.4), 7.74 (4H, m), 7.30 (2H, d, ³*J* 8.0), 7.07 (2H, d, ³*J* 8.0), 2.37 (3H, s) and 2.26 (3H, s); δ_C (63 MHz) 147.18 (2 × quat), 146.53 (CH), 141.49 (quat), 140.21 (2 × quat), 136.66 (CH), 133.36 (2 × quat), 131.40 (CH), 130.59 (CH), 130.49 (2 × CH), 128.73 (2 × CH), 128.43 (2 × CH), 125.84 (2 × CH), 125.53 (CH), 121.81 (CH), 21.70 (CH₃) and 21.17 (CH₃); *m/z* (EI) 299 (53), 172 (41), 155 (86), 145 (27), 116 (62) and 91 (100); *m/z* (FAB) 472 (MH⁺, 22%) and 300 (100).

4-(*p*-Toluenesulfonyloxy)isoquinoline 32



Isoquinoline *N*-oxide dihydrate **29** (1 g, 5.5 mmol) and *p*-toluenesulfonyl chloride (1.1 g, 5.7 mmol) were reacted as above, but the tosylate salt was not isolated, and the addition of sodium carbonate was not made. The solution obtained after addition of the tosyl chloride was stirred at room temperature for 30

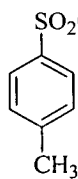
min, and was then washed several times with dilute sodium hydroxide solution (20% w/v) to remove the tosylate salt. The organic layer was separated off, dried with MgSO₄ and evaporated to give a pale yellow solid, which was identified as 4-(*p*-toluenesulfonyloxy)isoquinoline **32** (0.5 g, 30%) mp 91 °C [lit.,⁵⁰ 92-93 °C]; δ_H (250 MHz) 9.05 (1H, s), 8.02 (1H, s), 7.92 (2H, d, ³J 8.4), 7.71 (2H, d, ³J 8.3), 7.56-7.67 (2H, m), 7.24 (2H, d, ³J 8.0) and 2.37 (3H, s); δ_C (63 MHz) 151.09 (CH), 145.82 (quat), 141.87 (quat), 135.69 (CH), 131.89 (CH), 131.04 (quat), 130.32 (quat), 129.90 (2 × CH), 129.63 (quat), 128.44 (2 × CH), 128.04 (CH), 127.09 (CH), 120.99 (CH) and 21.59 (CH₃); *m/z* 299 (M⁺, 23%), 163 (37), 145 (47), 129 (21), 116 (72) and 91 (100). The ¹³C spectrum matched that in the literature.³²

4-(*p*-Toluenesulfonyloxy)isoquinoline **32**

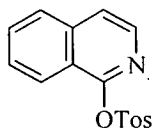
Isoquinoline *N*-oxide dihydrate **29** (0.5 g, 2.8 mmol) and *p*-toluenesulfonyl chloride (1.4 g, 2 eq., 5.7 mmol) were reacted as above. The chloroform layer obtained was washed several times with dilute sodium hydroxide solution (20% w/v) to remove the tosylate salt. The organic layer was separated off, dried with MgSO₄ and evaporated to give a yellow solid, which was identified from the ¹H NMR spectrum as a mixture of 4-(*p*-toluenesulfonyloxy)isoquinoline **32**, and an excess of *p*-toluenesulfonyl chloride.

4-(*p*-Toluenesulfonyloxy)isoquinoline **32**

Isoquinoline *N*-oxide dihydrate **29** (1 g, 5.5 mmol) and *p*-toluenesulfonyl chloride (1.1 g, 5.7 mmol) were reacted as above. The crude solid obtained was purified by

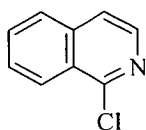
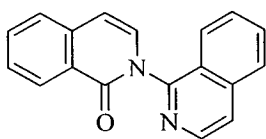


dry-flash chromatography, which yielded several compounds: *p*-toluenesulfonyl chloride **82** (73 mg, 9%); δ_H (250 MHz) 7.85 (2H, d, ³J 10.7), 7.32 (2H, d, ³J 9.7) and 2.41 (3H, s); δ_C (63 MHz) 146.71 (quat), 141.44 (quat), 130.08 (2 × CH), 126.85 (2 × CH) and 21.61 (CH₃); *m/z* 190 (M⁺, 54%), 163 (62), 155 (71), 145 (41), 128 (59) and 91 (100), 1-(*p*-toluenesulfonyloxy)isoquinoline **83** (61 mg, 4%); δ_H (250 MHz) 8.32 (1H, d, ³J 8.1),



7.90 (1H, d, ³J 8.3), 7.70 (1H, d, ³J 8.3), 7.20-7.64 (5H, m), 7.10 (1H, d, ³J 7.1), 6.47 (1H, d, ³J 7.1) and 1.96 (3H, s); δ_C (63 MHz) 171.00

(quat), 137.99 (quat), 132.45 (CH), 131.09 (CH), 129.87 (CH), 128.40 (CH), 128.06 (CH), 127.55 (CH), 127.08 (CH), 126.57 (CH), 126.02 (CH), 120.49 (CH), 106.62 (CH) and 20.86 (CH₃); *m/z* 299 (M⁺, 58%), 155 (87), 146 (66), 116 (87) and 91 (100); 4-(*p*-toluenesulfonyloxy)isoquinoline **32** (1.2 g, 76%); a mixture of products (70 mg) tentatively identified as 1-chloroisoquinoline **84**; *m/z* 165 (M⁺, 83%), 163 (M⁺, 100%), and 128 (90); isocarbostyryl *N*-isoquinoline **85**; *m/z* 271 (M⁺, 1%) and 145 (88). These by-products **83**, **84** and **85** have been previously identified.³²



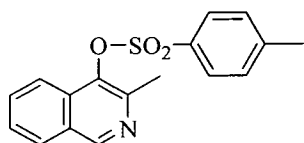
Attempts have been made to try to improve the work-up using various combinations of silica and methanol. The crude mixture obtained after addition of the *p*-toluenesulfonyl chloride was a.) refluxed in methanol and b.) stirred in a methanol/silica mixture, both resulting in very messy ¹H NMR spectra and unidentified products. The crude mixture was c.) absorbed onto silica and purified by dry-flash chromatography, by immediately washing off the column with methanol. The work-up then proceeded as above, for the synthesis of 4-(*p*-toluenesulfonyloxy)isoquinoline **32**, resulting in an improved 55% yield. The crude mixture was d.) absorbed onto silica and left on the dry-flash column for 24 h, before being washed off the column with methanol, but did not improve the yield further (46%).

4-(*p*-Toluenesulfonyloxy)isoquinoline **32**

Isoquinoline *N*-oxide dihydrate **29** (10 g, 0.055 mol) and *p*-toluenesulfonyl chloride (14.4 g, 0.07 mol) in chloroform (200 cm³), were reacted as above. The crude mixture was washed with dilute sodium hydroxide solution (10%, 3 × 200 cm³), the organic layer was separated off, dried with MgSO₄ and evaporated to give 4-(*p*-toluenesulfonyloxy) isoquinoline **32** (5 g, 30%). The aqueous layer was diluted with water (500 cm³), dichloromethane (500 cm³) was added, and the solution was continuously liquid-liquid extracted for 6 h, giving an unknown solid (1.1 g) after

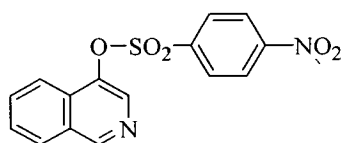
removal of the solvent, and messy NMR spectra. The aqueous layer was then acidified with concentrated hydrochloric acid, and continuously extracted with dichloromethane for a further 6 h. After removal of the solvent, 4-(*p*-toluenesulfonyloxy)isoquinoline **32** (0.5 g, 3%) was obtained.

3-Methyl-4-(*p*-toluenesulfonyloxy)isoquinoline **86**



3-Methylisoquinoline *N*-oxide **25** (100 mg, 0.63 mmol) was dissolved in chloroform (10 cm³) and cooled to 0 °C. *p*-Toluenesulfonyl chloride (127 mg, 6.6 mmol) was dissolved in chloroform (5 cm³) and added dropwise to the *N*-oxide solution, which was stirred at room temperature for 1 h, and then at 45 °C for a further 1 h. The solvent was removed *in vacuo* to give an orange solid, which was washed several times with dilute sodium hydroxide solution (20% *w/v*) to remove the tosylate salt. The organic layer was separated off, dried with MgSO₄ and evaporated to give a pale yellow solid that was identified as 3-methyl-4-(*p*-toluenesulfonyloxy) isoquinoline **86** (60 mg, 30%) mp 197-198 °C (from methanol) (Found: M⁺ 313.0775 C₁₇H₁₅N₄O₆S requires *M* 313.0773); δ_H (250 MHz) ([²H]₆DMSO) 9.62 (1H, s), 8.41 (1H, d, ³*J* 8.1), 7.93 (1H, t, ³*J* 8.4), 7.92 (2H, d, ³*J* 8.4), 7.86 (1H, t, ³*J* 8.1), 7.82 (1H, d, ³*J* 8.4), 7.55 (2H, d, ³*J* 8.5), 2.47 (3H, s) and 2.45 (3H, s); δ_C (63 MHz) 148.35 (CH), 146.65 (quat), 140.97 (quat), 139.62 (quat), 137.70 (quat), 134.17 (CH), 131.43 (quat), 130.48 (2 × CH), 128.97 (quat), 128.13 (2 × CH), 127.94 (CH), 125.29 (CH), 120.73 (CH), 21.05 (CH₃) and 16.78 (CH₃); *m/z* 313 (M⁺, 39%), 177 (67), 158 (54), 142 (41), 130 (64) and 91 (100). The regioselectivity of this reaction was confirmed by NOESY, which showed no correlation to the methyl group.

4-(*p*-Nitrobenzenesulfonyloxy)isoquinoline **88**

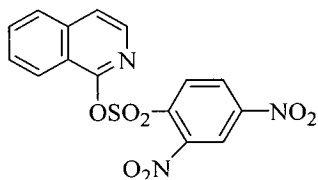


Isoquinoline *N*-oxide dihydrate **29** (0.5 g, 2.8 mmol) was dissolved in chloroform (10 cm³) and stirred in the presence of MgSO₄ overnight. The MgSO₄ was filtered off, and the solution was cooled to 0 °C. *p*-Nitrobenzenesulfonyl chloride (0.81 g, 2.8 mmol) was dissolved in chloroform (5

cm³) and added dropwise to the *N*-oxide solution, which was heated to reflux for 1 h. A precipitate formed during this time, which was filtered off and washed several times with dilute sodium hydroxide solution (20% w/v). The organic layer was separated off, dried with MgSO₄ and evaporated to give pale yellow solid, which was identified as 4-(*p*-nitrobenzenesulfonyloxy)isoquinoline **88** (0.2 g, 22%) mp 151 °C (Found: M⁺ 330.0315 C₁₅H₁₀N₂O₅ requires M 330.0310); δ_H (250 MHz) ([²H]₆DMSO) 9.36 (1H, s), 8.45 (2H, d, ³J 7.1), 8.29 (4H, m) and 7.81 (3H, m); δ_C (63 MHz) 151.98 (CH), 151.06 (quat), 140.76 (quat), 138.97 (quat), 135.39 (CH), 131.87 (CH), 130.02 (2 × CH), 129.23 (quat), 128.89 (quat), 128.57 (CH), 127.63 (CH), 124.96 (2 × CH) and 119.79 (CH); *m/z* 330 (M⁺, 56%), 203 (31), 186 (33), 144 (65), 116 (100) and 89 (87).

The solvent from the mother liquor was removed *in vacuo* to give a yellow solid (0.7 g), which contained *p*-nitrobenzenesulfonyl chloride, δ_H (250 MHz) ([²H]₆DMSO) 8.25 (2H, d, ³J 8.6) and 7.89 (2H, d, ³J 8.6); *m/z* 223 (M⁺, 9%), 221 (M⁺, 24%), 186 (78), 122 (64), 101 (72), 50 (100) and 46 (40). The procedure was repeated, with the reaction mixture being heated to reflux for 3 h, but there was no improvement in the yield.

1-(2,4-Dinitrobenzenesulfonyloxy)isoquinoline **91**



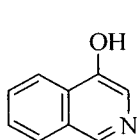
Isoquinoline *N*-oxide dihydrate **29** (0.5 g, 2.8 mmol) was dissolved in chloroform (10 cm³) and stirred in the presence of MgSO₄ overnight. The MgSO₄ was filtered off, and the solution was cooled to 0 °C. *p*-2,4-Dinitrobenzenesulfonyl chloride (0.97 g, 3.6 mmol) was dissolved in chloroform (5 cm³), and added dropwise to the *N*-oxide solution, which was heated to reflux for 1 h. 2,4-Dinitrosulfonyl chloride was not particularly soluble in chloroform, and a precipitate was obtained very quickly, which was identified as 1-(2,4-dinitrobenzenesulfonyloxy)isoquinoline **91** (0.4 g, 40%) mp 215 °C; δ_H (250 MHz) ([²H]₆DMSO) 8.56 (1H, d, ⁴J 4.5), 8.41 (1H, dd, ³J 6.3 ⁴J 2.3), 8.28 (1H, d, ³J 5.7), 8.25 (1H, d, ³J 7.5), 8.11 (1H, d, ³J, 8.6), 7.90 (1H, d, ³J 5.3), 7.83 (1H, t, ³J 5.7) and 7.81 (1H, t, ³J 5.7) (Another signal at δ_H 8.11 ppm (1H, d) in the ¹H NMR spectrum was overlapping); δ_C (63 MHz) 149.99 (quat), 147.27 (quat), 144.49 (quat), 141.31

(CH), 137.31 (CH), 131.58 (CH), 130.61 (CH), 129.21 (CH), 127.54 (CH), 126.47 (quat), 125.83 (quat), 125.54 (CH), 125.32 (CH), 121.23 (CH) and 118.20 (CH); m/z (FAB) 376 (MH^+ , 4%).

Upon removal of the solvent from the filtrate, a yellow solid was obtained (0.8 g), which was a mixture of products, the majority of which was 1-(2,4-dinitrobenzenesulfonyloxy) isoquinoline **91**. The reaction was repeated in acetonitrile to try to overcome the solubility problem, but gave similar results.

3.6 Hydrolysis reactions

Isoquinolin-4-ol **33**

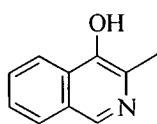
 Dilute sulfuric acid (40%, 10 cm³) was added to 4-(*p*-toluenesulfonyloxy)isoquinoline **32** (0.4 g, 1.33 mmol), and the mixture was heated to reflux for 8 h. After cooling, the solution was diluted with water (10 cm³), and then made strongly alkaline with sodium carbonate. The resulting precipitate was washed thoroughly with hot water, giving a brown coloured solid, which was identified as isoquinolin-4-ol **33** (0.12 g, 62%) mp 224 °C (from ethanol) [lit.,⁵⁰ 223 °C]; δ_H (360 MHz) ([²H]₆DMSO) 10.49 (1H, brs), 8.81 (1H, brs), 8.15 (1H, d, ³*J* 8.2), 8.10 (1H, brs), 8.07 (1H, d, ³*J* 7.3), 7.75 (1H, t, ³*J* 6.8) and 7.68 (1H, t, ³*J* 6.9); δ_C (90 MHz) 149.86 (quat), 143.76 (CH), 130.61 (CH), 128.39 (CH), 128.34 (quat), 128.13 (quat), 127.79 (CH), 127.75 (CH) and 121.83 (CH); m/z 145 (M^+ , 100%), 117 (61), 90 (85), 63 (44) and 43 (35).

Attempted synthesis of Isoquinolin-4-ol **33**

A solution of potassium hydroxide (0.56 g, 10 mmol) in ethanol (15 cm³) was added under an atmosphere of nitrogen to 4-(*p*-toluenesulfonyloxy)isoquinoline (0.27 g, 1 mmol).⁵⁴ The mixture was stirred and heated to reflux for 150 min, cooled to room temperature, and while still under nitrogen, quenched with dilute hydrochloric acid solution (5M, 3 cm³). It was then poured into water, extracted with dichloromethane, dried with MgSO₄ and evaporated, to give a solid (130 mg). ¹H NMR spectroscopy indicated that this was a 1:1 mixture of 4-(*p*-toluenesulfonyloxy)isoquinoline and

isoquinolin-4-ol. The solid obtained was then hydrolysed with base again (as above), but a mixture still resulted.

3-Methylisoquinolin-4-ol **28**



Dilute sulfuric acid (40%, 8 cm³) was added to 3-methyl-4-(*p*-toluenesulfonyloxy)isoquinoline **86** (0.3 g, 0.91 mmol), and the mixture was heated to reflux for 8 h. After cooling, the solution was diluted with water (5 cm³), and then made strongly alkaline with sodium carbonate. The expected precipitate did not form; dichloromethane was then added to the aqueous solution, which was continuously liquid-liquid extracted for 6 h. The solvent was removed *in vacuo* to give a yellow solid which was identified as 3-methylisoquinolin-4-ol **28** (60 mg, 42%) mp 176 °C [lit.,²⁷ 179 °C]; δ_{H} (250 MHz) ([²H]₆DMSO) 8.74 (1H, s), 8.14 (1H, d, ³*J* 8.0), 7.97 (1H, d, ³*J* 8.1), 7.64 (1H, t, ³*J* 8.4), 7.55 (1H, t, ³*J* 8.1) and 2.53 (3H, s); δ_{C} (90 MHz) 144.65 (quat), 142.52 (CH), 136.38 (quat), 129.19 (CH), 128.41 (quat), 128.21 (quat), 127.11 (CH), 126.34 (CH), 120.91 (CH) and 19.25 (CH₃); *m/z* 159 (M⁺, 70%), 143 (92), 130 (50) and 115 (100).

Hydrolysis of 4-(*p*-nitrosulfonyloxy)isoquinoline **88**

Dilute sulfuric acid (10%, 10 cm³) was added to 4-(*p*-nitrosulfonyloxy)isoquinoline **88** (0.2 g, 0.60 mmol), and the mixture was heated to reflux for 12 h. After cooling, the solution was diluted with water (2 cm³), and then made strongly alkaline with sodium carbonate. The resulting precipitate (75 mg) was filtered off, and from the crude ¹H NMR spectrum, an approximate 3:1 mixture of isoquinolin-4-ol **33** to 4-(*p*-nitrosulfonyloxy)isoquinoline **88** was obtained.

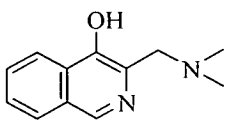
3.7 Reactions of isoquinolin-4-ol **33**

Attempted sulfonation of isoquinolin-4-ol **33**

A mixture of isoquinolin-4-ol **33** (100 mg, 0.7 mmol), manganese dioxide (150 mg, 1.72 mmol) and sodium sulfite (1.9 g, 15 mmol) in water (3 cm³), was heated at 90 °C for 1 h.⁴⁰ The mixture was filtered, neutralised with dilute hydrochloric acid solution (2M), and sodium chloride was added to give a small amount of an

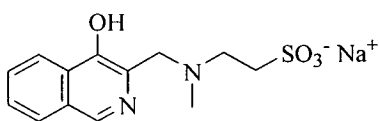
unidentified precipitate (10 mg). NMR spectroscopy proved inconclusive as messy spectra resulted, and no molecular ion peak corresponding to the sulfonated product was found in the FAB mass spectrum.

3-(Dimethylaminomethyl)isoquinolin-4-ol **93**



Aqueous dimethylamine solution (25%, 0.67 cm³) and aqueous formaldehyde solution (36%, 0.33 cm³) were added to a suspension of isoquinolin-4-ol **33** (0.5 g, 3.45 mmol) in methanol (10 cm³) at 0 °C.³⁹ The mixture was stirred at 0 °C for 30 min, then at room temperature for a further 2 h. This mixture was then acidified with concentrated hydrochloric acid and evaporated to dryness, giving a dark coloured residue. The residue was recrystallised to give a pale yellow solid, which was identified as 3-(dimethylaminomethyl)isoquinolin-4-ol **93** (0.36 g, 52%) mp 184 °C (from ethanol) [lit.,³⁹ 184-185 °C]; δ_{H} (250 MHz) ([²H]₆DMSO) 9.36 (1H, s), 8.65 (1H, d, ³J 8.5), 8.42 (1H, d, ³J 7.8), 8.09 (1H, t, ³J 6.9), 7.97 (1H, t, ³J 7.0), 4.85 (2H, s) and 2.92 (6H, s); δ_{C} (63 MHz) 150.75 (quat), 140.77 (CH), 132.82 (CH), 129.93 (CH), 129.61 (quat), 128.93 (CH), 128.66 (quat), 123.04 (quat), 122.60 (CH), 53.06 (CH₂) and 42.18 (2 × CH₃); m/z 202 (M⁺, 32%), 187 (14), 159 (100), 129 (54) and 89 (61).

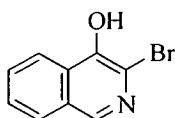
Sodium 3-aza-3-methyl-4(4-hydroxyisoquinolin-3-yl)butane-1-sulfonate **95**



Aqueous *N*-methyltaurine sodium salt **94** (0.34 g, 1.38 mmol) and aqueous formaldehyde solution (36%, 0.14 cm³) were added to a suspension of isoquinolin-4-ol (0.2 g, 1.38 mmol) in methanol (10 cm³) at 0 °C. A brown solid (0.6 g) was obtained after evaporation of the solvent, which was boiled in ethanol, in an attempt to recrystallise the crude material. The insoluble white solid that remained was filtered off, and identified as *sodium 3-aza-3-methyl-4(4-hydroxyisoquinolin-3-yl)butane-1-sulfonate* **95** (160mg, 40%) mp (decomposes) 205-210 °C (Found: MH⁺ (FAB) 319.0728 C₁₃H₁₆N₂O₄ requires *M* 319.0729); δ_{H} (250 MHz) ([²H]₆DMSO) 9.17 (1H, s), 8.53 (1H, d, ³J 8.3), 8.28 (1H, d, ³J 7.7), 7.97 (1H, t, ³J 6.9), 7.86 (1H, t, ³J 7.2), 4.78 (2H, s), 3.47-3.53 (2H, t, ³J 8.3), 3.01-3.07 (2H, t, ³J 8.0) and 2.87 (3H, s); δ_{C} (63 MHz) 149.27 (quat), 141.96 (CH), 131.50 (CH), 129.13 (CH), 128.90

(CH), 128.71 (quat), 128.20 (quat), 125.38 (quat), 122.40 (CH), 53.54 (CH₂), 52.37 (CH₂), 45.17 (CH₂) and 39.59 (CH₃); *m/z* (FAB) 319 (MH⁺, 25%).

3-Bromoisoquinolin-4-ol 67



Isoquinolin-4-ol **33** (0.16 g, 1.1 mmol) was dissolved in dilute sodium hydroxide solution (10%, 10 cm³), and the yellow/brown coloured solution was cooled to -5 °C using a sodium chloride/ice mixture.⁵⁸ Bromine (0.18 g, 0.057 cm³, 1.1 mmol) was dissolved in dilute sodium hydroxide solution (10%, 10 cm³), and was added dropwise *via* a syringe, to the isoquinolin-4-ol solution. During the bromine addition, the temperature of the reaction was not allowed to exceed 0 °C. The salt/ice bath was removed, the solution was allowed to warm to room temperature, and was stirred for 3 h. The solution was then cooled to -10 °C, and brought to pH 3 with concentrated hydrochloric acid, not allowing the solution temperature to exceed 0 °C. A pale yellow solution was obtained, and a small amount of precipitated solid was apparent, but not enough to filter off. Dichloromethane was added to the aqueous solution, which was continuously liquid-liquid extracted for 7 h. The solvent was removed *in vacuo* to give a light brown coloured solid, which was identified as 3-bromoisoquinolin-4-ol **67** (92 mg, 37%) mp 145 °C [lit.,³⁸ 145 °C]; δ_{H} (360 MHz) ([²H]₆DMSO) 10.49 (1H, brs), 8.72 (1H, s), 8.24 (1H, d, ³*J* 8.5), 8.12 (1H, d, ³*J* 8.2), 7.82 (1H, t, ³*J* 6.9) and 7.72 (1H, t, ³*J* 6.9); δ_{C} (90 MHz) 145.37 (quat), 143.46 (CH), 130.45 (CH), 128.92 (quat), 128.64 (quat), 128.05 (CH), 127.47 (CH), 124.26 (quat), 121.43 (CH); *m/z* 225 (M⁺, 62%), 223 (M⁺, 64%), 143 (74), 115 (100) and 89 (44).

3.8 Attempted coupling reactions of 67

Suzuki Coupling (1)

A mixture of 3-bromoisoquinolin-4-ol **67** (75 mg, 0.33 mmol), phenylboronic acid (41 mg, 0.33 mmol), potassium carbonate (270 mg, 2 mmol) and tetrakis(triphenylphosphonium)palladium (8 mg, 0.007 mmol) was heated to reflux in a 3:1 dioxane/water mixture for 4 h, under an atmosphere of nitrogen.⁵⁹ The mixture was allowed to cool, diluted with ether and filtered through a silica plug. The solvent

was removed *in vacuo* to give a yellow/brown solid which was identified as a mixture of 3-bromoisoquinolin-4-ol **67** and biphenyl **102** (47 mg); δ_{H} (250 MHz) 8.56 (1H, s), 8.24 (1H, d, 3J 8.0), 8.12 (1H, d, 3J 8.2), 7.82 (1H, t, 3J 6.9), 7.72 (1H, t, 3J 6.9), 7.10 (1H, d, 3J 8.2) and 6.80 (1H, d, 8.4); m/z 225 (M^+ , 27%), 223 (M^+ , 28%), 154 (36), 143 (32), 115 (41) and 94 (100). The ^1H NMR data was assigned from the crude spectrum, making the biphenyl **102** signals difficult to assign.

Suzuki Coupling (2)

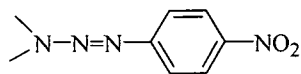
A mixture of 3-bromoisoquinolin-4-ol **67** (45 mg, 0.20 mmol), phenylboronic acid (25 mg, 0.20 mmol), cesium carbonate (130 mg, 0.4 mmol) and tetrakis(triphenylphosphonium)palladium (12 mg, 0.01 mmol) in a 3:1 THF/water (5 cm^3) mixture were heated at 120 $^{\circ}\text{C}$ (power 150 W) in a microwave for 10 min. The mixture was allowed to cool, and filtered through a silica plug. The solvent was removed *in vacuo* to give a brown solid. The crude ^1H NMR spectrum showed the presence of 3-bromoisoquinolin-4-ol in small amounts, but no other products could be easily identified. The mass spectrum also showed the presence of 3-bromoisoquinolin-4-ol **67**, m/z 223 (M^+ , 36%) and m/z 225 (M^+ , 35%), but no biphenyl **102** was seen. There was also a signal corresponding to 3-phenylisoquinolin-4-ol **42**, m/z 221 (M^+ , 12%).

3.9 Azo coupling reactions of Mannich derivatives **93** and **95**

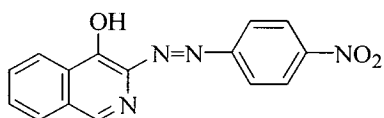
Reaction of 3-(Dimethylaminomethyl)-isoquinolin-4-ol **93** and *p*-nitroaniline

p-Nitroaniline (68 mg, 0.5 mmol) was suspended in water (5 cm^3), acidified to pH 1-2 with dilute hydrochloric acid solution (2M), and cooled to 0 $^{\circ}\text{C}$. Sodium nitrite (40 mg, 0.6 mmol) was dissolved in the minimum amount of water and added to the above suspension, where upon a pale yellow solution resulted.

3-(Dimethylaminomethyl)-isoquinolin-4-ol **93** (100 mg, 0.5 mmol) was dissolved in water at pH 8-9, and the diazonium solution was added dropwise to this solution, at 0 $^{\circ}\text{C}$. An instant colour change resulted from yellow to dark red, and the pH was maintained at 8-9. The resulting solution was stirred for 30 min and the precipitate



obtained was filtered off (135 mg) and identified as a mixture of products by ^1H NMR. This mixture was purified by dry-flash chromatography (ethyl acetate/hexane 1:1) to provide 3,3-dimethyl-1-(4-nitro-phenyl)-triazene **98** (35 mg, 36%), mp 143 °C [lit.,¹²² 143-144 °C]; δ_{H} (250 MHz) 8.19 (2H, d, 3J 9.1), 7.50 (2H, d, 3J 9.1), 3.60 (3H, s) and 3.28 (3H, s); δ_{C} (63 MHz) 155.84 (quat), 144.52 (quat), 124.72 (2 \times CH), 120.44 (2 \times CH), 43.45 (CH₃) and 36.17 (CH₃); lit.¹²² δ_{H} 8.10 (2H, d), 7.42 (2H, d), 3.50 (3H, s) and 3.28 (3H, s); δ_{C} 154 (quat), 146 (quat), 124 (2 \times CH), 120 (2 \times CH), 43 (CH₃) and 36 (CH₃); m/z 194 (M⁺, 51%), 178 (24), 150 (91), 122 (97), 76 (79) and 43 (100); 3-(*p*-nitrophenylazo)isoquinolin-4-ol **97** (35 mg, 25%); δ_{H} (250 MHz) ([^2H]₆DMSO) 8.92 (1H, s), 8.50 (2H, d, 3J 9.2), 8.37 (1H, d, 3J 7.4), 8.17 (1H, t, 3J 7.4), 8.14 (1H, t, 3J 6.3), 8.05 (1H, d, 3J 7.4) and 7.98 (2H, d, 3J 9.2); δ_{C} (63 MHz) 154.11 (CH), 147.50 (quat), 141.23 (quat), 138.70 (quat), 134.23 (CH), 133.45 (quat), 132.15 (CH), 129.63 (CH), 125.57 (2 \times CH), 125.44 (2 \times CH), 115.59 (CH);

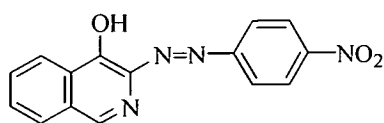


m/z 294 (M⁺, 33%), 249 (34), 144 (37), 138 (66), 122 (93) and 76 (100); unidentified compound (45 mg); δ_{H} (250 MHz) ([^2H]₆DMSO) 8.43 (2H, t, 3J 7.8), 8.20 (2H, d, 3J 8.9), 8.10 (2H, d, 3J 9.3), 8.04 (1H, d, 3J 7.8), 7.95 (1H, d, 3J 7.2), 7.83 (1H, t, 3J 6.9), 7.73 (2H, d, 3J 8.3), 7.68 (1H, d, 3J 7.2), 7.56 (1H, d, 3J 7.4) and 7.49 (2H, d, 3J 8.4). This reaction was also repeated at pH 7.5, but gave the same results.

Sodium 3-aza-3-methyl-4(4-hydroxyisoquinolin-3-yl)butane-1-sulfonate **95** and *p*-nitroaniline

This reaction was carried out as above, and proceeded similarly, with a dark red precipitate obtained (70 mg). A mixture of products was found again by ^1H NMR spectroscopy, and as above, none of the target azo coupled product was obtained. A singlet at 8.67 ppm was again identified, which suggests coupling did not take place at the 1-position, and no CH₂ or CH₃ peaks were identified. No triazene product was found due to its water soluble nature, but 3-(*p*-nitrophenylazo)isoquinolin-4-ol **97** was again identified, giving ^1H NMR spectra as above, m/z 294 (M⁺, 42%), 220 (57), 249 (58), 144 (52), 138 (72), 122 (71) and 89 (100).

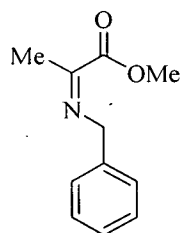
3-(*p*-Nitrophenylazo)isoquinolin-4-ol **97**



p-Nitroaniline (95 mg, 6.9 mmol) was suspended in water (5 cm³), acidified to pH 1-2 with dilute hydrochloric acid solution (2M) and cooled to 0 °C. Sodium nitrite (50 mg, 7.2 mmol) was dissolved in the minimum amount of water and added to the above suspension, where upon a pale yellow solution resulted. Isoquinolin-4-ol (100 mg, 6.9 mmol) was dissolved in dilute sodium hydroxide solution (10% w/v), the pH was adjusted to 7-8, and the solution was cooled to 0 °C. The *p*-nitrobenzene diazonium chloride solution was then added to the basic isoquinolin-4-ol solution, and immediately a dark red colour was observed. This solution was stirred for 30 min and the resulting precipitate was filtered off and identified as 3-(*p*-nitrophenylazo)isoquinolin-4-ol **97** (195 mg, 100%) mp 194 °C [lit.,⁴¹ 197-199 °C]; δ_{H} (250 MHz) ([²H]₆DMSO) 8.92 (1H, s), 8.50 (2H, d, ³*J* 9.2), 8.37 (1H, d, ³*J* 7.4), 8.17 (1H, t, ³*J* 7.4), 8.14 (1H, t, ³*J* 6.3), 8.05 (1H, d, ³*J* 7.4) and 7.98 (2H, d, ³*J* 9.2); δ_{C} (63 MHz) 154.11 (CH), 147.50 (quat), 141.23 (quat), 138.70 (quat), 134.23 (CH), 133.45 (quat), 132.15 (CH), 129.63 (CH), 125.57 (2 × CH), 125.44 (2 × CH), 115.59 (CH); *m/z* 294 (M⁺, 30%), 249 (74), 144 (22), 138 (83), 122 (96) and 76 (100).

3.10 Synthesis and FVP of Imine precursors

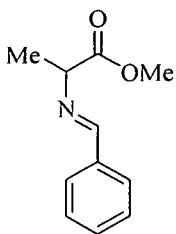
Methyl 2-Benzyliminopropionate **109**



Methyl pyruvate (0.56 g, 5.5 mmol) and benzylamine (0.65 g, 5.5 mmol) were stirred in dry THF (25 cm³) at 0 °C for 3 h with activated 5 Å molecular sieves (heated in the FVP furnace at 250 °C for 30 min). The sieves were filtered off through a celite pad and the solvent was removed *in vacuo*.⁶⁵ A yellow liquid resulted which solidified upon freezing. This yellow solid was then filtered dry to give a white solid, which was identified as methyl 2-benzyliminopropionate **109** (0.73 g, 70%) mp 53-54 °C (from hexane); δ_{H} (250 MHz) 7.30-7.37 (5H, m), 4.75 (2H, s), 3.88 (3H, s) and 2.24 (3H, s); δ_{C} (63 MHz) 165.33 (quat), 138.04 (quat), 129.01 (2 × CH), 128.31 (2 × CH), 127.52 (CH), 103.38 (quat), 57.03 (CH₂), 53.33 (CH₃) and 15.53 (CH₃); *m/z*

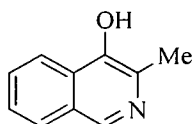
191 (M^+ , 31%), 176 (11), 131 (34), 106 (23), 91 (100) and 77 (15). There was no melting point or NMR data in the literature.

Methyl *N*-Benzylidenealanate 114



An ice-cold solution of methyl alanate hydrochloride (1.00 g, 7.27 mmol) in water (10 cm³), was treated with triethylamine (0.88 g, 8.72 mmol). After stirring for 10 min, benzaldehyde (1.12 cm³, 0.011 mol) was added, and the resultant mixture was allowed to warm to room temperature overnight. The reaction mixture was extracted into dichloromethane, dried over magnesium sulfate and the solvent was removed *in vacuo*.¹²¹ The resulting yellow oil was distilled (Kugelrohr) and identified as methyl *N*-benzylidenealanate **114** (0.71 g, 55%) bp 110 °C/1.5 mm (lit.,¹²¹ 138 °C/4 mm); δ_H (250 MHz) 8.25 (1H, s), 7.18-7.85 (5H, m), 4.11 (1H, q, ³*J* 7.0), 3.70 (3H, s) and 1.50 (3H, d, ³*J* 7.0). There was no NMR data in the literature.

FVP of Methyl 2-Benzyliminopropionate 109



[T_f 650 °C, T_i 60 °C, P 1×10^{-2} Torr, m_a 0.5 g, 2.62 mmol]
Small scale pyrolyses (50 mg) were carried out from 600-850 °C at 50 °C intervals, to identify the optimum conditions. At temperatures > 700 °C, the peaks corresponding to starting material **109** and the isoquinolin-4-ol **28** began to disappear; and 650 °C was identified as the optimum conditions for a preparative scale (0.5 g) pyrolysis. However, approximately half of the starting imine **109** decomposed in the FVP inlet. The crude ¹H NMR spectrum of the pyrolysate showed the target 3-methylisoquinolin-4-ol **28** and other unidentified products. The crude pyrolysate was distilled (Kugelrohr) and purified by dry-flash chromatography (silica), hexane/ethyl acetate (2:1). The ¹H NMR spectrum obtained matched the literature,¹²² showing 3-methylisoquinolin-4-ol **28** in very small amounts (11 mg, 3%) (Found: M^+ 159.0680. C₁₀H₉NO requires M 159.0684); δ_H (250 MHz) 8.67 (1H, s), 8.22 (1H, d, ³*J* 7.8), 7.83 (1H, d, ³*J* 7.6), 7.43-7.71 (2H, m) and 2.59 (3H, s); m/z 159 (M^+ , 19%), 132 (21), 86 (77) and 84 (100).

FVP of Methyl *N*-Benzylidenealanate 114

[T_f 600-800 °C, T_i 70 °C, P 1×10^{-2} Torr, m_a 50 mg, 0.262 mmol]

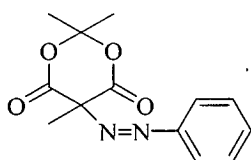
Small scale pyrolyses (50 mg) were carried out at 50 °C intervals over the temperature range shown. The optimum temperature identified was 600 °C, but the crude pyrolysate mainly consisted of starting material 114, with only very small signals corresponding to the isoquinolin-4-ol 28. At higher temperatures, less starting material 114 was present, but no peaks corresponding to the isoquinolin-4-ol 28 were evident. Therefore, this did not warrant a preparative scale reaction.

3.11 5-Arylazo-2,2,5-trimethyl-5-phenylazo-1,3-dioxane-4,6-dione derivatives

General Procedure

An aromatic amine was dissolved in a mixture of water and concentrated hydrochloric acid, at 0 °C. Sodium nitrite (1 eq.) was then added dropwise to provide the diazonium salt. Methyl Meldrum's acid (1 eq.) was dissolved in the minimum amount of dilute sodium carbonate, to provide a solution that was neutral to slightly basic, and was cooled to 0 °C. The diazonium salt was then added dropwise to the methyl Meldrum's acid solution, which turned yellow, and the azo compound precipitated very quickly.⁷¹

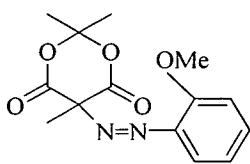
2,2,5-Trimethyl-5-phenylazo-1,3-dioxane-4,6-dione 120



The reaction of benzenediazonium chloride [(from aniline (1 cm³, 0.011 mol) and sodium nitrite (0.76 g, 0.011 mol) in water at 0 °C)] and methyl Meldrum's acid (1.74 g, 0.011 mol) yielded an orange precipitate, which was filtered off and recrystallised from cyclohexane, giving yellow needles of 2,2,5-trimethyl-5-phenylazo-1,3-dioxane-4,6-dione 120 (2.19 g, 76%) mp 59-61°C (from cyclohexane) (Found: C, 59.45; H, 5.4; N, 10.4. C₁₃H₁₄N₂O₄ requires C, 59.55; H 5.35; N, 10.7%); δ_H (250 MHz) 7.73-7.77 (2H, m), 7.47-7.53 (3H, m), 2.15 (3H, s), 1.78 (3H, s) and 1.75 (3H, s); δ_C (63 MHz) 164.87 (2 \times quat), 150.72 (quat), 132.86 (CH), 129.40 (2 \times CH), 123.31 (2 \times CH), 106.51 (quat), 78.92 (quat), 29.89 (CH₃), 29.12 (CH₃), and 20.08 (CH₃); m/z 262

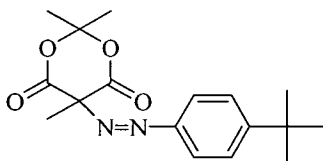
(M⁺, 4%), 204 (10), 182 (33), 169 (63), 160 (30), 154 (61), 143 (59), 132 (41), 104 (60) and 75 (100).

5-(2-Methoxyphenylazo)-2,2,5-trimethyl-1,3-dioxane-4,6-dione **120g**



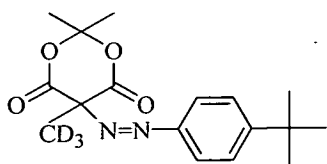
o-Methoxybenzenediazonium chloride [(from *o*-anisidine (0.91 cm³, 8.13 mmol) and sodium nitrite (0.56 g, 8.13 mmol) in water at 0 °C] and methyl Meldrum's acid (1.29 g, 8.13 mmol), yielded an orange solid which was recrystallised from cyclohexane, giving orange needles of 5-(2-methoxyphenylazo)-2,2,5-trimethyl-1,3-dioxane-4,6-dione **120g** (1.67 g, 70%) mp 74-76°C (from cyclohexane) (Found: M⁺ 292.1047. C₁₄H₁₆N₂O₅ requires *M* 292.1059); δ_H (250 MHz) 7.34-7.48 (2H, m), 6.89-7.05 (2H, m), 3.91 (3H, s), 1.98 (3H, s) and 1.80 (6H, s); δ_C (63 MHz) 164.86 (2 × quat), 156.92 (quat), 140.02 (quat), 134.04 (CH), 120.40 (CH), 117.31 (CH), 113.15 (CH), 106.34 (quat), 78.78 (quat), 56.24 (CH₃), 29.50 (CH₃), 28.86 (CH₃) and 20.11 (CH₃); *m/z* 292 (M⁺, 2%), 234 (15), 190 (5), 162 (5), 135 (69), 120 (67), 108 (100), 92 (75) and 77 (19).

5-(4-*t*-Butylphenylazo)-2,2,5-trimethyl-1,3-dioxane-4,6-dione **120f**



4-*t*-Butylbenzenediazonium chloride [(from 4-*t*-butylaniline (200 mg, 1.34 mmol) and sodium nitrite (92 mg, 1.34 mmol) in water at 0 °C] and methyl Meldrum's acid (212 mg, 1.34 mmol), yielded a yellow gum which solidified upon trituration with ether, and was identified as 5-(4-*t*-butylphenylazo)-2,2,5-trimethyl-1,3-dioxane-4,6-dione **120f** (0.47 g, 98%) mp 65-66 °C (Found: M⁺ 318.1581. C₁₇H₂₂N₂O₄ requires *M* 318.1580); δ_H (250 MHz) 7.61-7.66 (2H, d, ³*J* 8.90), 7.40-7.45 (2H, d, ³*J* 8.90), 1.87 (3H, s), 1.74 (3H, s), 1.70 (3H, s) and 1.26 (9H, s); δ_C (63 MHz) 164.72 (2 × quat), 156.51 (quat), 148.39 (quat), 126.08 (2 × CH), 122.86 (2 × CH), 106.18 (quat), 78.55 (quat), 35.02 (quat), 30.98 (3 × CH₃), 29.58 (CH₃), 28.91 (CH₃) and 19.75 (CH₃); *m/z* 318 (M⁺, 1%), 266 (30), 260 (1), 251 (57), 216 (3), 188 (3), 133 (61), 91 (63), 56 (76) and 43 (100).

5-(4-*t*-Butylphenylazo)-2,2-dimethyl-5-^{[2]H}₃methyl-1,3-dioxane-4,6-dione **137**



4-*t*-Butylbenzenediazonium chloride [(from 4-*t*-butylaniline (104 mg, 0.64 mmol) and sodium nitrite (44 mg, 0.64 mmol) in water at 0 °C] and 2,2-dimethyl-5-^{[2]H}₃methyl-1,3-dioxane-4,6-dione (105 mg, 0.64 mmol), yielded a yellow gum which solidified upon trituration with ether, and was identified as 5-(4-*t*-butylphenylazo)-2,2-dimethyl-5-^{[2]H}₃methyl-1,3-dioxane-4,6-dione **137** (140 mg, 70%) mp 68-69 °C; δ_{H} (250 MHz) 7.64 (2H, d, ³*J* 8.9), 7.43 (2H, d, ³*J* 8.9), 1.74 (3H, s), 1.70 (3H, s) and 1.27 (9H, s); δ_{C} (63 MHz) 165.51 (2 × quat), 156.50 (quat), 148.39 (quat), 126.07 (2 × CH), 122.85 (2 × CH), 106.18 (quat), 78.43 (quat), 35.01 (quat), 30.98 (3 × CH₃), 29.57 (CH₃) and 28.90 (CH₃); *m/z* 321 (MH⁺, 1%), 161 (19), 147 (30), 131 (50), 119 (42), 91 (52), 57 (98) and 43 (100). (2,2-Dimethyl-5-^{[2]H}₃methyl-1,3-dioxane-4,6-dione **136** was prepared by Miss Beeta Bolali Mood, see Section 2.12.10).⁸⁰

Attempted Hydrogenation of 2,2,5-Trimethyl-5-phenylazo-1,3-dioxane-4,6-dione **120**

A mixture of 2,2,5-trimethyl-5-phenylazo-1,3-dioxane-4,6-dione (200 mg, 0.76 mmol) and Adam's catalyst (PtO₂) (12 mg, 0.05 mmol) in toluene (20 cm³) was hydrogenated overnight at room temperature, at a pressure of 3 atmospheres.⁷⁷ The catalyst was filtered off through a celite pad and the solvent was removed *in vacuo*. ¹H NMR revealed that the major product was starting material.

Attempted reduction of 2,2,5-Trimethyl-5-phenylazo-1,3-dioxane-4,6-dione **120**

A mixture of sulfanilic acid (1.73 g, 0.01 mol), sodium carbonate (0.53 g, 5 mmol) and water (15 cm³) was heated and stirred until all the sulfanilic acid had dissolved, after which the solution was cooled to 0 °C. A solution of sodium nitrite (0.8 g, 0.01 mol) in water (3 cm³) was added, and the resulting solution was poured onto a mixture of concentrated hydrochloric acid (2 cm³) and ice. The solution was then stirred for 15-25 min at 0 °C, giving a yellow solution containing a pale yellow precipitate, which was the *p*-benzenediazonium sulfonate. Methyl Meldrum's acid (1.58 g, 0.01 mol) was dissolved in dilute sodium hydroxide solution (2M) and

cooled to 0 °C. The benzenediazonium sulfonate was then added, resulting in a dark red solution. This solution was stirred at room temperature for 1 h, but no precipitate formed. Nevertheless, the reduction to the amine was attempted by the dropwise addition of sodium hydrosulfite (4 g, 0.018 mol), and stirred until the frothing had subsided. The solution gradually lost the intense red colour and eventually became pale yellow.⁵² The expected precipitate did not form and the attempted extraction of the product into organic solvents was not successful. As a result, no analysis has been possible.

3.12 FVP of methyl Meldrum's acid derivatives

General Method

Small scale pyrolyses (80 mg) were carried out over the temperature ranges shown below at 50 °C intervals. The azo compounds however, were unstable in the inlet tube, and a large amount of decomposition accompanied all of these experiments, resulting in low product yields; thus making the synthesis unsuitable in a preparative sense. Only the reduced aromatic product was identified in each of the pyrolyses, at all the temperatures studied.

FVP of 2,2,5-Trimethyl-5-phenylazo-1,3-dioxane-4,6-dione **120**

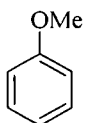
[T_f 450-750 °C, T_i 60 °C, P 1×10^{-2} Torr, m_a 80 mg, 0.30 mmol]



The crude ¹H NMR spectra all showed very weak signals, suggesting a volatile product, which was assumed to be benzene, but was too volatile under the conditions of the experiment to isolate.

FVP of 5-(2-Methoxyphenylazo)-2,2,5-trimethyl-1,3-dioxane-4,6-dione **120g**

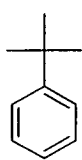
[T_f 450-750 °C, T_i 60 °C, P 1×10^{-2} Torr, m_a 80 mg, 0.27 mmol]



The crude ¹H and ¹³C NMR spectra matched that of the literature and showed anisole **126** as the only product (12 mg, 41%); δ_H (250 MHz) 7.29-7.37 (2H, m), 6.92-7.01 (3H, m), and 3.84 (3H, s); δ_C (63 MHz) 159.39 (quat), 129.32 (2 × CH), 120.52 (CH), 113.75 (2 × CH) and 55.01 (CH₃), anisole; δ_C (63

MHz) 159.63 (quat), 129.46 (2 × CH), 120.68 (CH), 113.95 (2 × CH) and 55.14 (CH₃).⁵³

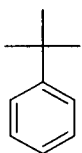
FVP of 5-(4-*t*-Butylphenylazo)-2,2,5-trimethyl-1,3-dioxane-4,6-dione **120f**



[*T_f* 650 °C, *T_i* 85 °C, *P* 1×10⁻² Torr, *m_a* 100 mg, 0.31 mmol]

The ¹H and ¹³C NMR spectra matched that of the literature⁵³ and showed *t*-butylbenzene **138** as the only product (11 mg, 27%); δ_H (250 MHz) 7.44 (2H, d, ³*J* 7.9), 7.34 (2H, t, ³*J* 7.2) and 7.21 (1H, t, ³*J* 7.0); δ_C (63 MHz) 150.90 (quat), 127.90 (2 × CH), 125.26 (CH), 125.09 (2 × CH) 34.54 (quat) and 30.78 (3 × CH₃); lit:⁵³ *t*-butylbenzene; δ_H 7.43 (2H, d), 7.34 (2H, t) and 7.21 (1H, t); δ_C 150.99 (quat), 127.99 (2 × CH), 125.34 (CH), 125.16 (2 × CH) and 34.62 (quat), 31.34 (3 × CH₃).

FVP of 5-(4-*t*-Butylphenylazo)-2,2-dimethyl-5-[²H]₃-methyl-1,3-dioxane-4,6-dione **137**

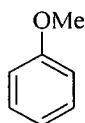


[*T_f* 650 °C, *T_i* 90 °C, *P* 1×10⁻² Torr, *m_a* 50 mg, 0.16 mmol]

The ¹H NMR spectrum matched that of the literature,⁵³ showing *t*-butylbenzene **138** as the only product. No incorporation of deuterium was observed (8 mg, 30%); δ_H (360 MHz) 7.44 (2H, d, ³*J* 7.9), 7.34 (2H, t, ³*J* 7.20) and 7.21 (1H, t, ³*J* 7.05), *t*-butylbenzene δ_H (360 MHz) 7.44 (2H, d, ³*J* 7.9), 7.34 (2H, t, ³*J* 7.2) and 7.21 (1H, t, ³*J* 7.0)

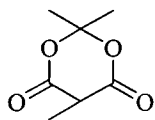
Condensed phase pyrolysis of 5-(2-Methoxyphenylazo)-2,2,5-trimethyl-1,3-dioxane-4,6-dione **120g**

5-(2-Methoxyphenylazo)-2,2,5-trimethyl-1,3-dioxane-4,6-dione **120g** (150 mg, 0.51 mmol) was heated in a Kugelrohr oven and volatalised (60 °C) at a pressure of 1×10⁻² Torr, using a modification of the standard FVP apparatus without the furnace (the U-tube from which the products were collected was connected directly to the inlet tube, and not *via* the furnace). The ¹H and ¹³C NMR spectra of the product mixture



matched that of the literature,⁵³ revealing anisole **126** as the major product (2:1), along with some methyl Meldrum's acid; anisole **126** (20 mg, 35%);

δ_{H} (250 MHz) 7.27-7.33 (2H, m), 6.89-6.95 (3H, m), 3.81 (3H, s); δ_{C} (63 MHz) 159.49 (quat), 129.30 (2 \times CH), 120.50 (CH), 113.73 (2 \times CH) and 54.99 (CH₃);



methyl Meldrum's acid (12 mg, 15%); δ_{H} (250 MHz) 3.52 (1H, q, 3J 7.0), 1.74 (3H, s), 1.69 (3H, s), 1.50 (3H, d, 3J 7.0); δ_{C} (63 MHz) 165.90 (quat), 104.73 (quat), 41.21 (CH), 28.44 (CH₃), 26.28 (CH₃) and 10.64 (CH₃).

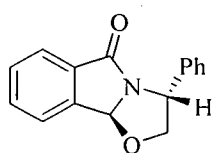
3.13 3-Substituted-tetrahydro[1,3]oxazolo[2,3-a]isoindol-5-ones

General Procedure

An equimolar amount of the ethanolamine (5 mmol) and 2-carboxybenzaldehyde (5 mmol) was slurried in toluene (100 cm³), and this mixture was heated to reflux under Dean-Stark conditions for 24 h. The resulting yellow solution was allowed to cool, and the toluene was removed *in vacuo*. No further purification was carried out unless stated otherwise.⁴³

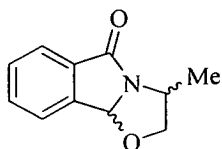
The following compounds were prepared by the standard method.

(3R,9bS)-3-Phenyl-2,3,5,9bH-tetrahydro[1,3]oxazolo[2,3-a]isoindol-5-one 151



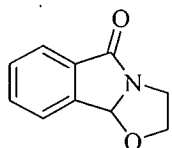
R-Phenylglycinol (0.702 g, 5.12 mmol) and 2-carboxybenzaldehyde (0.769 g, 5.12 mmol) yielded a yellow oil as a single isomer, which solidified upon freezing, and was identified as (3R,9bS)-3-phenyl-2,3,5,9bH-tetrahydro[1,3]oxazolo[2,3-a]isoindol-5-one **151** (1.15 g, 89%) mp 112-113 °C (from dichloromethane) [lit.,⁸² 112-116 °C]; δ_{H} (250 MHz) 7.86 (1H, d, 3J 5.3), 7.55-7.63 (3H, m), 7.25-7.41 (5H, m), 6.04 (1H, s), 5.20 (1H, t, 3J 7.4), 4.84 (1H, dd, 3J 8.8, 7.5) and 4.16 (1H, dd, 3J 8.8, 7.4); δ_{C} (63 MHz) 174.00 (quat), 142.28 (quat), 139.86 (quat), 133.20 (CH), 130.92 (CH), 128.99 (2 \times CH), 127.85 (CH), 126.17 (2 \times CH), 124.60 (CH), 124.31 (CH), 92.03 (CH), 78.21 (CH₂) and 58.19 (CH); m/z 251 (M⁺, 17%), 221 (100), 193 (75), 106 (55), 91 (98), 92 (83), 90 (60) and 77 (47). One quaternary peak at ~132 ppm was overlapping.⁸²

3-Methyl-2,3-dihydro-9bH-oxazolo[2,3-a]isoindol-5-one 154



R,S-2-Aminopropanol (0.41 cm³, 5.12 mmol) and 2-carboxybenzaldehyde (0.768 g, 5.12 mmol) gave an oil, which after Kugelrohr distillation, was identified as a 7:1 mixture of product diastereomers, which were not analysed further (0.81 g, 84%) bp 155 °C/4.5 mm; δ_{H} (250 MHz) (major isomer) 7.75 (1H, d, ³*J* 7.2), 7.54-7.58 (3H, m), 5.86 (1H, s), 4.46 (1H, dd, ³*J* 8.6, 7.0), 4.22 (1H, m), 3.86 (1H, dd, ³*J* 8.6, 6.6) and 1.39 (3H, d, ³*J* 6.5); δ_{C} (63 MHz) 172.78 (quat), 141.41 (quat), 132.52 (quat), 132.13 (CH), 129.89 (CH), 123.50 (CH), 123.31 (CH), 89.75 (CH), 76.91 (CH₂), 49.72 (CH) and 18.91 (CH₃); *m/z* 189 (M⁺, 33%), 188 (47), 174 (40), 159 (79), 133 (43), 130 (100), 104 (57) and 77 (59). No boiling point was reported in the literature. The NMR data matched those in the literature.¹²⁴

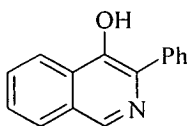
2,3-Dihydro-9bH-oxazolo[2,3-a]isoindol-5-one 155



2-Carboxybenzaldehyde (0.77 g, 5.12 mmol) and ethanolamine (0.31 g, 5.12 mmol) yielded an oil (1 g), which from the ¹H NMR spectrum, revealed a mixture of starting material and **155**. After purification by dry-flash chromatography (4:1 hexane/ethyl acetate gradient as eluent), 2,3-dihydro-9bH-oxazolo[2,3-a]isoindol-5-one **155** was obtained as a clear oil (0.1 g, 11%); δ_{H} (250 MHz) 7.85 (1H, d, ³*J* 7.0), 7.65-7.70 (3H, m), 5.92 (1H, s), 4.33 (2H, m), 4.06 (1H, m) and 3.51 (1H, m). The ¹H spectrum obtained matched the literature spectrum.¹²⁵ No further analysis was carried out, as the majority of the product was used for FVP experiments.

3.14 FVP of isoindolone precursors.

FVP of (3*R*,9*bS*)-3-Phenyl-2,3,5,9*bH*-tetrahydro[1,3]oxazolo[2,3-*a*]isoindol-5-one 151



[*T_f* 650 °C, *T_i* 105 °C, *P* 1×10⁻² Torr, *m_a* 0.43 g, 1.72 mmol]

Small scale (50 mg) pyrolysis experiments were carried out at 50 °C intervals from 650-800 °C to identify the optimum conditions. At lower temperatures (650-700 °C), signals in the ¹H NMR spectrum corresponding to

starting material **151** and the isoquinolin-4-ol **42** were evident. At higher temperatures, the starting material **151** and isoquinolin-4-ol **42** signals decreased in intensity, and were accompanied by a lot of decomposition products; 650 °C was identified as the optimum temperature. The crude ¹H NMR spectrum of the pyrolysate showed the major products to be a mixture of starting material **151** and 3-phenylisoquinolin-4-ol **42**. Unvolatilised starting material **151**(10-20%) remained in the furnace tube entry. The crude pyrolysate was then purified by dry-flash chromatography using a 2:1 hexane/ethyl acetate gradient as eluent. Starting material **151** (90 mg, 21%) was recovered along with 3-phenylisoquinolin-4-ol **42** (70 mg, 20%) mp 154-156°C (lit.,³⁴ 158-160 °C) (Found: MH⁺ (FAB) 222.0918. C₁₅H₁₂NO requires *M* 222.0919); δ_H (250 MHz) 8.81 (1H, s), 8.20 (1H, d, ³*J* 8.1), 7.33-7.93 (8H, m) and 5.0 (1H, brs); δ_C ([²H]₆DMSO) (63 MHz) 144.76 (quat), 143.39 (CH), 138.41 (quat), 136.74 (quat), 129.33 (CH), 129.09 (2 × CH), 128.72 (quat), 128.38 (quat), 127.66 (2 × CH), 127.10 (CH), 127.03 (CH), 126.98 (CH) and 121.36 (CH); *m/z* 221 (M⁺, 91%), 220 (100), 193 (52), 165 (59), 77 (64) and 89 (64).

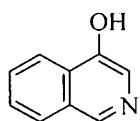
FVP of 3-Methyl-2,3-dihydro-9*bH*-oxazolo[2,3-*a*]isoindol-5-one **154**

[*T_f* 650-800 °C, *T_i* 150 °C, *P* 1 × 10⁻² Torr, *m_a* 60 mg, 0.317 mmol]

Several small scale experiments (50 mg) were carried out at 50 °C intervals over the temperature range shown above. The crude ¹H NMR spectra showed starting material **154** present at lower temperatures along with other unidentified aromatic products. At higher temperatures, messy spectra resulted, and very little of the target 3-methylisoquinolin-4-ol **28** was identified at any temperature, therefore, this did not warrant a preparative scale reaction.

FVP of 2,3-Dihydro-9*bH*-oxazolo[2,3-*a*]isoindol-5-one **155**

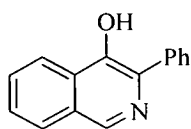
[*T_f* 700-850 °C, *T_i* 140 °C, *P* 1 × 10⁻² Torr, *m_a* 30 mg, 0.17 mmol]



Small scale pyrolyses (25 mg) were carried out over the temperature range shown above. The crude ¹H NMR spectra at temperatures greater than 700 °C showed no product peaks. At 700 °C mostly starting material **155** was recovered, which was soluble in CDCl₃. A very small amount of a white film (insoluble in CDCl₃) was also formed, which was the target isoquinolin-4-ol **33**; δ_H

(250 MHz) ($[\text{H}]_6\text{DMSO}$) 8.81 (1H, s), 8.07-8.15 (2H, m) and 7.68-7.75 (3H, m). Due to the very small amounts of product formed, no preparative scale reaction was done.

FVP of 3-Phenylisoquinolin-4-ol **42**



$[T_f 650\text{ }^\circ\text{C}, T_i 100\text{ }^\circ\text{C}, P 1 \times 10^{-2}\text{ Torr}, m_a 15\text{ mg}, 0.068\text{ mmol}]$

$^1\text{H NMR}$ spectroscopy showed only starting material **42** present.

$[T_f 750\text{ }^\circ\text{C}, T_i 100\text{ }^\circ\text{C}, P 1 \times 10^{-2}\text{ Torr}, m_a 12\text{ mg}, 0.054\text{ mmol}]$

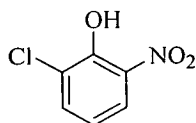
$^1\text{H NMR}$ spectroscopy showed only starting material **42** present.

$[T_f 850\text{ }^\circ\text{C}, T_i 100\text{ }^\circ\text{C}, P 1 \times 10^{-2}\text{ Torr}, m_a 5\text{ mg}, 0.026\text{ mmol}]$

$^1\text{H NMR}$ spectroscopy showed unidentified products, probably decomposed starting material **42**. This experiment was carried out as it was thought that **42** was unstable at high temperatures.

3.15 Synthesis of 2-Amino-6-chloro-4- sulfonamidophenol **163**

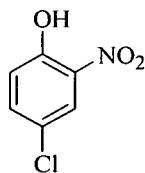
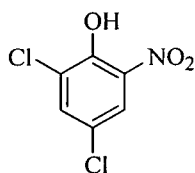
6-Chloro-2-nitrophenol **158**



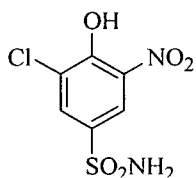
Nitric acid (150 cm³) was added slowly to a solution of 2-chlorophenol (250 g, 1.94 mol) in glacial acetic acid (600 cm³), keeping the temperature below 5 °C, and the mixture was stirred for 5 h. The mixture was then poured into water (4 l) and the precipitated nitro compounds were filtered off. The precipitate was washed with cold water and then steam distilled for four days. 6-Chloro-2-nitrophenol **158** crystallised out of the cold distillate as a yellow solid, which was filtered off (83 g, 25%) mp 67-68 °C (lit.,⁸⁵ 69 °C); δ_{H} (250MHz) ($[\text{H}]_6\text{DMSO}$) 7.98 (1H, dd, 3J 8.6, 4J 1.6), 7.86 (1H, dd, 3J 7.8, 4J 1.6) and 7.10 (1H, t, 3J 8.2); δ_{C} (63 MHz) 148.01 (quat), 137.75 (quat), 135.44 (CH), 123.73 (CH), 123.59 (quat) and 119.75 (CH); m/z 173 (100%), 156 (44), 143 (71), 115 (61), 99 (78) and 91 (65).

6-Chloro-4-nitrophenol **159** and 6-chloro-2,4-dinitrophenol **160** were also formed, but left behind as a mixture. The crude $^1\text{H NMR}$ spectroscopy revealed a 4:2:1 ratio of 6-chloro-4-nitrophenol **159**: 6-chloro-2-nitrophenol **158**: 6-chloro-2,4-dinitrophenol **160**. 6-chloro-4-nitrophenol **159**: δ_{H} ($[\text{H}]_6\text{DMSO}$) 8.18 (1H, d, 3J

2.78), 8.05 (1H, dd, 3J 9.0, 4J 2.8) and 7.10 (1H, d, 3J 9.0); 6-chloro-2,4-dinitrophenol **160**: δ_{H} ($[\text{H}]_6\text{DMSO}$) 8.60 (1H, d, 3J 3.0) and 8.34 (1H, d, 3J 3.0).

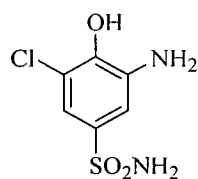


6-Chloro-2-nitro-4-sulfonamidophenol **162**



6-Chloro-2-nitrophenol **158** (21.7 g, 0.12 mol) was added slowly to chlorosulfonic acid (34 cm³, 0.5 mol), keeping the temperature below 40 °C, and was stirred at this temperature for 1 h. The mixture was cooled to room temperature and concentrated sulfuric acid was added to the stiff mixture to make it more fluid. It was then poured onto ice and the precipitated solid was filtered off. After washing acid free with cold water, the filter cake was added to ammonia solution (32%, 30 cm³) keeping the temperature below 10 °C, and was stirred at room temperature for 2 h. It was then heated on a steam bath for 1 h and allowed to cool, before being acidified with concentrated hydrochloric acid. The mixture was filtered and the dark filter cake was washed acid free with cold water to give 6-chloro-2-nitro-4-sulfonamidophenol **162** (10.5 g, 35%) mp 225 °C (lit.,⁸⁵ 230 °C); δ_{H} (250 MHz) ($[\text{H}]_6\text{DMSO}$) 8.31 (1H, d, 4J 2.2) and 8.14 (1H, d, 4J 2.2); δ_{C} (63 MHz) ($[\text{H}]_6\text{DMSO}$) 162.52 (quat), 135.20 (quat), 129.90 (quat), 128.83 (CH), 124.21 (CH) and 120.28 (quat); m/z 252 (M⁺, 100%), 236 (59), 218 (53), 125 (70) and 97 (56).

2-Amino-6-chloro-4-sulfonamidophenol **163**

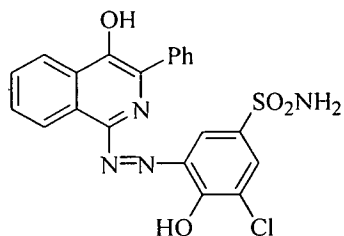


A mixture of 6-chloro-2-nitro-4-sulfonamidophenol **162** (1.5 g, 5.94 mmol), ethanol (50 cm³) and Pd/C (10%, 150 mg) was hydrogenated at room temperature for 6 h at a pressure of 3 atmospheres.⁸⁶ The catalyst was filtered off through a celite pad and the solvent was removed *in vacuo*. A dark solid resulted which was purified by dry-flash chromatography (silica), hexane/ethyl acetate (1:1) to give 2-amino-6-chloro-4-sulfonamidophenol **163** (1.15 g, 87%) mp 181 °C (lit.,⁸⁵ 184 °C); δ_{H} (250 MHz)

($[\text{H}]_6\text{DMSO}$) 7.15 (2H, brs), 7.01 (1H, d, 4J 2.2) and 6.97 (1H, d, 4J 2.2); δ_{C} (63 MHz) ($[\text{H}]_6\text{DMSO}$) 142.03 (quat), 139.47 (quat), 136.31 (quat), 119.99 (quat), 114.02 (CH) and 109.81 (CH); m/z (FAB) 223 (MH^+ , 5%), 154 (100), 138 (34), 137 (63), 136 (82) and 107 (22). FAB mass spectroscopy was used as the compound decomposed under EI conditions.

3.16 Synthesis of azo dye

3-Phenyl-1-(2-chloro-1-hydroxy-4-sulfonamidophenylazo)isoquinolin-4-ol **164**



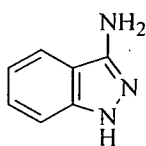
2-Amino-6-chloro-4-sulfonamidophenol **163** (0.17 g, 0.75 mmol) was dissolved in dilute sodium hydroxide solution (10%, 10 cm³), and the pH was lowered to 1.5 with concentrated hydrochloric acid. The material stayed in solution, was cooled to 0 °C, and sodium nitrite (60 mg, 0.87 mmol), dissolved in the minimum amount of

water, was added dropwise. Monitoring by HPLC showed that diazotisation readily occurred.

Due to its insoluble nature 3-phenylisoquinolin-4-ol **42** (0.166 g, 0.75 mmol) was dissolved in a mixture of acetonitrile and water at pH 9.5, and cooled to 0 °C. The diazonium solution derived from **163**, was then added dropwise over a period of 1 h, while maintaining the pH at 9.5 by the addition of very dilute sodium hydroxide and hydrochloric acid solutions. HPLC monitoring indicated that no reaction occurred at pH < 9. The reaction mixture was then stirred at room temperature overnight, with HPLC revealing > 90% conversion to product next day. A blue precipitate, 3-phenyl-1-(2-chloro-1-hydroxy-4-sulfonamidophenylazo)isoquinolin-4-ol **164** resulted, which was filtered off (0.22 g, 65%) mp 238-242 °C (Found: MH^+ (FAB) 455.0582. $\text{C}_{21}\text{H}_{16}\text{ClN}_3\text{O}_4\text{S}$ requires M 455.0581); (λ_{max} 619 nm, $w_{1/2}$ 133 nm, ϵ 15 700 l mol⁻¹ cm⁻¹) (ligand); (λ_{max} 637 nm, $w_{1/2}$ 100 nm, ϵ 25 600) (metallised); m/z (FAB) 455 (MH^+ , 1%).

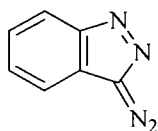
3.17 Synthesis of 3-aminoindazole 168 and diazoindazole 170

3-Aminoindazole 168



A solution of sodium nitrite (11.25 g, 0.15 mol), in the minimum amount of water (20 cm³), was added to a mixture of *o*-aminobenzonitrile (17.25 g, 0.15 mol) and concentrated hydrochloric acid (188 cm³), at 0 °C. The diazonium solution was added dropwise to a solution of stannous chloride (228 g, 1.2 mol) in concentrated hydrochloric acid (105 cm³), at 0 °C. A white solid formed, identified as the tin double salt from the elemental analysis: results, (Found: C, 23.0; H, 2.1; N, 11.0 C₇H₇Cl₄N₃Sn requires C, 21.4; H, 1.8; N, 10.7%), which was filtered without washing, and then dissolved in water. The aqueous solution was boiled for 10 min, cooled and made strongly alkaline with sodium hydroxide. The precipitated white solid that resulted was filtered, redissolved in water (not all the solid was soluble but was still added to the extraction mixture) and then continuously liquid-liquid extracted with dichloromethane for 12 h. The dichloromethane solution was stored overnight at -20 °C, after which time a white precipitate formed (identified as 3-aminoindazole) and was filtered off. The solvent was then removed from the filtrate *in vacuo*, to give a combined total of 3-aminoindazole **168** (14.2 g, 66%) mp 155 °C (from toluene) [lit.,⁹⁰ 154-156 °C]; (Found: M⁺ 133.0640. C₇H₇N₃ requires M 133.0640); δ_H (250 MHz) ([²H]₆DMSO) 11.40 (1H, s), 7.71 (1H, d, ³J 8.05), 7.20-7.29 (2H, m), 6.95 (1H, m) and 5.29 (2H, s); δ_C (63 MHz) 146.68 (quat), 139.05 (quat), 123.71 (CH), 117.76 (CH), 115.01 (CH), 111.55 (quat), and 106.96 (CH); *m/z* 133 (M⁺, 100%), 116 (32), 104 (58) and 77 (51). This procedure was an improved version of the literature method,⁹⁰ increasing the yield from 42% to 66%. This improvement was due to the continuous liquid-liquid extraction to remove the tin salt.

Diazoindazole 170



3-Aminoindazole **168** (4 g, 0.03 mol) was dissolved in a mixture of dilute hydrochloric acid solution (2M, 48 cm³), concentrated hydrochloric acid (12 cm³) and water (60 cm³), at 0 °C. A solution of sodium nitrite (2.10 g, 0.03 mmol) in water (21 cm³) was then added,

and the solution was left to stir for 20 min. Potassium acetate (43 g) was dissolved in water (19 cm³) and added to the diazonium solution, resulting in a golden brown coloured precipitate, which was identified as diazoindazole **170** (3.74 g, 87%) mp 105 °C (from acetone) [lit.,⁸⁸ 105-106 °C]; δ_{H} (250 MHz) 8.19 (1H, d, ³J 8.6), 8.03 (1H, d, ³J 8.5), 7.42-7.54 (2H, m); δ_{C} (63 MHz) 150.69 (quat), 126.06 (CH), 125.54 (CH), 124.50 (2 × quat), 119.86 (CH) and 118.08 (CH); *m/z* 144 (M⁺, 99%), 116 (100), 89 (80) and 62 (98).

3.18 Coupling reactions of diazoindazole **170**

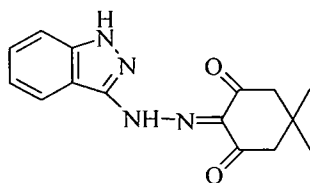
Method 1

Diazoindazole **170** was dissolved in the minimum amount of ethanol. The appropriate coupler (1 eq.) was then added to the brown solution at room temperature, resulting very quickly in a yellow precipitate, which was filtered off.^{88,89}

Method 2

Diazoindazole **170** was dissolved in the minimum amount of ethanol. The appropriate sulfonic acid derivative (1 eq.) was dissolved in the minimum amount of water, and was added *via* a syringe to the brown solution at room temperature, resulting very quickly in a precipitate, which was filtered. The water soluble azo products were analysed in their crude state, as they were insoluble in organic solvents, and therefore not suitable for purification. These compounds were also very hygroscopic and various quantities of water had to be added to their molecular formulae for the elemental analysis, which is standard practise in industry.

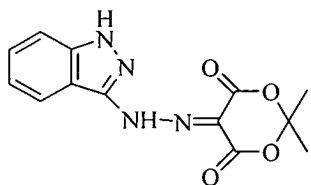
5,5-Dimethyl-1,3-cyclohexanedione -1,2,3-trione-2(indazol-3-yl)hydrazone **221**



Using method 1, diazoindazole (56 mg, 0.39 mmol) and dimedone (55 mg, 0.39 mmol) provided a yellow solid which was identified as 5,5-dimethyl-1,3-cyclohexanedione-1,2,3-trione-2(indazol-3-yl)hydrazone **221** (90 mg, 85%) mp 173-174 °C (from ethanol) [lit.,⁸⁹ 175 °C]; λ_{max} 422 nm (ϵ 19 400 l mol⁻¹ cm⁻¹) ($w_{1/2}$ 90 nm) (methanol); δ_{H} (250 MHz) ([²H]₆DMSO) 15.45 (1H, s),

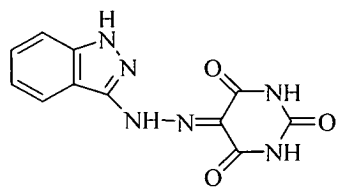
13.20 (1H, s), 8.28 (1H, d, 3J 8.2), 7.41-7.54 (2H, m), 7.23 (1H, m), 2.62 (4H, s) and 1.05 (6H, s); δ_C (63 MHz) 157.11 (2 \times quat), 141.36 (quat), 139.18 (quat), 127.81 (quat), 125.48 (CH), 119.36 (CH), 119.22 (CH), 111.04 (quat), 110.36 (quat), 108.31 (CH), 49.25 (2 \times CH₂) and 25.55 (2 \times CH₃); m/z 284 (M⁺, 16%), 200 (11), 140 (20), 133 (16) and 83 (100).

2,2-Dimethyl-1,3-dioxane-4,5,6-trione-5(indazol-3-yl)hydrazone **222**



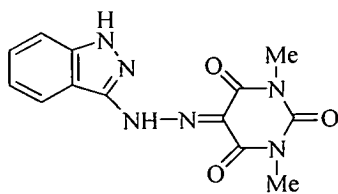
Using method 1, diazoindazole (47 mg, 0.32 mmol) and Meldrum's acid (47 mg, 0.32 mmol) provided a yellow solid which was identified as *2,2-dimethyl-1,3-dioxane-4,5,6-trione-5(indazol-3-yl)hydrazone* **222** (50 mg, 65%) mp 216-217 °C (from ethanol) (Found: C, 54.0; H, 4.10; N, 18.95. C₁₃H₁₂N₄O₄·0.2H₂O requires C, 53.6; H, 4.2; N, 19.2%); λ_{\max} 398 nm (ϵ 21 600 l mol⁻¹ cm⁻¹) (w_{1/2} 85 nm) (methanol); δ_H (250 MHz) ([²H]₆DMSO) 13.76 (1H, s), 13.24 (1H, s), 8.19 (1H, d, 3J 8.2), 7.43-7.55 (2H, m), 7.25 (1H, m) and 1.77 (6H, s); δ_C (63 MHz) 156.71 (2 \times quat), 141.06 (quat), 139.13 (quat), 125.50 (CH), 119.38 (CH), 118.90 (CH), 110.21 (quat), 110.11 (quat), 108.37 (CH), 103.12 (quat) and 24.54 (2 \times CH₃); m/z 288 (M⁺, 5%), 159 (39), 158 (31), 103 (62), 77 (29) and 43 (100).

Pyrimidine-2,4,5,6-tetraone-5(indazol-3-yl)hydrazone **223**



Using method 1, diazoindazole (53 mg, 0.37 mmol) and barbituric acid (47 mg, 0.37 mmol) provided a yellow solid which was identified as *pyrimidine-2,4,5,6-tetraone-5(indazol-3-yl)hydrazone* **223** (74 mg, 74%) mp (decomposed) > 340 °C (Found: M⁺ 272.0656. C₁₁H₈N₆O₃ requires M 272.0658); λ_{\max} 411 nm (ϵ 23 600 l mol⁻¹ cm⁻¹) (w_{1/2} 80 nm) (methanol); δ_H (250 MHz) ([²H]₆DMSO) 14.76 (1H, s), 13.11 (1H, s), 11.39 (2H, s), 8.23 (1H, d, 3J 8.2), 7.41-7.55 (2H, m) and 7.22 (1H, m); δ_C (63 MHz) 147.37 (2 \times quat), 141.35 (quat), 139.14 (quat), 125.42 (CH), 119.23 (CH), 119.06 (CH), 115.44 (quat), 110.06 (quat) and 108.24 (CH); m/z 272 (M⁺, 10%), 144 (17), 128 (57), 118 (71) and 42 (100).

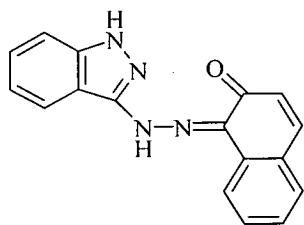
1,3-Dimethylpyrimidine-2,4,5,6-tetraone-5(indazol-3-yl)hydrazone **224**



Using method 1, diazoindazole (51 mg, 0.35 mmol) and 1,3-dimethyl barbituric acid (55 mg, 0.35 mmol) provided a yellow solid which was identified as 1,3-dimethylpyrimidine-2,4,5,6-tetraone-5(indazol-3-yl)hydrazone **224** (82 mg, 78%) mp (sublimed) > 280 °C;

(Found: M^+ 300.0971. $C_{13}H_{12}N_6O_3$ requires M 300.0971); λ_{\max} 411 nm (ϵ 20 800 l mol⁻¹ cm⁻¹) ($w_{1/2}$ 80 nm) (methanol); δ_H (250 MHz) ($[^2H]_6$ DMSO) 14.63 (1H, s), 13.16 (1H, s), 8.27 (1H, d, 3J 8.1), 7.47-7.53 (2H, m), 7.26 (1H, m) and 3.20 (6H, s); δ_C (63 MHz) 160.51 (quat), 158.40 (quat), 150.42 (quat), 143.59 (quat), 141.48 (quat), 127.84 (CH), 121.51 (2 \times CH), 117.29 (quat), 112.43 (quat), 110.62 (CH), 27.95 (CH₃) and 27.06 (CH₃); m/z 300 (M^+ , 16%), 156 (77), 99 (20), 71 (47) and 42 (100).

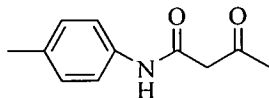
1,2-Napthoquinone-1(indazol-3-yl)hydrazone **225**



Using method 1, diazoindazole (56 mg, 0.39 mmol) and β -naphthol (56 mg, 0.39 mmol) provided an orange solid which was identified as 1,2-napthoquinone-1(indazol-3-yl)hydrazone **225** (80 mg, 70%) mp 257-258 °C (from ethanol:xylene 2:1) [lit.,⁸⁸ 257 °C]; λ_{\max} 457 nm (ϵ 20 700 l

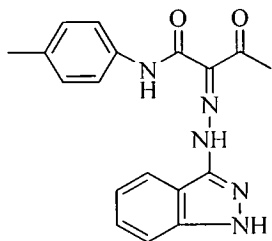
mol⁻¹ cm⁻¹) ($w_{1/2}$ 113 nm) (methanol); δ_H (250 MHz) ($[^2H]_6$ DMSO) 8.93 (1H, brd), 8.67 (1H, brd), 8.17-8.26 (2H, m), 7.90-7.94 (2H, brm) 7.76-7.80 (2H, brm), 7.48 (1H, brd) and 7.32 (1H, brd); δ_C (63 MHz) 154.24 (quat), 152.45 (quat), 141.81 (quat), 135.80 (CH), 131.84 (quat), 128.56 (2 \times CH), 127.94 (quat), 127.63 (CH), 124.75 (CH), 123.85 (CH), 121.86 (CH), 120.87 (CH), 120.25 (CH), 112.93 (quat) and 111.09 (CH); m/z 288 (M^+ , 100%), 270 (26), 259 (44), 231 (26), 144 (100) and 118 (33). Coupling constants could not be calculated due to the broad signals obtained.

N-p-Tolylacetoacetamide **226**



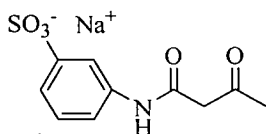
A stirred solution of ethyl acetoacetate (0.58 g, 4.5 mmol) and *p*-toluidine (0.48 g, 4.5 mmol) in *p*-xylene (18 cm³) was heated under a Dean-Stark head for 5 h in an oil bath at 185 °C.¹³ The solution was allowed to cool to room temperature, petroleum-ether (bp 60-80 °C) (20 cm³) was added, and the solution was stirred overnight, during which time a precipitate formed. The precipitate was filtered, washed with petroleum-ether (bp 60-80 °C) and dried to afford *N-p*-tolylacetoacetamide **226** (0.26 g, 31%) mp 93-94 °C (from xylene:ethanol 1:2) [lit.,¹²³ 95 °C]; δ_{H} (250 MHz) 8.99 (1H, s), 7.34 (2H, d, ³*J* 8.1), 7.08 (2H, d, ³*J* 8.1), 3.49 (2H, s) and 2.23 (6H, s); δ_{C} (63 MHz) 205.11 (quat), 163.31 (quat), 134.74 (quat), 134.10 (quat), 129.32 (2 × CH), 120.11 (2 × CH), 49.66 (CH₂), 31.06 (CH₃) and 20.72 (CH₃); *m/z* 191 (M⁺, 78%), 133 (65), 107 (100), 77 (54) and 43 (88).

2-[(1*H*-Indazol-3-yl)-hydrazono]-3-oxo-*N-p*-tolylbutyramide **227**



Using method 1, diazoindazole **170** (50 mg, 0.35 mmol) and *N-p*-tolylacetoacetamide **226** (67 mg, 0.35 mmol) provided a yellow solid which was identified as 2-[(1*H*-indazol-3-yl)-hydrazono]-3-oxo-*N-p*-tolylbutyramide **227** (0.1 g, 85%) mp 240-260 °C (from ethanol:xylene 2:1) (Found: M⁺ 335.1387. C₁₈H₁₇N₅O₂ requires *M* 335.1382); λ_{max} 390 nm (ϵ 25 000 l mol⁻¹ cm⁻¹) (*w*_{1/2} 75 nm) (methanol); δ_{H} (250 MHz) ([²H]₆DMSO) 14.91 (1H, s), 12.95 (1H, s), 11.28 (1H, s), 8.08 (1H, d, ³*J* 7.9), 7.45-7.39 (4H, m), 7.23-7.14 (3H, m), 2.50 (3H, s) and 2.29 (3H, s); δ_{C} (63 MHz) 129.30 (2 × CH), 127.50 (CH), 120.85 (CH), 120.19 (2 × CH), 111.44 (CH) and 27.06 (CH₃); *m/z* 335 (M⁺, 5%), 317 (87), 300 (39), 157 (62), 133 (30), 116 (84) and 107 (100). Due to the insoluble nature of this compound, even after heating the sample, only the signals reported above were apparent in the ¹³C spectrum.

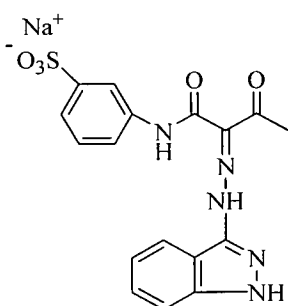
Sodium *N*-acetylacetomidoaniline-3-sulfonic acid **230**



Dilute sodium hydroxide solution (2M, 35 cm³) was added to a mixture of metanilic acid (12.6 g, 0.073 mol) and water (70

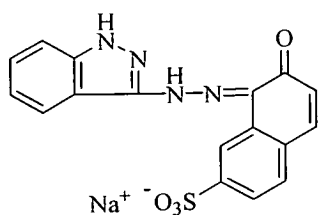
cm³) until the pH = 9, at which point all the metanilic acid dissolved, resulting in a dark brown solution. This solution was cooled to -3 °C using a sodium chloride/ice mixture and diketene (6.8 g, 0.08 mol) was added. The ice bath was removed and the solution was allowed to warm to 10 °C, at which point more diketene (2.23 g, 30 mmol) was added. This was then warmed to 20 °C, where a further addition of diketene (0.8 g, 9.5 mmol) was made, and the solution was stirred for 1 h. The solvent was then removed *in vacuo*, resulting in a white solid, which was dissolved in methanol, heated to reflux for 1 h and left overnight to cool.¹¹³ The resulting solid was filtered and washed with methanol until a pale yellow colour was obtained, to give *sodium N-acetylacetomidoaniline-3-sulfonic acid* **230** (7.6 g, 75%) mp 231-233 °C (Found: MH⁺ (FAB) 280.0259. C₁₀H₁₁NO₅ requires *M* 280.0256); δ_H (250 MHz) ([²H]₆DMSO) 10.42 (1H, s), 8.10 (1H, s), 7.82 (1H, d, ³*J* 7.8), 7.57-7.47 (2H, m), 3.83 (2H, s) and 2.45 (3H, s); δ_C (63 MHz) 202.73 (quat), 164.94 (quat), 148.35 (quat), 138.13 (quat), 127.96 (CH), 120.46 (CH), 119.00 (CH), 116.36 (CH), 52.16 (CH₂) and 30.00 (CH₃); *m/z* (FAB) 280 (MH⁺, 48%).

Sodium 3-{2-[(1*H*-Indazol-3-yl)-hydrazono]-3-oxo-butyrylamino}-benzenesulfonic acid **231**



Using method 2, diazoindazole **170** (50 mg, 0.35 mmol) and sodium *N-m*-sulfacetoacetamide **230** (100 mg, 0.35 mmol) provided a yellow solid which was identified as *sodium 3-{2-[(1*H*-indazol-3-yl)-hydrazono]-3-oxo-butyrylamino}-benzenesulfonic acid* **231** (0.115 g, 79%) mp > 350 °C (Found: C, 43.0; H, 4.1; N, 14.6. C₁₇H₁₄N₅O₅S.3H₂O requires C, 42.8; H, 3.6; N, 14.65%); λ_{max} 380 nm (ε 14 100 l mol⁻¹ cm⁻¹) (w_{1/2} 71 nm); δ_H (250 MHz) ([²H]₆DMSO) 15.01 (1H, s), 13.20 (1H, s), 11.62 (1H, s), 8.33 (1H, d, ³*J* 8.2), 8.17 (1H, s), 7.61-7.86 (5H, m), 7.51 (1H, t, ³*J* 7.4) and 2.79 (3H, s); δ_C (63 MHz) 197.73 (quat), 162.07 (quat), 148.78 (quat), 143.68 (quat), 141.41 (quat), 136.36 (quat), 120.22 (CH), 128.35 (CH), 127.95 (CH), 127.34 (quat), 121.59 (CH), 121.05 (quat), 120.70 (CH), 117.43 (CH), 112.04 (CH), 110.54 (CH) and 26.25 (CH₃); *m/z* (FAB) 424 (MH⁺, 5%).

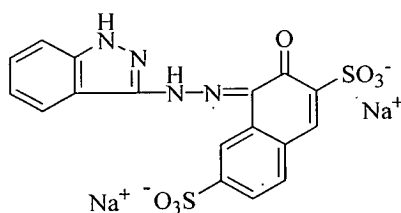
Sodium 1,2-naphthoquinone-7-sulfonate-1(indazol-3-yl)hydrazone **246**



Using method 2, diazoindazole **170** (50 mg, 0.35 mmol) and F-acid (85 mg, 0.35 mmol) provided a red solid which was identified as *sodium 1,2-naphthoquinone-7-isulfonate-1(indazol-3-yl)hydrazone* **246** (80 mg, 60%) mp (decomposed) > 325 °C (Found:

C, 48.0; H, 3.6; N, 13.0 C₁₇H₁₁N₄NaO₄S.2H₂O requires C, 47.9; H, 3.1; N, 13.1%); λ_{\max} 447 nm (ϵ 15 800 l mol⁻¹ cm⁻¹) (w_{1/2} 127 nm); δ_{H} (250 MHz) ([²H]₆DMSO) 14.81 (1H, s), 14.10 (1H, s), 9.14 (1H, s), 8.52 (1H, d, ³J 8.1), 8.09 (1H, d, ³J 9.2), 7.96 (1H, d, ³J 8.4), 7.72-7.80 (2H, m), 7.59 (1H, t, ³J 6.9), 7.45 (1H, t, ³J 7.1) and 7.31 (1H, d, ³J 9.1); δ_{C} (63 MHz) 178.71 (quat), 153.96 (quat), 152.42 (quat), 147.39 (quat), 141.74 (quat), 135.37 (CH), 131.27 (quat), 130.04 (quat), 128.31 (CH), 127.84 (CH), 123.90 (CH), 122.55 (CH), 121.96 (CH), 120.64 (CH), 118.04 (CH), 112.99 (quat) and 111.13 (CH); *m/z* (FAB) 391 (MH⁺, 63%).

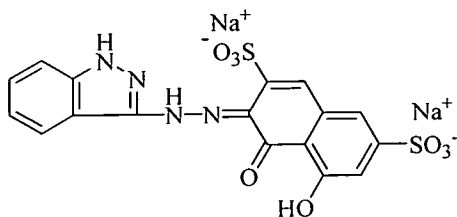
Disodium 1,2-naphthoquinone-3,7-disulfonate-1(indazol-3-yl)hydrazone **247**



Using method 2, diazoindazole **170** (0.63 g, 4.4 mmol) and sulfo F-acid (1.53 g, 4.4 mmol) provided a red coloured solid which was identified as *disodium 1,2-naphthoquinone-3,7-disulfonate-1(indazol-3-yl)hydrazone* **247** (2.18 g, 98%) mp

(decomposed) 280-310 °C (Found: C, 36.2; H, 3.1; N, 9.6. C₁₇H₁₀N₄Na₂O₇S₂.4H₂O requires C, 36.2; H, 2.5; N, 9.95%); λ_{\max} 467 nm (ϵ 15 600 l mol⁻¹ cm⁻¹) (w_{1/2} 178 nm); δ_{H} (250 MHz) ([²H]₆DMSO) 15.47 (1H, s), 13.83 (1H, s), 9.02 (1H, s), 8.47-8.51 (2H, m), 8.07 (1H, d, ³J 8.4), 7.73-7.80 (2H, m), 7.59 (1H, t, ³J 8.3) and 7.43 (1H, t, ³J 7.3); δ_{C} (63 MHz) 155.61 (quat), 150.85 (quat), 148.16 (quat), 141.69 (quat), 137.42 (quat), 133.97 (CH), 131.68 (quat), 130.31 (quat), 129.29 (CH), 127.83 (CH), 126.06 (quat), 123.56 (CH), 123.01 (CH), 121.77 (CH), 117.95 (CH), 113.08 (quat) and 111.14 (CH); *m/z* (FAB) 493 (MH⁺, 3%).

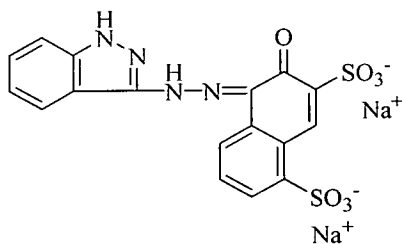
Disodium 1,2-naphthoquinone-3,6-disulfonate-8-hydroxy-2(indazol-3-yl)hydrazone 248



Using method 2, diazoindazole **170** (40 mg, 0.28 mmol) and chromotropic acid (100 mg, 0.28 mmol) provided a purple coloured solid which was identified as *disodium 1,2-naphthoquinone-3,6-disulfonate-8-hydroxy-*

2(indazol-3-yl)hydrazone (90 mg, 64%) mp (decomposed) > 350 °C (Found: C, 35.55; H, 2.55; N, 9.7. C₁₇H₁₀N₄Na₂O₈S₂·4H₂O requires C, 35.2; H, 3.1; N, 9.65%); λ_{max} 530 nm (ε 27 900 l mol⁻¹ cm⁻¹) (w_{1/2} 102 nm); δ_H (250 MHz) ([²H]₆DMSO) 16.73 (1H, s), 13.45 (1H, s), 12.94 (1H, s), 9.60 (1H, d, ³J 8.2), 7.48-7.59 (3H, m), 7.43 (1H, s), 7.22 (1H, t, ³J 7.4) and 7.10 (1H, s); δ_C (63 MHz) 162.17 (2 × quat), 154.12 (quat), 142.90 (CH), 141.42 (quat), 136.23 (quat), 127.73 (CH), 127.63 (CH), 124.50 (quat), 121.54 (CH), 121.26 (CH), 116.27 (CH), 113.23 (quat), 110.13 (quat) and 109.66 (CH); *m/z* (FAB) 509 (MH⁺, 16%). Not all quaternary carbon signals were identified due to the insoluble nature of this compound.

Disodium 1,2-naphthoquinone-3,5-disulfonate-1(indazol-3-yl)hydrazone



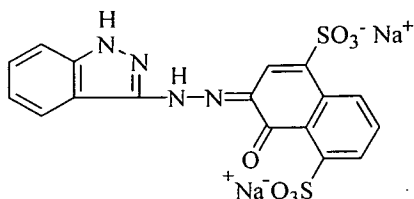
Using method 2, diazoindazole **170** (50 mg, 0.35 mmol) and R-acid (105 mg, 0.35 mmol) provided a red solid which was identified as *disodium 1,2-naphthoquinone-3,5-disulfonate-1(indazol-3-yl)hydrazone 249* (0.102 g, 60%) mp (decomposed) > 325 °C; (Found: MH⁺ (FAB)

492.9861 C₁₇H₁₁N₄O₇ requires *M* 492.9865); λ_{max} 467 nm (ε 9 300 l mol⁻¹ cm⁻¹) (w_{1/2} 160 nm) (ligand); λ_{max} 541 nm (ε 15 536) (w_{1/2} 107 nm) (metallised); δ_H (250 MHz) ([²H]₆DMSO) 9.02 (1H, brs), 8.80 (1H, brs), 8.62 (1H, brs), 8.35 (1H, brs), 8.18 (1H, brs) and 7.29-7.90 (3H, brm); δ_C (63 MHz) 178.15 (2 × quat), 163.21 (quat), 156.73 (quat), 144.48 (quat), 134.67 (CH), 127.60 (CH), 127.10 (quat), 125.71 (CH), 123.53 (CH), 121.90 (CH), 120.68 (CH) and 111.01 (CH); *m/z* (FAB) 493 (MH⁺, 6%). Due to the insoluble nature of this compound, not all of the quaternary peaks were identified in the ¹³C spectrum.

Ring opening/Coupling of 1,8-naphthosultone-4-sulfonic acid; sodium salt

Sodium 1,8-naphthosultone-4-sulfonic acid **239** (2.0 g, 7 mmol) was dissolved in dilute sodium carbonate solution (1 eq.), and the resulting solution was heated to reflux for 45 min, giving a dark red solution, which was allowed to cool to room temperature. Procedure then followed method 2 above.

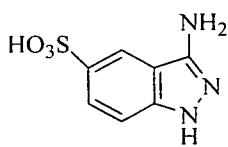
Disodium 1,2-naphthoquinone-4,8-disulfonate-2(indazol-3-yl)hydrazone **241**



Using method 2, diazoindazole **170** (1 g, 7 mmol) and a solution of disodium 1-naphthol-4,8-disulfonic acid **240** derived from sodium 1,8-naphthosultone-4-sulfonic acid **239** (2 g, 7 mmol) provided a dark red solid which was identified as

disodium 1,2-naphthoquinone-4,8-disulfonate-2(indazol-3-yl)hydrazone **249** (2.68 g, 78%) mp > (decomposed) 330 °C (Found: C, 36.55; H, 2.45; N, 10.05. C₁₇H₁₀N₄Na₂O₇S₂·4H₂O requires C, 36.2; H, 3.2; N, 9.95%); λ_{max} 507 nm (ε 14 600 l mol⁻¹ cm⁻¹) (w_{1/2} 131 nm); δ_H (250 MHz) ([²H]₆DMSO) 13.89 (1H, brs), 9.08 (1H, d, ³J 8.5), 8.62 (1H, s), 8.59 (1H, d, ³J 8.1), 8.26 (1H, d, ³J 7.3) 7.60-7.68 (2H, m), 7.51 (1H, t, ³J 8.2) and 7.40 (1H, t, ³J 6.9); δ_C (63 MHz); 158.80 (2 × quat), 142.69 (quat), 135.81 (quat), 135.15 (quat), 133.52 (quat), 130.91 (CH), 127.39 (CH), 126.16 (CH), 125.91 (CH), 123.63 (CH), 123.39 (CH), 122.31 (quat), 117.86 (quat), 114.17 (CH) 113.19 (quat) and 110.48 (CH); m/z (FAB) 493 (MH⁺, 1%).

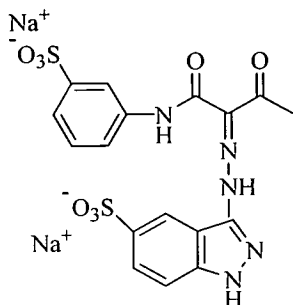
3.19 Synthesis and coupling reaction of 3-aminoindazole-5-sulfonic acid **233**



3-Aminoindazole **168** (3.0 g, 0.02 mol) was added in portions to a stirred oleum (20%, 15 cm³) solution. A stiff paste formed which gradually dissolved, and the resulting solution was stirred overnight at room temperature. Next day, it was drowned into an ice/water mixture and stirred for 1 h.¹¹⁴ A precipitate formed which was filtered and dried *in vacuo*, and was identified as 3-aminoindazole-5-sulfonic acid **233** (2.95 g, 60%) mp (sublimed) > 300 °C; δ_H (250 MHz) 8.20 (1H, s), 7.67 (1H, d, ³J 8.8) and 7.29 (1H, d, ³J 8.8); δ_C (63 MHz) 144.17 (quat), 141.70 (quat), 141.21 (quat), 129.32 (CH), 118.63 (CH), 111.02 (quat) and 110.54 (CH); m/z (FAB)

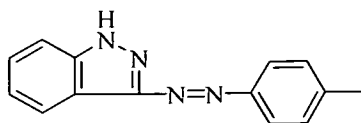
214 (MH⁺, 35%). The regioselectivity was established by a fully coupled ¹H-¹³C spectrum.

Disodium 3-{N'-[2-Oxo-1-(3-sulfophenylcarbamoyl)-propylidene]-hydrazino}-1H-indazole-5-sulfonic acid 234



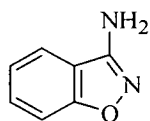
3-Aminoindazole-5-sulfonic acid **233** (1.15 g, 5.4 mmol) was dissolved in dilute aqueous sodium hydroxide solution (10%, 5 cm³), and the pH was adjusted to 7. The solution was cooled to 0 °C and the pH was dropped to 1-2 using concentrated hydrochloric acid. Sodium nitrite (0.4 g, 5.8 mmol) was added, resulting in an orange coloured solution, which was stirred for 45 min. Sodium *N*-acetylacetimidooaniline-3-sulfonic acid **230** (1.5 g, 5.4 mmol) was dissolved in the minimum amount of an aqueous solution of sodium hydroxide (10%), and the pH was adjusted to 7-8. This solution was cooled to 0 °C and the diazonium solution was added, resulting in a very dark coloured solution which was stirred for 20 min. The pH was dropped to 3, and then to 1, after which sodium chloride (15% w/v) solution was added to precipitate out the product, which was filtered and dried *in vacuo*, to give *disodium 3-{N'-[2-oxo-1-(3-sulfophenylcarbamoyl)-propylidene]-hydrazino}-1H-indazole-5-sulfonic acid 234* (2 g, 70%) mp (decomposed) > 300 °C (Found: C, 23.9; H, 2.7; N, 8.1. C₁₇H₁₃N₅Na₂O₈S₂ requires C, 38.9; H, 2.5; N, 13.3%); (Found: C, 23.9; H, 2.7; N, 8.1. C₁₇H₁₃N₅Na₂O₈S₂.5H₂O.4NaCl requires C, 24.0; H, 2.7; N, 8.2%); λ_{max} 360 nm (ε 11 700 l mol⁻¹ cm⁻¹); δ_H (360 MHz) ([²H]₆DMSO) 11.26 (1H, s), 8.78 (1H, s), 8.33 (1H, s), 8.05-8.15 (2H, m), 7.83 (1H, d, ³J 7.6), 7.38-7.49 (2H, m) and 3.26 (3H, s); δ_C (90 MHz) 162.05 (quat), 150.61 (quat), 148.20 (quat), 145.11 (quat), 143.23 (quat), 139.84 (quat), 137.82 (quat), 136.31 (quat), 129.96 (CH), 128.18 (CH), 121.56 (CH), 120.82 (CH), 117.77 (CH), 117.32 (CH), 117.28 (quat), 116.52 (CH) and 13.60 (CH₃); *m/z* (FAB) 526 (MH⁺, 3%); L = 99.8, a = -5.5, b = 10.3, C = 11.7 and h = 118.3. For the elemental analysis results, various amounts of water and sodium chloride were added to the molecular formula, due to the hygroscopic nature of the compound and the quantities of sodium chloride added during isolation. The additions shown above gave the best results.

3.20 3-(*p*-Toluidineazo)indazole 237



p-Toluidine (0.82 g, 7.63 mmol, 3 eq.) was dissolved in dilute hydrochloric acid solution (1M, 25 cm³) and water (11 cm³), at 0 °C. Sodium nitrite (0.63 g, 9.13 mmol) was added, and the solution was stirred for 20 min. Indazole (0.3 g, 2.54 mmol) was dissolved in dilute hydrochloric acid solution (1M, 12 cm³), and was cooled to 0 °C. The diazonium solution (1 eq.) was added, followed by sodium hydroxide, until a precipitate was formed. This precipitate was redissolved by the addition of concentrated hydrochloric acid. A further addition of the diazonium solution (1 eq.) was then made, followed by the addition of sodium hydroxide, and then hydrochloric acid again. This step was repeated for a third time, and after the final addition of sodium hydroxide, the resulting precipitate was filtered. The solid obtained was purified by dry-flash chromatography (hexane/ethyl acetate 3:1) to give 3-(*p*-toluidineazo)indazole **237** (0.14 g, 23%) mp 210-211 °C (Found: M⁺ 236.10603 C₁₄H₁₂N₄O requires *M* 236.10620); λ_{max} 357 nm (ε 22 700 l mol⁻¹ cm⁻¹) (w_{1/2} 61 nm); δ_H (250 MHz) 12.85 (1H, s), 8.36 (1H, d, ³*J* 8.2), 7.86 (2H, d, ³*J* 8.2), 7.65 (1H, d, ³*J* 8.3) 7.31-7.62 (4H, m) and 2.36 (3H, s); δ_C (63 MHz) 155.03 (quat), 150.48 (quat), 141.22 (quat), 139.61 (quat), 129.79 (2 × CH), 127.68 (CH), 122.64 (2 × CH), 122.01 (CH), 120.84 (CH), 112.82 (quat), 110.45 (CH) and 20.83 (CH₃); *m/z* 236 (M⁺, 41%), 208 (42), 145 (15), 118 (28), 90 (32) and 91 (100).

3.21 3-Amino-1,2-benzisoxazole 253



Acetone oxime (1 g, 1.4 mmol) was dissolved in DMF (13 cm³), potassium *tert*-butoxide (1.57 g, 1.4 mmol) was added, and the mixture was stirred for 30 min. *o*-Fluorobenzonitrile (1.57 g, 1.3 mmol) was then added, and the mixture was stirred for a further 1 h. The reaction mixture was poured onto a mixture of saturated ammonium chloride and ether; the organic layer was separated, washed with water and dried. The ether was removed *in vacuo* to give an oil **252**.¹¹⁸

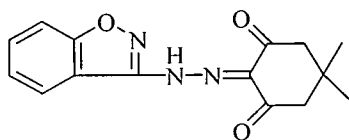
The oil **252** (1.82 g, 0.01 mol) was heated to reflux in a mixture of ethanol (22.5 cm³) and dilute hydrochloric acid (5%, 22.5 cm³) for 45 min. The ethanol was removed *in vacuo*, and the remaining aqueous phase was made basic with solid potassium

carbonate, and extracted with ethyl acetate ($3 \times 25 \text{ cm}^3$). The combined organic layers were washed with water, dried and evaporated to give a residue, which was triturated with ether and dried *in vacuo* several times, resulting in a brown solid, which was identified as 3-amino-1,2-benzisoxazole **253** (1.01 g, 72%) mp 108-110 °C [lit., ¹¹⁸ 110 °C]; δ_{H} (250 MHz) ($[\text{H}]_6\text{DMSO}$) 7.86 (1H, d, ³J 7.8), 7.44-7.56 (2H, m), 7.26 (1H, d, ³J 7.8) and 6.44 (2H, s); δ_{C} (63 MHz) 161.63 (quat), 158.38 (quat), 129.61 (CH), 121.78 (CH), 121.51 (CH), 116.62 (quat) and 109.15 (CH); m/z 134 (M^+ , 100%), 119 (43), 91 (85), 79 (77), 64 (72) and 56 (92).

3.22 General Method For Coupling reactions of 3-Amino-1,2-benzisoxazole **253**

3-Amino-1,2-benzisoxazole **253** was dissolved in a mixture of concentrated hydrochloric acid and a small amount of water. The solution was cooled to 0 °C, sodium nitrite (1 eq.) was added, and the solution was stirred for 20 min. The appropriate coupler (1 eq.) was dissolved in dilute sodium hydroxide solution (2M) to take the pH to approximately 8. The diazonium solution was then added dropwise to the alkaline solution and stirred at 0 °C for 30 min. A precipitate formed, which was filtered and dried *in vacuo*.

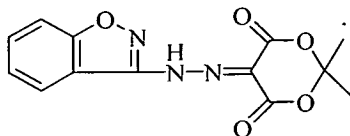
5,5-Dimethyl-1,3-cyclohexanedione-1,2,3-trione-2(benzisoxazol-3-yl)hydrazone **254**



Following the general method, 3-amino-1,2-benzisoxazole **253** (100 mg, 0.75 mmol), sodium nitrite (55 mg, 0.8 mmol) and dimedone (104 mg, 0.75 mmol) provided a yellow solid which was identified as 5,5-dimethyl-1,3-cyclohexanedione-1,2,3-trione-2(benzisoxazol-3-yl)hydrazone **254** (0.18 g, 82%) mp 188-190 °C (from methanol) (Found: C, 61.5; H, 5.1; N, 14.2 $\text{C}_{15}\text{H}_{15}\text{N}_3\text{O}_3 \cdot 0.5\text{H}_2\text{O}$ requires C, 61.2; H, 5.3; N, 14.3%); λ_{max} 351 nm (ϵ 11 400 $\text{l mol}^{-1} \text{cm}^{-1}$) ($w_{1/2}$ 85 nm) (methanol); δ_{H} (250 MHz) ($[\text{H}]_6\text{DMSO}$) 14.53 (1H, s), 8.28 (1H, d, ³J 7.2), 7.68 (2H, m), 7.43 (1H, m), 2.66 (2H, s), 2.59 (2H, s) and 0.98 (6H, s); δ_{C} (63 MHz) 163.16 (2 \times quat), 157.09 (quat), 132.62 (quat), 131.49 (CH), 126.16 (quat), 124.49 (CH), 124.00 (CH), 113.06 (quat), 110.03 (CH), 102.89 (quat), 51.70 (2 \times CH_2) and

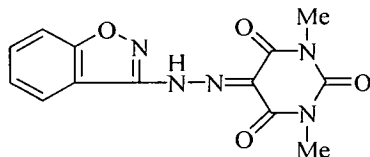
27.78 ($2 \times \text{CH}_3$); m/z 285 (M^+ , 52%), 242 (22), 173 (42), 145 (34), 134 (20), 119 (100) and 91 (79).

2,2-Dimethyl-1,3-dioxane-4,5,6-trione-5(benzisoxazol-3-yl)hydrazone 255



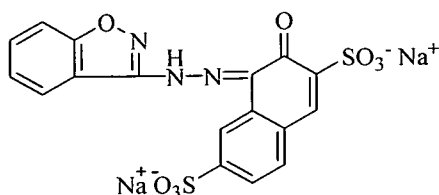
Following the general method, 3-amino-1,2-benzisoxazole **253** (100 mg, 0.75 mmol), sodium nitrite (55 mg, 0.8 mmol) and Meldrum's acid (108 mg, 0.75 mmol) provided a yellow solid which was identified as 2,2-dimethyl-1,3-dioxane-4,5,6-trione-5(benzisoxazol-3-yl)hydrazone **255** (0.11 g, 51%) mp (decomposed) 210-220 °C (from methanol) (Found: M^+ 289.0699. $\text{C}_{13}\text{H}_{11}\text{N}_3\text{O}_5$ requires M 289.0699); λ_{max} 344 nm (ϵ 11 900 $\text{l mol}^{-1} \text{cm}^{-1}$) ($w_{1/2}$ 64 nm) (methanol); δ_{H} (250 MHz) ($[\text{}^2\text{H}]_6\text{DMSO}$) 8.29 (1H, d, 3J 8.0), 7.77-7.91 (2H, m), 7.54 (1H, t, 3J 7.8) and 1.82 (6H, s); δ_{C} (63 MHz) 163.98 ($2 \times$ quat), 157.89 (quat), 132.30 (CH), 131.53 (quat), 125.82 (CH), 125.76 (CH), 124.62 (quat), 113.54 (quat), 110.82 (CH), 105.94 (quat) and 27.06 (CH_3); m/z 289 (M^+ , 10%), 253 (7), 221 (85), 159 (15), 119 (29), 103 (30) and 91 (100).

1,3-Dimethylpyrimidine-2,4,5,6-tetraone-5(benzisoxazol-3-yl)hydrazone 256



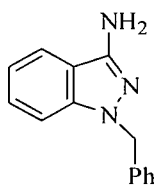
Following the general method, 3-amino-1,2-benzisoxazole **253** (100 mg, 0.75 mmol), sodium nitrite (55 mg, 0.8 mmol) and 1,3-dimethylbarbituric acid (117 mg, 0.75 mmol) provided a yellow solid which was identified as 1,3-dimethylpyrimidine-2,4,5,6-tetraone-5(benzisoxazol-3-yl)hydrazone **256** (0.112 g, 50%) mp (decomposed) 218-230 °C (from methanol) (Found: MH^+ (FAB) 301.0811. $\text{C}_{13}\text{H}_{11}\text{N}_5\text{O}_4$ requires M 301.0811); λ_{max} 355 nm (ϵ 22 000 $\text{l mol}^{-1} \text{cm}^{-1}$) ($w_{1/2}$ 98 nm) (methanol); δ_{H} (250 MHz) ($[\text{}^2\text{H}]_6\text{DMSO}$) 8.42 (1H, brd), 7.96 (2H, m), 7.72 (1H, m) and 3.44 (6H, s); δ_{C} (63 MHz) 124.52 (CH); m/z 301 (M^+ , 5%), 273 (9), 216 (7), 182 (37), 156 (17), 119 (100) and 91 (97). Due to the insoluble nature of this compound, the ^{13}C NMR spectrum proved very difficult to analyse, with only one CH signal easily identifiable.

Disodium 1,2-naphthoquinone-3,7-disulfonate-1(benzisoxazol-3-yl)hydrazone 257



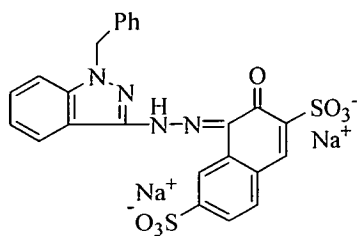
Following the general method, 3-amino-1,2-benzisoxazole **253** (2 g, 0.015 mol), sodium nitrite (1.1 g, 0.016 mol) and sulfo F-acid (5.2 g, 0.015 mol) provided an orange coloured solid which was identified as *disodium 1,2-naphthoquinone-3,7-disulfonate-1(benzisoxazol-3-yl)hydrazone 257* (5.8 g, 78%) mp 220-240 °C (Found: MH⁺ (FAB) 493.9706. C₁₇H₁₀N₃O₈ requires *M* 493.9705); λ_{max} 459 nm (ε 9 200) (w_{1/2} 125 nm) (ligand); λ_{max} 530 nm (ε 10 800 l mol⁻¹ cm⁻¹) (w_{1/2} 100 nm) (metallised); δ_H (250 MHz) ([²H]₆DMSO) 8.91 (1H, s), 8.61 (2H, s), 7.96-8.14 (4H, m) and 7.78 (1H, t, ³*J* 6.2); δ_C (63 MHz) 173.98 (quat), 163.62 (quat), 158.06 (quat), 149.64 (quat), 140.42 (CH), 132.41 (quat), 131.83 (quat), 131.63 (CH), 130.43 (CH), 126.91 (quat), 125.09 (CH), 124.80 (CH), 123.12 (CH), 119.11 (CH), 113.68 (quat) and 110.44 (CH); *m/z* (FAB) 494 (MH⁺, 1%).

3.23 Synthesis and coupling reaction of 3-amino-1-benzylindazole 258



3-Aminoindazole **168** (0.4 g, 3 mmol) was added to a solution of powdered potassium hydroxide (0.45 g, 8 mmol) in DMSO (60 cm³), and stirred for 10 min. Benzyl chloride (0.43 cm³, 3.75 mmol) was added and the mixture was stirred for 2 h, after which the solution was diluted with water (90 cm³). The resulting red/orange coloured emulsion was extracted with (3 × 45 cm³) portions of chloroform, and the combined organic layers were washed with (3 × 45 cm³) water portions.¹²² The organic layer was then dried with MgSO₄ and evaporated to give 3-amino-1-benzylindazole **258** as a deep orange coloured solid, which was purified by dry-flash chromatography (ethyl acetate:hexane 1:1) (0.36 g, 54%) mp 115-116 °C (from ethanol) [lit.,¹²² 116 °C]; δ_H (250 MHz) ([²H]₆DMSO) 7.45 (1H, d, ³*J* 8.1), 7.06-7.21 (7H, m), 6.85 (1H, t, ³*J* 8.1), 5.27 (2H, s) and 4.01 (2H, s); δ_C (63 MHz) 147.26 (quat), 141.13 (quat), 137.35 (quat), 134.28 (CH), 128.44 (2 × CH), 127.31 (CH), 126.86 (2 × CH), 119.43 (CH), 118.51 (CH), 114.76 (quat), 108.74 (CH) and 51.88 (CH₂); *m/z* 223 (M⁺, 80%), 146 (27), 132 (63), 118 (27), 104 (59), 91 (100) and 77 (62).

Disodium 1,2-naphthoquinone-3,7-disulfonate-1(1-benzylindazole-3-yl)hydrazone 259



3-Amino-1-benzylindazole **258** (0.91 g, 4.1 mmol) was dissolved in acetonitrile (7 cm³) at pH 7. Concentrated hydrochloric acid was added until the pH dropped to 1-2, and the solution was cooled to 0 °C. Sodium nitrite (0.34 g, 4.93 mmol) was added, and the solution was left to stir for 1 h. Disodium 2-naphthol-3,7-disulfonic acid (1.41 g, 4.1 mmol) was dissolved in dilute sodium hydroxide solution (10%, 10 cm³), and the pH was adjusted to 7-8, at 0 °C. The diazonium solution was then added dropwise to the alkaline solution, where upon the pH dropped quickly and was adjusted after each addition, back to 7-8. A red/brown solution resulted which was stirred for 30 min, and the pH was then dropped to 3-4. A precipitate formed which was filtered, and dried *in vacuo* to give *disodium 1,2-naphthoquinone-3,7-disulfonate-1(1-benzylindazole-3-yl)hydrazone 259* (1.78 g, 75%) mp (decomposed) > 230 °C; λ_{\max} 475 nm (ϵ 11 500 l mol⁻¹ cm⁻¹) ($w_{1/2}$ 183 nm); δ_{H} (250 MHz) ([²H]₆DMSO) 15.55 (1H, s), 9.11 (1H, s), 8.60 (1H, d, ³J 8.1), 8.56 (1H, s), 8.07 (1H, d, ³J 8.4), 7.87 (1H, d, ³J 6.9), 7.75 (1H, t, ³J 6.2), 7.58 (1H, t, ³J 7.4), 7.40-7.48 (6H, m) and 5.95 (2H, s); δ_{C} (63 MHz) 156.05 (quat), 149.89 (quat), 148.28 (quat), 141.20 (quat), 137.39 (quat), 136.58 (quat), 134.28 (CH), 131.61 (quat), 130.52 (quat), 129.32 (CH), 128.62 (2 × CH), 128.15 (CH), 127.73 (2 × CH), 127.38 (CH), 126.07 (quat), 123.91 (CH), 123.09 (CH), 122.11 (CH), 118.04 (CH), 114.04, (quat), 110.77 (CH) and 52.39 (CH₂).

3.24 UV Studies of model yellow derivatives and industry standard

The UV-Vis spectra of **221**, **222**, and **224** were recorded in methanol and the data obtained are shown in Table 19.

Indazole Derivatives

Derivative	Mass used	Conc. (dm ⁻³)	Methanol	
			λ_{\max} (nm)	ϵ (l mol ⁻¹ cm ⁻¹)
221	1.9 mg	0.006	422	19 400
222	1.7 mg	0.006	398	21 600
224	1.3 mg	0.004	411	20 000

Table 19 UV-Vis data and quantities used for the indazole derivatives.

The UV-Vis spectra of compounds **254**, **255**, and **256** were recorded in DMF and the data obtained are shown in Table 20.

Benzisoxazole Derivatives

Derivative	Mass used	Conc. (dm ⁻³)	DMF	
			λ_{\max} (nm)	ϵ (l mol ⁻¹ cm ⁻¹)
254	0.9 mg	0.006	383	38 000
255	1.6 mg	0.005	369/467	33 000
256	1.1 mg	0.004	371	47 000

Table 20 UV-Vis data and quantities used for benzisoxazole derivatives.

Industry standard yellow

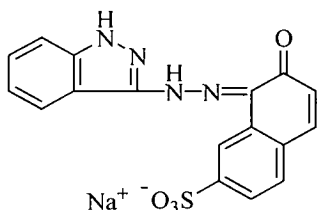
An industry standard yellow dye of unknown structure was then studied for comparison to those above. The dye (4 mg) was dissolved in deionised water, made

up to the mark in a volumetric flask (100 cm³), and the UV-Vis spectrum was recorded. The curve obtained was a single peak with a λ_{max} of 402 nm, and a half-band width of 112 nm. The high wavelength end of the spectrum was not of particularly steep gradient.

3.25 UV Studies – General Method (1) – Preliminary metallisation studies in methanol

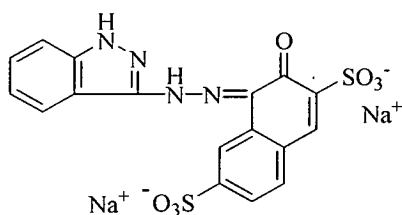
The ligand was dissolved in methanol, made up to the mark in a volumetric flask (100 cm³), and the UV-Vis spectrum was recorded. A vast excess of solid nickel (II) acetate tetrahydrate (10 eq.) was then added to the ligand solution and the resulting UV-Vis spectrum was recorded. The following experiments were carried out using this method.

Sodium 1,2-naphthoquinone-7-sulfonate-1(indazol-3-yl)hydrazone 246



The ligand **246** (6.8 mg, 0.017 mmol) gave an orange coloured solution (conc. 0.17 mmol dm⁻³), and a very broad absorption curve (λ_{max} 443 nm, ϵ 5 800, $w_{1/2}$ 104 nm). After the addition of nickel (II) acetate, an immediate colour change resulted from orange to purple. An increase of about 80 nm in the λ_{max} was observed, along with a small increase in the intensity, but the curve also became broader (λ_{max} 547 nm, ϵ 7 500, $w_{1/2}$ 137 nm). The intensity began to fall after the spectrum was recorded again after 5 min, 10 min and several hours. After a few days the spectrum was recorded again, where the intensity had fallen further, but seemed to have settled at an equilibrium value. The increase in λ_{max} , the increase in intensity and the colour change that was observed indicated that metallisation was successful.

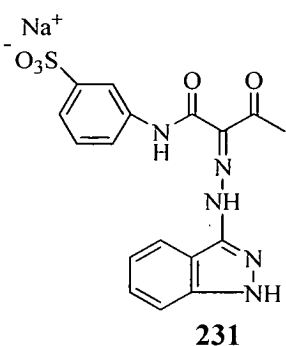
Disodium 1,2-naphthoquinone-3,7-disulfonate-1(indazol-3-yl)hydrazone 247



The ligand **247** (8.1 mg, 0.016 mmol) gave an orange solution (conc. 0.16 mmol dm⁻³), and a broad absorption curve (λ_{max} 467 nm, ϵ 15 600 l mol⁻¹ cm⁻¹, $w_{1/2}$ 148 nm). An immediate colour

change from orange to magenta, an increase in intensity of the absorption and a sharpening of the curve were observed, upon addition of the nickel (II) acetate (λ_{\max} 544 nm, ϵ 24 900 l mol⁻¹ cm⁻¹, $w_{1/2}$ 94 nm).

Sodium *N-m*-sulfacetoacetamide-3(indazol-3-yl)hydrazone **231**

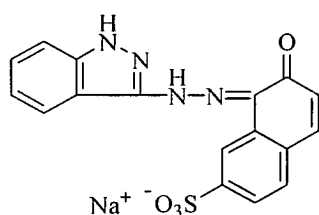


The ligand **231** (3 mg, 0.008 mmol) gave a yellow colour in solution (conc. 0.08 mmol dm⁻³) and an excellent curve, which was sharp and narrow (λ_{\max} 390 nm, ϵ 26 900 l mol⁻¹ cm⁻¹, $w_{1/2}$ 78 nm). Upon metallisation, the solution became a golden yellow colour, and the λ_{\max} value did increase as normal, but the curve became less intense with time, and eventually reached an equilibrium value after approximately 3 days, (λ_{\max} 454 nm, ϵ 17 050 l mol⁻¹ cm⁻¹, $w_{1/2}$ 96 nm).

3.26 UV- General Method (2) – Preliminary metallisation studies in water at pH 6.

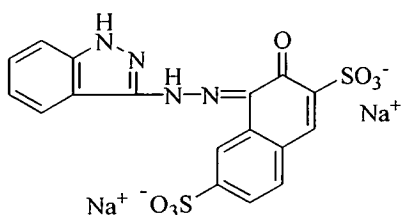
The ligand was dissolved in deionised water, made up to the mark in a volumetric flask (100 cm³), and the UV-Vis spectrum was recorded. A (10 ×) (unless otherwise stated) excess of nickel (II) acetate tetrahydrate was dissolved in the minimum amount of deionised water, and added to the ligand solution, after which the UV-Vis spectrum was recorded.

Sodium 1,2-naphthoquinone-7-sulfonate-1(indazol-3-yl)hydrazone **246**



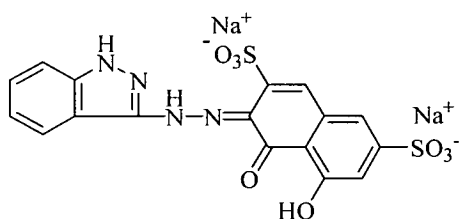
The ligand **246** (2.9 mg, 0.007 mmol) gave an orange solution (conc. 0.07 mmol dm⁻³) and a broad absorption curve, (λ_{\max} 448 nm, ϵ 15 800 l mol⁻¹ cm⁻¹, $w_{1/2}$ 127 nm). After addition of the metal, the solution became purple in colour, with a sharper and more intense curve observed, along with an increase in λ_{\max} , (λ_{\max} 532 nm, ϵ 23 600 l mol⁻¹ cm⁻¹, $w_{1/2}$ 97 nm). After about 15 minutes, the absorption began to decrease, and continued to decrease with time. A dark coloured precipitate eventually formed, and the solution lost its intense colour (ϵ 4 800).

Disodium 1,2-naphthoquinone-3,7-disulfonate-1(indazol-3-yl)hydrazone **247**



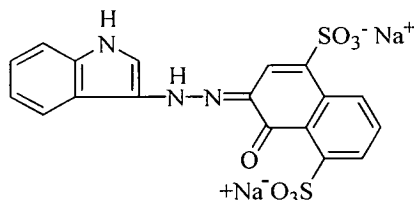
The ligand **247** (2.7 mg, 0.005 mmol) gave an orange colour in solution (conc. 0.05 mmol dm⁻³) and a broad flat curve, (λ_{\max} 467 nm, ϵ 12 400 l mol⁻¹ cm⁻¹, $w_{1/2}$ 178 nm). The solution colour changed to purple/magenta upon addition of the metal, with the now expected increase in intensity and λ_{\max} , (λ_{\max} 545 nm, ϵ 21 900 l mol⁻¹ cm⁻¹, $w_{1/2}$ 90 nm).

Disodium 1,2-naphthoquinone-3,6-disulfonate-8-hydroxy-2(indazol-3-yl)hydrazone **248**



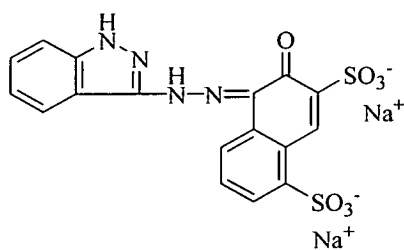
The ligand **248** (3 mg, 0.006 mmol) gave a magenta/red colour in solution (conc. 0.06 mmol dm⁻³), and a curve which was sharper, narrower and more intense than those described above, (λ_{\max} 530 nm, ϵ 29 700 l mol⁻¹ cm⁻¹, $w_{1/2}$ 102 nm). Upon addition of the metal, a colour change to purple was observed, but the λ_{\max} value did not increase much, and the ϵ value remained constant, (λ_{\max} 544 nm, ϵ 29 400 l mol⁻¹ cm⁻¹, $w_{1/2}$ 112 nm).

Disodium 1,2-naphthoquinone-4,8-disulfonate-2(indazol-3-yl)hydrazone **241**



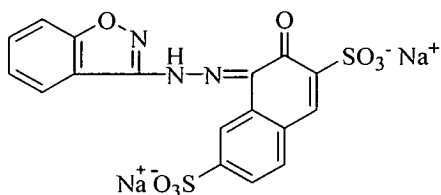
The ligand **241** (3.4 mg, 0.007 mmol) gave an orange/red colour in solution (conc. 0.07 mmol dm⁻³). A fairly high λ_{\max} value of 507 nm was obtained, along with $w_{1/2}$ 131 nm and ϵ 14 600 l mol⁻¹ cm⁻¹. A colour change to purple was observed after addition of the nickel (II) solution, (λ_{\max} 566 nm, ϵ 20 200 l mol⁻¹ cm⁻¹, $w_{1/2}$ 112 nm).

Disodium 1,2-naphthoquinone-3,5-disulfonate-1(indazol-3-yl)hydrazone 249



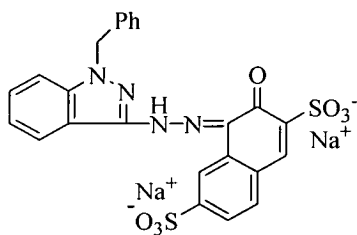
The ligand **249** (2.0 mg, 0.004 mmol) gave an orange solution (conc. 0.04 dm^{-3}) and a very broad curve of low intensity (λ_{max} 467 nm, ϵ $9\,300 \text{ l mol}^{-1} \text{ cm}^{-1}$, $w_{1/2}$ 160 nm). After addition of nickel (II) acetate tetrahydrate the λ_{max} and the intensity increased dramatically (λ_{max} 559 nm, ϵ $15\,500 \text{ l mol}^{-1} \text{ cm}^{-1}$, $w_{1/2}$ 107 nm).

Disodium 1,2-naphthoquinone-3,7-disulfonate-1(benzisoxazol-3-yl)hydrazone 257



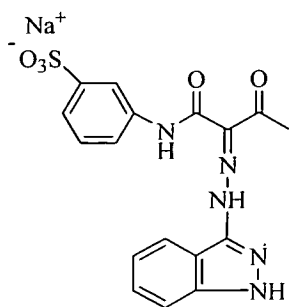
The ligand **257** (3.5 mg, 0.007 mmol) gave a yellow/orange colour in solution (conc. $0.07 \text{ mmol dm}^{-3}$), (λ_{max} 459 nm, ϵ $9\,200 \text{ l mol}^{-1} \text{ cm}^{-1}$, $w_{1/2}$ 122 nm). An immediate colour change from orange to purple/magenta was observed, after addition of the nickel (II) acetate tetrahydrate solution, indicating that metallisation was successful, (λ_{max} 530 nm, ϵ $10\,800 \text{ l mol}^{-1} \text{ cm}^{-1}$, $w_{1/2}$ 98 nm).

Disodium 1,2-naphthoquinone-3,7-disulfonate-1(1-benzylindazol-3-yl)hydrazone 259



The ligand **259** (3.9 mg, 0.007 mmol) was dissolved in deionised water (conc. $0.07 \text{ mmol dm}^{-3}$), and made up to the mark in a volumetric flask (100 cm^3), (λ_{max} 475 nm, ϵ $10\,000 \text{ l mol}^{-1} \text{ cm}^{-1}$, $w_{1/2}$ 182 nm). Nickel (II) acetate tetrahydrate (1.7 mg, 0.007 mmol) was then added to the ligand solution. Upon metallisation the orange coloured solution changed to the familiar purple/magenta colour, (λ_{max} 558 nm, ϵ $14\,500 \text{ l mol}^{-1} \text{ cm}^{-1}$, $w_{1/2}$ 110 nm).

Sodium *N*-*m*-sulfacetoacetamide-3(indazol-3-yl)hydrazone 231



The ligand **231** (3 mg, 0.008 mmol) gave a yellow colour in solution (conc. 0.08 mmol dm⁻³) and an excellent curve, which was sharp and narrow, (λ_{\max} 380 nm, ϵ 14 100 l mol⁻¹ cm⁻¹, $w_{1/2}$ 71 nm). Upon metallisation, not much change in the curve was observed. The colour of the solution did not change, and the curve became less intense but the λ_{\max} value did increase as normal, (λ_{\max} 434 nm, ϵ 10 300 l mol⁻¹ cm⁻¹, $w_{1/2}$ 112 nm). After 90 minutes the intensity had reduced further (ϵ 8 500 l mol⁻¹ cm⁻¹), and after 5 days, the λ_{\max} had reduced to 360 nm and the intensity to (ϵ 6 600 l mol⁻¹ cm⁻¹).

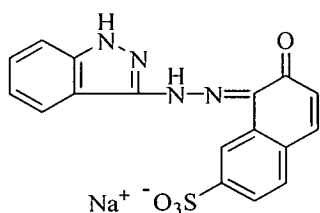
Industry standard magenta (1)

An industry standard metallised magenta dye (1) of unknown concentration and structure was then studied for comparison at pH 6.7. A small portion (0.5 cm³) of this dye solution was diluted with deionised water in a volumetric flask (10 cm³). A small portion (1 cm³) was taken from this solution and diluted in a volumetric flask (100 cm³). A curve with a very sharp peak was obtained, (λ_{\max} 532 nm, $w_{1/2}$ 76 nm), which also had a steep slope at the high wavelength side. A shoulder was present at the low wavelength side, but of much lower intensity.

Industry standard magenta (2)

An industry standard metallised magenta dye (2) of unknown concentration and structure was then studied for further comparison. A small portion (0.25 cm³) of this solution was diluted in a volumetric flask (10 cm³). A small portion of this solution (1 cm³) was then taken and diluted in a volumetric flask (100 cm³). The curve obtained had (λ_{\max} 546 nm, $w_{1/2}$ 87 nm) and also had a shoulder at low wavelength.

3.27 Identification of precipitate from sodium 1,2-naphthoquinone-7-sulfonate-1(indazol-3-yl)hydrazone 246 complex



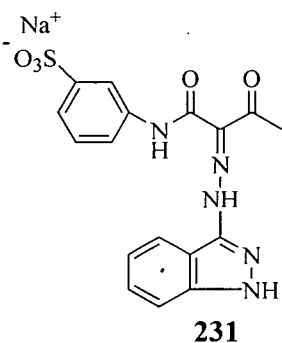
The ligand **246** was assumed to be ~90% strength from the elemental analysis results. The ligand **246** (87 mg,

0.22 mmol) was dissolved in deionised water (150 cm³) and nickel (II) acetate tetrahydrate (1 eq., 50 mg, 0.22 mmol) was added. This solution was then left overnight and a precipitate (50 mg) formed, which was filtered off and after elemental analysis, was tentatively identified as the 1:1 metallised complex, (-1H) (Found: C, 42.2; H, 2.9; N, 11.6. C₁₇H₁₀N₄NaNiO₄S.2H₂O requires C, 42.1; H, 3.1; N, 11.5%); 1:2 complex (-2H) (Found: C, 42.4; H, 3.5; N, 11.6. C₃₄H₁₆N₈Na₂NiO₈S₂.7H₂O requires C, 42.4; H, 3.3; N, 11.5%). The elemental analysis results above fit best for a 1:1 metallised complex, where one hydrogen was removed from the molecular formula. FAB mass spectroscopy however, proved inconclusive, as no peaks corresponding to the 1:1 or 1:2 complexes were observed.

3.28 UV- General Method (3) - Kinetic effects

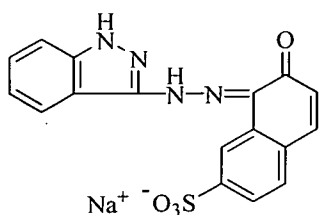
The ligand was dissolved in deionised water (100 cm³), (unless otherwise stated) and a (10 ×) excess of nickel (II) acetate tetrahydrate was added to each of the solutions below, at pH 6. The UV-Vis spectra were recorded every minute initially, then at various intervals.

Sodium *N*-*m*-sulfacetoacetamide-3(indazol-3-yl)hydrazone **231**



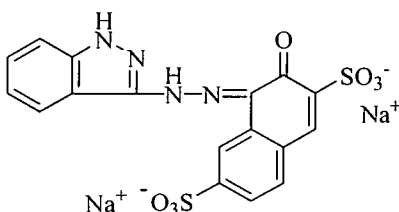
The ligand **231** (3 mg, 0.008 mmol) was dissolved in methanol (100 cm³), which gave a yellow solution (conc. 0.08 mmol dm⁻³). After addition of nickel (II) acetate tetrahydrate, a progression from starting material towards product was observed. The first spectrum recorded after 1 min showed starting material, but after 5 min most of it had reacted. After 50 min no starting material remained. After 4 h, the λ_{max} value had increased from 388 nm to 448 nm. After 3 days, the λ_{max} value had increased further to 454 nm. The absorption intensity had however, decreased a little. After 8 days, the curves characteristics remained the same, (see above for values).

Sodium 1,2-naphthoquinone-7-sulfonate-1(indazol-3-yl)hydrazone **246**



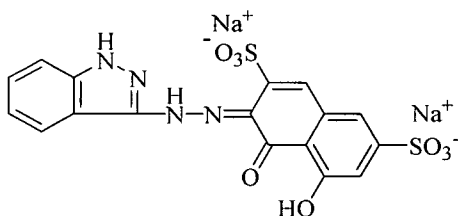
The ligand **246** (3.5 mg, 0.009 mmol) gave an orange solution (conc. $0.09 \text{ mmol dm}^{-3}$). After nickel (II) acetate was added, the curve changed very quickly and metallisation was deemed to be instantaneous. No starting material was observed. The absorption began to decrease with time, and after 30 min it had noticeably changed; the solution had lost its colour and a precipitate formed. The curve eventually becoming almost flat, (see above for values).

Disodium 1,2-naphthoquinone-3,7-disulfonate-1(indazol-3-yl)hydrazone **247**



The ligand **247** (3.1 mg, 0.006 mmol) gave an orange solution (conc. $0.06 \text{ mmol dm}^{-3}$). Upon metallisation the curve became instantly that of the metallised complex. This complex was extremely stable, and the spectrum recorded after 1 min was identical to that recorded after 8 days, (see Section 3.26 for values).

Disodium 1,2-naphthoquinone-3,6-disulfonate-8-hydroxy-2(indazol-3-yl)hydrazone **248**

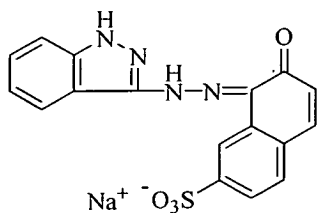


The ligand **248** (3.1 mg, 0.006 mmol) gave an orange solution (conc. $0.06 \text{ mmol dm}^{-3}$). The complex was extremely stable and the spectrum was identical from 1 min to after 8 days, similar to the sulfo F-acid **247** complex above, (see Section 3.26 for values).

3.29 UV – General Method (4) – Metallisation studies at pH 9

The ligand was dissolved in deionised water (100 cm^3) containing one pH 9.2 buffer tablet. A (10 ×) excess of nickel (II) acetate tetrahydrate solution (dissolved in unbuffered deionised water) was added and the UV-Vis curves were recorded.

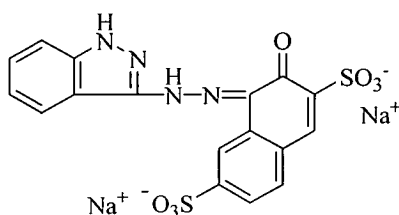
Sodium 1,2-naphthoquinone-7-sulfonate-1(indazol-3-yl)hydrazone 246



The ligand **246** (2.8 mg, 0.007 mmol) gave an orange solution (conc. 0.07 dm^{-3}) similar to that at pH 6, (λ_{max} 444 nm, ϵ 12 000 $\text{l mol}^{-1} \text{ cm}^{-1}$, $w_{1/2}$ 133 nm). After addition of nickel (II) acetate, the λ_{max} and the intensity both increased (λ_{max} 536 nm, ϵ 17 900 $\text{l mol}^{-1} \text{ cm}^{-1}$).

However, the intensity began to decrease very quickly and after 30 min had fallen by ~33%, and a precipitate formed. The curve of the complex did not return to the baseline at the low wavelength side, and therefore a $w_{1/2}$ value was not recorded.

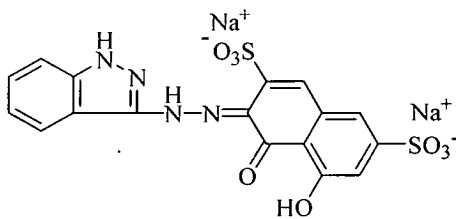
Disodium 1,2-naphthoquinone-3,7-disulfonate-1(indazol-3-yl)hydrazone 247



The ligand **247** (2.2 mg, 0.004 mmol) gave an orange solution (conc. 0.04 dm^{-3}) and a very broad curve of low intensity (λ_{max} 447 nm, ϵ 12 000 $\text{l mol}^{-1} \text{ cm}^{-1}$, $w_{1/2}$ 150 nm). The curve of the metallised complex was of a similar shape to that

observed at pH 6. The spectrum was then recorded again after 2 days where it seemed to have settled at an equilibrium value, (λ_{max} 568 nm, ϵ 20 600 $\text{l mol}^{-1} \text{ cm}^{-1}$, $w_{1/2}$ 104 nm).

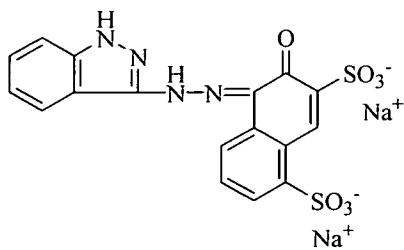
Disodium 1,2-naphthoquinone-3,6-disulfonate-8-hydroxy-2(indazol-3-yl)hydrazone 248



The ligand **248** (3 mg, 0.006 mmol) gave an orange solution (conc. 0.06 dm^{-3}) and a very broad curve of low intensity (λ_{max} 447 nm, ϵ 12 000 $\text{l mol}^{-1} \text{ cm}^{-1}$, $w_{1/2}$ 150 nm). After addition of nickel (II) acetate the λ_{max} and the

intensity increased dramatically (λ_{max} 553 nm, ϵ 28 600 $\text{l mol}^{-1} \text{ cm}^{-1}$, $w_{1/2}$ 101 nm). The complex was stable, similar to that at pH 6.

Disodium 1,2-naphthoquinone-3,5-disulfonate-1(indazol-3-yl)hydrazone **249**

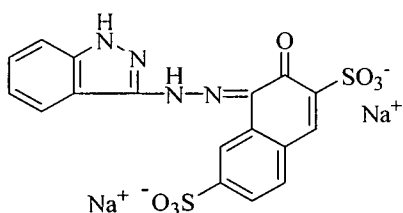


The ligand **249** (2.3 mg, 0.005 mmol) gave an orange solution (conc. 0.05 dm^{-3}) and a very broad curve of low intensity (λ_{max} 471 nm, ϵ $7\,800 \text{ l mol}^{-1} \text{ cm}^{-1}$, $w_{1/2}$ 180 nm). After addition of nickel (II) acetate the λ_{max} and the intensity increased dramatically (λ_{max} 559 nm, ϵ $15\,000 \text{ l mol}^{-1} \text{ cm}^{-1}$, $w_{1/2}$ 109 nm). The complex was stable similar to that at pH 6.

Industry standard magenta (1)

The industry standard metallised magenta dye (1) was then studied for comparison. A small portion (0.5 cm^3) of this dye solution was diluted with deionised water in a volumetric flask (10 cm^3). A small portion (1 cm^3) of this solution was then taken and diluted in a volumetric flask (100 cm^3). A λ_{max} value of 540 nm was observed with a very sharp peak and steep gradient on the right hand side of the curve, ($w_{1/2}$ 80 nm). A second peak was also observed at 513 nm which was previously a shoulder at pH 6.

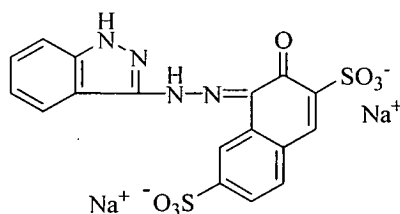
3.30 Quantitative addition of nickel to disodium 1,2-naphthoquinone-3,7-disulfonate-1(indazol-3-yl)hydrazone **247**



This experiment involved titrating calculated amounts of nickel (II) solution to the ligand **247** in pH 9 buffered deionised water. The ligand was assumed to be ~85% strength from the elemental analysis results. The ligand **247** (3.6 mg, 0.007 mmol) was dissolved in deionised water (10 cm^3) (conc. 0.6 mmol dm^{-3}) in a volumetric flask (10 cm^3). An aliquot (1 cm^3) was then taken from this solution and made up to the mark in a volumetric flask (10 cm^3). The resulting solution (conc. 0.06 mmol l^{-1}) was then placed in a burette. Nickel (II) acetate tetrahydrate (76 mg, 0.30 mmol) was dissolved in deionised water (conc. 3 mmol dm^{-3}) and made up to the mark in a volumetric flask (100 cm^3). An aliquot (1 cm^3) was then taken and made up to the mark in a volumetric flask (10 cm^3). From the resulting solution, a

further aliquot (1 cm³) was taken and made up to the mark in a volumetric flask (10 cm³). This solution was then placed in a second burette. The ligand solution (1 cm³) was added to a volumetric flask (10 cm³), and an appropriate volume of the nickel solution was also added to the volumetric flask. This was then made up to the mark with deionised water. 0.25, 0.5, 0.65, 0.75, 1 and 1.25 equivalents of nickel were added and the UV-Vis spectra were recorded. No isobestic points were observed, and at 1 equivalent, the spectrum was similar to that recorded previously with a 10-fold excess of nickel. A gradual increase in the absorption intensity was observed as the number of equivalents was increased. A large shift in the λ_{\max} value was found at 0.5 equivalents.

3.31 Variation of pH of disodium 1,2-naphthoquinone-3,7-disulfonate-1(indazol-3-yl)hydrazone 247

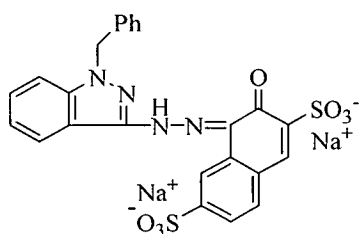


The ligand **247** (19 mg, 0.04 mmol) was dissolved in deionised water (25 cm³) (conc. 1.60 mmol dm⁻³). The ligand was assumed to be ~85% strength from the elemental analysis results. A small portion (10 cm³) of this solution was then placed in the

burette. Nickel (II) acetate tetrahydrate (380 mg, 1.53 mol) was dissolved in deionised water (100 cm³). A small portion (1 cm³) of this solution was taken and made up to the mark in a volumetric flask (25 cm³). A small portion (10 cm³) of this solution was then placed in a burette. The ligand solution (0.5 cm³) and the nickel solution (1 cm³, 1eq.) were then run into a volumetric flask (10 cm³) and made up to the mark with deionised water. The pH was then altered with < 1% sodium hydroxide and hydrochloric acid solutions. The pH values studied: 2.75, 4.0, 4.76, 5.65, 6.60, 8.0, 9.9, 11.0 and 12.0. At pH 3 the curve represented that of the unmetallised ligand and the solution was orange in colour. At pH 4.6 a significant change occurred with the curve becoming more product like as the absorption and λ_{\max} values both increased. From pH 3 to 5.3, isobestic points were observed. The absorption continued to increase as the pH was increased, but the λ_{\max} value remained constant up to pH 8, and the isobestic points were no longer apparent. From pH 8-10, the λ_{\max} value increased to 567 nm and the absorption intensity

increased further. At pH 11-12, the λ_{\max} value was similar to that at pH 8-10, but the absorption intensity decreased slightly. Noticeable colour changes were observed from orange at pH 3 to pink at pH 4.8, to purple at pH 5.65 and magenta at pH 8-11. The industry standard metallised magenta dye (1) was then studied for comparison. The dye solution (0.5 cm^3) was diluted with deionised water in a volumetric flask (10 cm^3). A small portion (1 cm^3) of this solution was then taken and diluted in a volumetric flask (100 cm^3). The pH was varied as above and the spectra were recorded for pH's 2.30, 5.13, 6.70, 8.50, 10.15 and 11.14. At pH 3, the solution lost its deep magenta colour and became yellow/orange, giving a very broad curve. The λ_{\max} value increased quickly with pH, as did the absorption, to become more product like. The colour of the solution changed also. At pH 5-7 the λ_{\max} value was stable, but the absorption was still increasing. At pH 9-11, the curve became very stable with not much change being observed.

3.32 Variation of pH of disodium 1,2-naphthoquinone-3,7-disulfonate-1(1-benzylindazole-3-yl)hydrazone 259



The ligand **259** (21 mg, 0.04 mmol) was dissolved in deionised water (25 cm^3) (conc. $1.44 \text{ mmol dm}^{-3}$). The procedure then followed that for the pH studies above, with similar dilutions being made, and the same equipment being used. A pH range of 2-11 was studied. At pH 2, a curve corresponding to the ligand was observed. Two peaks were observed at pH 3, with the ligand peak decreasing in intensity, and the complex curve beginning to form. At pH 4, all the ligand had reacted, and a curve similar to the metallised complex previously studied was found. This curve increased in intensity as the pH was increased, where it eventually became stable and no further changes were observed from pH 7-11. Once the curve corresponding to the metallised complex was observed, the λ_{\max} value did not vary as the pH was increased further.

pH 5 Buffer Solution.

Solution 1 (1M Acetic Acid). Glacial acetic acid (6 g) was added to a volumetric flask (100 cm³), and made up to the mark with deionised water.

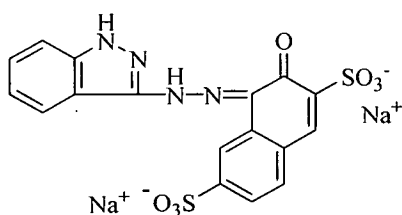
Solution 2 (1M Sodium Acetate Trihydrate). Sodium acetate tetrahydrate (13.6 g) was added to a volumetric flask (100 cm³) and made up to the mark with deionised water.

Using a burette, solution 1 (29.6 cm³) was then combined with solution 2 (70.4 cm³), resulting in pH 5 1M acetate buffer solution. The pH was measured using a pH meter.

3.33 General method for quantitative addition of nickel (II).

The ligand (1 g, 2 mmol) was dissolved in deionised water (200 cm³) and the pH was adjusted to 7, using < 1% sodium hydroxide and hydrochloric acid solutions. The ligand was analysed by HPLC and the UV-Vis spectrum was recorded. Nickel acetate tetrahydrate (0.51 g, 2 mmol) was dissolved in deionised water (10 cm³). The nickel solution (1 cm³, 0.1 eq.) was added sequentially to the ligand solution, and the pH was maintained at 7. Not all the ligand was immediately soluble in water, but became soluble when the first nickel aliquot was added. After each addition the solution was stirred for 15 min and samples were analysed by HPLC and UV-Vis spectroscopy. All UV-vis spectra were recorded in pH 5 acetate buffer solution (1 cm³ of sample, 2 cm³ of buffer in a 100 cm³ volumetric flask). In general, HPLC did not provide a successful method for following the metallisation processes, as only the ligands appeared on the trace; the metallised complexes were not apparent. Therefore, UV-Vis spectroscopy provided the best method for monitoring the process, with the L, a, b values and the absorption being used as indicators as to when the reaction was complete. The following reactions were monitored in this way.

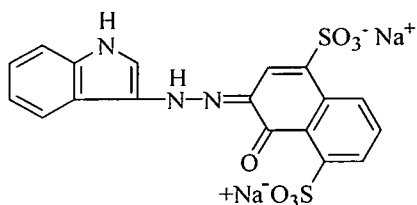
Disodium 1,2-napthoquinone-3,7-disulfonate-1(indazol-3-yl)hydrazone 247



The reaction was monitored up to 1.2 equivalents of nickel, where the complex began to precipitate. After inspection of the curves, it was concluded

that the metallisation process required ~ 0.85 equivalents of nickel, λ_{\max} 544 nm (ϵ 24 900 l mol⁻¹ cm⁻¹); L = 58.3, a = 61.7, b = -28.1, C = 67.8 and h = 335.6

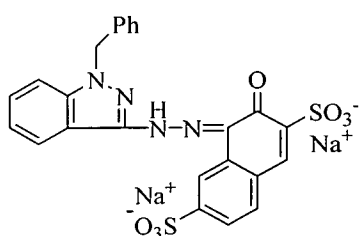
Disodium 1,2-naphthoquinone-4,8-disulfonate-2(indazol-3-yl)hydrazone 241



The reaction was monitored up to 1.2 equivalents, which proceeded very similar to above. After inspection of the curves, it was concluded that the metallisation process required ~ 0.85 equivalents of nickel, λ_{\max} 553 nm (ϵ 22 700); L = 55.2, a = 54.2,

b = -50.0, C = 73.8 and h = 317.3.

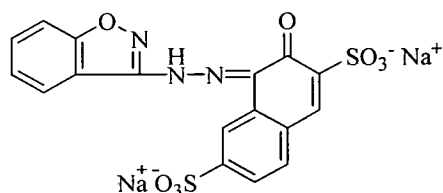
Disodium 1,2-naphthoquinone-3,7-disulfonate-1(1-benzylindazole-3-yl)hydrazone 259



The UV-Vis curves became very quickly product like (~ 0.3 eq). This was the only complex which could be analysed by HPLC, the ligand **259** appeared at 13.47 min, and a small peak appeared at 12.93 min, after the addition of 0.1 equivalents. This peak at 12.93 min

increased in intensity as the number of equivalents was increased, whereas the ligand peak at 13.47 min decreased in intensity. The peak at 12.93 min was assumed to be the metallised complex, as this pattern was also seen in the UV-Vis curves, where the ligand curve disappeared and the complex curve began to form. The process was monitored up to 0.6 equivalents where extra peaks began to appear in the HPLC. This thought to be due to contamination, as the curves did not correspond to those obtained previously. Unfortunately, the end-point could not be predicted, so it was assumed to be 0.85 equivalents, as with the others above, λ_{\max} 557 nm (ϵ 16 800 l mol⁻¹ cm⁻¹); L = 51.0, a = 35.7, b = -45.2, C = 57.7 and h = 308.3.

Disodium 1,2-naphthoquinone-3,7-disulfonate-1(benzisoxazol-3-yl)hydrazone 257



The metallisation process proved to be extremely slow, and mostly ligand **257** remained after the addition of 1 equivalent of

nickel (II), as shown by the UV-Vis spectra. Further additions of nickel were made up to 2 equivalents, but the metallisation was not even 50% complete. The metallised complex also precipitated out of solution at higher concentrations of nickel. It was concluded that this compound was no use for further metallisation studies as it required high concentrations of the toxic nickel compound.

3.34 General method for small scale isolation of metallised complexes

The ligand (0.2 mmol) was dissolved in deionised water (20 cm³) at pH 7. Nickel (II) acetate tetrahydrate (43 mg, 0.17 mmol, 0.85 eq.) was dissolved in the minimum amount of deionised water and was added to the ligand solution. The pH was maintained at 7, and the now dark purple coloured solution was stirred for ~ 30 min, after which a small sample was taken, and the UV-Vis spectrum was recorded. The metallised complex solution was then heated in the oven at 40 °C (~1 day) until all the solvent had evaporated, and a dark red coloured solid resulted. The dyes derived from **241** and **247** were then successfully reconstituted in water, and their UV-Vis spectra were recorded again, to see if they matched those obtained earlier when in solution. Both complexes were stable to these conditions as they gave good spectra that matched those previously obtained.

3.35 Large Scale Metallisations

Method 1

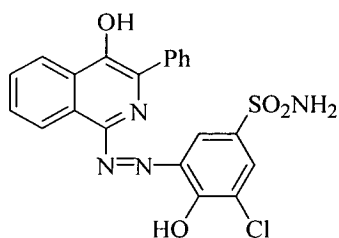
The ligand (5 mmol) was dissolved in deionised water (250 cm³) and the pH was adjusted to 7. Nickel (II) acetate tetrahydrate (0.85 eq.) was then added, resulting in a dark coloured solution. The pH was adjusted to 7, and the solution was stirred for 45 min. The UV-Vis spectrum was recorded at this point. The solution was then heated in an oven at 40 °C until all the solvent had evaporated (~2 days), resulting in the metallised complex. The ligands **247** and **241** were both scaled up in this manner, giving 2.9 g and 2.6 g of the respective metallised complexes.

Method 2

Ligand **259** (0.85 g, 1.46 mmol) was dissolved in deionised water (100 cm³) and the pH was adjusted to 7. Nickel (II) acetate tetrahydrate (0.31 g, 1.24 mmol, 0.85 eq.) was added, and the procedure then followed the general method above (1), giving the metallised complex (0.9 g).

3.36 Metallisation of azo cyan **164**

3-Phenyl-1-(2-chloro-1-hydroxy-4-sulfonamidophenylazo)isoquinolin-4-ol **164** (180



mg, 0.4 mmol) was dissolved in deionised water (20 cm³) and the pH was adjusted to 7. Nickel (II) acetate tetrahydrate (1 eq.) was then added, resulting in a dark coloured solution. The pH was adjusted to 7, and the solution was stirred for 45 min. The UV-Vis spectrum

was recorded at this point. The solution was then heated in an oven at 40 °C until all the solvent had evaporated (~2 days), resulting in the metallised complex (180 mg), (λ_{max} 637 nm, ϵ 25 600 l mol⁻¹ cm⁻¹, $w_{1/2}$ 100 nm).

Industrial Cyan Dye

An industrial standard metallised cyan dye of unknown structure, was then studied by UV-Vis for comparison to **164**. The dye (6 mg) was dissolved in deionised water and made up to the mark in a volumetric flask (100 cm³). The UV-Vis spectrum was then recorded. A double peaked curve was obtained, with the more intense peak giving a λ_{max} value of 616 nm. The less intense peak absorbed at a wavelength of around 660 nm. A half-band width of 106 nm was found, but again, the extinction coefficient could not be calculated.

3.37 Stability studies

Addition of Industrial Ligand to Metallised Complexes of **247** and **241**

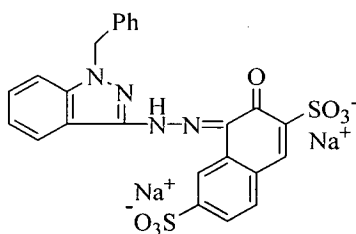
The ligand (0.1 mmol) (experiment done for ligands **247** and **241**) was dissolved in deionised water (10 cm³) and the pH was adjusted to 7 by < 1% sodium hydroxide and hydrochloric acid. Nickel (II) acetate tetrahydrate (0.85 eq.) was then added, and

the solution was stirred for 20 min, at pH 7. Samples were taken at this point for HPLC and UV-Vis spectroscopy. The industrial ligand (1 eq.) was then added to the metallised solution, resulting in a more magenta like colour being observed. The pH was adjusted to 7, and the solution was stirred for 20 min. Samples were then taken for HPLC and UV-Vis spectroscopy, with HPLC indicating a mixture of products. The industrial ligand was not observed on the HPLC, but the metallised complex was apparent at 3 min. Ligands **247** and **241** were seen on the HPLC at 8 min and 10 min respectively. The final UV-Vis curve was not exclusively either of the metallised complexes, and it was concluded that a mixture of products was obtained.

Addition of **241** to Metallised Industry standard complex (3).

The industrial ligand (0.1 mmol) was dissolved in deionised water (10 cm³) at pH 7. Nickel (II) acetate tetrahydrate (0.85 eq.) was then added, and the solution was stirred for 20 min at pH 7. Samples were taken for HPLC and UV-Vis. Ligand **241** (50 mg, 1 eq.) was then added to the metallised industrial solution, resulting in a darker coloured solution. The pH was adjusted to 7, and the solution was stirred for 20 min. Samples were taken for HPLC and UV-Vis. As above, a mixture of products were obtained on the HPLC trace, and the UV-Vis spectrum proved inconclusive, as the curve observed was not exclusively that of either metallised complex.

Disodium 1,2-naphthoquinone-3,7-disulfonate-1-(1-benzylindazole-3-yl)hydrazone **259**

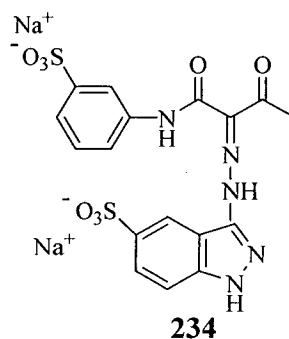
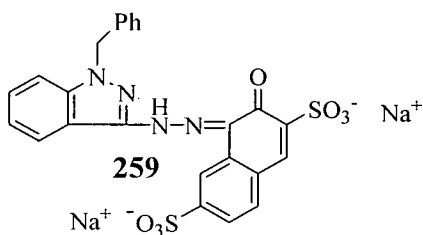
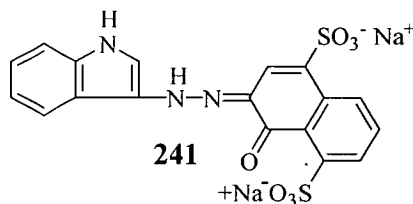
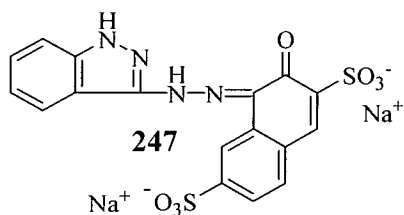


The metallised complex of **259** (32 mg, 0.05 mmol) was dissolved in deionised water and made up to the mark in a volumetric flask (100 cm³). A small aliquot of this stock solution was taken (conc. = 0.5 mmol dm⁻³), and the UV-Vis spectrum was recorded. The concentration was then varied by taking another aliquot (8 cm³), making up to the mark in a volumetric flask (10 cm³) (conc. = 0.4 mmol dm⁻³), and recording the UV-Vis spectrum. Further dilutions were made, and the UV-Vis spectra were recorded at the following concentrations; 0.30 mmol dm⁻³, 0.25 mmol dm⁻³, 0.15 mmol dm⁻³ and

0.07 mmol dm⁻³. A plot of absorbance versus concentration showing that the complex followed the Beer-Lambert law gave a straight line through the origin.

3.38 Dye Testing

The four metallised dyes to be tested were the metallised complexes of **247**, **241** and **259** (all magentas); and the yellow dye **234**.



3.39 Formulation of the Generic Inks

Method 1 (Dyes **247**, **241** and **259**)

The dye (0.3 g, 3% w/v) was added to a 5:5:1 solution (9.7 cm³) of 2-pyrrolidone, diethylene glycol and Surfynol 465. The strengths of each ligand used were estimated from the elemental analysis results. The pH of this suspension was adjusted to 8.5 using dilute sodium hydroxide solution (2M) and then sonicated for 1 h. A dark coloured solution resulted similar to that observed after metallisation. Not all the dye went into solution; crystals/aggregates were observed under a microscope. A further addition of 2-pyrrolidone (1 g) was then made to the dye. Next day, dyes **247** and **259** were filtered (through a syringe), whereas filtration was not required for

241. These filtrations however, meant that the strength of the dyes in the inks became weaker.

Method 2 (Dye 234)

The dye (0.3 g, 3% w/v) was added to a 5:5:1 solution (9.7 cm³) of 2-pyrrolidone, diethylene glycol and Surfynol 465. The strength of the ligand was estimated from the elemental analysis, although the dye strength in the ink was weakened by the addition of salt during the isolation of the dye. The pH of this suspension was adjusted to 8.5 using dilute sodium hydroxide solution (2M) and then sonicated for 1 h, resulting in a yellow coloured solution. Due to the highly water soluble nature of this dye, no filtration or further additions of 2-pyrrolidone was required.

Each of the 4 inks described above (5 cm³) were injected *via* a syringe into the ink cartridge, and then loaded into an HP 5550 printer, from which all the prints were obtained on 7 different types of paper. Three plain papers were used: Xerox Acid, HP Printing Paper and HP Multipurpose. Three microporous papers were used: Canon HG 201 (alumina humidity microporous), Canon PR101 (alumina microporous) and SEC Premium (silica microporous). One swellable paper was used: HP Premium. All the various tests below were performed on all 7 of these papers, for each of the 4 inks.

3.40 Applications testing

Wet Fastness

The prints were held at an angle of 45 ° on a glass plate. Water (0.5 cm³) was dripped down across the horizontal bars, after 0 min and 15 min for dyes 247 and 259, and after 0 min, 15 min and 24 h for dyes 241 and 234. (See Appendix 1 for results)

Light and Ozone Fastness

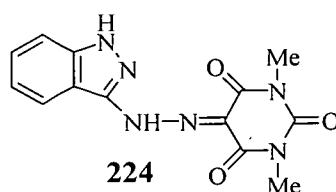
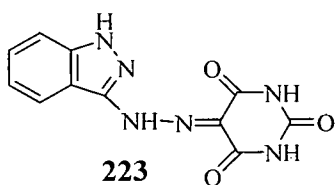
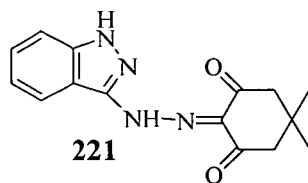
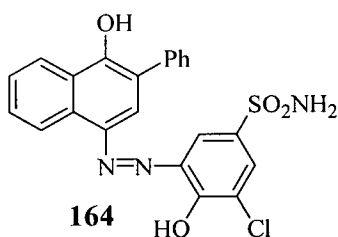
Small squares of each of the prints on all 7 papers were cut out and mounted on cardboard, placed in the appropriate bracket and placed in the machine. They were removed after 100 h and 24 h respectively. Colour measurements were then taken of the prints. (See Appendix 1 for results)

Colour Measurements

The instrument was firstly calibrated, and the ROD values were then recorded for all 4 dyes on all 7 papers at 100% print strength. The ROD values of all 7 papers were also recorded, which had to be subtracted from the value obtained for the wet fastness results. The ROD values for the ozone and light fastness samples were recorded directly. The ROD values for the wet fastness samples were recorded between the second last and last horizontal bars of the prints. (See Appendix 1 for results).

High Through-Put Testing

Testing of the four dyes below was also carried out on a small scale. This could be done on a high through put test requiring only around 200 mg of sample. The metallised azo cyan dye, plus the unmetallised yellow indazole dyes, were all tested. However, all four compounds proved too insoluble for this purpose, and no further analysis was done.



4. REFERENCES

References

1. a.) P. Gregory, *Chemistry in Britain*, 2000, **36**, 39. b.) P. Gregory, *Proceedings Royal Microscopical Society*, 2001, 36.
2. www.creativepro.com/printerfriendly/story/20511.html.
3. R. W. Kenyon, *Chemistry and Technology of Printing and Imaging Systems*, Chapter 5, p 113, Blackie, Glasgow, 1996.
4. H. P. Lue, *J. Imaging Science and Technology*, 1998, **42**, 49.
5. R. N. Mills, Proc. IS&T's NIP 12: *International Congress on Digital Printing Technologies*, 1996, 262.
6. P. Gregory, *High Technology Applications of Organic Colourants* Chapter 9, p 175, New York and London: Plenum, 1991.
7. S. F. Pond, *Inkjet Technology*, Torrey Pines Research, California, 2000.
8. J. Provost, R. Docherty, J. Watkinson and A. Lavery, Unpublished work, Zeneca Specialist Colours.
9. P. F. Gordon and P. Gregory, *Organic Chemistry in Colour*, Springer-Verlag, Heidelberg, 1987.
10. R. L. M. Allen, *Studies in Modern Chemistry, Colour Chemistry*, Chapter 1, p 1-3 and 11, Chapter 2, p 14-20, Chapter 3, p 21, Nelson, London, 1971.
11. J. March, *Advanced Organic Chemistry*, 4th Edition, p 139, Wiley-Interscience, New York, 1992.
12. S. Ege, *Organic Chemistry*, p 930, D. C. Heath & Co., USA, 1984.
13. X-Rite Inc., *The Colour Guide and Glossary*, USA, 1998.
14. X-Rite Inc., *A Guide to Understanding Colour Communication*, 2000.
15. Gretag Macbeth, *Fundamentals of Colour and Appearance*, 1998.
16. D.J. Palmer, 4th International Congress on advances in non-impact printing technologies, "Development of Ink/Media for Paintjet Printers", p 127, California, 1988.
17. www.photo-i.co.uk/Reviews.
18. F. Beffa and G. Back, *Rev. Prog. Coloration*, "Metal-Complex Dyes for Wool and Nylon – 1930 - Date", 1984, **14**, 33.
19. J. Griffiths, *Colour and Constitution of Organic Molecules*, Academic Press,

- London, 1976.
20. K. Baettig and G. Jan, US Patent 5824785, 1996. (*Chem. Abstracts.*, 1996, 621396).
 21. a.) K. Carr, *Dyes For Ink-Jet Printing*, Colourants for non-textile applications, 2000, 1, b.) R. M. Christie, *Colour Chemistry*, The Royal Society of Chemistry, Cambridge, 2001.
 22. W. Bauer, IS+T's NIP 12: *International Conference on Digital Printing Technologies*, "Magenta Dyes for Ink-Jet Applications" p 60, 1998.
 23. M. Kenworthy and C. D. Robertson, UK Patent 9967334, 1999. (*Chem. Abstracts.*, 1999, 819452).
 24. Z. Csepregi, P. Aranyosi, I. Ruznak, L. Toke, J. Frankl and A. Vig, *Dyes and Pigments*, 1998, **37**, 1.
 25. R. Price, *The Chemistry of Synthetic Dyes*, Vol. 3, p 303, Academic Press, London, 1970.
 26. P. Doll, F. Shi, S. Kelly and W. Wnek, IS+T's NIP 4: *International Conference on Digital Printing Technologies*, p 118, 1998.
 27. M. M. Robison and B. L. Robison, *J. Org. Chem.*, 1957, **21**, 1337.
 28. T. L. Gilchrist, G. E. Gymer and C. W. Rees, *J. Chem. Soc. Perkin Trans 1*, 1975, 1.
 29. S. Oae, T. Kitao and Y. Kitaoka, *Tetrahedron*, 1963, **19**, 827.
 30. S. Ikehera, *Chem. Pharm. Bull.*, 1959, **7**, 501.
 31. S. Kozuka, S. Oae, K. Ogino and S. Tamagaki, *Tetrahedron*, 1969, **25**, 5761.
 32. W. J. Jones, G. C. Leo, B. E. Maryanoff, A. B. Reitz and H. C. Zhang, *Tetrahedron Lett.*, 1993, **34**, 7247.
 33. M. M. Robison and B. L. Robison, *J. Am. Chem. Soc.*, 1958, **80**, 3443.
 34. H. Sard, *J. Heterocycl. Chem.*, 1994, **31**, 1085.
 35. P. B. Terent'ev, N. P. Lomakina and A. N. Kost, *Org. Mass. Spectrom.*, 1976, **11**, 281.
 36. R. Beugelmans, J. Chastanet and G. Roussi, *Tetrahedron*, 1984, **40**, 311.
 37. H. O. House, *Modern Synthetic Reactions*, p 230, W. A. Benjamin Inc., New York, 1965.

38. N. A. Andronova, L. D. Smirnov, V. P. Lezina and B. E. Zaitsev, *Bull. Acad. Sci. USSR, Div. Chem. Sci.*, 1971, **20**, 395.
39. Y. Suzuki, *Yakugaki Zasshi*, 1961, **81**, 792. (*Chem. Abstracts*, 1961, 24746).
40. N.A.Andronova, L.D.Smirnov, U.P.Lezima and K.M.Dyumaev, *Bull. Acad. Sci. USSR Div. Chem. Sci.*, 1972, **21**, 404.
41. N. A. Andronova, L. D. Smirnov, U. P. Lezima and K. M. Dyumaev, *Bull. Acad. Sci. USSR, Div. Chem. Sci.*, 1972, **21**, 452.
42. S. B. Ferguson, E. M. Seward, F. Diedrich, E. M. Sanford, A. Chou, P. Inocencio-Szweda and C. B. Knobler, *J. Org. Chem.*, 1988, **53**, 5595.
43. C. Naumann and H. Langhals, *Synthesis*, 1990, 279.
44. A. Banerji and S. Maiti, *Tetrahedron*, 1994, **50**, 9079.
45. G. H. L. Nefkens and B. Zwanenburg, *Tetrahedron*, 1985, **41**, 6063.
46. D. D. Chapman, J. K. Elwood and J. A. Friday, US Patent, 1979, 4148642. (*Chem. Abstracts*, 1979, 66274).
47. P. Bergthaller, H. V. Runzheimer, G. Schenk and G. Wolfrum, *DE Patent*, 1982, 3107540. (*Chem. Abstracts.*, 1987, 431094).
48. D. D. Chapman and E. Wu, *US Patent*, 1981, 4273706. (*Chem. Abstracts*, 1981, 9965).
49. D. Heber, V. Holzgrabe and W. Werra, *Magn. Res. Chem.* 1992, **30**, 640.
50. M. Ikehera and E. Ochiai, *Chem. Pharm. Bull.*, 1955, **3**, 454.
51. M. Bolte, K. Hensen and R. Mayer-Stein, *Acta. Crystallogr. Sect. C*, 1999, **55**, 1565.
52. G. Smets and J. Vansant, *J. Org. Chem.*, 1980, **45**, 1557.
53. The Aldrich Library of ^1H and ^{13}C FT NMR spectra.
54. K. Paruch, *J. Org. Chem.*, 2000, **65**, 8774.
55. M. Cheung, T. Fukuyama, Y. Hidai, C. Jow and T. Kan, *Tetrahedron Lett.*, 1997, **38**, 5831.
56. A. G. Giumanini, L. Lassiani, C. Nisi, A. Petric and B. Stanovnik, *Bull. Chem. Soc. Japan*, 1983, **56**, 1887.
57. N. A. Andranova, K. M. Dyumaev, V. P. Lezina, L. D. Smirnov and B. E. Zaitsev, *Bull. Acad. Sci. USSR. Div. Chem. Sci.*, 1970, 2244.

58. H. Langhals and C. Naumann, US Patent 5266700, 1993. (*Chem. Abstracts.*, 1991, 122078).
59. H. McNab and F. McMillan, Unpublished work, University of Edinburgh, 2004.
60. M. Moreno-Manas, M. Perez and R. Pleixats, *J. Org. Chem.*, 1996, **61**, 2346.
61. C. Dai, G. C. Fu and A. F. Littke, *J. Am. Chem. Soc.*, 2000, **122**, 4020.
62. H. McNab, *Aldrichimica Acta*, 2004, **37**, 19.
63. R. F. C. Brown, *Pyrolytic Methods in Organic Chemistry*, Academic Press: New York, 1980.
64. T. T. Tidwell, *Ketenes*, Chapter 3, p 70, John Wiley & Sons, Inc., Canada, 1995.
65. S. Yamada and S. Hashimoto, *Tetrahedron.*, 1976, 997.
66. D. S. Campbell and C. Lawrie, *J. Chem. Soc., Chem. Commun.*, 1971, 355.
67. S. J. Blanksby and G. B. Ellison, *Acc. Chem. Res.*, 2003, **36**, 355.
68. J. W. Tilley, P. Levitan and R. W. Kierstead, *J. Heterocycl. Chem.*, 1979, **16**, 333.
69. O. Tsuge, S. Kanemasa and M. Yoshioka, *J. Org. Chem.*, 1988, **53**, 1384.
70. A. M. Gaber and H. McNab, *Synthesis*, 2001, 2059.
71. R. J. Clemens and J. S. Witzeman, *J. Am. Chem. Soc.*, 1989, **111**, 2186.
72. B. Eistert and F. Geiss, *Chem. Ber.* 1961, **94**, 929.
73. H. McNab and K. Wilson, Unpublished Work, University of Edinburgh, 2002.
74. S. Bozzini, M. Calligaris, S. Gratton, G. Nardin, A. Risaliti and A. Stener, *J. Chem. Soc. Perkin Trans. 1*, 1977, 1377.
75. P. D. Boyle and C. E. Pfluger, *J. Chem. Soc. Perkin Trans. 2*, 1985, **10**, 1547.
76. C. J. Brown, *Acta Crystallogr.*, 1966, **21**, 146.
77. B. T. Newbold, *The Chemistry of Hydro, Azo and Azoxy Compounds Part 2*, ed. S. Patai, Wiley, London, 1975, p 631.
78. L. F. Fieser, *Org. Synth. Coll.*, Vol. II, 1943, 35.
79. R. A. Marty and P. de Mayo, *J. Chem. Soc., Chem. Commun.*, 1971, 127.
80. B. Balali-Mood and H. McNab, Unpublished Work, University of Edinburgh 2002.
81. M. Joucla and J. Mortier, *Tetrahedron Lett.*, 1987, **28**, 2973.
82. S. M. Allin, C. J. Northfield, M. I. Page and A. M. Z. Slamin, *J. Chem. Soc. Perkin Trans. 1*, 2000, 1715.

83. S. M. Allin, C. J. Northfield, M. I. Page and A. M. Z. Slamin, *Tetrahedron Lett.*, 1997, **38**, 3627.
84. S. Hunsch, W. Richter, I. Ugi and J. Chattopadhyaya, *Liebigs Ann. Chem.*, 1994, 269.
85. Internal Report Avecia Ltd.
86. H. McNab and C. Sommerville, Unpublished work, University of Edinburgh Thesis 1995.
87. Internal Report Avecia Ltd.
88. E. Bamberger, *Ber.Dtsch. Chem. Ges.*, 1899, **32**, 1773.
89. D. Fortuna, B. Stanovnik and M. Tisler, *J. Org. Chem.*, 1974, **39**, 1833.
90. C. E. Kwartler and P. Lucas, *J. Am. Chem. Soc.*, 1943, **65**, 1804.
91. I. Leban, B. Stanovnik and M. Tisler, *Acta Crystallogr. Sect. B*, 1978, **34**, 293.
92. L. Horner, U. Simon and O. Sus, *Liebigs Ann. Chem.*, 1966, **697**, 17.
93. R.J. Cox, C. Bridges, R.G.D. Moore, C. Forks and M.L. Moskowitz, US Patent 2997467, 1961. (*Chem. Abstracts*, 1962, 31369).
94. R. G. D. Moore and P. T. Woitach, US Patent 816382, 1959. (*Chem. Abstracts*, 1961, 1185).
95. J. M. Tedder and B. Webster, UK Patent 988221, 1964. (*Chem. Abstracts.*, 1965, 87769).
96. T. Ankenbrand and R. Neidlein, *Heterocycles*, 1999, **51**, 513.
97. A. Padwa, T. Kumagai and A.D. Woolhouse, *J. Org. Chem* 1983, **48**, 2330.
98. H. Durr and H. Schmitz, *Chem. Ber.*, 1978, **111**, 2258.
99. G. Ege and K. Gilbert, *J. Heterocycl. Chem.*, 1981, **18**, 675.
100. G. Ege and K. Gilbert, *Tetrahedron. Lett.*, 1979, **18**, 1567.
101. G. Ege and K. Gilbert, *Tetrahedron. Lett.*, 1979, **44**, 4253.
102. D. Janzeic, S. Polanc, B. Stanovnik and M. Tisler, *J. Heterocycl. Chem.*, 1978, **15**, 349.
103. M. V. Gorelik, V. I. Lomzakova, E. A. Khamidova and M. G. Kuznetsova, *Russian J. Org. Chem.*, 1996, **32** (11), 1682. (*Zh. Otg. Khimii.*, 1996, **32** (11), 1734.)
104. M. Bester, V. Kermavner, M. Kocevar, B. Koren, B. Stanovnik and M. Tisler, *Synth. Commun.*, 1979, 194.

105. G. Ege, K. Gilbert and R. Heck, *Chem. Ber.*, 1984, **117**, 1726.
106. L. N. Divaeva, S. N. Kolodyazhnaya, A. M. Simonov and R. A. Sogomonova, *Chem. Heterocycl. Compounds*, 1990, **5**, 538.
107. S. N. Kolodyazhnaya, L. N. Podladchikova and A. M. Simonov, *Chem. Heterocycl. Compounds*, 1974, **10**, 596.
108. S. N. Kolodyazhnaya, A. M. Siminov and I. G. Uryukina, *Chem. Heterocycl. Compounds*, 1972, **8**, 1533.
109. L. N. Divaeva, S. N. Kolodyazhnaya, V. A. Polenov and A. M. Siminov, *Chem. Heterocycl. Compounds*, 1992, **28**, 58.
110. L. N. Divaeva, S. N. Kolodyazhnaya, A. M. Simonov and R. A. Sogomonova, *Chem. Heterocycl. Compounds*, 1983, **5**, 534.
111. I. C. Clelland and H. McNab, Unpublished results, Ph.D Thesis, 1999.
112. F. A. Cotton and G. Wilkinson, *Advanced Inorganic Chemistry*, 2nd Edition, p 460, John Wiley and Sons, Inc., London, 1966.
113. Avecia, Internal Report.
114. Avecia, Internal Report.
115. P. E. Hansen, *Progress in NMR Spectroscopy*, 1981, **14**, 175.
116. R. D. Brown, B. A. W. Coller and M. L. Heffernan, *J. Chem. Soc.*, 1958, 365.
117. P. Gregory, Personal Communication.
118. K. J. Kapples and G. M. Shutske, *J. Heterocycl. Chem.*, 1989, **26**, 1293.
119. P. Grunager and P. Vita-Finzi, "Isoxazoles: The Chemistry of Heterocyclic Compounds Part 2", p 114, John Wiley and Sons, Inc., 1999, **49**.
120. A. Albert, "Heterocyclic Chemistry", 2nd Edition, p 441, Melbourne University Press, 1968.
121. L. Crawford and H. McNab, Unpublished work, Ph.D Thesis, 2002.
122. O. V. Dyablo, M. A. Kolesnichenko, V. V. Kuz'menko and A. F. Pozharskii, *Kh. Geterotsiklicheskikh Soedinenii*, 2001, **5**, 619. (*Chem. Heterocycl. Compounds*, 2001, **37**, 567).
123. G. S. Calabrese, S. A. Harkaway and R. L. Reeves, *Inorg. Chem.*, 1983, **22**, 3076.
124. J. C. Pommelet, *Synth. Comm.*, 1999, **29**, 1785.
125. C. J. Wharton and R. Wrigglesworth, *J. Chem. Soc. Perkin. Trans. 1*, 1985, 809.

5. APPENDICES

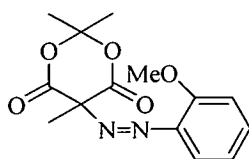
Appendix 1 Dye Results

Paper	Dye	Test	ROD	L	A	B	C	H	DE	ROD_LOSS	PCENT	WF initial	WF 15mins	WF 24 hours
SEC Premium	M1	initial	0.63	62	35	-27	44	322				0.00	0.00	
SEC Premium	M1	If 100hrs	0.66	61	39	-31	50	321	6		-5			
SEC Premium	M1	of 1ppm/24 hrs	0.08	94	1	-3	3	293	52		87			
Xerox acid	M1	initial	0.46	66	13	-22	25	302				0.03	0.03	
Xerox acid	M1	If 100hrs	0.38	74	16	-8	18	333	16		17			
Xerox acid	M1	of 1ppm/24 hrs	0.41	70	14	-14	20	315	9		11			
HP Printing paper	M1	initial	0.48	66	15	-26	30	300				0.04	0.03	
HP Printing paper	M1	If 100hrs	0.38	74	15	-10	18	328	19		21			
HP Printing paper	M1	of 1ppm/24 hrs	0.43	69	15	-18	24	308	9		10			
HP Multipurpose	M1	initial	0.46	66	14	-22	26	302				0.02	0.02	
HP Multipurpose	M1	If 100hrs	0.38	74	16	-7	17	334	17		17			
HP Multipurpose	M1	of 1ppm/24 hrs	0.41	71	14	-14	20	314	9		11			
Canon HG 201	M1	initial	0.63	62	35	-27	44	322				0.01	0.01	
Canon HG 201	M1	If 100hrs	0.45	72	26	-13	29	333	19		29			
Canon HG 201	M1	of 1ppm/24 hrs	0.07	95	3	-2	3	323	52		89			
Canon PR101	M1	initial	0.5	66	20	-20	28	315				0.01	0.01	
Canon PR101	M1	If 100hrs	0.53	66	22	-7	23	341	12		-6			
Canon PR101	M1	of 1ppm/24 hrs	0.06	95	0	-2	2	283	39		88			
HP Premium Plus	M1	initial	0.81	51	34	-40	53	311				0.00	0.01	
HP Premium Plus	M1	If 100hrs	0.75	54	30	-31	43	314	11		7			
HP Premium Plus	M1	of 1ppm/24 hrs	0.76	53	32	-34	47	313	7		6			
SEC Premium	M2	initial	0.98	44	44	-54	69	309				0.04	0.04	0.05
SEC Premium	M2	If 100hrs	0.95	46	45	-50	67	312	4		3			
SEC Premium	M2	of 1ppm/24 hrs	0.09	93	0	4	4	86	87		91			
Xerox acid	M2	initial	0.67	53	13	-36	38	290				0.05	0.07	0.08
Xerox acid	M2	If 100hrs	0.53	63	15	-22	27	304	17		21			
Xerox acid	M2	of 1ppm/24 hrs	0.63	56	13	-33	35	291	4		6			
HP Printing paper	M2	initial	0.68	53	15	-39	42	291				0.07	0.06	0.06
HP Printing paper	M2	If 100hrs	0.5	64	14	-23	26	301	20		26			
HP Printing paper	M2	of 1ppm/24 hrs	0.64	55	13	-37	39	290	4		6			
HP Multipurpose	M2	initial	0.67	54	14	-36	39	291				0.04	0.04	0.04
HP Multipurpose	M2	If 100hrs	0.51	64	14	-21	26	304	18		24			
HP Multipurpose	M2	of 1ppm/24 hrs	0.63	56	13	-33	36	291	4		6			
Canon HG 210	M2	initial	0.77	50	27	-40	48	303				0.05	0.04	0.03
Canon HG 210	M2	If 100hrs	0.52	64	20	-28	34	306	20		32			
Canon HG 210	M2	of 1ppm/24 hrs	0.05	96	1	1	1	53	66		94			
Canon PR101	M2	initial	0.81	47	21	-44	49	296				0.01	0.01	0.04
Canon PR101	M2	If 100hrs	0.77	48	18	-45	48	292	4		5			
Canon PR101	M2	of 1ppm/24 hrs	0.05	95	0	1	1	115	69		94			
HP Premium	M2	initial	1.07	39	37	-48	61	307				0.06	0.08	0.04
HP Premium	M2	If 100hrs	1	42	36	-44	57	309	5		7			
HP Premium	M2	of 1ppm/24 hrs	1.03	41	37	-43	57	311	5		4			
SEC Premium	M3	initial	0.24	81	8	-19	21	293				0.00	0.00	
SEC Premium	M3	If 100hrs	0.22	82	7	-17	18	294	3		8			
SEC Premium	M3	of 1ppm/24 hrs	0.07	94	1	-5	5	285	20		71			
Xerox acid	M3	initial	0.27	79	10	-17	20	302				0.02	0.01	
Xerox acid	M3	If 100hrs	0.2	85	9	-10	13	311	9		26			
Xerox acid	M3	of 1ppm/24 hrs	0.25	81	10	-15	18	304	2		7			
HP Printing paper	M3	initial	0.27	79	12	-21	24	298				0.01	0.01	
HP Printing paper	M3	If 100hrs	0.19	85	8	-12	14	303	12		30			
HP Printing paper	M3	of 1ppm/24 hrs	0.25	80	11	-20	23	299	2		7			
HP Multipurpose	M3	initial	0.27	79	11	-17	20	302				0.01	0.00	
HP Multipurpose	M3	If 100hrs	0.19	85	8	-10	13	310	9		30			
HP Multipurpose	M3	of 1ppm/24 hrs	0.25	81	10	-15	18	304	2		7			
Canon HG 210	M3	initial	0.19	84	6	-16	17	289				0.00	0.00	
Canon HG 210	M3	If 100hrs	0.14	88	5	-13	14	291	5		26			
Canon HG 210	M3	of 1ppm/24 hrs	0.11	91	4	-10	11	292	9		42			
Canon PR101	M3	initial	0.25	80	9	-19	21	294				0.00	0.00	
Canon PR101	M3	If 100hrs	0.22	82	7	-15	16	297	5		12			
Canon PR101	M3	of 1ppm/24 hrs	0.09	92	2	-6	6	287	19		64			
HP Premium	M3	initial	0.34	73	8	-21	23	292				0.00	0.01	

Dye: M1 = 247, M2 = 241, M3 = 259, M4 = 234

Appendix 2 X-Ray crystal data

Bond lengths [Å] and angles [deg] for 5-(2-Methoxyphenylazo)-2,2,5-trimethyl-1,3-dioxane-4,6-dione **120g**.

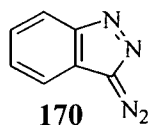


120g

O (1) - C (6)	1.335 (2)	C (6) - O (1) - C (2)	122.13 (13)
O (1) - C (2)	1.446 (2)	O (3) - C (2) - O (1)	110.69 (14)
C (2) - O (3)	1.438 (2)	O (3) - C (2) - C (22)	110.06 (15)
C (2) - C (22)	1.504 (3)	O (3) - C (2) - C (22)	110.09 (15)
C (2) - C (21)	1.506 (3)	O (1) - C (2) - C (21)	105.86 (15)
O (3) - C (4)	1.342 (2)	C (22) - C (2) - C (21)	114.59 (17)
C (4) - O (41)	1.195 (2)	C (4) - O (3) - C (2)	120.36 (14)
C (4) - C (5)	1.525 (3)	O (41) - C (4) - O (3)	119.54 (19)
C (5) - N (7)	1.505 (2)	O (41) - C (4) - C (5)	122.22 (19)
C (5) - C (6)	1.521 (2)	O (3) - C (4) - C (5)	118.17 (15)
C (5) - C (51)	1.524 (3)	N (7) - C (5) - C (6)	102.95 (13)
C (6) - O (61)	1.202 (2)	N (7) - C (5) - C (51)	114.29 (14)
N (7) - N (8)	1.2259 (1)	C (6) - C (5) - C (51)	110.20 (15)
N (8) - C (9)	1.425 (2)	N (7) - C (5) - C (4)	106.37 (15)
C (9) - C (14)	1.397 (2)	C (6) - C (5) - C (4)	113.01 (14)
C (9) - C (10)	1.403 (2)	C (51) - C (5) - C (4)	109.89 (15)
C (10) - O (15)	1.356 (2)	O (61) - C (6) - O (1)	118.72 (15)
C (10) - C (11)	1.392 (2)	O (61) - C (6) - C (5)	122.52 (16)
C (11) - C (12)	1.384 (3)	O (1) - C (6) - C (5)	118.75 (15)
C (12) - C (13)	1.386 (3)	N (8) - N (7) - C (5)	112.78 (14)
C (13) - C (14)	1.382 (2)	N (7) - N (8) - C (9)	114.88 (14)
O (15) - C (16)	1.433 (2)	C (14) - C (9) - C (10)	120.30 (15)
		C (14) - C (9) - N (8)	123.18 (15)
		C (10) - C (9) - N (8)	116.47 (14)

O (15) – C (10) – C (11)	124.47 (16)
O (15) – C (10) – C (9)	116.32 (14)
C (11) – C (10) – C (9)	119.21 (16)
C (12) – C (11) – C (10)	119.65 (17)
C (11) – C (12) – C (13)	121.46 (17)
C (12) – C (11) – C (10)	119.65 (17)
C (11) – C (12) – C (13)	121.46 (17)
C (14) – C (13) – C (12)	119.37 (17)
C (13) – C (14) – C (9)	120.00 (16)
C (10) – O (15) – C (16)	117.36 (13)

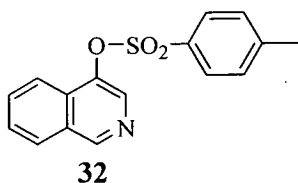
Appendix 3 X-Ray crystal data



Bond lengths [Å] and angles [deg] for diazoindazole **170**.

N (1) - N (2)	1.305 (6)	N (2) - N (1) - C (7a)	109.2 (4)
N (1) - C (7a)	1.398 (7)	N (1) - N (2) - C (3)	107.6 (4)
N (2) - C (3)	1.383 (7)	N (3) - C (3) - N (2)	119.8 (5)
C (3) - N (3)	1.335 (7)	N (3) - C (3) - C (3a)	128.5 (5)
C (3) - C (3a)	1.423 (7)	N (2) - C (3) - C (3a)	111.5 (4)
N (3) - N (4)	1.118 (6)	N (4) - N (3) - C (3)	179.4 (6)
C (3a) - C (4)	1.392 (8)	C (4) - C (3a) - C (7a)	121.1 (5)
C (3a) - C (7a)	1.402 (7)	C (4) - C (3a) - C (3)	137.7 (5)
C (4) - C (5)	1.375 (8)	C (7a) - C (3a) - C (3)	101.2 (4)
C (4) - H (4)	0.9500	C (5) - C (4) - C (3a)	117.7 (5)
C (6) - C (7)	1.360 (8)	C (5) - C (4) - H (4)	121.2
C (6) - H (6)	0.9500	C (3a) - C (4) - H (4)	121.2
C (7) - C (7a)	1.402 (7)	C (4) - C (5) - C (6)	121.3 (5)
C (7) - H (7)	0.9500	C (4) - C (5) - H (5)	119.4
		C (6) - C (5) - H (5)	119.4
		C (7) - C (6) - C (5)	121.4 (5)
		C (7) - C (6) - H (6)	119.3
		C (5) - C (6) - H (6)	119.3
		C (6) - C (7) - C (7a)	118.2 (5)
		C (6) - C (7) - H (7)	120.9
		C (7a) - C (7) - H (7)	120.9
		N (1) - C (7a) - C (7)	129.2 (5)
		N (1) - C (7a) - C (3a)	110.4 (5)
		C (7) - C (7a) - H (7a)	120.3(5)

Appendix 4 X-Ray crystal data



Bond lengths [Å] and angles [deg] for 4-(*p*-toluenesulfonyloxy)isoquinoline **32**.

S (1) - O (1)	1.6166 (12)	O (1) - S (1) - O (3)	108.32 (7)
S (1) - O (3)	1.4292 (12)	O (1) - S (1) - O (2)	102.56 (7)
S (1) - O (2)	1.4250 (12)	O (3) - S (1) - O (2)	120.33 (8)
S (1) - C (9)	1.7484 (16)	O (1) - S (1) - C (9)	104.11 (7)
O (1) - C (4)	1.4060 (19)	O (3) - S (1) - C (9)	109.27 (8)
C (9) - C (14)	1.390 (2)	O (2) - S (1) - C (9)	110.83 (8)
C (9) - C (10)	1.391 (2)	S (1) - O (1) - C (4)	118.24 (10)
C (4) - C (41)	1.414 (2)	S (1) - C (9) - C (14)	118.83 (13)
C (4) - C (3)	1.363 (2)	S (1) - C (9) - C (10)	119.29 (12)
C (14) - C (13)	1.389 (2)	C (14) - C (9) - C (10)	121.88 (15)
C (14) - C (41)	1.004	O (1) - C (4) - C (41)	117.38 (15)
C (10) - C (11)	1.389 (2)	O (1) - C (4) - C (3)	120.83 (16)
C (10) - H (101)	1.011	C (41) - C (4) - C (3)	121.70 (16)
C (12) - C (11)	1.398 (3)	C (9) - C (14) - C (13)	118.51 (16)
C (12) - C (13)	1.380 (3)	C (9) - C (14) - H (141)	120.454
C (12) - C (15)	1.509 (2)	C (13) - C (14) - H (141)	121.031
C (41) - C (5)	1.415 (2)	C (9) - C (10) - C (11)	118.38 (15)
C (41) - C (81)	1.420 (2)	C (9) - C (10) - H (101)	120.731
C (3) - N (2)	1.363 (2)	C (11) - C (10) - H (101)	120.890
C (3) - H (31)	1.011	C (11) - C (12) - C (13)	118.88 (16)
N (2) - C (1)	1.316 (3)	C (11) - C (12) - C (15)	120.15
C (5) - C (6)	1.373 (3)	C (13) - C (12) - C (15)	120.97
C (11) - H (51)	0.998	C (4) - C (41) - C (5)	124.55 (16)

C (11) - H (111)	1.006	C (4) - C (41) - C (81)115.79 (16)
C (13) - H (131)	1.012	C (5) - C (41) - C (81)119.65 (16)
C (81) - C (1)	1.418 (3)	C (4) - C (3) - N (2)122.41 (18)
C (81) - C (8)	1.413 (3)	C (4) - C (3) - H (31)118.624
C (1) - H (1)	1.014	N (2) - C (3) - H (31)118.967
C (15) - H (151)	1.008	C (3) - N (2) - C (1)117.39 (17)
C (15) - H (152)	1.004	C (41) - C (5) - C (6)119.41 (17)
C (15) - H (153)	0.997	C (41) - C (5) - H (51)120.195
C (7) - C (6)	1.413 (3)	C (6) - C (5) - H (51)120.394
C (7) - C (8)	1.367 (3)	C (12) - C (11) - C (10)121.14 (16)
C (7) - H (71)	1.010	C (12) - C (11) - H (111)120.045
C (6) - H (61)	1.007	C (10) - C (11) - H (111)118.811
C (8) - H (81)	1.003	C (12) - C (13) - C (14)121.21 (16)
		C (12) - C (13) - H (131)119.721
		C (14) - C (13) - H (131)119.071
		C (41) - C (81) - C (1) 117.95 (17)
		C (41) - C (81) - C (8)119.28 (17)
		C (1) - C (81) - C (8)122.77 (17)
		C (81) - C (1) - N (2)124.67 (17)
		C (81) - C (1) - H (11)117.864
		N (2) - C (1) - H (11)117.464
		C (12) - C (15) - H (151)109.323
		H (151) - C (15) - H (153)109.062
		H (152) - C (15) - H (153)109.400
		C (6) - C (7) - C (8)120.22 (19)
		C (6) - C (7) - H (71)135.259
		C (8) - C (7) - H (71)104.351
		C (7) - C (6) - C (5)121.11 (19)
		C (7) - C (6) - H (61)119.422
		C (5) - C (6) - H (61)119.465
		C (81) - C (8) - C (7)120.32 (18)
		C (81) - C (8) - H (81)118.230

